UNIVERSITY OF SOUTHAMPTON

FACULTY OF NATURAL AND ENVIRONMENTAL SCIENCES

Ocean and Earth Sciences

Chromium Isotope Behaviour in Natural Waters

by

Heather Jane Goring-Harford

Thesis for the degree of Doctor of Philosophy

June 2017

UNIVERSITY OF SOUTHAMPTON

ABSTRACT

FACULTY OF NATURAL AND ENVIRONMENTAL SCIENCES

Ocean and Earth Sciences

Doctor of Philosophy

CHROMIUM ISOTOPE BEHAVIOUR IN NATURAL WATERS

By Heather Jane Goring-Harford

The isotopes of chromium (Cr) fractionate during terrestrial oxidation reactions that require the presence of oxygen. The main source of Cr to the oceans is *via* rivers, and thus Cr isotopic signatures (expressed as $\delta^{53}Cr$) preserved in authigenic sediments are increasingly being used to reconstruct the oxygen levels of ancient environments. However, Cr can undergo various reactions in natural waters that may fractionate Cr isotopes. The contribution of these reactions to authigenic sediment $\delta^{53}Cr$ values is not well understood, and this limits the interpretation of $\delta^{53}Cr$ values measured in ancient archives. This thesis describes the development of a method to accurately and precisely measure Cr isotopic signatures in natural waters with extremely low Cr concentrations, and evaluates the behaviour of Cr isotopes in water samples from a range of environmental settings.

Seawater samples from the Atlantic Ocean Oxygen Minimum Zone (OMZ) were analysed to evaluate whether Cr isotopic fractionation was enhanced under depleted oxygen conditions. Results indicate that the Atlantic OMZ is not sufficiently depleted in oxygen to reduce and remove Cr from seawater, although $\delta^{53}Cr$ values (1.08 – 1.72‰) were variable due to adsorption of Cr(III) to particles on the shelf, and hydrological mixing. Black Sea seawater samples that had dissolved oxygen concentrations close to zero were enriched in ^{52}Cr, resulting in a $\delta^{53}Cr$ that was 0.38‰ lower than the overlying fully oxygenated waters.

Samples were also taken from the Celtic Sea to investigate the seasonal variation in the Cr isotopic composition of seawater from a biologically productive, oxic shelf sea. Chromium concentrations and $\delta^{53}Cr$ values were affected by organic matter cycling, and, as in the Atlantic OMZ region, interactions of Cr with particles on the shelf and hydrological mixing were locally important.

Finally, two transects of the Beaulieu River (UK), a relatively pristine river-estuary system, were sampled to assess the behaviour of Cr during estuarine mixing. Both redox species of Cr (Cr(III) and Cr(VI)) and $\delta^{53}Cr$ behaved conservatively during mixing between river water and seawater. The Beaulieu River had relatively low $\delta^{53}Cr$ (as low as -0.59‰) compared to most other rivers analysed to date, which suggests that the $\delta^{53}Cr$ of Cr supplied to the oceans from rivers may be more variable than previously thought.

List of Contents

List of Figures

Chapter 1: Introduction

Chapter 3: Behaviour of chromium isotopes in the North Atlantic Oxygen Minimum Zone

Chapter 4: Temporal and spatial variations in the chromium isotopic signature of seawater in the Celtic Sea

List of Tables

Chapter 4: Temporal and spatial variations in the chromium isotopic signature of seawater in the Celtic Sea

Chapter 5: Behaviour of chromium and chromium isotopes during estuarine mixing: Beaulieu estuary, UK

Declaration of Authorship

I, Heather Jane Goring-Harford, declare that this thesis entitled **Cr isotope behaviour in natural waters** and the work presented in it are my own and has been generated by me as the result of my own original research.

I confirm that:

1. This work was done wholly or mainly while in candidature for a research degree at this University;
2. Where any part of this thesis has previously been submitted for a degree or any other qualification at this University or any other institution, this has been clearly stated;
3. Where I have consulted the published work of others, this is always clearly attributed;
4. Where I have quoted from the work of others, the source is always given. With the exception of such quotations, this thesis is entirely my own work;
5. I have acknowledged all main sources of help;
6. Where the thesis is based on work done by myself jointly with others, I have made clear exactly what was done by others and what I have contributed myself;
7. None of this work has been published before submission.

Signed: ……

Date: ……..

Acknowledgements

First, a huge thank you to my supervisors Rachael James, Christopher Pearce and Douglas Connelly. I am especially grateful to Chris for teaching me so many essential lab skills early on, without which the (reasonably) timely finish of this project could not have been achieved. I am particularly indebted to Rachael for her tireless efforts during the write-up period in providing swift and detailed feedback, and for keeping me focussed on big ideas at times when minutia proved distracting. I am also grateful to Doug for the unique insight he was able to give on the art of co-precipitation and the taming of chromium, fickle beast that it is. In addition I am thankful to my panel chair Rachel Mills for her praise and encouragement for my work, which was I was always surprised and pleased to receive.

Next I would like to thank Andy Milton, Matt Cooper and Kate Peel, all of whom worked extremely hard to meet the heavy lab demands of my project. The skills I learned from Andy and Matt will be invaluable in my new role as Geochemistry Research Technician at NOCS and I hope to continue learning their dark and mysterious arts for a long time to come.

Many thanks to those who shared their expert advice with me on various topics – Ian Parkinson on double spike calculations, Anna Lichtschlag on coring and pore water sampling, Maeve Lohan on filtration and Aly Lough on UV digestion. Also thanks to Chris Holmden and Isabelle Baconnais at the University of Saskatchewan for their contributions to the inter-calibration study, and the friendly team at BODC for always supplying me with auxiliary data so promptly.

I am grateful to Rachael James, Peter Statham and Maeve Lohan for making my participation on the SSB cruise in March 2015 possible and for arranging the collection of samples on other cruises. Thanks are also due to the whole trace metal SSB team for collecting so many samples for me, I can only apologise for how heavy they were! I must also express my gratitude to Jessica Klar, who made practical contributions to every one of my science chapters through collecting samples and giving advice which helped me to maintain the highest standards in my lab work. When faced with clean lab doubts, I will always ask ‘what would Jessy do?’. I am also indebted to Hannah Donald, who sacrificed her precious time and energy to make my Beaulieu sample collections a success.

Next I would like to thank my office, demonstrating and conference companions over the years, especially Hannah Donald, Sarah Wright, Dave Reading and Aly Lough for all our long chats. They probably prevented long-term lunacy on my part.

Love to Mum, Dad and Meg for both keeping me grounded and lifting me up. Finally, no words are sufficient to properly thank my husband Anthony (a.k.a. Cecil) so I must fall to analogy: he is Mulder to my Scully, Kirk to my Spock (and often, Chewbacca to my Han). But through this project most of all, I have been Frodo and he has been long suffering Sam. I am grateful and amazed that you have chosen to walk with me so far.

Definitions and abbreviations

AAIW	Antarctic Intermediate Water
Al	Aluminium
Al_2O_3	Aluminium oxide
ASCS	Atlantic Seawater Conductivity Standard
BIF	Banded Iron Formation
$CaCl_2$	Calcium chloride
Chl-a	Chlorophyll-a
Cr	Chromium
Cr_{ORG}	Dissolved organic Cr concentration
Cr_T	Total dissolved Cr concentration, Cr(III) + Cr(VI)
DOC	Dissolved organic carbon
Fe	Iron
GOE	Great Oxidation Event
H_2O_2	Hydrogen peroxide
HCl	Hydrochloric acid
HDPE	High density polyethylene
HNO_3	Nitric acid
ID	Isotope dilution
LDPE	Low density polyethylene
M	Moles per litre
MC-ICP-MS	Multi-collector inductively coupled plasma mass spectrometry
Mg	Magnesium
Mn	Manganese
Mo	Molybdenum
MOW	Mediterranean Outflow Water
MQ	Milli-Q water, resistivity 18.2MΩ
MW	Mediterranean Water

Na_2CO_3	Sodium carbonate
NACW	North Atlantic Central Water
NADW	North Atlantic Deep Water
NBS979	Chromium nitrate standard distributed by NIST
NEACW	North East Atlantic Central Water
NEADW	North East Atlantic Deep Water
NH_4OH	Ammonium hydroxide
NIST	National Institute of Standards and Technology
NOCS	National Oceanography Centre, Southampton
O_2	Oxygen
OAE	Ocean Anoxic Event
OMZ	Oxygen Minimum Zone
PTFE	Polytetrafluoroethylene
Redox	Reduction and oxidation
S	Salinity
SACW	South Atlantic Central Water
SD	Standard deviation
SML	Surface mixed layer
Ti	Titanium
U	Uranium
UCDW	Upper Circumpolar Deep Water
V	Vanadium
$\delta^{53}Cr$	Cr isotopic signature relative to NBS979 reference standard
Δ	Fractionation factor

Chapter 1: Introduction

1.1 Utility of chromium isotopes as a redox proxy

The oxygenation of Earth's atmosphere and the evolution of life are strongly intertwined, however their timing and causes are still hotly debated (e.g. Robbins *et al.* 2016, Planavsky *et al.* 2016, Zhang *et al.* 2016). Moreover, several climatological events in the Phanerozoic Eon are associated with deoxygenation of the oceans (so called Ocean Anoxic Events, or OAEs) and these are thought to be linked with mass extinctions (e.g. Hough *et al.* 2006). Our understanding of the evolution and sustenance of life through Earth's history hinges on our ability to decipher changes and imbalances in the oxygen (O_2) cycle. In the context of modern climate change, such understanding may help to predict and manage the deoxygenation of the modern oceans that is occurring due to rising temperatures and decreased ocean circulation (Keeling *et al.*, 2010; Stramma *et al.*, 2008). Consequently significant attention has been paid to tracers which can be used to reconstruct O_2 levels in past environments in recent years. A whole host of reduction-oxidation (redox) sensitive metallic elements may be used (e.g. iron (Fe) and molybdenum (Mo)), and each exhibits a unique response to changing O_2 levels which affects their preservation in sedimentary sequences (e.g. Algeo and Maynard 2004; Nameroff *et al.* 2004; Tribovillard *et al.* 2006). Isotopic ratio measurements are regarded as particularly useful tracers because they are altered by a more limited range of processes than simple element concentrations, and the reactions that cause these alterations are different for specific elements. For example Fe isotopes are sensitive to a host of abiotic and microbial redox effects whereas Mo is known to respond primarily to adsorption onto manganese (Mn) oxide particles, and sulphide formation in euxinic waters (Anbar and Rouxel, 2007; Severmann and Anbar, 2009). Therefore a more precise interpretation of past environments is possible using isotopic tracers, as the confounding effects of multiple processes are reduced.

Chromium (Cr) isotopes occupy a useful niche within this framework. Its isotopes fractionate during redox reactions under relatively mild reducing conditions, which means it is more sensitive to subtle changes in O_2 levels than elements like Fe and Mo (Nameroff *et al.*, 2004; Piper, 1994). Furthermore the amount of O_2 required to kick-start terrestrial Cr oxidation appears to be similar to that required to support early animal life (Gilleaudeau

et al., 2016; Planavsky *et al.*, 2014) which may mean it can provide key information about the evolution of complex animals. Consequently it has been used in a wide range of studies over the last decade to contribute to our understanding of past O_2 levels (Crowe *et al.*, 2013; D'Arcy *et al.*, 2016; Frei *et al.*, 2016; Frei *et al.*, 2011; Frei *et al.*, 2009; Gilleaudeau *et al.*, 2016; Holmden *et al.*, 2016; Planavsky *et al.*, 2014; Rodler *et al.*, 2016; Rodler *et al.*, 2016; Sial *et al.*, 2015). However, the environmental processes that contribute to the fractionation of Cr isotopes relative to a Cr isotope reference standard (referred to as the Cr 'isotopic signature') are still not fully characterised. Cr undergoes diverse reactions at as it is transferred through the environment that are poorly understood in relation to the isotopic effect on sedimentary rocks (e.g. Gueguen *et al.* 2016, Rodler *et al.* 2016). This makes it difficult to quantify past O_2 levels and identify other potentially important causes of isotopic fractionation.

Preliminary studies have shown that there is significant global heterogeneity in the Cr isotopic signatures of modern seawater (Bonnand *et al.*, 2013; Scheiderich *et al.*, 2015). The reactions responsible for these isotopic variations are uncertain and it is unclear whether Cr isotopic signatures are best applied as a global-scale or local-scale redox proxy. As a result, the potential of the Cr isotope proxy has not yet been fully realised. Field studies of Cr behaviour in natural environments are required to clarify the mechanisms governing Cr isotope systematics, in particular its behaviour in natural waters as many redox reactions occur in aqueous solutions. These measurements are challenging to make because Cr concentrations in natural waters are generally in the nanomolar range (e.g. Bonnand *et al.* 2013; McClain and Maher 2016; Scheiderich *et al.* 2015) and precise isotopic measurements require significant quantities of all four Cr isotopes in the analyte (Bonnand, 2011). The aims of this thesis are to further develop methods for the accurate and precise measurement of Cr isotopes in low concentration natural samples (Bonnand *et al.*, 2013; Cranston and Murray, 1978), and to apply these methods to the analysis of a diverse range of natural waters in order to clarify the processes that control Cr isotopic signatures on Earth.

1.1.1 Chemistry of chromium in the natural environment

Chromium has two stable oxidation states in Earth surface environments, Cr(VI) and Cr(III). Most Cr bearing minerals (e.g. chromite, $(Fe,Mg)Cr_2O_4$) contain the Cr(III) form and this is

released into the environment *via* hydrolysis reactions which form aqueous Cr(III) octahedral complexes such as $CrOH^{2+}$, $Cr(OH)_3$ and $Cr(OH)_4^-$ (Rai *et al.*, 1987). The complex formed depends upon the standard potential and pH of the solution (**Figure 1.1**), and in seawater the most favourable form is $Cr(OH)_2^+$ (Elderfield, 1970). Based on thermodynamic calculations all of these species are unstable in oxic natural waters and should rapidly oxidise to Cr(VI), however the high crystal field stabilisation energy for Cr(III) means that its ligands are tightly bound, restricting mechanisms of oxidation (Elderfield, 1970; Pettine and Millero, 1990). Additionally, Cr(III) may be stabilised in solution by complexation with a wide range of organic ligands (Hug *et al.*, 1997; Kaczynski and Kieber, 1994; Remoundaki *et al.*, 2007). In practise therefore oxidation by dissolved O_2 is extremely slow, and it has been demonstrated that only 3% of Cr(III) is oxidised in this way over 30 days at environmentally relevant temperatures (22-26°C) (Schroeder and Lee, 1975). There are only two oxidants which are known to be effective in natural settings; manganese (Mn) oxides and hydrogen peroxide (H_2O_2) (Oze *et al.*, 2007; Pettine and Millero, 1990; Pettine *et al.*, 1991; Schroeder and Lee, 1975). In laboratory experiments oxidation of Cr by Mn oxides happens within minutes for aqueous Cr(III) (Schroeder and Lee, 1975) and within hours for Cr-bearing minerals (Oze *et al.*, 2007). This reaction is important in settings where Mn oxides are abundant, such as ultramafic soils and hydrothermal sediments (Fandeur *et al.*, 2009; Fantoni *et al.*, 2002; Jeandel and Minster, 1984). Oxidation by H_2O_2 may be more important in surface water environments where particulate Mn oxides are not abundant, as it can be generated by photochemical reactions (Pettine and Millero, 1990).

Once oxidised, the soluble CrO_4^{2-} ion is usually the dominant form of Cr(VI) in natural waters since Cr concentrations are typically too low to favour dimerization to the dichromate ion, $Cr_2O_7^{2-}$ (Elderfield, 1970). Both Cr(III) and Cr(VI) may adsorb to solid surfaces and do so at distinct pH ranges (**Figure 1.2**). Aqueous Cr(VI) may also undergo a number of reduction reactions. Iron in its reduced Fe(II) form is a particularly effective reductant in a wide range of settings, and may reduce Cr on mineral surfaces such as goethite (Basu and Johnson, 2012) or in solution, even under oxygenated conditions (Buerge and Hug, 1997; Fendorf and Li, 1996). The reaction is effective at high and low pH although the products are only soluble at low pH (Fendorf and Li, 1996):

$$Cr(VI)_{(aq)} + 3Fe(II)_{(aq)} \rightarrow Cr(III)_{(aq)} + 3Fe(III)_{(aq)} \text{ (pH 1-4)} \qquad \textbf{Equation 1.1}$$

$$Cr(VI)_{(aq)} + 3Fe(II)_{(aq)} + 3H_2O \rightarrow Cr_xFe_{1-x}(OH)_{3(s)} + 3H^+ \ (pH > 4) \qquad \textbf{Equation 1.2}$$

Co-precipitation of Cr(III) with Fe as $Cr_xFe_{1-x}(OH)_3$ (Sass and Rai, 1987) represents a more effective removal mechanism than adsorption or direct precipitation of CrO_3 over a wide pH range (4-11) (Crawford *et al.*, 1993). Fe may also catalyse reactions with organic reductants, causing the formation of inert organic Cr(III) species (Buerge and Hug, 1998). Chromium is not thought to be a nutrient for phytoplankton or bacteria but various studies have shown that biological activity can reduce Cr(VI) to Cr(III), either actively within biological cells (possibly as a consequence of the similar tetrahedral structures of chromate (CrO_4^{2-}) and sulphate (SO_4^{2-}) (Wang and Dei, 2001), or *via* the release of organic reductants into the water column (Li *et al.*, 2009; Semeniuk *et al.*, 2016). Hydrogen sulphide (Johnson *et al.*, 1992; Kim *et al.*, 2001; Smillie *et al.*, 1981) as well as a wide range of organic molecules (Deng and Stone, 1996; Kitchen *et al.*, 2012) are also known to reduce Cr in their own right. The effect of Cr redox reactions on Cr speciation and Cr isotopes will be discussed in depth in **Section 1.1.2**.

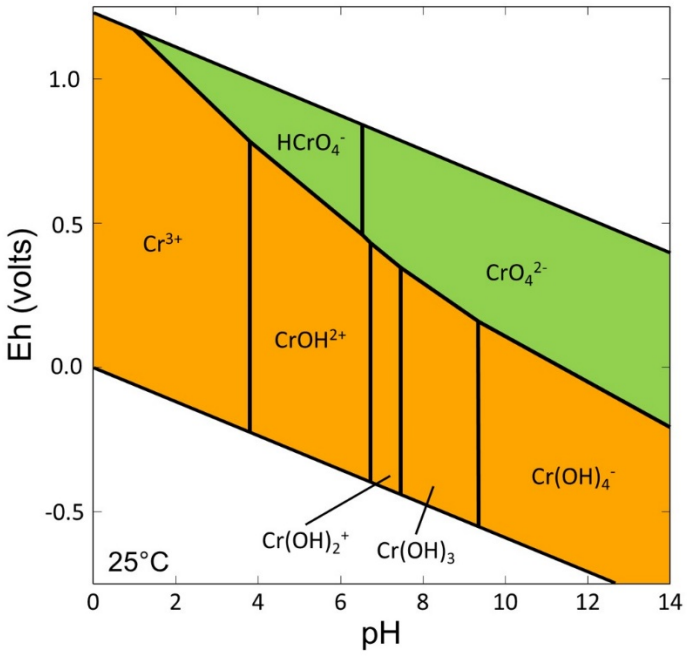

Figure 1.1 - Eh-pH diagram for aqueous species of Cr in water, modelled at 1bar pressure and Cr concentration of 1nM. Orange blocks represent Cr(III) species and green blocks represent Cr(VI) species. Generated using Geochemist's Workbench V11 with the Lawrence Livermore National Laboratory (LLNL) standard database.

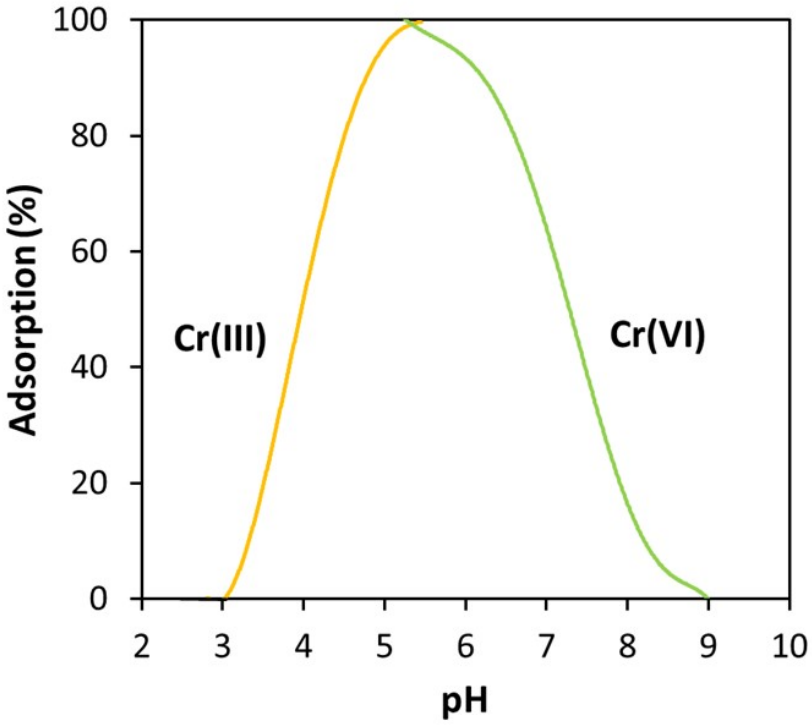

Figure 1.2 - Modelled adsorption of Cr(III) and Cr(VI) onto goethite as a fuction of pH. Adapted from Gaillardet *et al.* 2003, with adsorption constants taken from Dzomback and Morel 1990.

1.1.2 Chromium isotope systematics

Chromium has four stable isotopes: ^{50}Cr (4.35%), ^{52}Cr (83.79%), ^{53}Cr (9.50%) and ^{54}Cr (2.36%). Changes to the relative proportions of isotopes in a sample are expressed as δ^{53}Cr relative to a manufactured chromium standard (chromium nitrate, $Cr(NO_3)_3$, referred to as NBS979) (**Equation 1.1**).

$$\delta^{53}\mathrm{Cr} = \left[\frac{\left(\frac{53_{\mathrm{Cr}}}{52_{\mathrm{Cr}}}\right)_{sample} - \left(\frac{53_{\mathrm{Cr}}}{52_{\mathrm{Cr}}}\right)_{NBS979}}{\left(\frac{53_{\mathrm{Cr}}}{52_{\mathrm{Cr}}}\right)_{NBS979}} \right] \times 1000 \qquad \textbf{Equation 1.3}$$

Cr isotopic signatures in the natural environment are controlled by redox reactions and fractionations incurred as a result of other types of reaction are generally small (see **Table 1.1**). The amount of fractionation incurred by a specific reaction can be described in terms of the fractionation factor α (**Equation 1.4**), but for convenience these are expressed as Δ

values between the reactants and products in this work and elsewhere (**Equations 1.5** and **1.6;** reactants = R, products = P).

$$\alpha = \frac{\left(\frac{53_{Cr}}{52_{Cr}}\right)_R}{\left(\frac{53_{Cr}}{52_{Cr}}\right)_P} \qquad \textbf{Equation 1.4}$$

$$\Delta_{R-P} = 1000 \times (\alpha - 1) \qquad \textbf{Equation 1.5}$$

And for small values of Δ_{R-P},

$$\Delta_{R-P} \approx \delta^{53}Cr_R - \delta^{53}Cr_P \qquad \textbf{Equation 1.6}$$

If the reactants and products are in different phases (e.g. solid *versus* liquid, liquid *versus* gas) then isotopes cannot re-equilibrate over timescales of years (Wang *et al.*, 2015). Hence because of the high solubility of Cr(VI) and the low solubility of Cr(III), large changes in $\delta^{53}Cr$ of up to 10.2‰ have been observed in laboratory experiments (Kitchen *et al.*, 2012) and up to 7.9‰ in environmental samples (Ball and Bassett, 2000). Reduction of Cr(VI) is governed by kinetic fractionation: bonds between lighter isotopes possess a slightly higher vibrational frequency which allows them to be broken more easily, resulting in slightly faster reaction rates for the lighter isotopes such that the Cr(III) product has a lower $\delta^{53}Cr$ than the reactant Cr(VI) (**Table 1.1**). Conversely, is oxidation is thought to be governed by equilibrium fractionation: as a reaction proceeds in both directions, the isotopes are distributed to achieve the lowest overall energy in the system. Preferential oxidation of ^{53}Cr is thought to occur because the ^{53}Cr isotope forms stronger bonds as Cr(VI) within the CrO_4^{2-} oxyanion compared to Cr(III) (D'Arcy *et al.*, 2016). However, laboratory experiments indicate that Cr(VI) can be enriched in either ^{52}Cr or ^{53}Cr relative to Cr(III), and Cr(VI) products have $\delta^{53}Cr$ values of -2.5 - 0.7‰ (Bain and Bullen, 2005; Joshi *et al.*, 2011). This may be due to different reaction rates and mechanisms for different forms of Mn oxide (Joshi *et al.*, 2011), or partial back-reduction of the Cr(VI) that forms (Frei *et al.*, 2011).

Table 1.1 – Experimentally and theoretically determined fractionation factors (expressed as Δ_{R-P}) for different reaction types.

Reaction type	Reactant	Experimental conditions	Type of fractionation	Δ_{R-P}	Reference
Reduction of $Cr(VI)_{(aq)}$ to Cr(III)	-	Theoretical	Equilibrium	6 - 7	Schauble *et al.* 2004
	Fe(II) (magnetite/natural sediments)	Suspended sediment	Rayleigh	3.3 - 3.5	Ellis *et al.* 2002
	Fe(II) (contaminated sediments)	Sediment incubation	Rayleigh	2.4 - 3.1	Berna *et al.* 2010
	$Fe(II)_{(aq)}$	Batch	Rayleigh	3.1 - 4.5	Døssing *et al.* 2011
	$Fe(II)_{(aq)}$	Gradual Fe(II) addition	Rayleigh	1.5	Døssing *et al.* 2011
	Fe(II) (synthesised minerals FeS, FeCO3, goethite, green rust)	Suspended sediment	Rayleigh	2.1 - 3.9	Basu and Johnson 2012
	$Fe(II)_{(aq)}$	Batch, pH 4-5.3	Rayleigh	4.2	Kitchen *et al.* 2012
	H_2O_2	Batch	Equilibrium/Rayleigh	3.5 - 7.2	Zink *et al.* 2010
	Bacteria (Shewanalla oneidensis)	Variable lactate concentration	Rayleigh	1.8 - 4.5	Sikora *et al.* 2008
	Bacteria (Pseudomonas stutzeri)	Aerobic, cell suspension with lactate	Rayleigh	2	Han *et al.* 2012
	Bacteria (Pseudomonas stutzeri)	Denitrifying, cell suspension with lactate	Rayleigh	0.4	Han *et al.* 2012
	Bacteria (G. sulfurreducens, Shewanella sp., P. stutzeri, D. vulgaris)	Anaerobic, cell suspension with acetate/lactate	Rayleigh	2.2 - 3.1	Basu *et al.* 2014
	Bacteria (Bacillus sp.)	Variable glucose	Rayleigh	2 - 3.7	Xu *et al.* 2015

Table 1.1 - continued

Reaction type	Reactant	Experimental conditions	Type of fractionation	Δ_{R-P}	Reference
	Bacillus sp. QH-1	Variable temperature	Rayleigh	2 - 7.6	Xu *et al.* 2015
Reduction of $Cr(VI)_{(aq)}$) to Cr(III) (continued)	Organic molecules (deciduous tree mulch)	Batch	Rayleigh	3.5	Jamieson-Hanes *et al.* 2012
	Organic molecules (humic, fulvic, mandelic acids)	Batch, pH 4.5-5, goethite/Al_2O_3 catalysts	Rayleigh	3.1	Kitchen *et al.* 2012
Adsorption of $Cr(VI)_{(aq)}$	Goethite/Al_2O_3	Batch, pH 4-6	Equilibrium	≤ -0.1	Ellis *et al.* 2004
Ligand exchange, Cr(III)	Oxide, aquo, hydroxyl ligands	Theoretical	Equilibrium	< ±1	Schauble *et al.* 2004
Oxidation of $Cr(III)_{(aq)}$ to Cr(VI)	H_2O_2	Batch	Rayleigh?*	-0.6	Zink *et al.* 2010
Oxidation of Cr(III) to Cr(VI)	Manganese oxides	Theoretical (based on measured peridotites)	Equilibrium	-0.2 - -0.6	Wang *et al.* 2016
Acid dissolution of Cr(III)	Hydrochloric acid, chromite	Batch	?	≤ ±0.1	Crowe *et al.* 201
Precipitation of $Cr(VI)_{(aq)}$ in inorganic carbonate (calcite)	$CaCl_2$ + Na_2CO_3	Batch/silica hydrogel	Rayleigh	-0.1 - -0.3	Rodler *et al.* 201
Precipitation of Cr(VI) in biogenic carbonate	Green algae	Theoretical (based on measured carbonates)	?	0.5	Holmden *et al.* 2016

*Fractionation factors were different for products and reactants implying multi-step reaction/in situ back-reduction

1.2 Biogeochemistry of chromium in Earth surface environments

1.2.1 Behaviour of Cr during terrestrial weathering

The average abundance of Cr in continental crust is 97-126 ppm (Hans Wedepohl, 1995; Rudnick and Gao, 2003). Most of this Cr is contained within ultramafic rocks, which typically contain 2500-3000 ppm Cr as Cr(III) (Schoenberg *et al.*, 2008; Stueber and Goles, 1967). The δ^{53}Cr of igneous crust is -0.12 ± 0.10‰ (Schoenberg *et al.*, 2008) and is not affected by metamorphic alteration (Frei *et al.*, 2016; Wang *et al.*, 2016). Although chromite contains the largest proportion of Cr of any naturally occurring mineral it is highly refractory, so other minerals with a lower Cr content (such as Cr-magnetites and Cr-silicates) are thought to be important in supplying Cr to the environment (Oze *et al.*, 2004). During oxic weathering, Cr(III) is oxidised to Cr(VI) that can be incorporated into (and/or adsorbed onto) clay minerals and Fe oxyhydroxides (Oze *et al.*, 2004). The ^{53}Cr isotope is thought to be preferentially oxidised (**Section 1.1.2**; Berger and Frei 2014; Frei and Polat 2013), and Cr(VI) is highly soluble and mobile, so it tends to be transported away from the weathering site. This results in weathered materials that have δ^{53}Cr values lower than the protolith, and in support of this modern soils often have lower δ^{53}Cr values than continental crust (-0.44 to 0.23‰; D'Arcy *et al.* 2016; Frei *et al.* 2014; Berger and Frei 2014).

1.2.2 Ground waters and soil pore waters

The Cr chemistry of ground waters and soil pore waters is exceedingly complex due to the sensitivity of Cr to changes in dissolved O_2 levels and pH, and the abundant oxidants, reductants and reactive mineral surfaces available in these environments (as discussed in **Section 1.1.1**). Either species (Cr(III) or Cr(VI)) may dominate depending on local environmental conditions (Fantoni *et al.*, 2002; Izbicki *et al.*, 2008; Magar *et al.*, 2008; Masscheleyn *et al.*, 1992). For example, Cr(VI) was favoured in well oxygenated, alkaline ground waters of the Mojave Desert (USA) and any Cr(III) produced by reductants was effectively removed from solution by precipitation (Izbicki *et al.*, 2008). In contrast, Cr in sedimentary pore waters of the Lower Hackensack River catchment (USA) at uncontaminated and contaminated sites alike was found to be exclusively present as Cr(III) due to anoxia in the sediments (Martello *et al.*, 2007). In that case Cr did not oxidise even when the host sediment was aerated for several hours, due to the slow oxidation kinetics of Cr(III) with O_2 and the apparent dominance of reductants (e.g. organic molecules) over

oxidants (manganese oxides) in the sediments (Magar *et al.*, 2008). The speciation of Cr strongly affects its mobility in the environment, with reduction, adsorption and precipitation all effectively acting to curtail transport (Kent *et al.*, 1995) and oxidation acting to enhance transport. Thus the variability in the chemical composition of ground waters and soil pore waters explains in part why Cr concentrations in rivers are so variable (see **Section 1.2.3**).

The Cr concentration and δ^{53}Cr values of ground waters is very variable: uncontaminated ultramafic ground waters can contain around 1400nM Cr (Fantoni *et al.*, 2002; Izbicki *et al.*, 2008) whereas riverine pore waters may contain less than 200nM (Martello *et al.*, 2007), and δ^{53}Cr values range between 0.2 and 7.9‰ (Ball and Bassett, 2000; Ellis *et al.*, 2002; Izbicki *et al.*, 2008; Raddatz *et al.*, 2010; Villalobos-Aragón *et al.*, 2012). There is evidence that reduction of Cr(VI) by naturally occurring reductants is responsible for much of this variation (Heikoop *et al.*, 2014; Jamieson-Hanes *et al.*, 2012; Raddatz *et al.*, 2010), and oxidation of Cr(III) may also affect δ^{53}Cr (Frei *et al.*, 2014). Inorganic Cr(III) tends to precipitate from ground waters when it mixes with oxic seawater, resulting in lower concentrations being delivered to coastal waters and hence to the oceans (O'Connor *et al.*, 2015). However, Cr often does not conform to the redox behaviours expected in sedimentary redox sequences when it forms inert organic complexes (O'Connor *et al.*, 2015; Rigaud *et al.*, 2013). As a result submarine ground water may still act as a source of Cr to some parts of the coastal ocean, and can supply 0.01 - 4.43µmol day^{-1} m^{-2} Cr (O'Connor *et al.*, 2015; Rigaud *et al.*, 2013).

The global ground water flux of Cr to the oceans has been estimated at 2-9% of the total flux (Bonnand *et al.*, 2013) and ground waters are not expected to have a significant impact on ocean δ^{53}Cr values. However, ground water may make a significant contribution to the Cr inventory of the coastal zone if submarine ground waters have relatively high concentrations and δ^{53}Cr values (O'Connor *et al.*, 2015; Rigaud *et al.*, 2013). As yet, however, this is unknown.

1.2.3 Rivers and estuaries

Rivers represent the largest source of Cr to the oceans by far with 76-98% of the oceanic Cr budget delivered *via* this route (Bonnand *et al.*, 2013; Chester and Murphy, 1990; McClain and Maher, 2016). The initial isotopic signatures and any fractionating processes

that occur within rivers during transport to the ocean are therefore likely to be important in defining ocean $\delta^{53}Cr$. Chromium in rivers and estuaries occurs in three major forms: particulate, dissolved inorganic (Cr(III)/Cr(VI)), and dissolved organic. The Cr concentration of riverine suspended particle concentrations varies widely, with an average value of 130 ± 155 ppm (Viers *et al.*, 2009). The bulk $\delta^{53}Cr$ value of these particles is similar to that of crustal rocks (-0.1 to 0.1‰; Wu *et al.* 2017), but the $\delta^{53}Cr$ value of the reactive surface Cr fraction has yet to be determined.

Dissolved inorganic Cr concentrations in rivers are variable, with concentrations as low as 1.2nM in chalky catchments such as Southampton Water and the Humber Estuary (UK) (Bonnand *et al.*, 2013; Comber and Gardner, 2003), whereas ultramafic catchments in the USA and Central Europe commonly have concentrations of 100-500nM (McClain and Maher, 2016; Novak *et al.*, 2014). The proportions of Cr(III) and Cr(VI) are also highly variable (**Figure 1.3A**). Organic forms of Cr can be important in rivers that contain large quantities of organic acids; for example one study showed that an average of 65% and 72% of Cr in the Shark and Tamiami Rivers (USA) respectively was bound in organic complexes (Kaczynski and Kieber, 1994). The role of organic compounds in defining $\delta^{53}Cr$ in natural systems is yet to be explored, mainly due to the practical difficulties associated with separating organic and inorganic Cr from natural water samples.

To date, there are relatively few measurements of the Cr isotopic composition of river water (**Figure 1.4**) but they appear to have moderately positive $\delta^{53}Cr$; the overall range is -0.33 to 4.0‰. Positive $\delta^{53}Cr$ values are attributed to preferential oxidation of ^{53}Cr during oxidative weathering (Frei *et al.*, 2014), but it is also argued that reduction of Cr(VI) and removal of the Cr(III) that forms also increases the $\delta^{53}Cr$ value of the remaining Cr(VI) (Bonnand *et al.*, 2013; D'Arcy *et al.*, 2016). Reduction of Cr(VI) can occur in the presence of dissolved Fe(II) and/or organic matter (Kieber and Helz, 1992), or on the surface of Fe(II) containing minerals such as goethite and magnetite (Basu and Johnson, 2012; White and Peterson, 1996). Removal of Cr during transport in rivers and through the estuarine system may occur *via* several mechanisms. Adsorption of Cr(VI) is significantly inhibited by the presence of competing anions, and at pH >7, so it is thought to be negligible in river and estuarine waters (Masscheleyn *et al.*, 1992; Mayer and Schick, 1981; Zachara *et al.*, 1987). However adsorption of Cr(III) onto suspended matter and river sediments is highly efficient

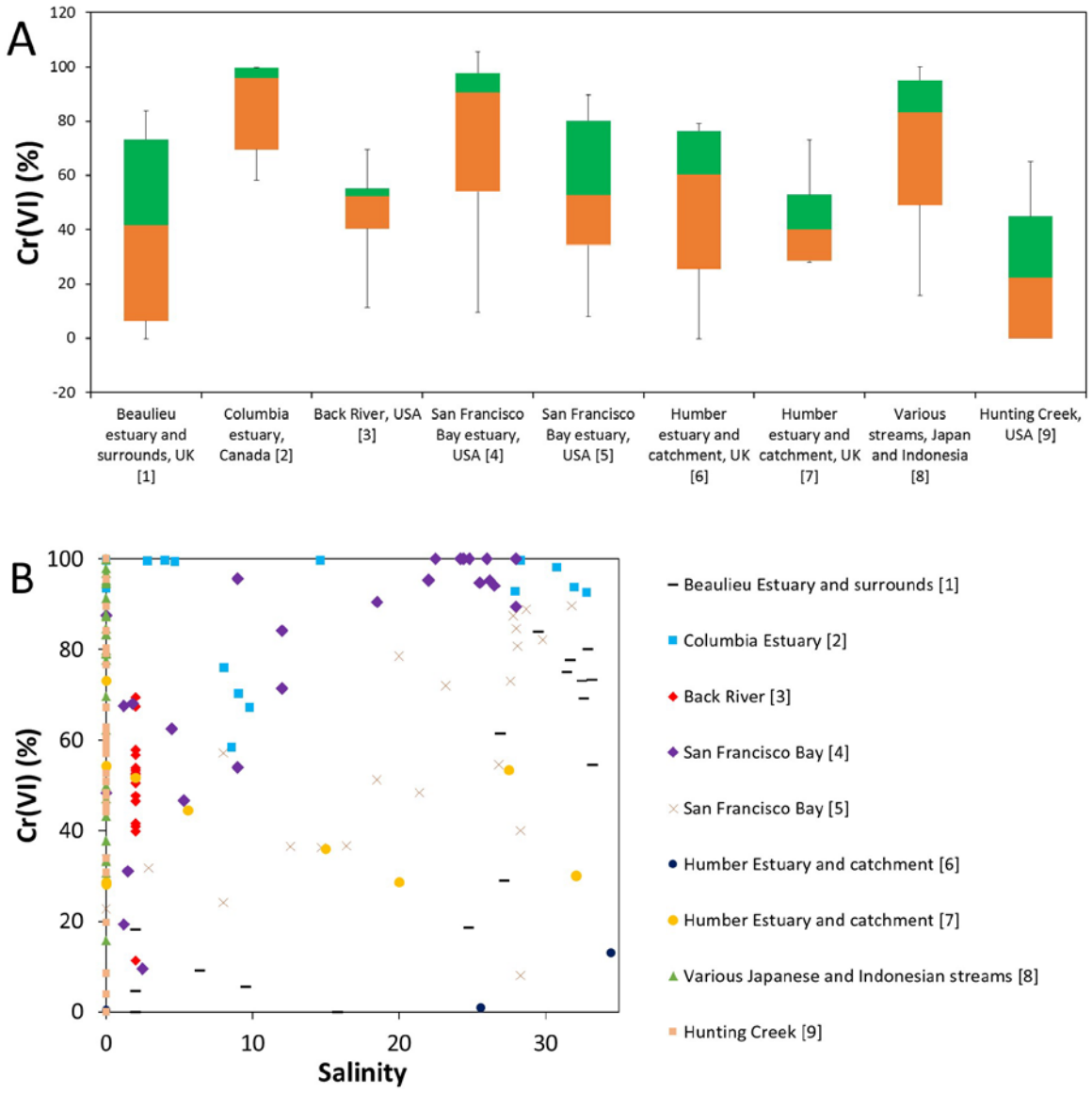

Figure 1.3 - (A) Box and whisker diagram showing the interquartile ranges for percentage of inorganic Cr(VI) (compared to total inorganic Cr) in selected rivers and estuaries. Orange and green boxes represent the 2nd and 3rd quartiles respectively, and the median is where they meet. Error bars indicate minimum and maximum values. (B) Cr(VI) in the same rivers and estuaries plotted against salinity (PSU). References: [1] Dolamore-Frank 1984, [2] Cranston and Murray 1980, [3] Kieber and Helz 1992, [4] Abu-Saba and Flegal 1995, [5] Abu-Saba and Flegal 1997, [6] Gardner and Ravenscroft 1996, [7] Comber and Gardner 2003, [8] Saputro et al. 2014, [9] McClain and Maher 2016.

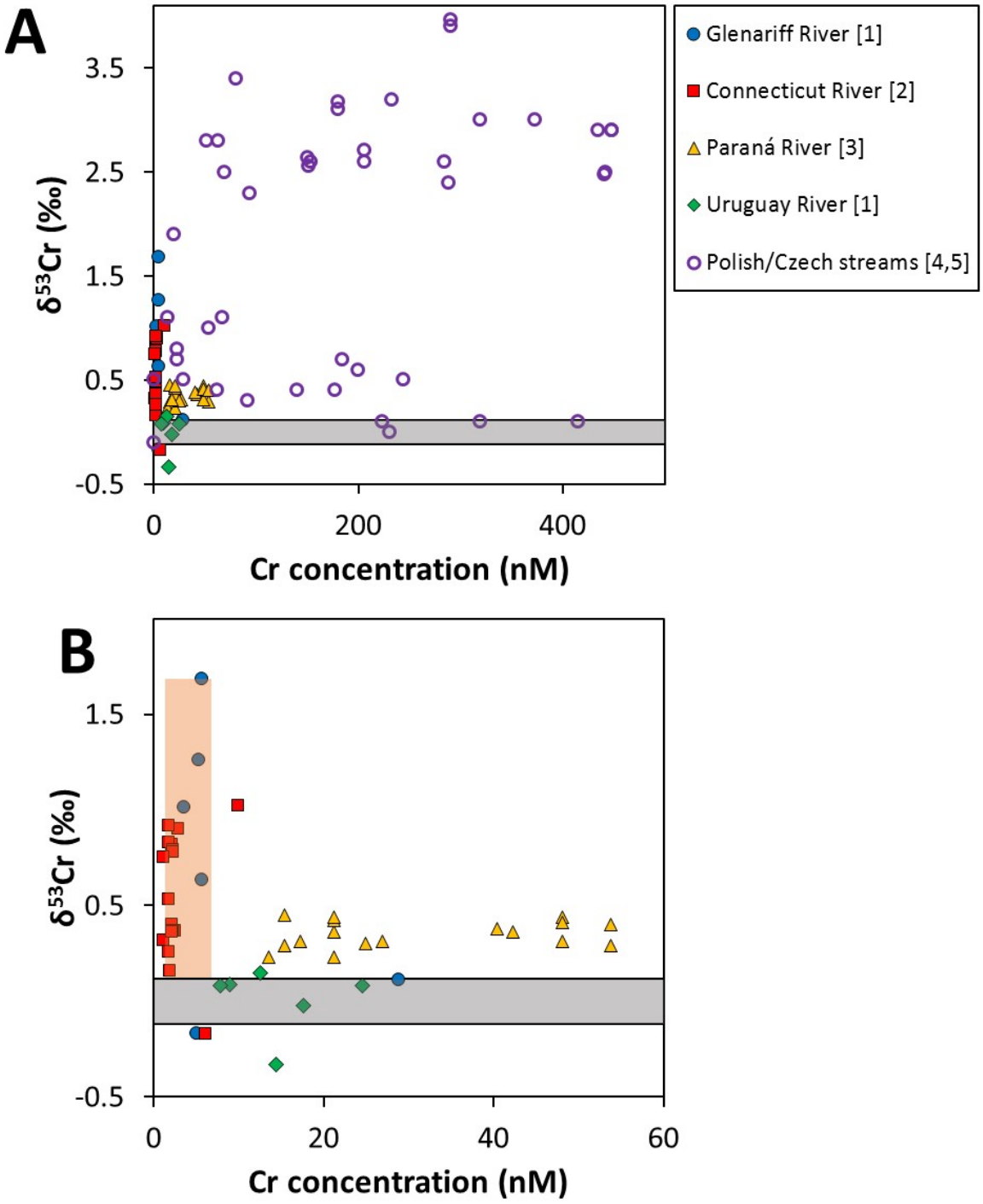

Figure 1.4 – (A) Previously published δ^{53}Cr data for rivers, as a function of Cr concentration. Data includes tributaries to the main rivers for the Glenariff, Connecticut and Paraná Rivers. Polish/Czech streams are geogenically contaminated due to ultramafic catchment zones. (B) Non-geogenically contaminated rivers only. Orange box represents δ^{53}Cr and Cr concentration range for seawater (see Figure 1.5 for seawater references). Horizontal grey bars in both A and B represent crustal δ^{53}Cr range and legend in A applies to both plots. References are as follows: [1] D'Arcy *et al.* 2016; [2] Wu *et al.* 2017; [3] Frei *et al.* 2014; [4] Farkaš *et al.* 2013; [5] Novak *et al.* 2014.

at pH >5 (Crawford *et al.* 1993, **Figure 1.2**), thus Cr(III) is effectively removed from solution *via* adsorption. Alternatively Cr(III) may form an insoluble inorganic precipitate with or without Fe (**Reaction 2**; Crawford *et al.* 1993; Rai *et al.* 1987; Sass and Rai 1987). A third removal route is *via* flocculation: during estuarine mixing the ionic strength of water significantly increases allowing humic acid molecules to aggregate, often in association with Fe (Sholkovitz, 1976; Sholkovitz *et al.*, 1978). At the same time this process removes Cr(III) from estuarine waters at salinities of <10 (Cranston and Murray, 1980; Dolamore-Frank, 1984).

The δ^{53}Cr range in estuaries is 0.08-1.02‰, however to date there are only 7 data points available. One study demonstrated that Paraná river and estuary δ^{53}Cr values were similar, indicating that reduction and removal of Cr were not significant (Frei *et al.*, 2014). However two other studies of the Brahmani and Glenariff river-estuary systems measured higher δ^{53}Cr in the rivers, which may be a result of reduction and removal of Cr during transport and/or conservative mixing with seawater (D'Arcy *et al.*, 2016; Paulukat *et al.*, 2015).

1.2.4 Oceans

Despite the relatively long residence time of Cr in seawater (~9500 years; Reinhard *et al.* 2013) Cr concentrations in the oceans are spatially heterogeneous, with a typical range of 1.7-6.5nM (Bonnand *et al.*, 2013). The δ^{53}Cr range for seawater is also quite large at 0.13-1.55‰, with the largest variations observed in surface waters (Bonnand *et al.*, 2013; Economou-Eliopoulos *et al.*, 2016; Holmden *et al.*, 2016; Paulukat *et al.*, 2015; Paulukat *et al.*, 2016; Pereira *et al.*, 2015; Scheiderich *et al.*, 2015). This implies that river δ^{53}Cr is not the only controlling factor on ocean δ^{53}Cr and *in situ* processes must also be important.

Chromium is known to associate with particulate organic material in marine environments, either through biological uptake or adsorption (Connelly *et al.*, 2006; Dauby *et al.*, 1994; Semeniuk *et al.*, 2016). Chromium concentrations are therefore often lowest in surface waters and higher in deep waters due to formation and remineralisation of organic material, and Cr concentrations can show a positive correlation with nutrients such as silicon at some locations (Achterberg and Berg, 1997; Campbell and Yeats, 1981; Cranston, 1983). Thus Cr is often categorised as a recycled element, despite the fact that it is not

thought to be a nutrient for marine phytoplankton. Higher proportions of dissolved Cr(III) have been observed in Sargasso seawater during periods of high biological activity, which implies that biological processes exert some control on Cr speciation in the oceans (Connelly *et al.*, 2006). Biological processes may therefore also regulate seawater $\delta^{53}Cr$, but this has not yet been confirmed due to a lack of detailed seawater $\delta^{53}Cr$ data for the upper part of the water column.

Although rivers deliver the majority of Cr to the oceans, other inputs can be locally important. For example, the Mediterranean Sea receives natural atmospheric Cr input from Saharan dusts that elevates surface water concentrations by around 0.5-1nM (Achterberg and Berg, 1997). Similarly hydrothermal activity in the Caribbean Sea elevates deep water Cr by up to 12nM (Sander *et al.*, 2003) despite the fact that Cr is removed from seawater *via* scavenging by Fe oxyhydroxides in the hydrothermal plume (German *et al.*, 1991). Marine sediments can act as both a sink and source of Cr, as adsorbed, precipitated and biogenic Cr(III) is delivered to sediments *via* sinking particles and may be re-released into the water column where sediment redox conditions favour oxidation back to soluble Cr(VI) (Jeandel and Minster, 1984). Whilst isotopic measurements have not been made for hydrothermal and atmospheric Cr sources, oxic marine sediments are globally thought to possess $\delta^{53}Cr$ values close to that of crustal rocks (-0.14 to 0.06‰; Schoenberg *et al.* 2008; Gueguen *et al.* 2016) because the detrital component of these sediments is much larger than that of the authigenic component. This also reflects the fact that most oxic seawater Cr is present as Cr(VI) (Sirinawin *et al.*, 2000) which is not generally transferred to sediments *via* adsorption to particles or precipitation. Conversely reducing marine sediments contain a larger proportion of Cr; these have average $\delta^{53}Cr$ values of 0.38‰ and 0.61‰ in the Cariaco Basin and Peru Margin respectively (Gueguen *et al.*, 2016). The authors argue that it is unclear whether partial or complete Cr reduction occurred to produce these signatures, since the $\delta^{53}Cr$ of the contemporaneous seawater is unknown. Complete reduction would result in authigenic sediments possessing the same $\delta^{53}Cr$ as seawater, however partial reduction would produce somewhat lighter $\delta^{53}Cr$ values due to the preferential incorporation of ^{52}Cr during reduction processes. The latter appears more likely based on previous studies of Cr in reducing seawater; Cr profiles from both the Pacific O_2 minimum zone (Rue *et al.*, 1997) and the Saanich Inlet (Emerson *et al.*, 1979) revealed reduction of

Cr in anoxic waters but some Cr(VI) persisted at both sites. The relationship between the $\delta^{53}Cr$ values of seawater and underlying authigenic sediments requires further research to resolve.

On a global scale, there appears to be a negative correlation between $\delta^{53}Cr$ values and Cr concentrations of seawater. This has been attributed to *in situ* reduction of Cr(VI) in surface waters and oxygen minimum zones followed by removal of the Cr(III) that forms, and return of this Cr(III) to the water column *via* desorption/oxidation in deeper waters. The apparent isotopic fractionation factor ($\Delta_{\text{seawater-removed Cr}}$) associated with this process is 0.8 (**Figure 1.5;** Paulukat *et al.* 2016; Scheiderich *et al.* 2015). However, the exact mechanisms that control this apparent relationship between $\delta^{53}Cr$ and Cr concentrations in seawater are poorly understood, and as yet there have been no studies of Cr isotope behaviour in O_2 depleted parts of the ocean that may be strongly affected by Cr redox cycling. It is also important to note that data acquired so far are mainly from the Atlantic (84 samples), with relatively few samples measured in the Pacific (11) and Indian (1) Oceans.

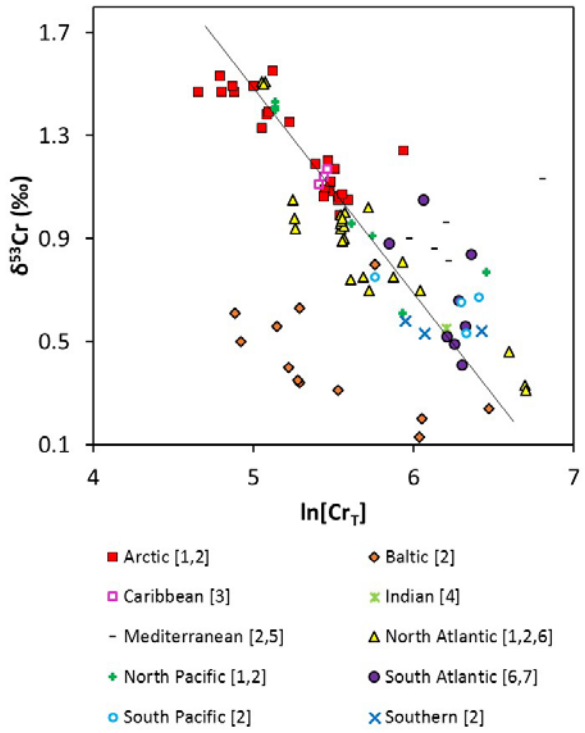

Figure 1.5 - Global seawater data for $\delta^{53}Cr$ plotted against the natural log of the Cr concentration ($\ln[Cr_T]$) with global correlation line ($\ln[Cr_T] = -0.8\ \delta^{53}Cr + 5.1$). References are as follows: [1] Scheiderich *et al.* 2015, [2] Paulukat *et al.* 2016, [3] Holmden 2013, [4] Paulukat *et al.* 2015, [5] Economou-Eliopoulos *et al.* 2016, [6] Bonnand *et al.* 2013, [7] Pereira *et al.* 2015.

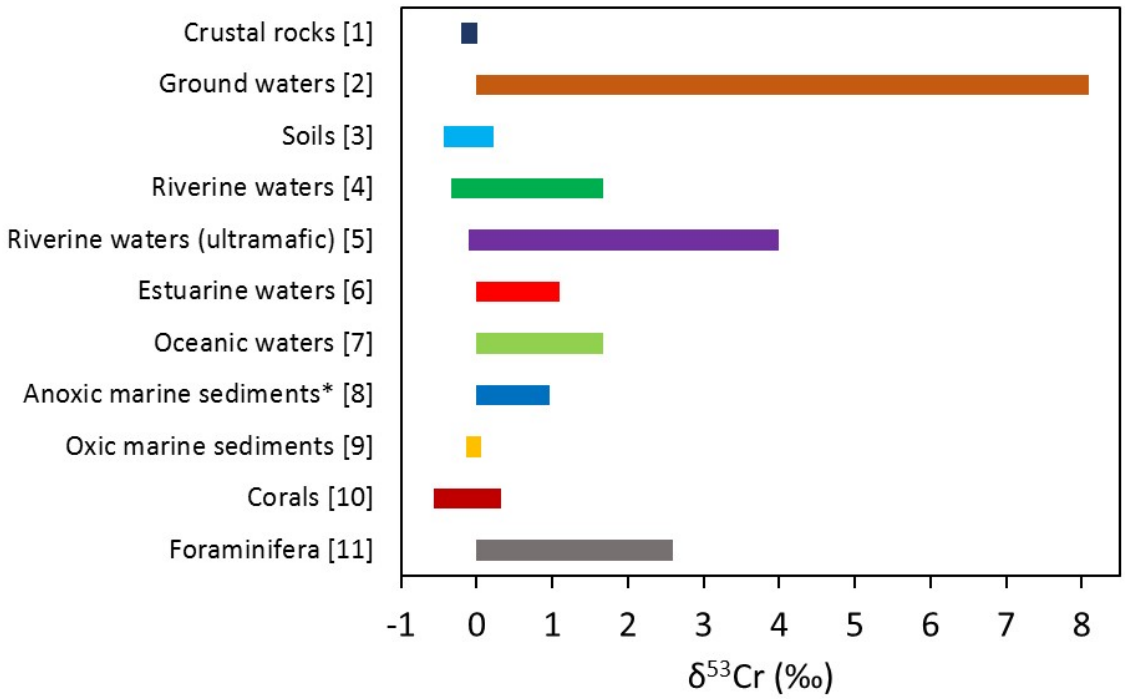

Figure 1.6 - Summary of the ranges of $\delta^{53}Cr$ values measured for different Cr reservoirs in the modern environment. *Anoxic marine sediment range is for the authigenic fraction only. References: [1] Schoenberg *et al.* 2008, [2] Ball and Bassett 2000, Ellis *et al.* 2002, Izbicki *et al.* 2008, Raddatz *et al.* 2010, Villalobos-Aragón *et al.* 2012, [3] Berger and Frei 2014, D'Arcy *et al.* 2016, Frei *et al.* 2014, [4] D'Arcy *et al.* 2016, Frei *et al.* 2014, Paulukat *et al.* 2015, Wu *et al.* 2017, [5] Farkaš *et al.* 2013, Novak *et al.* 2014, [6] D'Arcy *et al.* 2016, Frei *et al.* 2014, Paulukat *et al.* 2015, [7] Bonnand *et al.* 2013, Paulukat *et al.* 2016, Scheiderich *et al.* 2015, [8] Gueguen *et al.* 2016, Reinhard *et al.* 2014, [9] Gueguen *et al.* 2016, [10] Pereira *et al.* 2015, [11] Wang *et al.* 2016

1.3 The chromium isotope redox proxy

An important application of Cr isotopic signatures is their potential to act as a proxy for redox processes in ancient environments. Several authors have measured $\delta^{53}Cr$ in well-preserved sedimentary sequences in order to better understand the evolution of atmospheric O_2 over geological time, as well as more transient environmental events such as OAEs (Crowe *et al.*, 2013; D'Arcy *et al.*, 2016; Frei *et al.*, 2016; Frei *et al.*, 2011; Frei *et al.*, 2009; Gilleaudeau *et al.*, 2016; Holmden *et al.*, 2016; Planavsky *et al.*, 2014; Rodler *et al.*, 2016; Rodler *et al.*, 2016; Sial *et al.*, 2015). The systematics of the Cr isotope proxy, as applied to different authigenic rock types, will be described in the following sections. Note that in most studies, authigenic sediments also contain a detrital component that must be accounted for by normalisation, for example to Al or Ti (e.g. Gilleaudeau *et al.* 2016; Rodler *et al.* 2016; Wang *et al.* 2016).

1.3.1 Banded Iron Formations

Banded Iron Formations (BIFs) preserve Cr that weathered from terrestrial sources and was subsequently transferred to the ocean. Under an anoxic atmosphere, any Cr that was mobilised from crustal rocks by weathering would not have undergone redox reactions before transfer to BIFs, other than those which occur photochemically (for example in the presence of H_2O_2) that have been shown to impart extremely small fractionations (Frei *et al.*, 2016). Consequently BIFs deposited during periods with low atmospheric O_2 levels should have $\delta^{53}Cr$ close to that of crustal rocks (-0.12 ± 0.10‰). This has indeed been inferred for BIFs deposited in the Archean Eon (Frei *et al.*, 2009). In contrast, Cr that is weathered in the presence of Mn oxides should undergo partial oxidation, resulting in seawater that has higher $\delta^{53}Cr$ than crustal rocks (as is the case today; see **Section 1.2.4**). In times when the ocean was stratified with regards to O_2, aqueous Cr(VI) bearing high $\delta^{53}Cr$ values would have been transferred to oxic surface waters and reduced to Cr(III) in the presence of Fe(II). This would subsequently have been oxidised to Fe(III) forming a Cr(III)-Fe(III) precipitate at the oxic-anoxic boundary (**Reaction 2**) and so BIFs deposited in the late Neoproterozoic era have $\delta^{53}Cr$ values of 0.9-5.0‰ (**Figure 1.7**; Frei *et al.* 2009). It is estimated that <0.1% of the present atmospheric level of O_2 is required for Cr oxidation by Mn oxides to occur (Planavsky *et al.*, 2014). Thus, Cr isotopic signatures in BIFs may be used to trace fine-scale developments in atmospheric O_2 before and after the Great Oxidation Event (GOE), and potentially to clarify the evolutionary timing of oxygenic photosynthesis. BIF studies have yielded interesting results which suggest that the evolution of atmospheric O_2 was much more complicated than previously thought, with a return to low O_2 levels after the GOE and several fluctuations in atmospheric O_2 during the late Neoproterozoic era (Frei *et al.*, 2009; Frei *et al.*, 2013). These hypotheses remain controversial, however, due to uncertainties in the systematics of the Cr proxy. Specifically, (i) the amount of isotope fractionation associated with Cr oxidation is poorly characterised (Konhauser *et al.*, 2011; Lyons and Reinhard, 2009), and (ii) the assumption that Cr not is subjected to further fractionation within the oceans may not be valid. In particular it is notable that $\delta^{53}Cr$ in the modern ocean does not appear to reach values higher than 1.6‰ and authigenic marine sediments (even those deposited under anoxic conditions) also have $\delta^{53}Cr$ values of <1‰ (Gueguen *et al.*, 2016; Reinhard *et al.*, 2014). Therefore it is currently unclear how such large fractionations in BIFs occurred. The situation may be further

complicated for BIFs formed or altered in the presence of hydrothermal activity, as this may produce Cr isotope signatures lower than that of crustal rocks (Sial *et al.*, 2015).

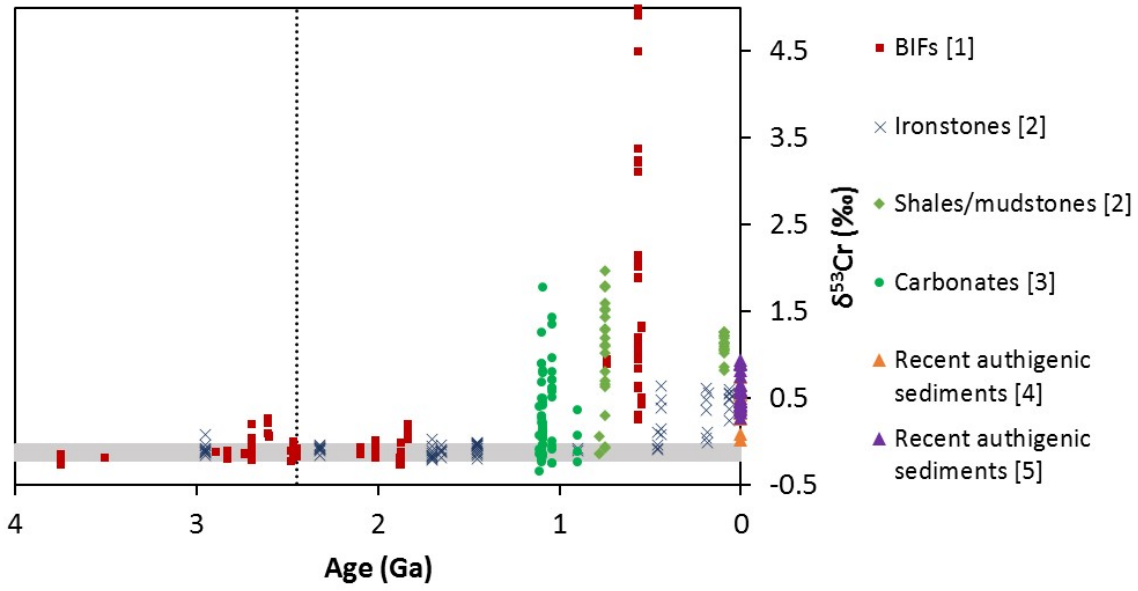

Figure 1.7 - $\delta^{53}Cr$ for marine authigenic deposits with well constrained ages. Dotted black line indicates the onset of the GOE at 2.4Ga (Holland 2006) and shaded grey area is the $\delta^{53}Cr$ range of crustal rocks. Ages for recent authigenic sediments are all <20ka. References: [1] Frei *et al.* 20092] Planavsky *et al.* 2014, [3] Gilleaudeau *et al.* 2016, [4] Reinhard *et al.* 2014, [5] Gueguen *et al.* 2016.

1.3.2 Paleosols

Paleosol (ancient lithified soil) sequences have primarily been studied in order to better understand Cr behaviour during oxidative weathering processes (Babechuk *et al.*, 2016; Berger and Frei, 2014; Crowe *et al.*, 2013; Frei and Polat, 2013). In the absence of conclusive fractionation factors for Cr oxidation (Bain and Bullen, 2005; Joshi *et al.*, 2011) they provide the best indirect evidence for the preferential release of ^{53}Cr during oxidative weathering, since $\delta^{53}Cr$ values as low as -1‰ (Crowe *et al.*, 2013; Frei and Polat, 2013) have been observed in the residual soil. These findings are in good agreement with modern studies, which have shown that soils, laterites and saprolites possess low $\delta^{53}Cr$ values in the range of -0.4‰ to -0.1‰ (Berger and Frei, 2014; D'Arcy *et al.*, 2016; Frei *et al.*, 2014). However, one study measured paleosol $\delta^{53}Cr$ values of up 2.4‰ which appears to be incompatible with the oxidative release of Cr (Babechuk *et al.*, 2016) and, in support of this, there was an apparent lack of Mn oxides present in the sequence. In this case it was proposed that

dissolved Cr(III) with a high $\delta^{53}Cr$ value was incorporated into secondary minerals during pedogenesis, while the lighter Cr isotopes were preferentially transported away as aqueous Cr(III). Serpentinized ultramafic rocks also have high isotopic signatures of up to 1.2‰ (Farkaš *et al.*, 2013) which was suggested to be because these rocks formed from serpentinizing or meteoric fluids that carried Cr(VI) with high $\delta^{53}Cr$, which could have been obtained during previous redox reactions. Alternatively the authors suggest that weathering may have preferentially released ^{52}Cr(III) into solution and become oxidised to Cr(VI), which was then removed along with other fluid mobile elements ($\delta^{53}Cr$ was well correlated with concentrations of fluid mobile elements rubidium and potassium). These studies suggest that there is much more to be learned about the mechanisms of Cr release into the environment from crustal rocks, and incorporation into secondary minerals.

1.3.3 Carbonates

Small amounts of Cr(VI) (typically 1-9 ppm, Holmden *et al.* 2016, Bonnand *et al.* 2013) are directly incorporated into marine carbonates as CrO_4^{2-}, meaning that they may capture the $\delta^{53}Cr$ value of the seawater in which they form (Tang *et al.*, 2007). Since carbonates are ubiquitous throughout Earth's history (unlike BIFs), they may contain a trove of information about past seawater oxygenation. Carbonates have been used to demonstrate the occurrence of significant atmospheric O_2 in understudied periods such as the mid-Proterozoic (Gilleaudeau *et al.*, 2016), and have also proven useful for inferring other important information about Earth's climate. For example, low Ediacaran carbonate $\delta^{53}Cr$ values are interpreted to reflect increased input of continental Cr due to high rates of physical weathering (and low O_2) during a glaciated period (Frei *et al.*, 2011). In another study, carbonates deposited during a Cretaceous OAE were found to have $\delta^{53}Cr$ values similar to igneous crust, presumably due to large hydrothermal inputs (Holmden *et al.*, 2016). Thus carbonate sediments may reveal information not only about Cr redox cycling but also past changes in Cr sources to the ocean.

A pre-requisite for carbonates to faithfully record seawater $\delta^{53}Cr$ is that the process of incorporation of Cr into carbonates does not fractionate Cr in its own right, or at least does so in a way which is predictable and can be accounted for. Laboratory experiments have demonstrated that Cr isotope fractionation during inorganic precipitation of carbonate (Δ_{R-}

$_P$, in this case $\Delta_{fluid\text{-}calcite}$) is between -0.1 and -0.3‰ with the lower end of this range most likely for seawater (Rodler *et al.*, 2015), implying authigenic sediments reflect coeval seawater with reasonable accuracy. In support of this, one study found that modern ooids had a δ^{53}Cr range (0.6-0.8‰; Bonnand *et al.* 2013) similar to that of modern seawater. In contrast, biogenic carbonates appear to significantly fractionate Cr compared to surrounding seawater; carbonates precipitated by green algae appear to have low isotopic signatures ($\Delta_{fluid\text{-}calcite}$ = 0.46‰, Holmden *et al.* 2016) whereas foraminiferal tests have variable δ^{53}Cr (0.1-2.5‰, Wang *et al.* 2016), extending to values higher and lower than those measured in seawater (0.1 – 1.6‰). Scleractinian corals also have variable δ^{53}Cr (-0.56 to 0.33‰), much lower than the seawater in which they grow (0.84 to 1.05‰; Pereira *et al.* 2015).

1.3.4 Black shales

Black shales are sedimentary rocks with a high organic carbon content. They arise where sinking organic material is not completely oxidised in sediments due to an insufficient supply of O_2 (Tourtelot, 1979). Black shales often have high Cr concentrations (up to 340 ppm, Cole *et al.* 2016) as very low O_2 levels (and high productivity) favour the accumulation of Cr in marine sediments (e.g. Shaw *et al.* 1990). Crucially, black shales are thought to be less susceptible to diagenetic alteration than other authigenic materials (Cole *et al.*, 2016) which makes them attractive for proxy studies. High δ^{53}Cr values in black shales are thought to arise in the same way as they do in BIFs (see **Section 1.3.1**), and Cr isotope evidence from black shales has recently been used to support a link between increased atmospheric O_2 levels and the onset of complex animal evolution (Cole *et al.*, 2016; Planavsky *et al.*, 2014). However, although authigenic Cr is strongly associated with organic carbon within black shales (Algeo and Maynard, 2004), large detrital Cr inputs can mask authigenic sedimentary δ^{53}Cr signatures (Wille *et al.*, 2013). Furthermore black shales can acquire high δ^{53}Cr values when weathered (Wang *et al.*, 2016).

1.4 Thesis outline

This thesis is divided into 6 chapters. Chapter 2 details the development of methods for the accurate and precise analysis of Cr concentration and Cr isotope ratios in low concentration natural samples. Chapters 3, 4 and 5 apply these techniques to assess the behaviour of Cr and Cr isotopes in aquatic systems. Chapter 3 investigates Cr isotope behaviour in O_2

depleted waters of the sub-tropical North Atlantic Ocean and the Black Sea. Chapter 4 explores the temporal and spatial variability of Cr and Cr isotopes in a shelf sea (the Celtic shelf sea, offshore south west UK). Chapter 5 examines Cr behaviour in the Beaulieu River (UK), and assesses how Cr speciation and Cr isotopes are modified by mixing with seawater in the Beaulieu estuary. Finally the key outcomes and scope for further work are discussed in Chapter 6.

Chapter 2: Methods

2.1 Introduction

The analysis of chromium (Cr) isotopic signatures requires measurement of all four isotopes of Cr, two of which have low abundances in nature (^{50}Cr – 4.35%, ^{52}Cr – 83.79%, ^{53}Cr – 9.50%, ^{54}Cr – 2.36%). Measurements can be done using high precision Multi-Collector Inductively Coupled Plasma Mass Spectrometry (MC-ICP-MS) or Thermal Ionisation Mass Spectrometry (TIMS). There are two basic prerequisites for Cr analysis using mass spectrometry: (i) a sufficient quantity of all Cr isotopes must be present in the analyte, and (ii) the analyte must contain minimal amounts of interfering isotopes, dissolved solids, particulates and organic material. Therefore, Cr derived from natural waters must be concentrated and separated from matrix materials before isotopic analysis can take place.

Separation of sufficient Cr from filtered natural waters is challenging, due to the low levels of Cr present and the differing chemistries of the two naturally occurring species, Cr(VI) and Cr(III). Several methods have been used to measure Cr concentrations, including co-precipitation with iron (Fe) hydroxide or magnesium hydroxide, organic complexation with 1,5-diphenyl-carbazide or methyl isobutyl ketone, and ion exchange separation (Cranston and Murray, 1978; Gómez and Callao, 2006; Semeniuk *et al.*, 2016; Walsh and O'Halloran, 1996). With the exception of a few low sensitivity on-line flow injection chromatography methods, each of these pre-concentration techniques can be used to measure only one of the two Cr species (Sperling *et al.*, 1992). For total Cr determination, all Cr is converted to one species. For speciation studies, total concentration and the concentration of one species is measured, and the second species is then determined by subtraction. None of the aforementioned methods are considered superior, as they may all be hampered by problems relating to low natural concentrations and the complex behaviour of Cr in natural waters. Yield losses during sample processing through adsorption of Cr(III) to container walls, incomplete recovery from ion exchange resins due to the presence of several Cr complexes, and insufficient detection limits are common problems (Cranston and Murray, 1978; Gómez and Callao, 2006; Larsen *et al.*, 2016; Marqués *et al.*, 2000), thus any method designed to measure the concentration of Cr must be carefully evaluated. Furthermore, adapting such a method to measure isotopic composition must also account for the greater

quantity of Cr required for analysis and any isotopic fractionation induced during sample processing.

The first isotopic study of seawater Cr was carried out in 2011 using an Fe(II) co-precipitation method modelled after that of Cranston and Murray 1978 (Bonnand *et al.*, 2013; Cranston and Murray, 1978). Briefly, the samples were spiked with a ^{50}Cr-^{54}Cr double spike and Cr was co-precipitated with Fe(II) hydroxide (Cranston and Murray, 1978). The redox reaction between Cr(VI) and Fe(II) formed an insoluble Fe-Cr precipitate, with any residual dissolved Cr(III) being adsorbed onto the precipitate resulting in quantitative recovery of Cr as Cr(III). The precipitate was removed from the seawater matrix by siphoning and centrifugation before ion exchange chromatography was used to remove Fe and residual salts. Other authors have since used an evaporation method where double spiked water samples are simply dried and all Cr is converted to Cr(VI) using saturated ammonium peroxidisulphate prior to ion exchange chromatography (D'Arcy *et al.*, 2016; Frei *et al.*, 2014), but a modified version of the former method (Bonnand *et al.*, 2013) was utilised in this study.

The modified method used in this study is described in the following sections (see also **Appendix A**). In short, water samples were first spiked with an appropriate amount of ^{50}Cr-^{54}Cr double spike to account for analytical mass bias and fractionation during processing (Albarède and Beard, 2004). Cr was then co-precipitated quantitatively with Fe(II) hydroxide and the precipitate was separated from seawater using vacuum filtration. Samples were then processed through an anion exchange chromatography procedure to remove the Fe, and through a cation exchange procedure to remove other residual salts before analysis. Isotopic signatures were acquired using a Thermo Fisher Neptune MC-ICP-MS instrument, and data was processed using the Newton-Raphson deconvolution technique (Albarède and Beard, 2004).

2.2 Isotopic procedures

2.2.1 Cleaning and storage

The low concentrations of Cr in natural waters (and representative standards) meant it was necessary to carry out all sample processing in a class 100 clean laboratory. Standard clean room procedures for the prevention of contamination were followed, with sample bottles

(LDPE or HDPE) being pre-cleaned for at least 3 nights each in (i) 2% Decon solution, (ii) 50% analytical grade hydrochloric acid (HCl) and (iii) analytical grade 50% nitric acid (HNO_3) interspersed with MQ water rinses. Cleaning procedures for capsule filters (used for the removal of natural particulate materials) were cleaned by pumping with 1L MQ water followed by a minimum of 500mL of sample. Savillex containers used during sample processing were cleaned using a 4 step procedure with MQ water rinses after each stage as follows: (i) 50% HCl (analytical grade) at 100°C, (i) MQ water at 100°C, (iii) sub-boiled HCl reflux at 130°C, (iv) MQ water reflux at 130°C (each for 24 hours). The cleaning procedure for membrane filters (used to capture Fe-Cr precipitates) required some investigation as described in **Section 2.2.3**. New column resins were batch cleaned by shaking in MQ water several times with removal of fine material by decanting, and were then soaked in 6M HCl for 2 days. In addition the normal column cleaning procedure was carried out twice before any samples were loaded (see **Section 2.2.4.**). Pipette tips were cleaned overnight in sub-boiled 10% HNO_3 at 85°C. All other equipment that came into contact with samples, standards or blanks, including Pasteur pipettes, tubing, vacuum filter flask, scintillation vials, centrifuge tubes and columns, were soaked for 1-7 days in sub-boiled 10% HNO_3 and rinsed with MQ water.

To prevent or reverse the adsorption of Cr to bottle walls, samples were acidified to pH 2 or lower using concentrated sub-boiled HCl (1-2ml L^{-1}) (Yeats, 1987). Samples which were processed within ~30 hours of collection were not subjected to this procedure as Cr concentrations have been found not to change significantly during this length of time (Comber and Gardner, 2003; Sirinawin and Westerlund, 1997). However the speciation of Cr may change rapidly following collection, so for Cr(III) determinations spiking and co-precipitation were done as soon as possible after sample collection (Kingston *et al.*, 1998; Sirinawin and Westerlund, 1997). These samples were usually processed within 2 hours of collection, though in some instances up to 4 hours was needed to convey samples from the field to a suitable laboratory.

2.2.2 Double spiking

'Double spiking' is the addition two isotopes of the same element as the analyte element (in this case Cr) in a known quantity and ratio. Double spiking samples before co-precipitation allows any fractionation incurred as a result of sample processing or

instrumental mass bias to be accounted for, as changes in spiked sample ratios can be tracked provided that the artificially added isotope ratio is accurately known. The advantages to this are threefold: (i) the requirement for 100% sample yield to determine accurate isotopic ratios is removed, (ii) sample-standard bracketing techniques to adjust for instrumental drift are no longer needed (though standard measurements are still made, see **Section 2.2.6** and **Appendix C**), and (iii) very precise sample concentrations can be obtained using isotope dilution calculations (see **Section 2.3.1**). Therefore double-spiking significantly reduces the difficulty in processing samples and the time required to analyse them.

Two ^{50}Cr-^{54}Cr double spikes were used during the course of this work. Early method development work and sample processing were done using the double spike of Bonnand 2011, here referred to as the OU double spike (Bonnand, 2011). A new double spike of similar composition was then made at the NOCS using ^{50}Cr and ^{54}Cr isotopes supplied by Oak Ridge National Laboratory. The two isotopes (supplied in a ground metallic form with cubic structure) were separately digested in sub-boiled HCl at 130°C. Sonication was used to aid digestion of the most insoluble particles. The concentration of the resulting single isotope stocks were determined using isotope dilution (ID) on the Thermo Element 2 ICP-MS. Appropriate quantities of each (diluted) stock were then weighed into 6M HCl to create a new double spike solution with a total Cr concentration of 50ppm. This double spike was calibrated using the Thermo Fisher Neptune MC-ICP-MS and a reversed deconvolution technique, yielding a composition detailed in **Table 2.1**. Henceforth this double spike is referred to as the NOCS double spike.

Table 2.1 - Isotopic compositions of OU and NOC double spikes.

Isotope	Proportion in OU double spike	Proportion in NOCS double spike
^{50}Cr	0.641654	0.669186
^{52}Cr	0.032497	0.033555
^{53}Cr	0.004686	0.004615
^{54}Cr	0.321162	0.292645

Optimal isotopic ratios in the spiked samples are required to reduce the error magnification term associated with double spike measurements. The optimal ratios were supplied by Dr Ian Parkinson at the University of Bristol (updated after Bonnand 2011) and used in this

work to determine the appropriate amount of double spike to add to each sample. The amount of Cr in the sample is also required for the calculation of optimal ratios, so the sample weight and concentration must be known. A single spike ID method was therefore developed to determine sample concentrations prior to isotopic processing (see **Section 2.2**). A more precise sample concentration can subsequently be calculated using double spiked isotopic sample data. To obtain 2 isotopic measurements of a single sample a minimum of 130ng Cr was required, and sample sizes were typically 1-3L to provide this amount.

Dilute (2.5ppm) double spike was added to samples using a dedicated set of adjustable volume Eppendorf Research pipettes. To ensure the accuracy of spike addition using this method, the mass of MQ water pipetted at each spike volume was weighed 3-5 times and averaged. A correction was applied to account for the greater density of the double spike solution in 6M HCl (1.098g/ml) and the amount of double spike Cr added to the sample was calculated from this. Typical seawater samples required a double spike volume of 20-30µl l^{-1}. After spiking the samples were left for ~24 hours to allow the sample and spike Cr isotopes to equilibrate, although complete equilibration was not expected at this stage if the sample contained Cr(VI) due to slow equilibration rates between Cr(VI) and Cr(III) (Wang *et al.*, 2015). In this case equilibration was expected to occur upon co-precipitation when Cr(VI) was converted to Cr(III).

2.2.3 Co-precipitation and filtration

To pre-concentrate Cr and remove the majority of the bulk seawater matrix, acidified samples were adjusted to pH 8-9 using Romil Ultrapure ammonium hydroxide (NH_4OH). Samples that were not acidified did not require pH adjustment.

An Fe(II) hydroxide precipitate was produced by addition of NH_4OH to freshly made 2mM ammonium Fe(II) sulphate solution (made from ammonium Fe(II) sulphate hexahydrate crystals; Sigma-Aldrich, 99.997% trace metals basis). 5-10mL L^{-1} of this precipitate (suspended in solution) was immediately added to samples, and reaction with Fe(II) caused Cr(VI) to be reduced to Cr(III), with simultaneous oxidation of Fe(II) to Fe(III). Cr(III) was then adsorbed onto the newly formed Fe(III) precipitate.

In the method of Bonnand *et al.* 2013, separation of the Cr-Fe precipitate was achieved using siphoning and centrifugation. In this work, collection of the precipitate was instead achieved *via* vacuum filtration as this was found to be more practical for processing large numbers of samples. In the past membrane filters have been found to contain high levels of Cr capable of contaminating samples and these filters may degrade during acid cleaning (Connelly, 1997; Yiğiterhan *et al.*, 2011). However, a number of filters are now available that are capable of withstanding acid cleaning and thus contribute only a negligible amount of Cr. Several combinations of filter type and cleaning methods were tested to obtain the lowest achievable blank (**Figure 2.1**). The results show that Cr filter blanks have a particularly large variability compared to other elements, as found by other studies (Cullen and Sherrell, 1999; Yiğiterhan *et al.*, 2011). However PTFE filters (Omnipore, 1µm) refluxed in 6M HCl and then in MQ water produced an acceptably low blank, so this procedure was selected for all further work.

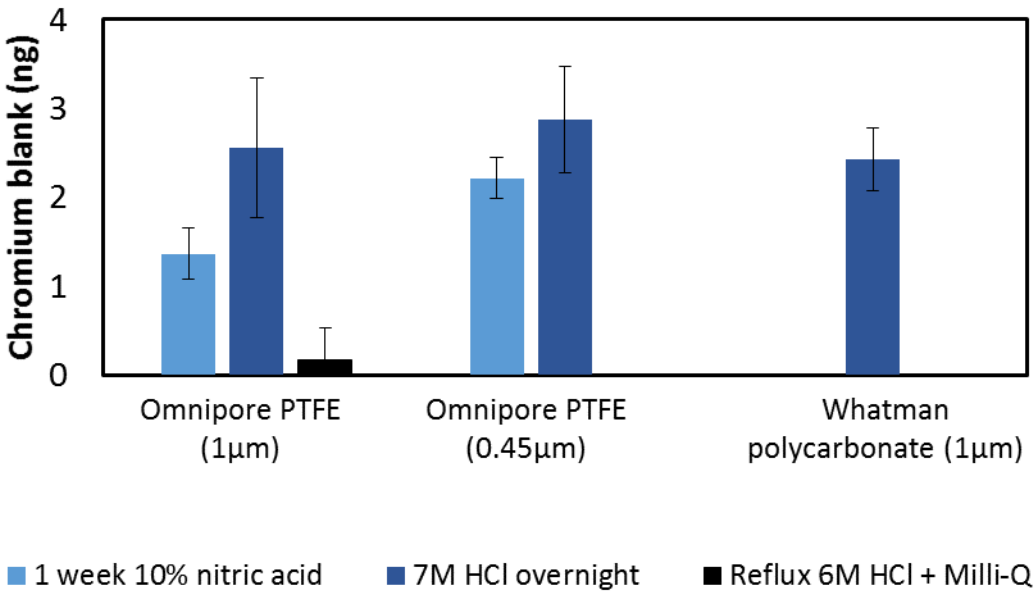

Figure 2.1 - Filter blanks (n=3 for all). All combinations of filter type and cleaning procedure that were tested are shown. Error bars show 2 standard deviations (2SD).

2.2.4 Column procedures

Fe in the Fe-Cr precipitate had to be removed before analysis, as the ^{54}Fe isotope is an isobaric interference when measuring ^{54}Cr. Separation was achieved using 2ml Bio-Rad

AG1-X8 (200-400 mesh size) resin packed into pre-cleaned Bio-Rad gravity flow columns. The resin has a charge capacity of 1.2mEq ml^{-1}, thus the charge capacity of the columns was 2.4mEq. The estimated negative charge in remaining seawater of a filtered sample (<0.5ml), plus the negative charge contributed from the 2mM Fe precipitate is <0.4mEq so this capacity was more than sufficient. The resin was stored in 0.5M HCl in the columns and used several times before being replaced. A long cleaning procedure was used to ensure the Cr blank derived from the resin was low. This involved washing the column with 5ml MQ water, 10ml 0.5M HCl, 5ml MQ water, 5ml concentrated HCl, and a final aliquot of 5ml MQ water in sequence. Meanwhile samples were refluxed at 130°C in 7M HCl for 24 hours to ensure all Cr was converted to Cr(III). After pre-conditioning the column with 10ml 7M HCl, sample Cr was loaded onto columns in the same 6ml 7M HCl used for refluxing using an adjustable volume pipette. This was followed by a 4ml 7M HCl wash that was also collected. All of the acids used in this procedure were sub-boiled, and the 0.5M and 7M HCl solutions were accurately titrated prior to use.

To remove residual salts from samples, the cation column procedure of Bonnand *et al.* (2011) was carried out after the anion column procedure using Biorad AG50W-X12 cation resin (200-400 mesh size) in 30ml Savillex columns. Columns were cleaned with 10mL 50% HNO_3 (made using sub-boiled concentrated HNO_3), 30mL 6M HCl, and 30mL MQ water before samples were loaded. All 6M HCl used in the procedure was accurately titrated from sub-boiled concentrated HCl. Samples were dissolved in 0.5mL 6M HCl and diluted to 6ml 0.5M HCl with MQ water using adjustable volume pipettes. It was essential to load the samples onto columns directly after this dilution to avoid Cr losses from speciation changes. A 4ml 0.5M HCl wash was also collected after samples had passed through (**Figure 2.2A**).

After column chemistry was complete, samples were dried down and then re-dissolved in 50µl concentrated Fluka TraceSELECT Ultra grade H_2O_2, as this was found to oxidise residual organic material that can interfere with measurement. This was dried down once more before samples were dissolved in 60µL concentrated HNO_3, and this was diluted to a 3% HNO_3 solution using 1.94mL MQ water for analysis.

Column calibrations were performed using the OSIL Atlantic Seawater Conductivity Standard (ASCS) to check the performance of both column procedures (**Figure 2.2**). This

standard is a filtered, UV-irradiated and homogenised seawater sample collected from just below the surface of the North Atlantic Ocean. It does not have a certified Cr concentration or isotopic signature, however these have been determined as part of this study and at the University of Saskatchewan (see **Section 2.4.4**), thus it provided the most appropriate standard for this work. The overall Cr yield after all seawater processing (including the co-precipitation and filtration steps) was 69%, which is slightly better than the average yield obtained for NBS979 standards (61%; **Appendix B, Table B1**). The anion column procedure gave a Cr yield of ~75% however most of the loss is likely due to the vacuum filtration step prior to columns, which did not recover 100% of the Fe-Cr precipitate. As expected only Fe was removed from the anion columns, while other metals and residual salts were collected. These were effectively removed during the cation column procedure. Of the Cr collected from the anion column, 89% was recovered from the cation column indicating a slightly better efficiency than previously found (Bonnand *et al.*, 2013). The results of this calibration are discussed further in **Section 2.4.3**.

2.2.5 Procedural blanks

The procedural blank accumulated during sample processing was investigated in order to identify, minimise and account for significant sources of contamination. Sample bottle blanks and acid solutions used in the procedure were measured using a standard calibration curve technique on the Thermo Element 2 ICP-MS. All chemical solutions used during processing (NH_4OH, H_2O_2, HCl and HNO_3) had extremely low Cr concentrations and therefore contributions from these sources were considered negligible (**Appendix B, Table B2**). The Cr contribution from pre-cleaned sample bottles was also found to be negligible, as leachates from these bottles gave Cr concentrations below the limit of detection (0.05ppb) even when pre-concentrated by a factor of 25 prior to analysis. Other contributing factors to the procedural blank are shown in **Figure 2.3**. Clearly the Fe(II) solution is the largest contributor to the blank, and appropriate corrections were therefore made for this component (see further discussion in **Section 2.4.1**). The combined sum of these blanks determined by a standard calibration curve was within error of the average total procedural blank determined separately by ID, demonstrating that all major sources of blank Cr have been identified.

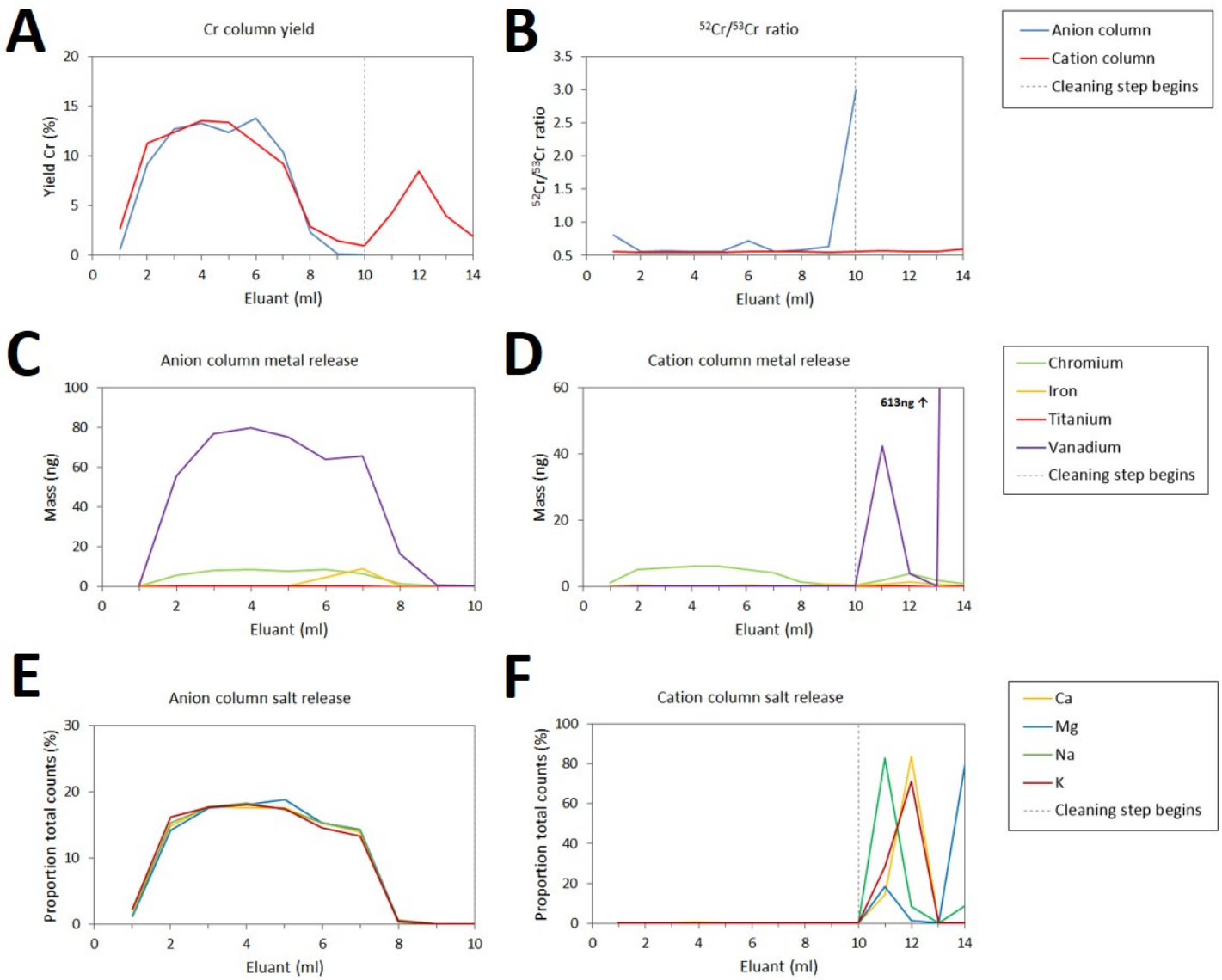

Figure 2.2 - OSIL ASCS seawater column calibration. (A) Percentage Cr yield from each column type, (B) $^{53}Cr/^{52}Cr$ ratio of each column type, (C) release of relevant metals from anion column (D) release of relevant metals from cation column, (E) release of major salt ions from anion column, (F) release of major salt ions from cation column. Note that the anion column waste fractions were not analysed as they contained large amounts of Fe and residual salts.

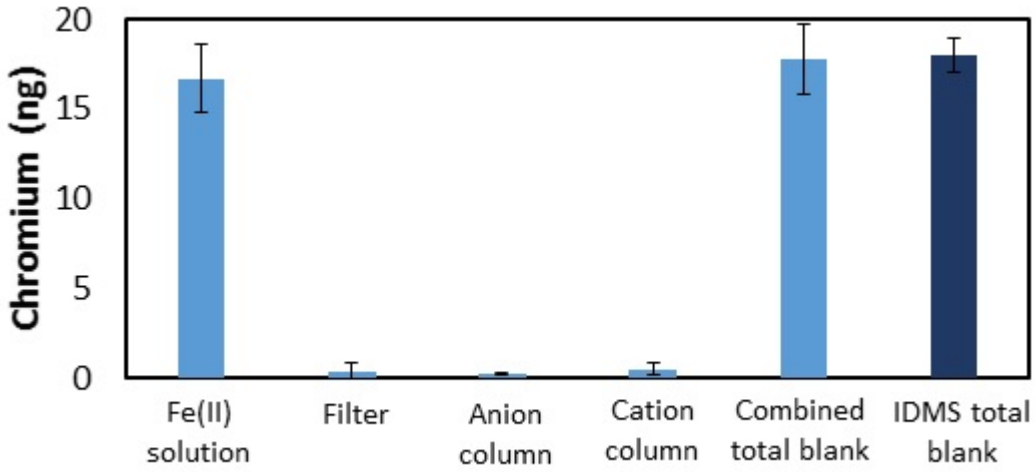

Figure 2.3 - Contributing factors to total isotopic procedural blank (n=3 for all measurements except Fe(II) solution, where n=5). Error bars show 2SD.

2.2.6 Isotopic analysis

Samples were introduced to the Thermo Fisher Neptune MC-ICP-MS using an Aridus 2 Desolvating Nebuliser system using argon as the carrier gas. The Aridus was pre-cleaned with hot 10% nitric acid before each session and nitrogen gas was omitted to minimise interferences from argon nitride (ArN^+), the largest of which was present on the ^{54}Cr isotope as $^{40}Ar^{14}N^+$. The intensities of all four isotopes of Cr were measured in medium resolution mode using $10^{11}\Omega$ amplifiers. In addition, signals from ^{49}Ti, ^{51}V and ^{56}Fe were measured in order to account for isobaric interferences from ^{50}Ti, ^{50}V and ^{54}Fe respectively. An unspiked 33ppb NBS979 Cr standard was used to correctly position the torch and source lenses to obtain an optimal Cr signal. Typically, an optimised ^{52}Cr beam using this standard gave a 6-8V signal. Polyatomic interferences on the ^{53}Cr, ^{54}Cr and ^{56}Fe peaks prevented the use of peak centres for measurement, therefore peak shoulders were used instead. A mass resolution ($M/\Delta M$) of >4800 is required to do this, mainly due to the ^{56}Fe peak shoulder which is too narrow to give a suitable measurement position at low mass resolutions. The range of $M/\Delta M$ values in this study was 5800-6500.

During each analytical session several measurements of a 33ppb spiked standard (alternated with blank measurements) were made prior to sample analysis in order to

check the quality and accuracy of data. A blank measurement consisted of 50 individual measurements or 'cycles', whereas standard and sample measurements consisted of 100 cycles. Prior to sample analysis, undiluted sample ^{52}Cr voltages were measured and dilutions were made to match the ^{52}Cr voltage with that of the 33ppb spiked NBS979 standard for that session. During sample analysis blocks of 3 samples were measured between NBS979 standards, with alternating blank measurements. A long wash time of 12 minutes was set after each standard and sample to prevent contamination of the blank solution and to avoid memory effects between each sample/standard. At least one repeat measurement was acquired for each sample in order to confirm analytical reproducibility, either within the same session or during subsequent sessions. Further details of analytical set-up for the Thermo Fisher Neptune MC-ICP-MS can be found in **Appendix C**.

2.2.7 Data processing and corrections

Baseline and gain corrections were done automatically by the Thermo Fisher Neptune software before further off-line data processing was carried out. Individual sample and standard cycles were blank corrected using the average of the 50 blank cycles measured immediately before and after the sample/standard. Corrections for interferences on the ^{50}Cr and ^{54}Cr peaks were then subtracted and a Newton-Raphson deconvolution technique was used to calculate the original isotopic composition of the sample. Initial isotopic signatures were then calculated using **Equation 1.1** (see **Chapter 1**).

Initial isotopic signatures were normalised against the daily average measurements for the NBS979 standard. The NBS979 standard itself according to **Equation 1** has a $\delta^{53}Cr$ defined as 0‰, but small offsets from the true $\delta^{53}Cr$ were routinely observed between each analytical session due to instrumental mass drift (**Figure 2.4**). NBS979 standard and sample measurements were normalised to account for this drift by subtracting the daily average offset of NBS979 standards from the initial isotopic signature. The normalised external reproducibility of the NBS979 standard was 0.000 ± 0.041‰ (n=520; **Figure 2.4**).

A further correction was made to isotopic signature values to account for the blank contribution. It was found that the Cr isotopic composition of the blank (mostly derived from the ammonium Fe(II) sulphate salt used in co-precipitation) was very different from the samples. This could skew measured $\delta^{53}Cr$ of samples to a greater or lesser extent

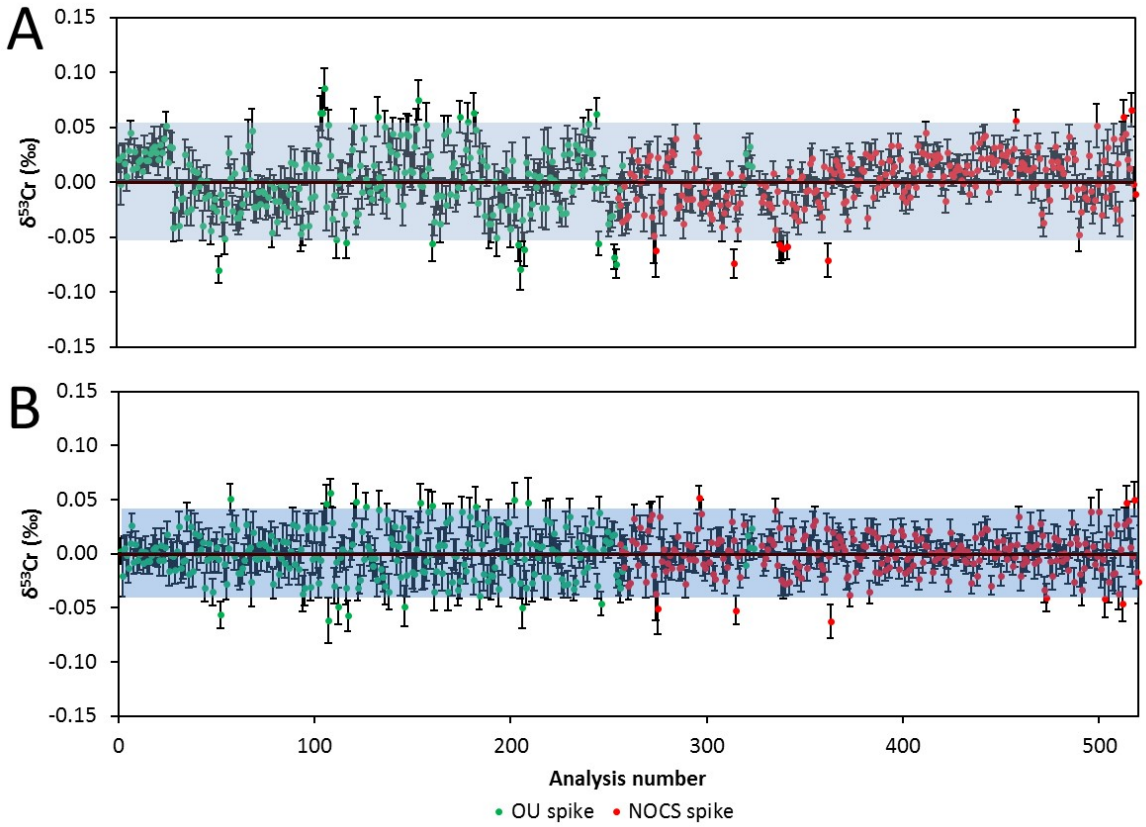

Figure 2.4 - (A) Long term uncorrected reproducibility of NBS979 δ^{53}Cr, (B) normalised reproducibility of NBS979 δ^{53}Cr. Values in green are standards were spiked with the OU double spike, and values in red are standards containing the NOCS double spike. Error bars are 2SE (standard error) of all valid individual cycles for each measurement. Blue shaded areas represent 2SD limits, and central black line marks long term average δ^{53}Cr value.

depending on the amount of Cr and δ^{53}Cr of the sample. Furthermore, the isotopic signature of the Fe(II) precipitate was not consistent, varying between -0.31 ±0.02‰ and -0.54 ±0.00‰ (2SD)**.** The inconsistency between batches is thought to arise from an uneven distribution of isotopes within the ammonium Fe(II) salt used to produce the precipitate. To account for this the isotopic signature of the Fe(II) precipitate was measured with each sample batch and its contribution to the isotopic signature of the sample was proportionally subtracted. This meant the size of the correction changed depending on how much the true δ^{53}Cr of the sample differed from that of the Fe(II) solution. For example, a sample with a normalised δ^{53}Cr of 0.50‰ would correct to 0.55‰, whereas a sample with a normalised δ^{53}Cr of 1.50‰ would correct to 1.62‰ (assuming the same proportion of Fe(II) solution was present in each). Sample concentrations determined using double spike

ID were also corrected according to the amount of Fe(II) hydroxide added in the co-precipitation procedure.

The reported isotopic signature of each sample is the average of all successful and corrected measurements for that sample. Sample errors are given as twice the standard deviation of these measurements (2SD).

2.3 Concentration procedures

The concentration of a sample was determined *via* ID as part of the double spike isotopic technique presented in **Section 2.2.** However, it was essential to know the Cr concentration of a sample before it was processed for isotopic analysis in order to add an optimal amount of double spike. It was therefore necessary to determine the Cr concentration of water samples before making isotopic measurements, whilst preserving as much sample as possible for the isotopic work.

A single spike ID technique was deemed most appropriate for determining initial concentrations as spiking removes the need for 100% Cr recovery, which is difficult to achieve in combination with ion exchange chromatography (Bonnand *et al.*, 2011; Larsen *et al.*, 2016). The sample processing procedure used to determine total Cr concentration was the same as described for isotopic measurements (**Section 2.2**), except that smaller volumes (200-500ml) and a single spike were used. ID concentrations were calculated using the same principles for both the initial single spike procedure and the final double spike isotopic procedure, and these are detailed in the following sections.

A slightly modified co-precipitation procedure using an oxidised Fe(III) hydroxide was required to measure Cr(III) only, and thus speciation could not be determined as part of the isotopic method; thus a single spike ID method was also used to determine Cr(III) concentrations. The procedure was similar to that used for total Cr analyses, except that the Fe(II) hydroxide precipitate was allowed to fully oxidise to Fe(III) hydroxide before addition to the samples. This was done by shaking the Fe(II) hydroxide solution in the presence of ample oxygen for 5-10 minutes, then allowing the precipitate to stand for 3-7 days before use. Cr(VI) does not react with Fe(III) thus only Cr(III) was collected *via* adsorption onto the oxidised precipitate.

2.3.1 Isotope dilution

Isotope dilution mass spectrometry (IDMS) involves spiking a sample with a known quantity of a reference isotope, measuring its concentration relative to a natural isotope and calculating the original quantity of Cr in the sample using the ID equation (**Equation 2.1**, Ohata *et al.* 1998).

$$C = \frac{W_{sp} M_t \left(A_{sp} - RB_{sp}\right)}{W_s M_{sp} (RB_t - A_t)} \qquad \textbf{Equation 2.1}$$

Where C is the concentration of Cr in the sample (ppb), W_{sp} is the weight of Cr in the spike (ng), W_s is the volume of the sample (ml), M_t is the average atomic weight of Cr in the sample, M_{sp} is the average atomic weight of Cr in the spike, A_t and B_t are the abundances of ^{52}Cr and ^{53}Cr in the sample, A_{sp} and B_{sp} are the abundances of ^{52}Cr and ^{53}Cr in the spike, and R is the measured $^{52}Cr/^{53}Cr$ ratio.

For this work ^{52}Cr was chosen as the natural isotope as (i) it is the most abundant isotope, and therefore the best count rate can be achieved using mass spectrometry, and (ii) it has no isobaric interferences, which simplifies analysis and data processing. ^{53}Cr was chosen as an appropriate spike isotope as it also has no isobaric interferences.

2.3.2 Error multiplication

It is important to add an appropriate amount of the spike to samples, because the amount added affects the error multiplication factor (EMF). This is a theoretical factor that influences the precision of the measured isotopic ratios (Bedson, 2007; Ohata *et al.*, 1998). **Figure 2.5** shows how the error multiplication factor is influenced by the $^{52}Cr/^{53}Cr$ ratio in a spiked sample. The optimal ratio is 0.59 (EMF = 1.2) according to **Equation 2.2**, and ratios between 0.1 and 3.7 were deemed acceptable (EMFs up to 1.7; Bedson 2007).

$$EMF_{opt} = \sqrt{\frac{B_{sp}}{A_{sp}} \times \frac{A_t}{B_t}} \qquad \textbf{Equation 2.2}$$

To ensure that the correct amount of spike was added to samples, the spike was calibrated using reverse ID with the NBS979 Cr standard and the sample concentration was estimated using appropriate literature values. These data were used to calculate the optimal spike quantity to be added to achieve the optimal ratio of 0.59.

Column chromatography as presented in **Section 2.2.4** was used to purify samples after co-precipitation as for isotopic work. This was necessary despite the fact that neither the ^{52}Cr or ^{53}Cr isotopes have isobaric interferences, because residual salts and Fe in the analyte solution result in high total dissolved solids that interfere with ionisation efficiency during ICP-MS analysis. Separate sets of columns were used in order to avoid contamination of double spiked samples with the ^{53}Cr spike. The anion procedure was otherwise identical. For the cation procedure only 2ml AG50W-X12 and correspondingly smaller cleaning/pre-conditioning volumes were used.

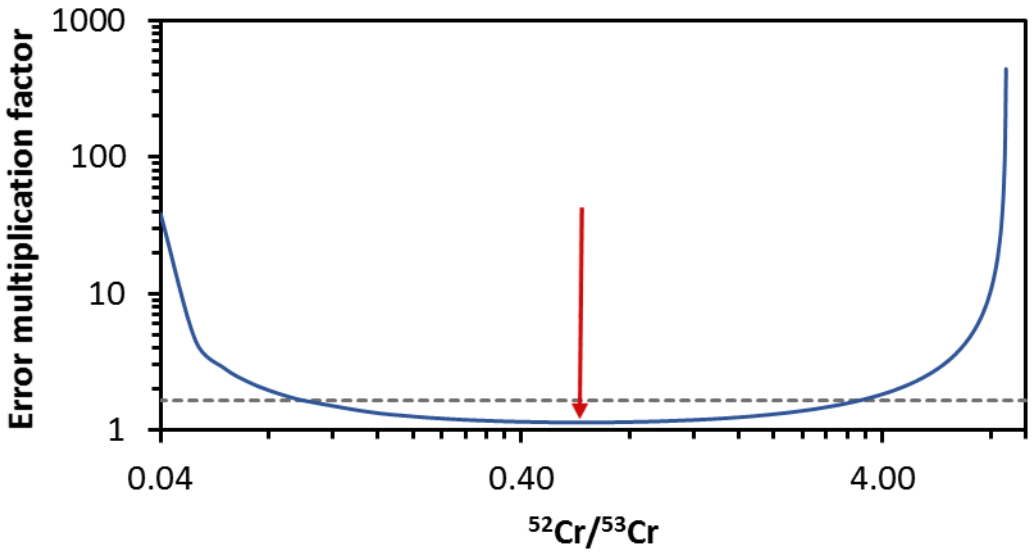

Figure 2.5 - Error multiplication factor variation with $^{52}Cr/^{53}Cr$ ratio. Note log scales on both axes. Dashed grey line shows the maximum acceptable error for this study and red arrow indicates optimal error at $^{52}Cr/^{53}Cr$ of 0.59.

Because only small quantities of Cr were processed for the initial ID procedure, it was important to minimise and account for the procedural blank. A typical sample contained

~40ng Cr and the blank contribution constituted ~10% of the total Cr analysed. In exceptional cases where the sample Cr concentration was very low, the blank contributed up to 40% of the total Cr analysed. To evaluate the blank size, individual blank components were measured and compared to the total procedural blank measured by ID (**Figure 2.6**). The greater variability observed in the total ID procedural blank compared to individual components reflects the fact that ID data were collected over a period of several months during different sample processing sessions, whereas the individual components were tested at the same time. To account for blank variability, two blanks were processed alongside each batch of samples. Blank variations within each batch never exceeded ±1.5ng and were typically less than ±1.0ng, therefore it was possible to make a satisfactory blank correction even when the blank size was relatively large compared to the amount of sample Cr. This was confirmed by processing 2 aliquots of a low concentration river sample, which gave a concentration of 0.26 ± 0.05nmol kg^{-1} demonstrating that good reproducibility could be achieved using the appropriate blank correction.

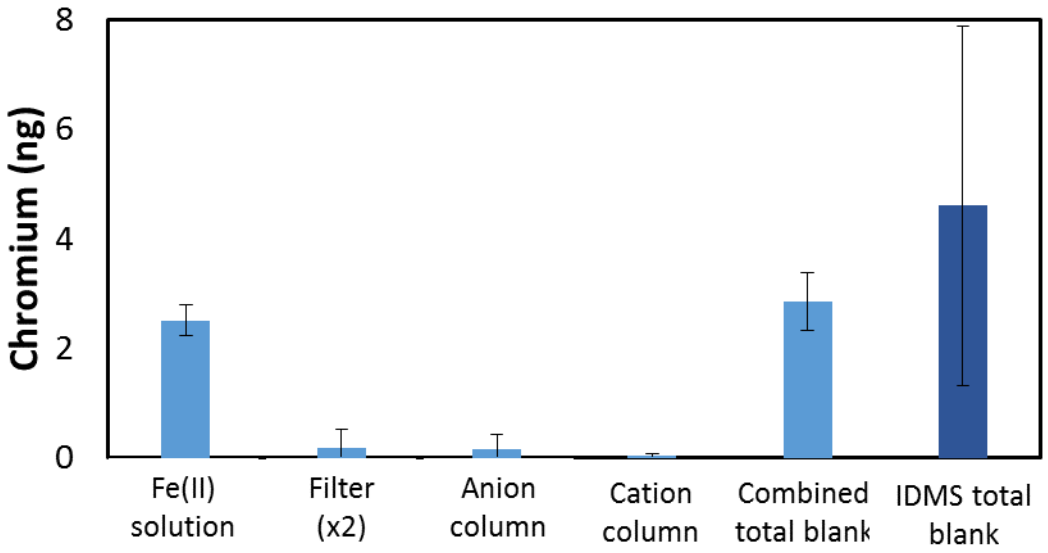

Figure 2.6 - Contributing factors to ID procedural blank (n=5 for Fe(II) solution, n=3 for filters, n=2 for anion and cation columns, n=13 for ID total blank).

2.4 Method validation

2.4.1 Isotopic signatures

A large quantity of Fe was added during co-precipitation of the samples and ^{54}Fe is an isobaric interference when measuring ^{54}Cr. It was therefore important to find out whether interference from residual ^{54}Fe could be effectively accounted for in the interference subtraction calculations. To this end, a number of Fe-doped NSB979 standards were tested during multiple analytical sessions. Fe-doped standards with a range of $^{56}Fe/^{54}Cr$ ratios of up to 0.5 gave $\delta^{53}Cr$ values that were indistinguishable (-0.008 ± 0.036‰ 2SD, n=35) from non-doped standards (0.000 ± 0.041‰ 2SD) (**Figure 2.7**). A weak relationship was found between $^{56}Fe/^{54}Cr$ and standard $\delta^{53}Cr$, however the shallow gradient over a large range of $^{56}Fe/^{54}Cr$ values renders the effect on $\delta^{53}Cr$ values negligible (**Figure 2.8**). Typically $^{56}Fe/^{54}Cr$ for processed seawater samples is <0.05 after column chemistry, and never exceeded 0.5. Therefore our Fe removal method and ^{54}Fe subtraction during data processing successfully prevented a significant systematic error in sample measurements.

As no seawater standard for $\delta^{53}Cr$ is currently available, it was necessary to verify the accuracy of isotopic measurements using alternative means. Analysis of the carbonate standard JDo-1 produced a value of 1.73 ± 0.04‰ (n=2), which is within error of published values (**Table 2.2**). However the sample processing procedure for carbonates is different than for seawater, so tests designed specifically to evaluate the effect of seawater processing were necessary (Bonnand *et al.*, 2011).

Table 2.2 - $\delta^{53}Cr$ values obtained for the JDo-1 carbonate standard in different studies.

Reference	$\delta^{53}Cr$ (‰)	Error (2SD)
Bonnand *et al.* 2011	1.72	0.06
Pereira *et al.* 2015	1.70	0.08
Rodler *et al.* 2015	1.69	0.05
Gilleaudeau *et al.* 2016	1.64	0.03
This study	1.73	0.04

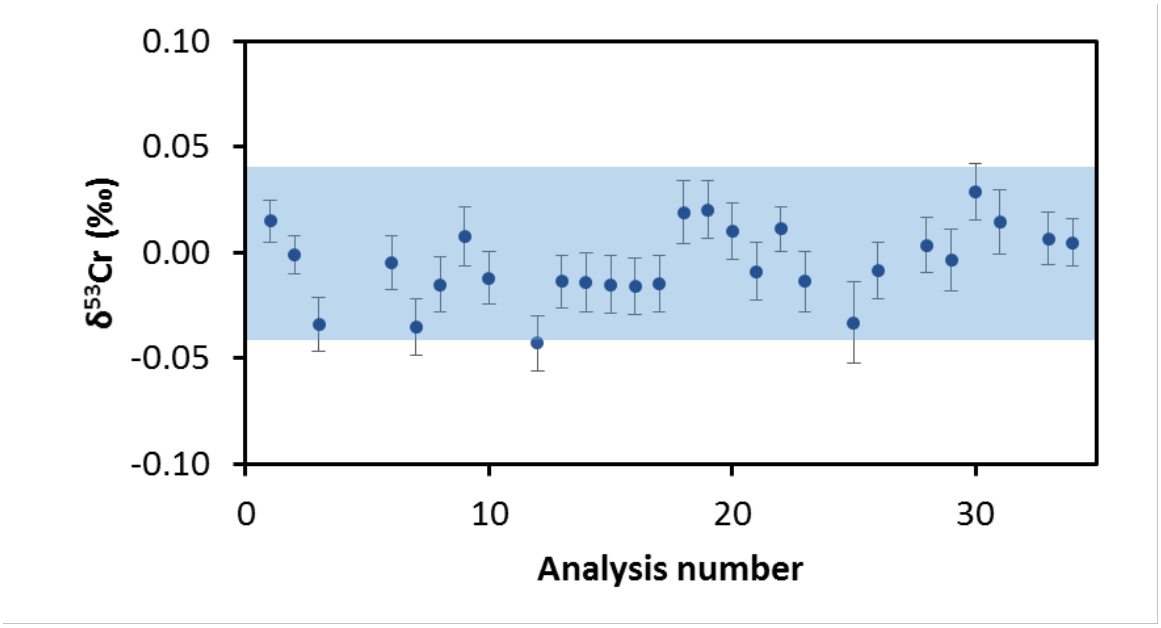

Figure 2.4 - $\delta^{53}Cr$ of NBS979 standards doped with variable quantities of Fe. Blue shading indicates 2SD range for non-doped NBS979 standards. Error bars are 2SE.

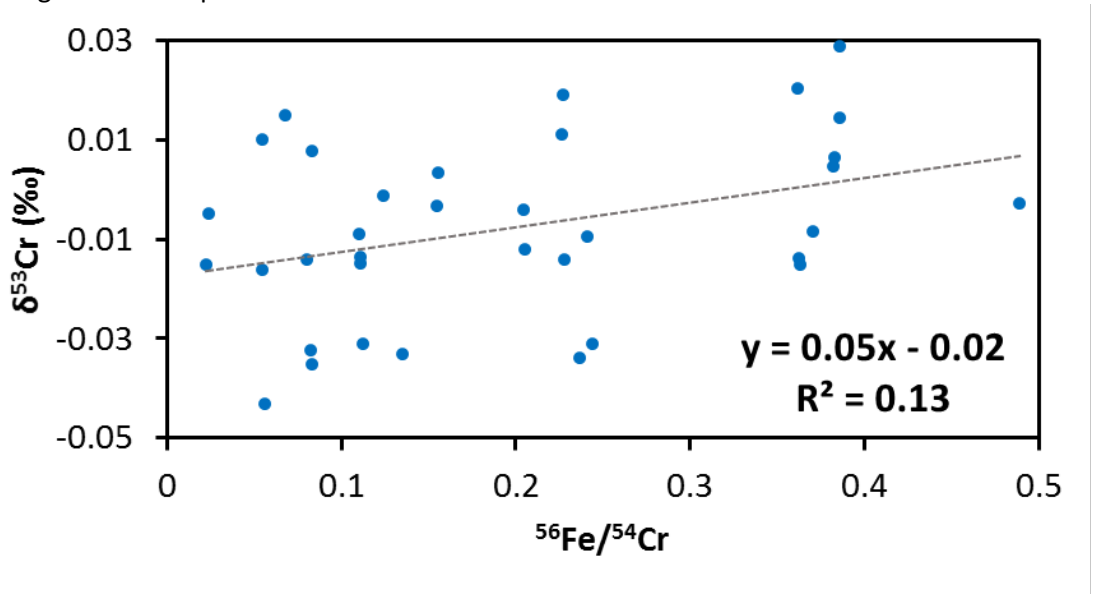

Figure 2.5 - $\delta^{53}Cr$ of Fe doped standards versus $^{56}Fe/^{54}Cr$.

Bonnand *et al.* (2013) processed the NBS979 standard in MQ water to test whether Cr isotopes were fractionated by the seawater processing procedure. It was found that co-precipitation caused no fractionation but column chemistry did cause a small negative fractionation (−0.056 ± 0.028‰, 2SD). To investigate whether fractionation occurs with a seawater matrix, a standard addition experiment was performed using a seawater sample from Southampton Water (**Figure 2.9**). Varying amounts of NBS979 standard were added

to this sample, and three aliquots were analysed without standard addition to represent the seawater end-member. Extrapolation of this data to predict the Cr isotopic composition of the NBS979 end-member reveals a negligible offset of 0.02‰. The linear behaviour of $\delta^{53}Cr$ over a large isotopic range indicates that this method is able to accurately measure $\delta^{53}Cr$ in seawater samples. Furthermore the analyses reveal that the end-member Southampton Water sample had an average isotopic signature of 1.48 ±0.06‰ (2SD), which is within error of the previously measured value of 1.51 ±0.05‰ (Bonnand *et al.*, 2013).

As a further check, 500mL of OSIL ASCS was doped with 10µg of NBS979 standard. Since the natural Cr concentration of this seawater is 1.3nmol kg^{-1}, doping rendered the original seawater isotopic signature insignificant and the expected $\delta^{53}Cr$ was therefore 0‰. This sample was then separated into 5 aliquots which were processed separately. A small offset from 0‰ was observed in these samples, 0.03 ± 0.02‰ (2SD), but this still smaller than the offset observed by Bonnand *et al.* (2013).

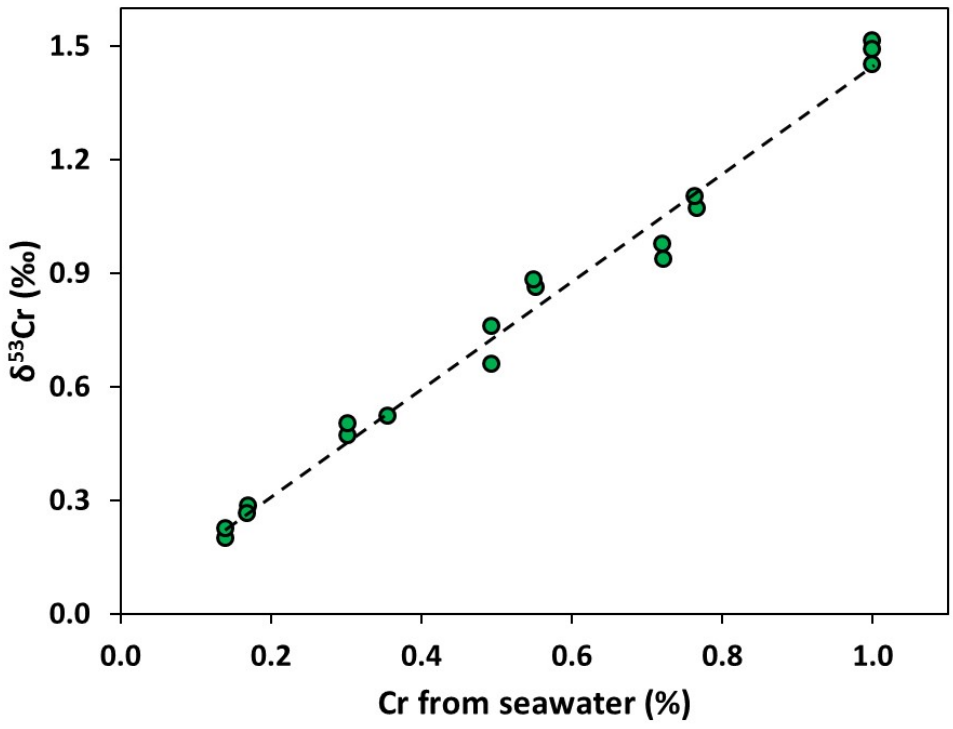

Figure 2.6 - Standard addition experiment with NBS979 standard in Southampton Water. Data points represent single measurements. 2SE error bars are smaller than the markers.

2.4.2 Accuracy of Cr concentrations determined by double spike ID

The OSIL ASCS doped with 10µg NBS979 (total Cr concentration 358.7nmol kg^{-1}) was processed 5 times and produced an average value of 360.3 ± 0.1nmol kg^{-1} (2SD). This demonstrates excellent external reproducibility and is within 0.4% of the true value. To evaluate the accuracy in a standard with a concentration closer to real seawater, a large sample of NBS979 in MQ water was processed 5 times (with an expected concentration 11.0nmol kg^{-1}). The averaged measured concentration was 10.5 ± 0.0nmol kg^{-1}, which again demonstrates excellent external reproducibility and good accuracy, since the Cr concentration was within 4% of the expected value.

A Cr(VI) standard (expected concentration 23.8nmol kg^{-1}) was also tested 3 times after seawater processing and produced a concentration of 18.4 ± 0.06nmol kg^{-1}, 23% lower than expected. A similar problem was experienced using the single spike method, and investigated further using that method (**Section 2.4.3**).

2.4.3 Accuracy of Cr concentrations determined by single spike ID

To assess the accuracy of concentration data obtained using the single spike method detailed in **Section 2.3**, the concentration of Cr(III) and Cr(VI) standards in MQ water were tested (NBS979 and Inorganic Ventures Certified Reference Material ammonium bichromate, respectively). Four 11.2nmol kg^{-1} Cr(III) standards were processed and their average concentration was determined to be 10.9 ± 0.2nmol kg^{-1}, within 4% of the true value. However, the Cr(VI) standard consistently returned values ~32% lower than expected. A second Cr(VI) standard (potassium chromate, Fluka TraceCERT® Certified Reference Material) was tested and this returned values 60-66% lower than expected.

All Cr in acidified seawater is expected to be present as Cr(III), meaning the loss of Cr(VI) should not present an issue in determining the total Cr concentration of natural waters (Semeniuk *et al.*, 2016; Sirinawin and Westerlund, 1997). However the concentration measured in NASS-6 seawater was 20% lower than the certified value, indicating that a similar problem may be present for both Cr(VI) standards and seawater samples. The loss of Cr(VI) during processing was therefore investigated further.

In the case of potassium chromate standards, the measured $^{52}Cr/^{53}Cr$ ratio consistently fell between 0.23-0.30, much lower than the desired ratio of 0.59. Contamination from a natural source would drive this ratio to higher values (>0.59) due to the higher natural abundance of ^{52}Cr (83.8%). Only the presence of a component with a high proportion of ^{53}Cr can drive the ratio to lower values (<0.59) as observed. ^{53}Cr contamination is an unlikely cause since all standards tested (n=15), at different times and under different experimental conditions, consistently produced this ratio (**Appendix B, Table B3**). A systematic error in the Cr(VI) concentration measurements is therefore considered to be more likely. There are three possible contributing factors: (i) Cr(VI) did not equilibrate with the ^{53}Cr spike, (ii) co-precipitation did not quantitatively collect Cr, and (iii) the spike and sample Cr became separated before or after co-precipitation. Equilibration rates between Cr(III) and Cr(VI) are extremely slow and therefore it is expected that the spike and sample Cr did not equilibrate until co-precipitation occurred (Wang *et al.*, 2015). This does not present a difficulty if co-precipitation collects Cr quantitatively as expected (Cranston and Murray, 1978), thus (i) is unlikely to be the cause. Similarly the problem affected Cr(VI) standards regardless of whether they were subjected to co-precipitation (**Appendix B, Table B3**) so (ii) can be ruled out as a cause. Therefore the issue must have occurred prior to co-precipitation or during column chromatography as a result of (iii), regardless of whether spike and sample Cr pools became equilibrated. A simple model shows that in a spiked potassium chromate standard, Cr(VI) loss of 60-66% during processing will produce $^{52}Cr/^{53}Cr$ ratios of 0.23-0.28 assuming no spike Cr is lost (**Figure 2.10**). This matches exactly with the observed ratios and lends support to the hypothesis that natural and spike Cr were fractionated during sample processing.

It was not clear whether this separation occurred before or after co-precipitation, thus column calibrations with Cr(VI) and Cr(III) were carried out to investigate where the problem occurred. For both anion and cation columns, a quantity of Cr similar to a typical sample (41-42ng) of either Cr(III) (NBS979) or Cr(VI) (potassium chromate) was used. This Cr was spiked with enough ^{53}Cr to produce the optimal $^{52}Cr/^{53}Cr$ ratio of 0.59. The resulting solution was dried down and given the same pre-column treatment as a sample. The standards were passed through identical columns 1ml at a time, and each 1ml fraction was collected separately for analysis using a Thermo Element 2 ICP-MS. Cr concentrations were

calculated with a calibration curve. In each calibration, the first 10 fractions represent the 10ml which would be collected as sample material, whilst later fractions represent the waste which is eluted when the column is cleaned after use.

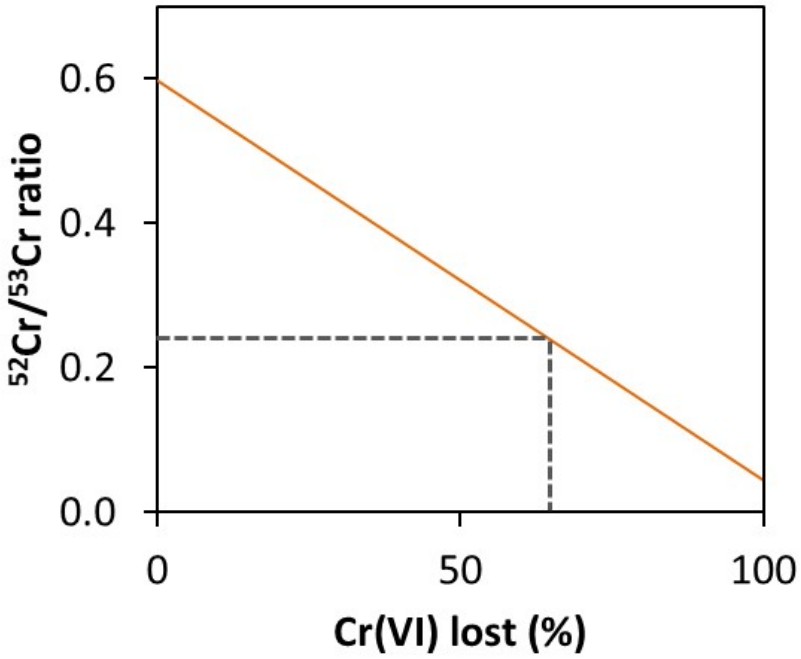

Figure 2.7 - Model showing expected $^{52}Cr/^{53}Cr$ ratio of a spiked Cr(VI) standard with varying Cr(VI) loss. Dashed line shows actual measured Cr(VI) standard $^{52}Cr/^{53}Cr$ ratio of 0.26 and corresponding percentage loss of Cr(VI).

The anion column results for the Cr(III) standard (NBS979; **Figure 2.11A+B**) show that 92% of Cr(III) was collected before the cleaning stage begins. This value is very close to the 95% found by Bonnand *et al.* 2011. The collected fraction of Cr(III) has a combined ratio of 0.58, very close to the intended 0.59, and the ratio is rather consistent in all fractions where a significant amount of Cr was collected (2-8ml fractions). During the cleaning step very low concentrations were observed reflecting the fact that Cr collection during the first 1-10ml is efficient. The column blank (approximately 0.01ng/ml) represents a significant proportion of the remaining Cr after these fractions. The higher ratios in fractions 11-14 can be explained by blank contamination with a natural $^{52}Cr/^{53}Cr$ ratio. Overall Cr(III) behaves as expected during anion column chemistry.

In contrast, the anion column yield for the Cr(VI) standard was only 50% despite an overnight reflux step in 7M HCl which should convert all Cr to Cr(III). If the low yield of Cr(VI)

in the collected fraction were due to incomplete conversion to Cr(III) during the reflux stage, the remaining 50% of the Cr(VI) would still be present as the CrO_4^{2-} anion and this would be eluted during the cleaning stage. This was not observed within the 11-14ml fractions where only 2.5% was recovered, suggesting that Cr(VI) was lost before column chemistry began. The collected fraction also had a $^{52}Cr/^{53}Cr$ ratio of 0.26, as for previously measured Cr(VI) standards.

The cation column yields were poor for both Cr(III) (27%) and Cr(VI) (33%) (**Figure 2.11C+D**). In the case of Cr(III) this is probably due to incomplete conversion to Cr(VI) before column chemistry, supported by the fact that a large quantity of Cr with the intended ratio of 0.59 was collected during the cleaning phase. A total of 91% of the Cr(III) was accounted for. On the other hand, little of the remaining Cr(VI) was eluted during the cleaning phase with only 56% of the Cr(VI) accounted for in total. Once again the collected fraction had $^{52}Cr/^{53}Cr$ of 0.28.

Cr(VI) standards produced a $^{52}Cr/^{53}Cr$ ratio of 0.26-0.28 in fractions 1-10 for both columns, consistent with co-precipitated samples. The balance of Cr(VI) was not recovered in the column waste. Overall these results suggest that a significant proportion of Cr(VI) was lost before column chemistry, and that this Cr had not equilibrated with the ^{53}Cr spike. To confirm Cr loss before column chemistry, three Cr(VI) spiked standards were tested without column chemistry or co-precipitation. These samples also had $^{52}Cr/^{53}Cr$ ratios of 0.23-0.26, confirming that loss occurs without any sample processing. Spiked standards exposed to hydrogen peroxide to oxidise the spike and promote equilibration suffered the same effect. The mechanism of Cr(VI) loss is unknown, but may be due to adsorption of Cr(VI) onto Savillex sample bottle/pipette tip surfaces. Rigorous cleaning of containers was performed, and this has been noted to create available adsorption sites for Fe in natural waters (Achterberg *et al.*, 2001). A similar phenomenon may affect Cr.

A column calibration using an OSIL seawater salinity standard was also carried out to see if the effect was similar in a natural sample (**Figure 2.2**). The expected $^{52}Cr/^{53}Cr$ ratios for the anion and cation OSIL samples in this experiment were 0.84 and 0.82 respectively. $^{52}Cr/^{53}Cr$ ratios of 0.59 and 0.55 were actually measured. This resulted in a concentration ~15% lower than that determined for this standard using the double spike method in this work and another study (Scheiderich *et al.*, 2015). Along with comparable results for the NASS-6

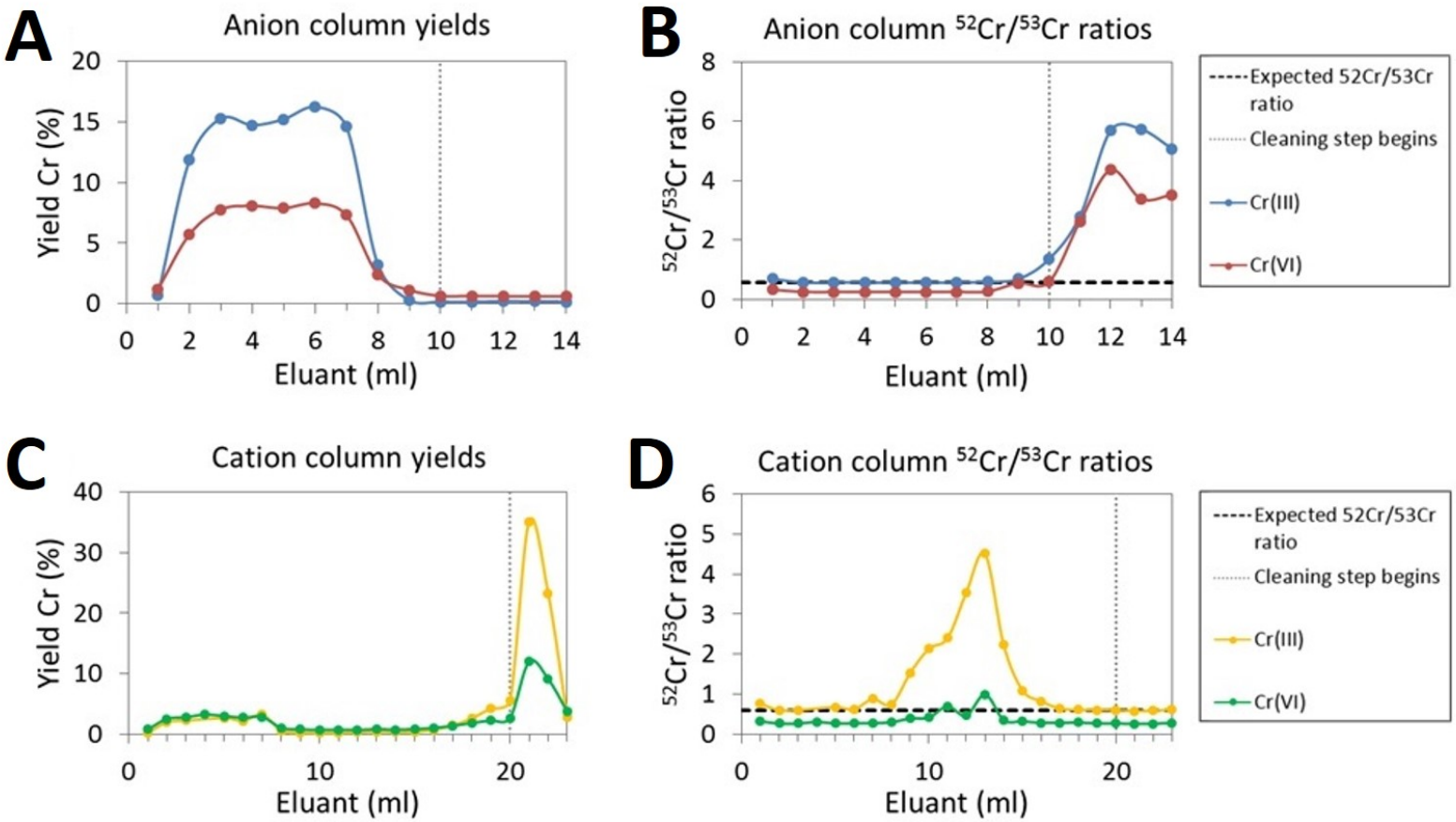

Figure 2.11 - (A) Cr yield in each fraction as a proportion of Cr loaded onto the anion column, (B) $^{52}Cr/^{53}Cr$ ratio of each anion fraction, (C) Cr yield in each fraction as a proportion of Cr loaded onto the cation column, and (D) $^{52}Cr/^{53}Cr$ ratio of each fraction in the cation column.

standard (20% loss), this suggests that the issue may manifest itself in seawater samples although the effect is less extreme than in the potassium chromate Cr(VI) standard.

It remains unexplained how exactly Cr(VI) is lost, and why the effect is less pronounced in double spike ID concentrations. Overall the single spike ID method was unable to accurately determine total Cr concentration in samples which contain a proportion of Cr(VI), although it was still useful for obtaining indicative sample concentrations prior to double spiking, and was suitable for the determination of Cr(III) in natural waters.

2.4.4 Inter-calibration study

To evaluate the robustness of the Fe(II) co-precipitation method between laboratories, an inter-calibration exercise was performed in collaboration with University of Saskatchewan, Canada. First, six samples of the OSIL ASCS were measured at the University of Southampton to compare against the values reported by Scheiderich *et al.* (2015). The isotopic signatures and concentrations of these standards fell within 2SD error of the published values (**Table 2.3**). Secondly, three samples from a depth profile in the Beaufort Sea were also measured at both universities. This was conducted as a semi-blind test at Southampton. Samples were processed and measured without prior knowledge of the values obtained at the University of Saskatchewan by a similar Fe(II) co-precipitation technique. Comparison of the results indicated that isotopic signatures were in good agreement (within 2SD error), however it was not possible to match the concentration values, which were determined to be 12-14% lower at Southampton. The Saskatchewan and Southampton double spike concentrations are both considered to be well calibrated and this is an unlikely cause of the discrepancy. It could arise from Cr adsorption to container walls during prolonged storage (despite acidification), or preferential loss of sample Cr during processing as discussed in **Section 2.4.3**. Further investigation is required.

Table 2.3 - Results of inter-calibration study with University of Saskatchewan (External 2SD errors given for OSIL, internal (analytical) 2SD given for Beaufort waters).

Sample	Concentration (nmol kg^{-1})		δ^{53}Cr (‰)	
	Univ. Saskatchewan	Univ. Southampton	Univ. Saskatchewan	Univ. Southampton
OSIL	3.01 ± 0.06	3.08 ± 0.03	0.96 ± 0.06	0.97 ± 0.10
Beaufort 10m	1.50	1.29	1.34 ± 0.06	1.33 ± 0.03
Beaufort 1400m	2.73	2.40	1.10 ± 0.07	1.09 ± 0.05
Beaufort 3000m	2.90	2.58	1.05 ± 0.05	1.08 ± 0.07

2.5 Summary

An Fe(II) co-precipitation method has been developed for the measurement of Cr isotopic compositions in natural waters. Rigorous testing of the method shows that Cr fractionation is not induced during sample processing over a wide range of isotopic values, and that the isotopic compositions determined by this method may be considered to be accurate. The external reproducibility of the method is ±0.1‰ which is comparable with similar studies (Bonnand *et al.*, 2013; Scheiderich *et al.*, 2015).

Concentration measurements were also obtained using this method, employing either a single (^{53}Cr) spike or a double (^{50}Cr-^{54}Cr) spike. The method accurately measures Cr(III) in natural waters but is unable to accurately determine the concentration of Cr(VI) standards, and NASS-6 standard seawater concentrations were also lower than the certified value by 20%. An inter-calibration study revealed that some seawater sample concentrations match those measured at the University of Saskatchewan, whereas others were up to 14% lower in this study. It is possible that the conversion of Cr(III) to Cr(VI) during sample processing is responsible for the discrepancy, but further research is required. The total Cr concentrations determined by this method should therefore be considered minimum estimates.

Chapter 3: Behaviour of chromium isotopes in the North Atlantic Oxygen Minimum Zone

3.1 Introduction

The chromium (Cr) isotopic composition of ancient marine deposits is increasingly being used to help constrain the evolution of atmospheric oxygen and to establish redox conditions in ancient seawater (e.g. Crowe *et al.* 2013; Frei *et al.* 2009; Planavsky *et al.* 2014). This is because Cr has two stable valence states at Earth surface conditions, Cr(III) and Cr(VI), and mass dependent fractionation of Cr isotopes occurs during oxidation and reduction reactions (e.g. Kitchen *et al.* 2012; Zink *et al.* 2010). For example natural reduction of Cr(VI) to Cr(III) enriches the remaining Cr(VI) in the heavier isotope by up to 7.9‰ on the $^{53}Cr/^{52}Cr$ ratio (Ball and Bassett, 2000). The degree of fractionation for oxidation is less well characterised but appears to be smaller (fractionation factor ($\Delta_{Cr(III)-Cr(VI)}$) for Cr(VI) product ≈ -0.2‰; Zink *et al.* 2010). Oxidation may enrich Cr(VI) relative to Cr(III) in ^{52}Cr or ^{53}Cr depending on the structure of the oxidant, rendering $\delta^{53}Cr$ in the remaining Cr(III) high or low relative to its starting value (Bain and Bullen, 2005; Joshi *et al.*, 2011).

The vast majority of dissolved Cr is supplied to the oceans *via* rivers (Bonnand *et al.*, 2013; Chester and Murphy, 1990; McClain and Maher, 2016), and is derived from the terrestrial weathering of Cr(III) in mafic rocks that have a narrow range of $\delta^{53}Cr$ values (-0.12 ± 0.10‰; Schoenberg *et al.* 2008). During the weathering process Cr(III) is hydrolysed to $CrOH^{2+}$, $Cr(OH)_2^{+}$ and/or $Cr(OH)_3$ which are reactive species that may be oxidised to Cr(VI) (forming $HCrO_4^-$ and CrO_4^{2-}) under oxic conditions. Oxidation of Cr(III) by O_2 is slow (Magar *et al.*, 2008; Schroeder and Lee, 1975), but it is more rapid with manganese (Mn) oxides and hydrogen peroxide (Oze *et al.*, 2007; Pettine and Millero, 1990). As noted above the differences in the $\delta^{53}Cr$ values of the Cr(VI) produced and residual Cr(III) appear to be small, but the overall effect of Cr(III) oxidation during oxic weathering appears to be the production of a ^{53}Cr enriched fluid and retention of ^{52}Cr in the solid phase (e.g. Frei *et al.* 2014, Frei and Polat 2013), consistent with an equilibrium fractionation mechanism (Schauble *et al.*, 2004). This effect can be further enhanced by partial back-reduction of Cr(VI) which also enriches ^{53}Cr in the dissolved phase (e.g. D'Arcy *et al.* 2016, Kitchen *et al.*

2012, Zink *et al.* 2010). Thus river waters that are delivered to the ocean are generally enriched in ^{53}Cr relative to source rocks, with a $\delta^{53}Cr$ range of -0.33 to 1.68‰ (D'Arcy *et al.* 2016, Frei *et al.* 2014, Paulukat *et al.* 2015, Wu *et al.* 2017). Seawater and ancient marine authigenic precipitates are thought to inherit positive $\delta^{53}Cr$ values from these processes under oxic terrestrial conditions (Frei *et al.*, 2009; Frei *et al.*, 2013; Gilleaudeau *et al.*, 2016). However the nature and extent of Cr reduction-oxidation reactions within the oceans themselves may further influence the $\delta^{53}Cr$ of marine deposits (Scheiderich *et al.*, 2015), yet these are poorly understood. A full interpretation of Cr isotope signatures in these deposits requires a process-based understanding of the behaviour of Cr and its isotopes in seawater.

The distribution of dissolved Cr in seawater is heterogeneous despite a relatively long residence time of ~9500 years (Reinhard *et al.*, 2013) and concentrations usually range between 0.9 and 6.5nM (e.g. Achterberg and Berg 1997; Bonnand *et al.* 2013; Campbell and Yeats 1981; Connelly *et al.* 2006; Cranston 1983; Jeandel and Minster 1984; Sirinawin *et al.* 2000). Small surface depletions in Cr concentration are common and are often correlated with nutrient depletion (e.g. Campbell and Yeats 1981, Cranston 1983, Achterberg and Berg 1997) leading to the classification of Cr as a recycled element. However in some parts of the ocean relatively high surface Cr can also occur due to atmospheric inputs (Achterberg and Berg, 1997). Similarly, inputs of Cr from marine sediments can result in relatively high concentrations close to the seabed at some locations (Jeandel and Minster, 1984). If there are no external inputs of Cr and rates of biological activity are low, then concentrations may simply reflect those of newly formed water masses that are subducted into the interior ocean (Sirinawin *et al.*, 2000).

Reduction of Cr(VI) is expected to occur under roughly the same conditions as nitrate reduction (standard potentials for $CrO_4^{2-}/Cr(OH)_3$ = -0.12V, NO_3^-/NO_2^- = 0.01V; Bratsch 1989, Fanning 2000). In oxic waters Cr(VI) is generally the dominant species, but under some circumstances Cr(III) can constitute up to ~50% of the dissolved Cr inventory in the upper water column (Connelly *et al.*, 2006). Cr(III) may form in the presence of reductants such as Fe(II) (Døssing *et al.*, 2011) and organic material. Organic molecules can reduce Cr in their own right or support reduction by other mechanisms (Jamieson-Hanes *et al.*, 2012; Kitchen *et al.*, 2012), and they can also act to stabilise Cr(III) in solution (Kaczynski and

Kieber, 1994). Although Cr is not thought to be a nutrient for marine bacteria and phytoplankton, inadvertent biological reduction is also well documented (Basu *et al.*, 2014; Li *et al.*, 2009; Sikora *et al.*, 2008; Wang and Dei, 2001). While Cr(VI) is not significantly particle reactive at seawater pH and is only weakly held on most mineral surfaces (Gaillardet *et al.*, 2003; Zachara *et al.*, 1988), Cr(III) aquahydroxyl and hydroxyl species readily adsorb to particle surfaces or precipitates as CrO_3 or with Fe (hydr)oxides (Crawford *et al.*, 1993).

The separation of Cr(VI) and Cr(III) into aqueous and sedimentary phases by oxidation and reduction can result in the preservation of $\delta^{53}Cr$ values that reflect the redox processes the Cr has been through, hence the $\delta^{53}Cr$ composition of ancient marine deposits is considered to be a proxy for redox conditions in past environments. For instance, high $\delta^{53}Cr$ values in banded iron formations (BIFs) are thought to reflect oxidative weathering on land, with quantitative reduction of Cr(VI) to Cr(III) in redox stratified basins and co-precipitation of the Cr(III) with iron minerals (e.g. Frei *et al.* 2009). By contrast $\delta^{53}Cr$ values close to crustal rocks are suggested to indicate the absence of oxidative weathering, and thus low atmospheric O_2 (Crowe *et al.*, 2013; Frei *et al.*, 2009; Planavsky *et al.*, 2014). Authigenic carbonates on the other hand are thought to reflect seawater $\delta^{53}Cr$, since CrO_4^{2-} is directly incorporated into them; seawater $\delta^{53}Cr$ itself is the culmination of all redox processes that affected Cr during terrestrial weathering and transport (Bonnand *et al.*, 2013; Holmden, 2013).

Studies of the behaviour of dissolved Cr in the Oxygen Minimum Zone (OMZ) of the tropical East Pacific revealed that the concentrations of Cr(VI) were depleted by ~30% within the OMZ core (that has 5µmol kg^{-1} dissolved oxygen) whereas the concentration of Cr(III) and particulate Cr were highest at the top of the OMZ (Murray *et al.*, 1983; Rue *et al.*, 1997). In the Saanich Inlet, an intermittently anoxic fjord, Cr(VI) concentrations fell to zero in the suboxic zone and Cr(III) concentrations increased about 15m above this zone (Emerson *et al.*, 1979). The reactivity of Cr in suboxic waters has previously been used to make distinctions between suboxic and anoxic conditions in past environments (e.g. Algeo and Maynard 2004, Tribovillard *et al.* 2006), and knowledge of corresponding changes in $\delta^{53}Cr$ may also prove highly useful in paleo-oceanographic studies.

The range of $\delta^{53}Cr$ values observed in seawater to date is 0.13 to 1.55‰ (Bonnand *et al.*, 2013; Economou-Eliopoulos *et al.*, 2016; Holmden *et al.*, 2016; Paulukat *et al.*, 2015; Paulukat *et al.*, 2016; Pereira *et al.*, 2015; Scheiderich *et al.*, 2015). Overall there appears to be a negative correlation between Cr concentrations and $\delta^{53}Cr$, which has been interpreted to reflect reduction of Cr(VI) in surface waters and OMZs, with small to negligible fractionation resulting from re-oxidation and release from marine sediments in deeper waters (Scheiderich *et al.*, 2015). The behaviour of Cr isotopes in dysoxic, suboxic and anoxic marine environments is, however, as yet unknown (see **Table 3.1** for definitions of these terms). To address this we have determined the Cr concentration and Cr isotopic composition of oxic and dysoxic water column samples collected within the OMZ of the eastern North Atlantic Ocean and oxic, suboxic and anoxic samples from the Black Sea. We show that O_2 concentrations are insufficiently low in the Atlantic OMZ to reduce and fractionate Cr but that a change in $\delta^{53}Cr$ values does occur across the oxic-suboxic boundary of the Black Sea. We also demonstrate that deep water $\delta^{53}Cr$ values show less variation in comparison with intermediate, surface and shelf waters. The implications of our results for the interpretation of Cr isotopic compositions in sedimentary archives are also discussed.

Table 3.1 - Terminology for the different oxygen regimes discussed in this work, after Tyson and Pearson 1991. Values converted from ml L^{-1} to mol kg^{-1} using a seawater density value of 1.035kg L^{-1}.

Oxygen concentration (µmol kg^{-1})	Term used
92 - 370	Oxic
9.2 - 92	Dysoxic
0.0 – 9.2	Suboxic
0.0 (+ H_2S)	Anoxic

3.2 Sampling locations

3.2.1 Northeast and South Atlantic Ocean

Water samples were collected in the vicinity of the eastern Atlantic OMZ at six stations during RRS Discovery cruise D361 (GA06) between 7 February and 19 March 2011 as part of the GEOTRACES project. Four stations (stations 2-5) were located above the Senegalese shelf and a fifth (station 18) in the North Atlantic Ocean approximately halfway between the Senegalese coast and the mid-Atlantic ridge, all at a latitude of ~12°N. A sixth station (station 11.5) was located in the South Atlantic Ocean at a latitude of 3°S (**Figure 3.1A**).

Senegalese coastal waters are located in the southern extent of the North West African upwelling system. Upwelling only occurs there in the boreal winter and spring when trade winds are strong, and the vertical extent of upwelling is relatively shallow compared to more northerly regions, with the deepest upwelled waters originating from the top of the thermocline (~100m; Pelegrí and Benazzouz 2015). Nonetheless, elevated nutrient levels in the top 100m allow enhanced biological activity on the shelf and shelf slope. In addition to coastal upwelling, the Guinea Dome upwelling system is also located in the study area.

Below the coastal upwelling system, South Atlantic Central Water (SACW) is found at depths of ~150-500m. This water mass is transferred to the South Atlantic Ocean from the Indian Ocean *via* the Aghulas current. It crosses the Atlantic basin *via* the Benguela current, and travels north with the North Brazilian Undercurrent. Beyond, in the sub-tropical and equatorial regions, the pathways of SACW are highly complex and seasonably variable (Stramma and England, 1999).

Table 3.2 - Summary of stations sampled during this work. Contains data supplied by the Natural Environment Research Council (cruise D361) and the GEOTRACES project.

Cruise	Station	Latitude	Longitude	Sea floor depth (m)	Description
D361 (RRS *Discovery*)	2	12.5942	-17.9199	2656	Shelf slope
	3	12.6100	-17.7157	1041	Shelf slope
	4	12.6120	-17.5728	51	Shelf
	5	12.5882	-17.5724	164	Shelf
	11.5	-2.9625	-25.6148	5300	Open ocean
	18	12.0325	-28.9805	5717	Open ocean
PE370 (RV *Pelagia*)	1	39.7333	-14.1664	5265	Open ocean
PE373 (RV *Pelagia*)	10	42.7387	32.5052	2180	Semi-enclosed sea

The SACW meets well-ventilated North Atlantic Central Water (NACW) at the Cape Verde Convergence Zone at approximately 20°N (**Figure 3.1B**). The NACW is consequently deflected towards the west forming the south-eastern corner of the North Atlantic sub-tropical gyre. This means that NACW inputs at 12°N are negligible and subsequent ventilation of SACW is prevented (Stramma *et al.*, 2005). This contributes to the presence

of a poorly ventilated 'shadow zone' between the sub-tropical gyre and equatorial current systems, in which our study area lies (Zenk *et al.*, 1991). O_2 concentrations on the shelf and shelf slope are also depleted as large quantities of organic matter sink and decay. The combined effects of poor ventilation and high biological productivity in surface waters cause a dysoxic OMZ (45-90µmol kg^{-1} O_2) at 200-800m depth, though the waters do not become suboxic as in the Indian and Pacific Oceans (Helly and Levin, 2004). Highly oxygenated Antarctic Intermediate Water (AAIW) bounds the OMZ from below and is identified by a salinity minimum at 600-1000m, whilst NADW occurs between 1000m and the seafloor, though the deepest stations may be influenced by Antarctic Bottom Water (ABW) (Stramma and England, 1999; Stramma *et al.*, 2005).

At 3°S (station 11.5) the water column structure is similar to that at 12°N, with the exception that Upper Circumpolar Deep Water (UCDW) is found between AAIW and NADW at 1000-1300m. SACW at this station is fed by both oxygen poor equatorial waters and oxygen rich waters from the south (Stramma and Schott, 1999). This results in higher average O_2 concentrations within the SACW compared to the other stations, though the OMZ is still well defined between 200 and 600m.

3.2.2 The Black Sea and adjacent North Atlantic

Three seawater samples (oxic, suboxic and anoxic) were taken from the Black Sea as part of a GEOTRACES inter-comparison exercise on the RV Pelagia Medblack cruise PE373 (leg 2) on 22 July 2013 (**Figure 3.1**). Two additional samples of the nearest adjacent open ocean seawater were collected at 39°44.00N, 14°09.99W in the North Atlantic Ocean PE370 (leg 1) at 25m and 1500m depth. The 25m sample represents surface waters whilst the 1500m sample consists of mixed AAIW and Mediterranean Outflow Water (MOW; van Aken 2000).

The Black Sea is strongly stratified due to large riverine inputs and a restricted flow of seawater into the basin *via* the Bosphorus Strait (Murray *et al.*, 1991). The strong density gradient that results prevents the oxygenation of water below the surface, giving rise to anoxic conditions below ~100m depth. In the transition from oxic to anoxic conditions, there is a suboxic zone of narrow vertical extent (~20m). A fine particulate layer is known to occur in the suboxic layer due to the upward diffusion and re-oxidation of Mn(II) and Fe(II), reinforced by horizontal advective transport from the shelf (Tankéré *et al.*, 2001).

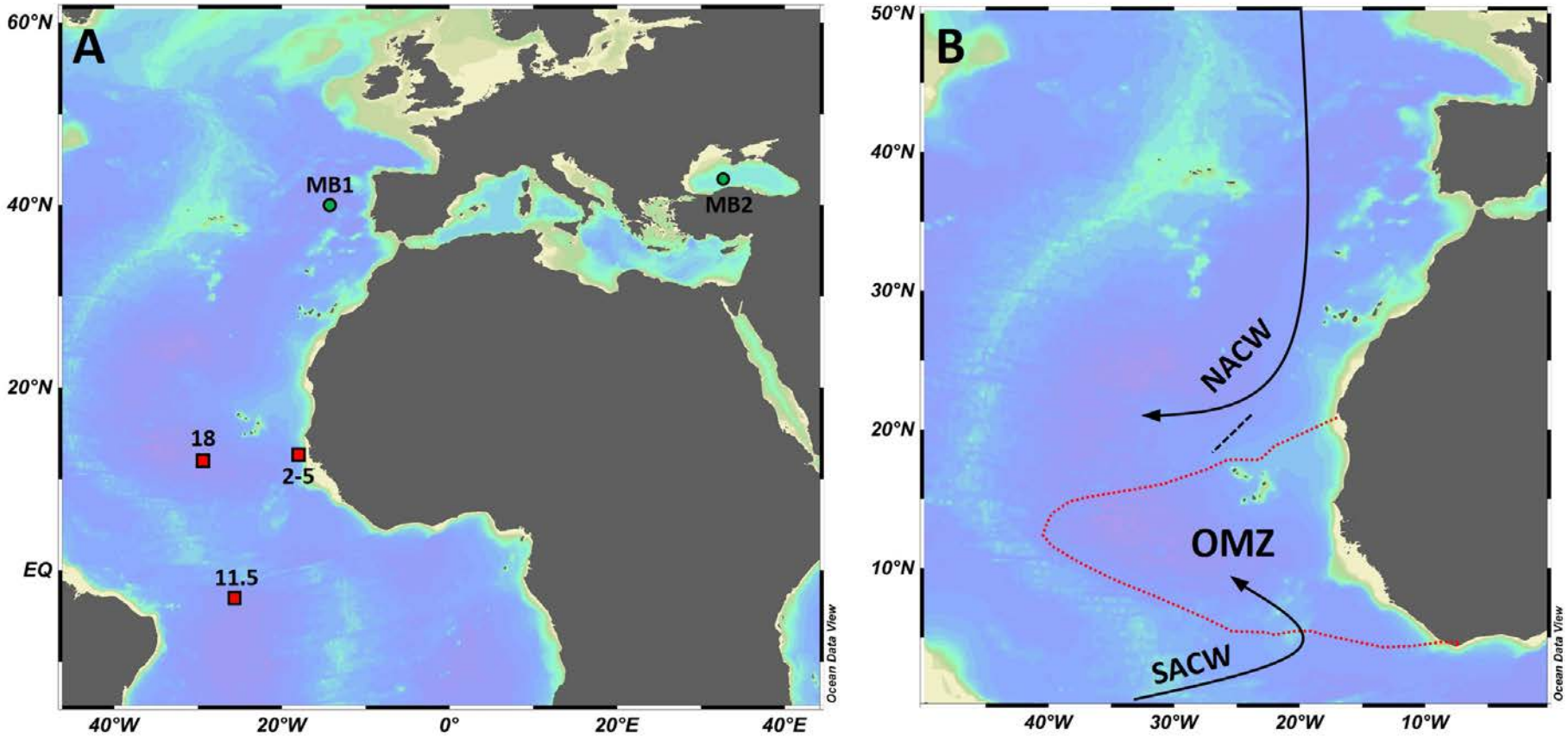

Figure 3.1 - (A) Locations of stations sampled in this study. Red markers are stations sampled as part of RRS *Discovery* cruise D361 stations (squares labelled 2-5, 11.5, 18) and green markers are stations samples as part of the GEOTRACES Medblack cruises (Labelled MB1 and MB2). (B) Schematic of generalised central water mass movement (100-500m water depth) in the North Atlantic OMZ region (Stramma *et al.*, 2008). Dashed black line is the Cape Verde Convergence Zone (Zenk *et al.*, 1991) and red dashed line marks the approximate outline of the OMZ region.

3.3 Methods

3.3.1 Sample collection

3.3.1.1 D361 (eastern Atlantic OMZs)

A trace metal clean CTD system equipped with modified Ocean Test Equipment Inc. (OTE) bottles was used to collect the water samples. The OTE bottles were transferred to a class 100 clean container aboard the RRS Discovery and seawater was filtered through pre-rinsed Supor Acropak filters (0.2µm) or acid cleaned polyethersulpone filters (0.45µm) into acid washed 1L bottles. Samples were acidified to pH 2 (Romil UpA HCl) and double bagged for storage at the National Oceanography Centre, Southampton (Klar, 2014).

3.3.1.2 Medblack (Black Sea and North Atlantic)

An ultra-clean CTD system was used to collect five ≥100L bulk seawater samples. Each sample was homogenised in a pre-rinsed container after filtration (through Sartorius Sartobran 300 capsule filters) inside a class 100 clean container. The bulk samples were acidified (Seastar Baseline grade HCl) and sub-sampled for Cr isotopes into acid-washed 1L bottles. The samples were double bagged for storage at the National Oceanography Centre, Southampton.

3.3.2 Analysis of Cr concentration and isotopic composition

The total Cr concentration (Cr_T, where Cr_T = Cr(VI) + Cr(III)) and Cr isotopic composition of seawater samples were determined by multi-collector inductively coupled plasma mass spectrometry (MC-ICP-MS) using a double spike technique based on that described by Bonnand *et al.* 2013. Processing of the samples was carried out in a class 100 clean laboratory. All acid reagents were sub-boiled while ammonia and hydrogen peroxide (H_2O_2) were Romil UpA and Fluka TraceSELECT grades respectively.

3.3.3 Preliminary determination of Cr_T

In order to optimise the ratio of natural Cr to double spike Cr for isotopic measurements, Cr_T of the seawater sample must be known. This was achieved using a single spike isotope dilution technique which followed a similar procedure to that described in **Chapter 2** but used a single ^{53}Cr spike and smaller sample volumes (~200mL). $^{52}Cr/^{53}Cr$ ratios were used to calculate seawater concentrations and these were measured using an Element 2 ICP-MS.

3.3.4 Preparation of seawater samples for Cr isotope analysis

As the Cr content of seawater is relatively low, it was necessary to pre-concentrate the Cr by co-precipitation with Fe using a modified version of the method described in Bonnand *et al.* 2013. Briefly, an appropriate amount of a ^{50}Cr-^{54}Cr double spike was first added to the seawater samples and left to equilibrate for ~24 hours. The samples were then adjusted to pH 8-9 to facilitate precipitation of Cr, then a freshly prepared suspended precipitate of Fe(II) hydroxide (made by the addition of ammonia to a fresh ammonium Fe(II) sulphate solution) was added (10ml L^{-1} of seawater). Under these conditions any Cr(VI) is reduced to Cr(III) by Fe(II) which is in turn oxidised to Fe(III), forming an Fe(III)-Cr(III) precipitate. Any Cr(III) remaining in solution is adsorbed onto this precipitate (Cranston and Murray, 1978; Crawford *et al.*, 1993). The precipitate was removed from seawater *via* vacuum filtration through Millipore Omnipore filters (1µm), which were pre-cleaned in 6M sub-boiled HCl at 95°C followed by Milli-Q water at 95°C (Scheiderich *et al.*, 2015). The precipitate was then leached from the filters using 6M HCl before being dried down and taken up in 7M HCl. The Cr was separated from the Fe *via* anion exchange chromatography (Biorad AG1-X8, 200-400 mesh size; Bonnand *et al.* 2013). Remaining cations were then removed by exchange chromatography in 0.5M HCl (Biorad AG50-X12, 200-400 mesh size; Bonnand *et al.* 2011). Finally, 30µmol H_2O_2 was added to the dried Cr samples and the solution was dried down once again in order to oxidise any remaining organic material. This step was found to prevent a loss of voltage encountered during MC-ICP-MS analysis of seawater, which is thought to be caused by the interaction of residual organic material with the sampling probe and/or the Aridus 2 nebuliser system.

3.3.5 MC-ICP-MS analysis

Cr isotopic compositions and concentrations were measured at the University of Southampton using a method similar to that described in Bonnand *et al.* 2011. Samples were introduced to a Thermo Fisher Neptune MC-ICP-MS using an Aridus 2 desolvating nebuliser system with argon (Ar) as the carrier gas. Nitrogen (N) was omitted to reduce the size of ArN^+ polyatomic interferences. The intensities of the four naturally occurring stable isotopes of Cr (^{50}Cr, ^{52}Cr, ^{53}Cr, ^{54}Cr) were measured in addition to ^{49}Ti, ^{51}V and ^{56}Fe in order to correct for isobaric interferences. Medium resolution settings and $10^{11}\Omega$ amplifiers were used and mass resolution ($M/\Delta M$) was maintained at 5800-6500. The signal intensity of

^{52}Cr for a 50ppb solution was ~6-7V. Each analytical session began with at least three spiked NBS979 standards, and then one spiked NBS979 standard after every three samples. Intensities of the blank solution (3% HNO_3) were measured before and after each sample or standard, and subtracted from the sample/standard data. A Newton-Raphson deconvolution calculation was performed to extract the sample $\delta^{53}Cr$ from that of the spiked sample (Albarède and Beard, 2004) and this was normalised against the session average NBS979 $\delta^{53}Cr$ value to account for instrumental drift.

3.4 Results

3.4.1 Method validation

The Cr blank for the Fe(II) co-precipitation method was 18 ± 0.9ng, the majority of which (~93%) was contributed by the ammonium Fe(II) sulphate salt (Sigma-Aldrich) used to generate the Fe(II) hydroxide precipitate. The isotopic composition of this salt varies slightly between batches, presumably due to an uneven distribution of isotopes within the crystals. For this reason, the Cr_T and $\delta^{53}Cr$ of the ammonium Fe(II) sulphate solution was regularly determined (respectively, 16nmol kg^{-1}, -0.34 ±0.32‰ 2SD, n=6) and appropriate corrections to the final data were applied to account for its contribution to Cr_T and $\delta^{53}Cr$ of the samples.

Despite the large quantities of Fe added to the samples during co-precipitation, efficient removal of Fe by anion exchange chromatography ensured that the $^{56}Fe/^{54}Cr$ of the samples was always between 0.01 and 0.50. Several Fe doped NBS979 standards were tested to confirm that accurate $\delta^{53}Cr$ values could be retrieved by the double spike procedure for $^{56}Fe/^{54}Cr$ ratios of between 0.02 and 0.50. These solutions produced an average $\delta^{53}Cr$ value of -0.01 ± 0.04‰ (2SD, n=35), within error of NBS979 standards containing no additional Fe (0.00 ± 0.04‰, n=477) indicating that $^{56}Fe/^{54}Cr$ ratios of up to 0.5 can be successfully tolerated.

In the absence of a seawater Cr isotope standard, several tests were carried out to evaluate the accuracy and precision of the method. First, a standard addition experiment was performed using a seawater sample from Southampton Water mixed with the NBS979 Cr standard. Southampton Water is ideal for this purpose as it has a high $\delta^{53}Cr$ value (Bonnand *et al.*, 2013), allowing a wide range of standard-seawater $\delta^{53}Cr$ values to be tested. The

relationship between measured $\delta^{53}Cr$ and the proportion of seawater present was linear, with a gradient (0.014) similar to that expected from mixing calculations (0.015; **Figure 3.2**). Furthermore a negligible offset from 0‰ for NBS979 is predicted by the y-intercept of the graph (+0.02‰). For a true $\delta^{53}Cr$ value of 2‰, this offset increases to 0.05‰. Nevertheless, this indicates that accurate $\delta^{53}Cr$ measurements are achievable for the entire range for seawater, which to date has spanned values of 0.13 - 1.55‰ (Bonnand *et al.*, 2013; Paulukat *et al.*, 2016; Scheiderich *et al.*, 2015).

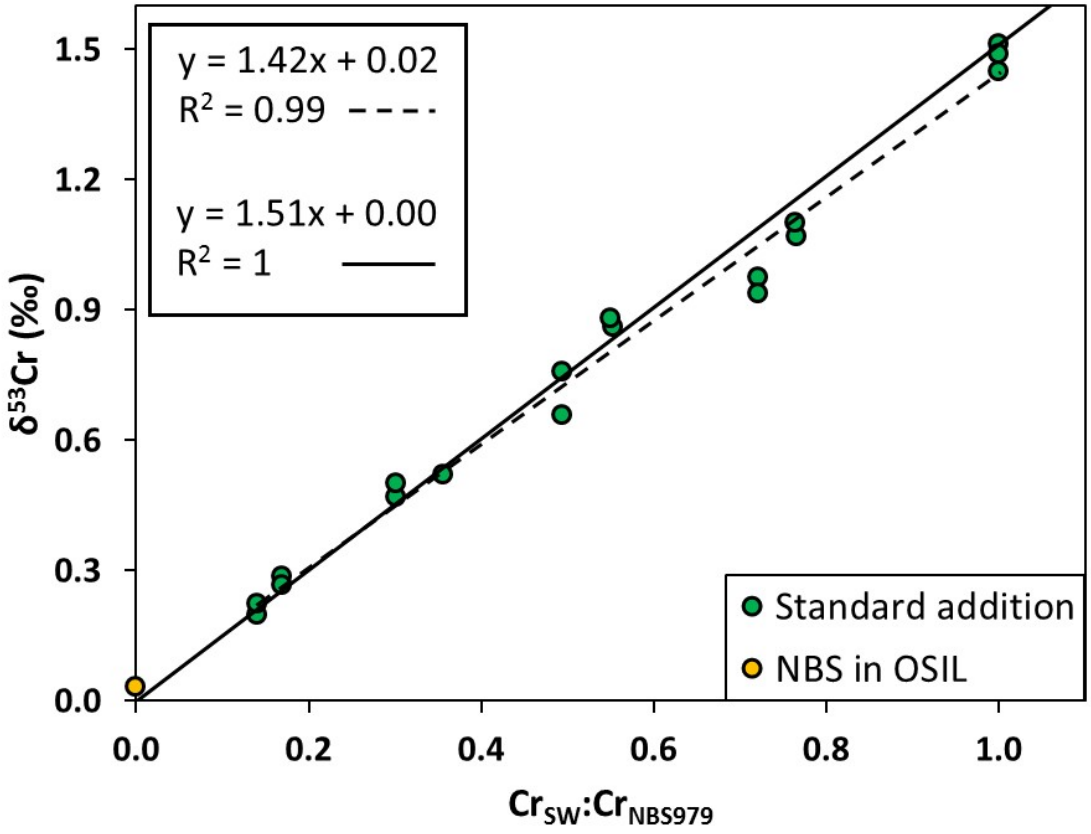

Figure 3.2 - $\delta^{53}Cr$ values of various seawater:standard mixtures (green circles). Seawater is from Southampton Water (SW) and the standard is NBS979. Solid black line indicates expected relationship and dashed line indicates the linear trend through measured values. Error bars are smaller than markers. Yellow circle shows Southampton Water doped with 10µg NBS979.

In order to confirm that the $\delta^{53}Cr$ composition of the NBS979 endmember could be replicated in a seawater matrix as predicted by the standard addition experiment, a 500mL sample of the OSIL salinity standard seawater was doped with a large amount of NBS979 (10µg) in order to render the original seawater isotopic signature negligible. The solution was split into 5 aliquots and these were processed separately. The average $\delta^{53}Cr$ of 0.03 ±

0.02‰ (2SD) was within error of the predicted value and this indicates that the NBS979 standard behaves in the same way as seawater Cr during processing. The concentration of this solution was also measured at 360.4 ± 0.1nmol kg^{-1} (2SD), which was within 0.4% of the expected value (359.1nmol kg^{-1}).

Finally, the Cr_T and $\delta^{53}Cr$ values that we measured for Southampton Water and the OSIL Atlantic Salinity Standard seawater (**Table 3.3**) were within error of previously published values with the exception of the Cr_T of Southampton Water. The sample used in this study was different from those used in a previous study (Bonnand *et al.*, 2013) and had a lower salinity (30 *versus* 34) that accounts for lower Cr_T. These validation experiments show that the Fe(II) co-precipitation method produces accurate results for seawater samples, with comparable precision to previously published seawater values.

Table 3.3 - Comparison of seawater $\delta^{53}Cr$ and Cr_T measurements from this study and others.

Sample	Reference	Cr_T (nmol kg^{-1})	2SD	$\delta^{53}Cr$ (‰)	2SD	n
OSIL Atlantic Salinity Standard	This work	3.10	0.04	0.97	0.10	6
	Scheiderich et al. 2015	3.02	0.06	0.96	0.06	8
Southampton Water	This work	1.31	0.06	1.48	0.06	3
	Bonnand et al. 2013	1.85	0.02	1.51	0.05	4

3.4.2 Cr_T and $\delta^{53}Cr$ in the eastern Atlantic Oxygen Minimum Zone

All CTD sensor data for cruise D361 was supplied by the British Oceanographic Data Centre, courtesy of the Natural Environment Research Council. The distribution of salinity along a section at 12°N that encompasses all of the shelf and shelf slope stations sampled on cruise D361 is shown in **Figure 3.3A**. The Guinea Dome circulation can be identified by the doming of isohalines in the surface waters around 22°W and the mixing of shelf and open ocean waters can be seen at 0-300m, 18-20°W. Profiles of salinity (**Figure 3.3B)** for stations 18 and 11.5 show sub-surface salinity peaks which originate from Tropical Surface Water and South Atlantic waters, respectively, and both peaks are overlain by low-salinity

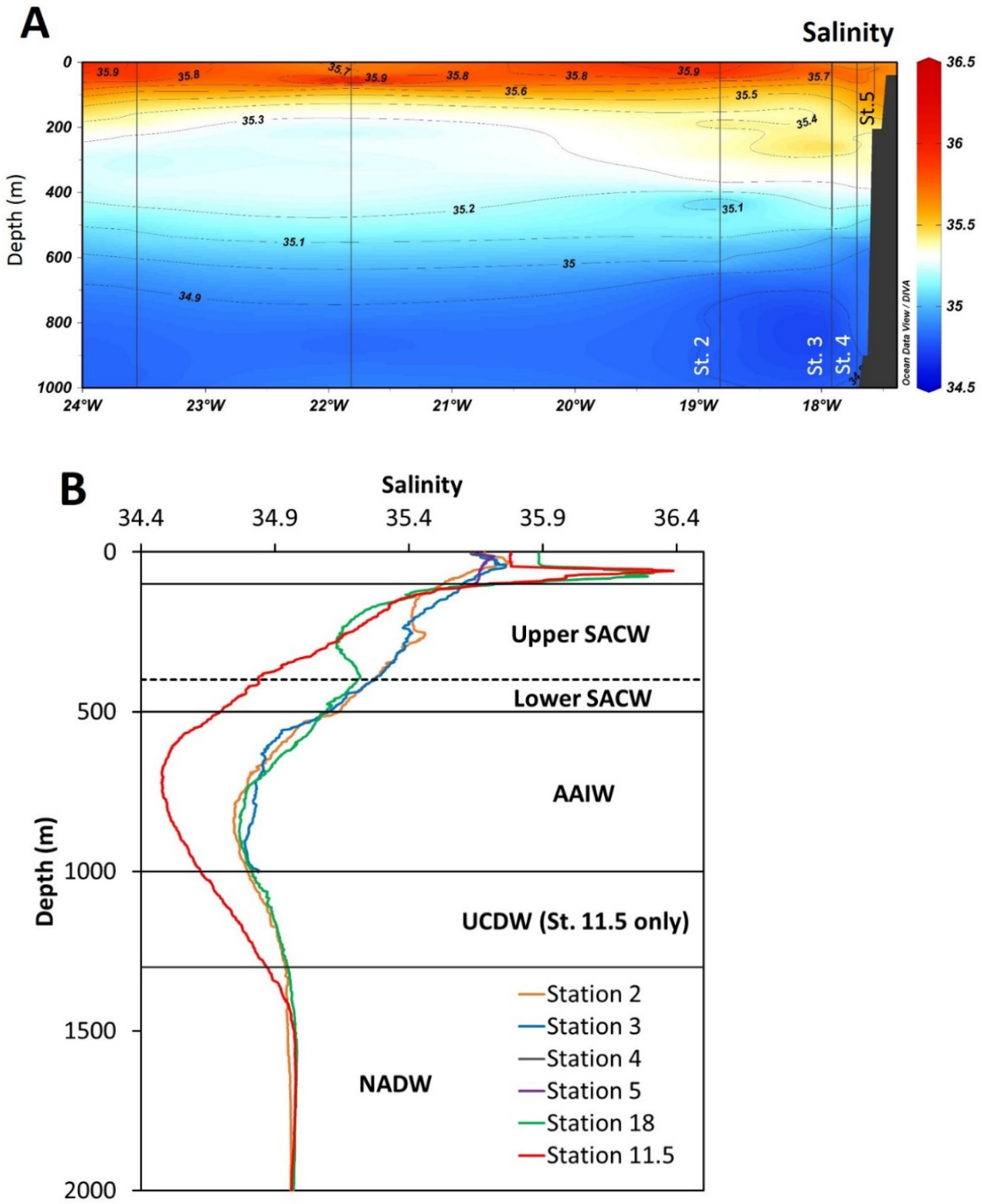

Figure 3.3 - (A) Salinity distribution in the upper 1000m of the water column along ~12°N in the eastern tropical Atlantic showing shelf influenced North-West African waters. Stations 2-5 are shown by the solid black vertical lines (left-right). (B) Salinity profiles between 0 and 2000m water depth for all D361 stations sampled in this study. Approximate locations of different water masses are shown by horizontal black lines. SACW = South Atlantic Central Water, AAIW = Antarctic Intermediate Water, UCDW = Upper Circumpolar Deep Water, NADW = North Atlantic Deep Water. Contains data supplied by the Natural Environment Research Council.

equatorial sourced waters which have experienced high levels of precipitation (Stramma *et al.*, 2005). The SACW has variable salinity whereas AAIW and NADW salinity is consistent across all stations except for 11.5, where the AAIW salinity minimum is more prominent because the water mass has travelled less far from its source and has experienced less mixing.

During cruise D361 the core of the OMZ was at ~450m for the shelf slope and off-shelf stations (**Figure 3.4**). The lowest O_2 concentrations (46-51µmol kg^{-1}) were found at stations 2, 3 and 18. Concentrations of O_2 within the OMZ were higher than those typically measured within the eastern tropical Pacific (~15µmol kg^{-1}) and northern Indian Ocean (~13-16 µmol kg^{-1}) OMZs (Paulmier and Ruiz-Pino, 2009). At shelf stations 4 and 5 the lowest O_2 concentrations (66-93µmol kg^{-1}) were found at the closest to the sea bed, as upwelling supplied waters which were already somewhat oxygen depleted and there was no ventilation from deeper water masses. At Station 11.5 the OMZ had a higher O_2 concentration of (90-100 µmol kg^{-1}) and there was a secondary, smaller O_2 minimum at 1000-1300m due to the presence of UCDW. Chlorophyll-a (Chl-a) concentrations of up to 2.1mg m^{-3} were recorded on the shelf slope where upwelling actually occurs, and concentrations of up to 1.5 mg m^{-3} were also observed on the shelf itself. Away from the upwelling area Chl-a concentrations were ≤0.5mg m^{-3} (**Figure 3.4**).

Profiles of Cr_T and $\delta^{53}Cr$ are presented in **Figures 3.5** and **3.6**. Seawater $\delta^{53}Cr$ values ranged from 1.08 to 1.72‰, at the upper end of the range measured for seawater to date (0.13 – 1.55‰; e.g. Bonnand *et al.* 2013; Paulukat *et al.* 2015; Scheiderich *et al.* 2015). Cr_T showed only limited variation, ranging from 2.1 to 2.9nmol kg^{-1}, which is within the range previously measured for seawater (0.9-6.5nmol kg^{-1}; (e.g. Achterberg and Berg 1997; Bonnand *et al.* 2013; Campbell and Yeats 1981; Connelly *et al.* 2006; Cranston 1983; Jeandel and Minster 1984; Sirinawin *et al.* 2000). Relatively high $\delta^{53}Cr$ values were present at all depths at shelf stations 4 and 5 (1.21-1.62‰), and on average Cr_T was 15% lower on the shelf compared to shelf slope and open ocean stations. At shelf slope stations 2 and 3, intermediate $\delta^{53}Cr$ and Cr_T values were found in the top 300m compared to shelf and open ocean stations. This represents mixing of open ocean and shelf Cr as high salinity shelf waters mixed with deeper, lower salinity waters at 18-20°W (**Figure 3.3A**). Within the OMZ at 400-500m water depth, $\delta^{53}Cr$ values at stations 2 and 3 were very different. Station 2 had a distinct $\delta^{53}Cr$

maximum (1.71‰) that coincided with a small increase in Cr_T, but little change in $\delta^{53}Cr$ or Cr_T was observed within the OMZ relative to the enveloping waters at station 3 despite similar O_2 concentrations within the OMZ. At open ocean stations 11.5 and 18, the $\delta^{53}Cr$ range was quite narrow throughout the water column (1.08 to 1.26‰) with the exception of one sample from within UCDW at station 11.5 which had notably higher $\delta^{53}Cr$ (1.72‰). The concentrations of Cr_T at the open ocean stations occupied the higher end of the range for this study (2.5-2.9nmol kg^{-1}).

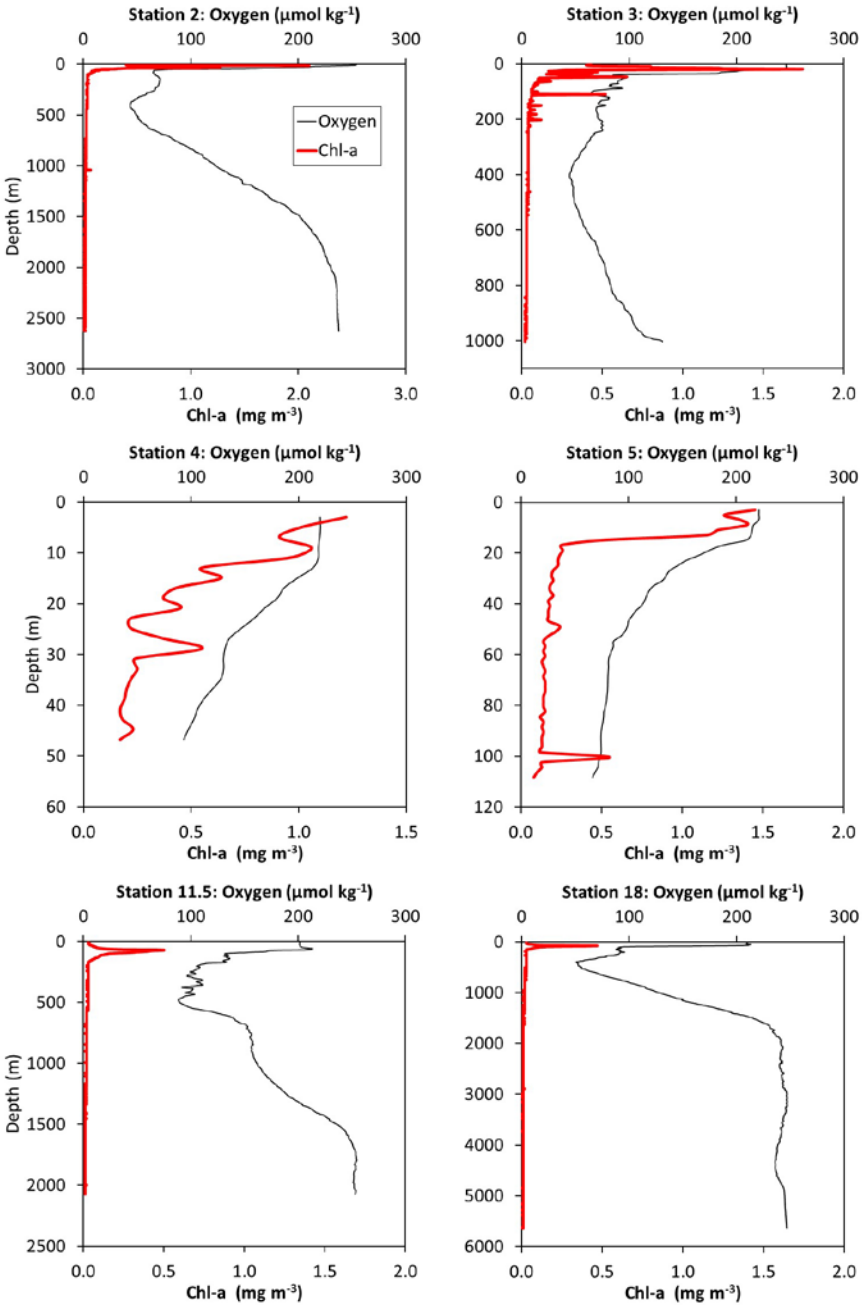

Figure 3.4 - Profiles of O_2 concentrations and Chl-a for all stations sampled on D361. Contains data supplied by the Natural Environment Research Council.

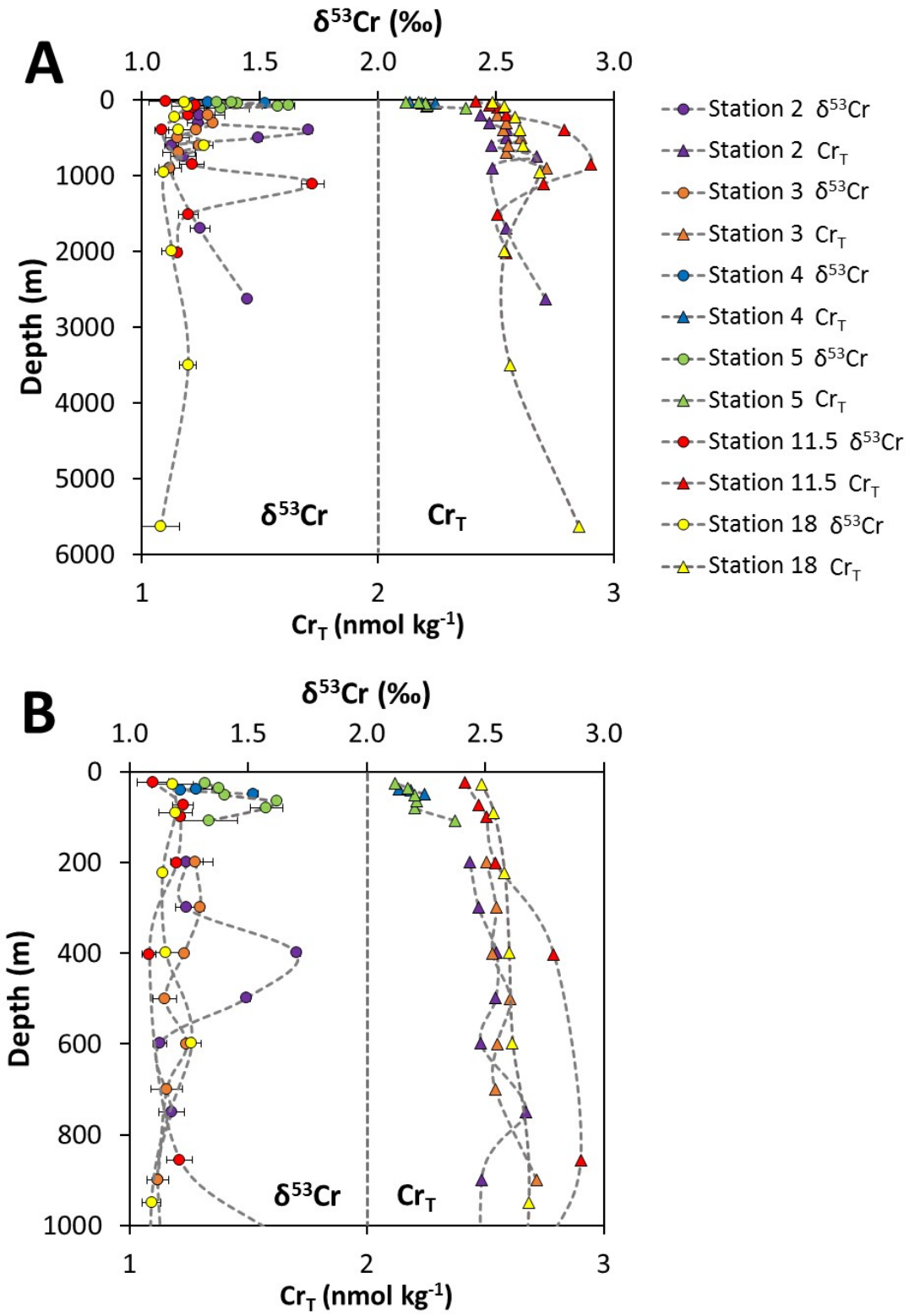

Figure 3.5 - (A) Profiles of $\delta^{53}Cr$ and Cr_T for all stations sampled on D361 (B) $\delta^{53}Cr$ and Cr_T in the top 1000m water depth.

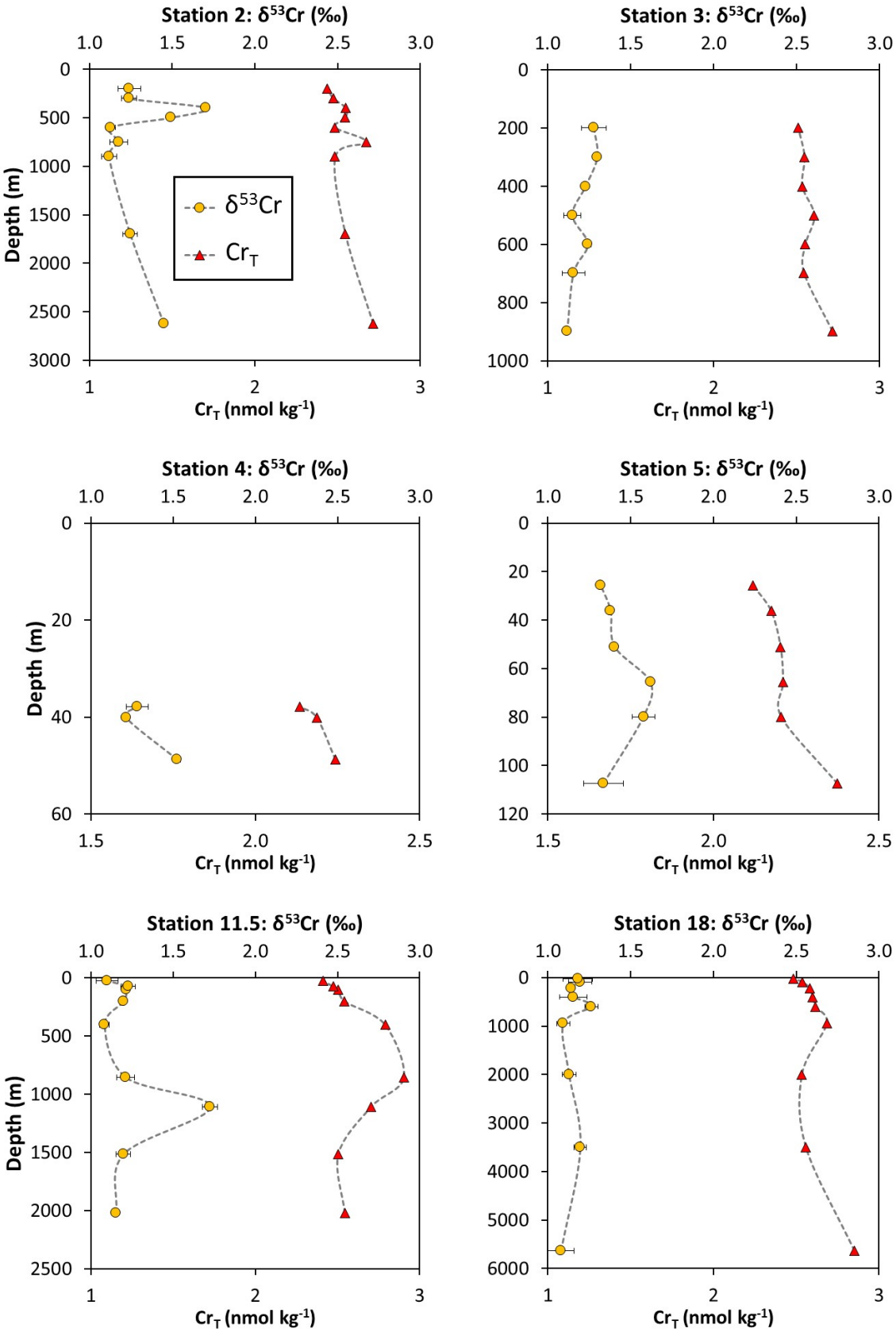

Figure 3.6 - Individual $\delta^{53}Cr$ and Cr_T profiles for D361 stations. Note different scales for depth and Cr_T.

Table 3.4 - Chromium data for all samples measured in this study. 2SD for δ53Cr is calculated from two MC-ICP-MS measurements. Contains data supplied by the Natural Environment Research Council and the GEOTRACES project.

Station	Depth (m)	O_2 (µmol kg^{-1})	O_2 classification	Cr_T (nmol kg^{-1})	$\delta^{53}Cr$ (‰)	2SD	Water mass
North Atlantic (Medblack)	25	210	Oxic	2.31	1.16	0.03	SML
	1500	245	Oxic	2.48	1.14	0.03	AAIW+MOW
Black Sea	30	328	Oxic	1.02	1.69	0.05	
	100	0	Suboxic	0.88	1.42	0.03	
	150	0 (+20µmol kg^{-1} H_2S)	Anoxic	1.67	1.32	0.01	
D361 St. 2	200	70	Dysoxic	2.44	1.24	0.07	SACW
	300	58	Dysoxic	2.48	1.24	0.04	SACW
	400	44	Dysoxic	2.54	1.71	0.02	SACW
	500	50	Dysoxic	2.54	1.49	0.02	SACW
	600	57	Dysoxic	2.48	1.13	0.03	AAIW
	750	85	Dysoxic	2.67	1.18	0.05	AAIW
	900	111	Oxic	2.48	1.12	0.05	AAIW
	1700	216	Oxic	2.54	1.25	0.04	NADW
	2625	237	Oxic	2.71	1.45	0.00	NADW
D361 St.3	200	72	Dysoxic	2.50	1.28	0.07	SACW
	300	59	Dysoxic	2.54	1.30	0.01	SACW
	400	45	Dysoxic	2.54	1.23	0.01	SACW
	500	49	Dysoxic	2.62	1.15	0.05	SACW
	600	60	Dysoxic	2.56	1.24	0.02	AAIW
	700	73	Dysoxic	2.54	1.16	0.07	AAIW
	900	98	Dysoxic	2.71	1.12	0.01	AAIW
D361 St. 4	38	128	Oxic	2.13	1.28	0.00	SML
	40	112	Oxic	2.19	1.21	0.07	SML
	49	93	Oxic	2.25	1.52	0.12	SML
D361 St. 5	26	146	Oxic	2.12	1.32	0.07	SML
	36	117	Oxic	2.17	1.38	0.03	SML
	51	97	Oxic	2.21	1.40	0.09	SML
	66	82	Dysoxic	2.21	1.62	0.07	SML
	80	80	Dysoxic	2.21	1.58	0.01	SML
	107	69	Dysoxic	2.37	1.34	0.02	SML
D361 St. 18	30	210	Oxic	2.48	1.18	0.09	SML
	90	119	Oxic	2.54	1.19	0.07	SML
	225	91	Dysoxic	2.58	1.14	0.00	SACW
	400	51	Dysoxic	2.60	1.15	0.08	SACW
	600	68	Dysoxic	2.62	1.26	0.04	AAIW
	960	121	Oxic	2.69	1.09	0.04	AAIW
	2020	241	Oxic	2.54	1.13	0.04	NADW
	3550	243	Oxic	2.56	1.20	0.04	NADW
	5740	246	Oxic	2.85	1.08	0.08	NADW
D361 St. 11.5	25	202	Oxic	2.40	1.10	0.07	SML
	75	177	Oxic	2.48	1.23	0.07	SML
	100	132	Oxic	2.50	1.22	0.02	SML
	200	107	Oxic	2.54	1.20	0.02	SACW
	400	101	Oxic	2.79	1.08	0.01	SACW
	855	158	Oxic	2.90	1.21	0.02	AAIW
	1110	170	Oxic	2.71	1.72	0.05	UCDW
	1515	236	Oxic	2.50	1.20	0.09	NADW
	2020	252	Oxic	2.54	1.15	0.02	NADW

3.4.3 Black Sea and adjacent North Atlantic Ocean

All CTD sensor and H_2S data in this section is from the GEOTRACES project (supplied by the British Oceanographic Data Centre and funded by NERC). The Black Sea oxic zone extended to 90m at station MB2 (**Figure 3.7**). Suboxic conditions prevailed between 90-100m and hydrogen sulphide was present below 100m, marking the start of the anoxic zone. The transition between the oxic and anoxic zones is characterised by a marked increase in attenuance (an indicator for particle concentrations; **Figure 3.7**) that is likely due to precipitation of Fe- and Mn- oxyhydroxides (Tankéré *et al.*, 2001). $\delta^{53}Cr$ values and Cr_T for the Medblack samples can be found in **Table 3.4**. The North Atlantic (MB1) samples have $\delta^{53}Cr$ values similar to other Atlantic waters (1.14-1.16‰; see **Section 3.4.2**) and their Cr_T values (2.31-2.48nmol kg^{-1}) fall within the range measured previously for nearby North Atlantic surface waters (1.9-2.6nM; Achterberg and Berg 1997). Cr_T values in the Black Sea were significantly lower (0.88-1.67nmol kg^{-1}), with a minimum in the suboxic zone. $\delta^{53}Cr$ values were higher (1.32-1.69‰) than in the adjacent North Atlantic waters, with the highest value occurring in oxic surface water (1.69‰).

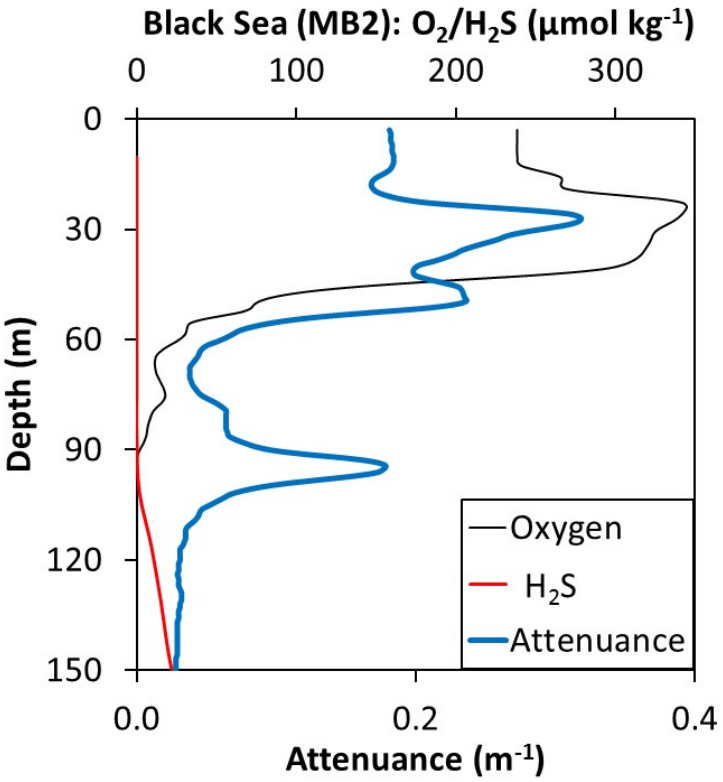

Figure 3.7 - O_2 concentrations and attenuance at the Black Sea sampling station MB2 in the top 150m water depth. Contains data supplied by the Natural Environment Research Council and the GEOTRACES project.

3.5 Discussion

3.5.1 Behaviour of Cr isotopes in the eastern Atlantic Oxygen Minimum Zone

In keeping with other studies, all of the seawater samples from the eastern Atlantic Ocean had positive $\delta^{53}Cr$ values that are consistent with the preferential release of ^{53}Cr during oxidative weathering and/or preferential ^{52}Cr reduction of Cr(VI) to Cr(III) in seawater (e.g. Frei *et al.* 2014; Scheiderich *et al.* 2015). Concentrations of Cr_T were relatively low and ranged from 2.12-2.90nmol kg^{-1} whereas the range of $\delta^{53}Cr$ values was relatively large (1.08-1.72‰; **Figure 3.8**; **Table 3.4**).

All of the shelf slope and open ocean stations sampled in this study were located within the eastern Atlantic OMZ. As a result, the dissolved O_2 concentration of the waters was highly variable, ranging from 45 to 250nmol kg^{-1}. Critically however, the low O_2 waters did not have Cr_T or $\delta^{53}Cr$ values that were distinctly different from the waters outside the OMZ (**Figure 3.9B**). This suggests either that reduction of Cr(VI) to Cr(III) is insignificant in the eastern Atlantic OMZ, or that reduction of Cr(VI) to Cr(III) could occur but particle concentrations within the OMZ are low, preventing the Cr(III) that forms from being segregated from the residual Cr(VI). The average nitrite concentration was negligible at all shelf slope and open ocean stations within the OMZ (0.01µmol L^{-1}), indicating that nitrate reduction did not occur there; thus it is unlikely that Cr(VI) was reduced either given the similar standard reduction potentials for NO_3^- and CrO_4^{2-} ($CrO_4^{2-}/Cr(OH)_3$ = -0.12V, NO_3^-/NO_2^- = 0.01V; Bratsch 1989, Fanning 2000). Nonetheless, a range of $\delta^{53}Cr$ values was observed (between 1.08 and 1.72‰) and the reasons for this will be discussed below.

3.5.2 Enhanced Cr removal in shelf waters

Concentrations of Cr_T were slightly lower on the shelf (2.21 ± 0.07nmol kg^{-1}) than in open ocean waters at the same water depth (between 0 and 160m, 2.48 ± 0.07nmol kg^{-1}). The shelf waters also had higher $\delta^{53}Cr$ values (1.41 ± 0.14nmol kg^{-1} compared to 1.18 ± 0.05nmol kg^{-1} for open ocean waters shallower than 160m). This is consistent with partial reduction of Cr(VI) to Cr(III), with subsequent removal of the ^{52}Cr enriched Cr(III) onto particle surfaces (e.g. Døssing *et al.* 2011; Kitchen *et al.* 2012; Paulukat *et al.* 2016; Scheiderich *et al.* 2015; Sikora *et al.* 2008) in shelf waters.

However, there was no significant relationship between dissolved O_2 and $\delta^{53}Cr$ in shelf water. It seems more likely that reduction of Cr(VI) and removal of Cr(III) is accomplished through photochemical or biological processes. Light transmittance is low on the shelf and is generally inversely proportional to Chl-a concentrations, indicating there is a high abundance of biogenic particles on the shelf. Phytoplankton have been shown to reduce Cr(VI) to Cr(III) and particulate organic matter is known to sequester Cr (Connelly *et al.*, 2006; Dauby *et al.*, 1994; Semeniuk *et al.*, 2016), thus reduction and/or adsorption of Cr to biogenic particles may be more prevalent in shelf waters than in the open ocean. In support of this, there is a negative correlation between transmittance and $\delta^{53}Cr$ when comparing shelf, shelf slope and open ocean stations (R^2 = 0.5, **Figure 3.9A**), i.e. $\delta^{53}Cr$ increases with particle concentrations. Photochemical reactions also produce H_2O_2 and Fe(II) in surface waters which can also reduce Cr(VI) to Cr(III) (Li *et al.*, 2009; Pettine and Millero, 1990), and Cr(III) produced in this way may also subsequently adsorb to biogenic particles (Semeniuk *et al.*, 2016).

Oxidation *via* Mn oxides or oxygen are likely to be suppressed in dysoxic waters (Schroeder and Lee, 1975; Sunda and Huntsman, 1994), and rapid sequestration of Cr(III) onto biogenic particles means that the Cr(III) and Cr(VI) pools become segregated, with enrichment of ^{53}Cr in Cr(VI) in the dissolved phase. Arctic shelf waters and coastal waters of the UK (Southampton Water) and Oregon display similarly high $\delta^{53}Cr$ and low Cr_T values (Bonnand *et al.*, 2013; Scheiderich *et al.*, 2015), which may imply that removal of Cr(III) onto particles is important in other shelf seas, even without low O_2 conditions.

3.5.3 Intermediate and deep water masses

The $\delta^{53}Cr$ values of intermediate and deep water masses in the eastern Atlantic shelf slope and open ocean stations are relatively consistent compared to surface and central waters (shallower than ~1000m). AAIW has slightly higher Cr_T compared to central and deep water masses, with Cr_T values ranging from 2.48-2.71nmol kg^{-1} and $\delta^{53}Cr$ = 1.16 ± 0.06‰ (1SD, n=8) at Stations 2, 3 and 18 (at ~12°N). Cr_T and $\delta^{53}Cr$ values for AAIW are higher at station1 1.5 (2.90nmol kg^{-1}, 1.21‰ respectively) which probably reflects a 'purer' AAIW signal as the water mass is less attenuated at this site. Average $\delta^{53}Cr$ and Cr_T values for NADW (sampled at stations 2, 18 and 11.5, n=7) are also consistent (2.61 ± 0.13nmol kg^{-1}, 1.21 ±

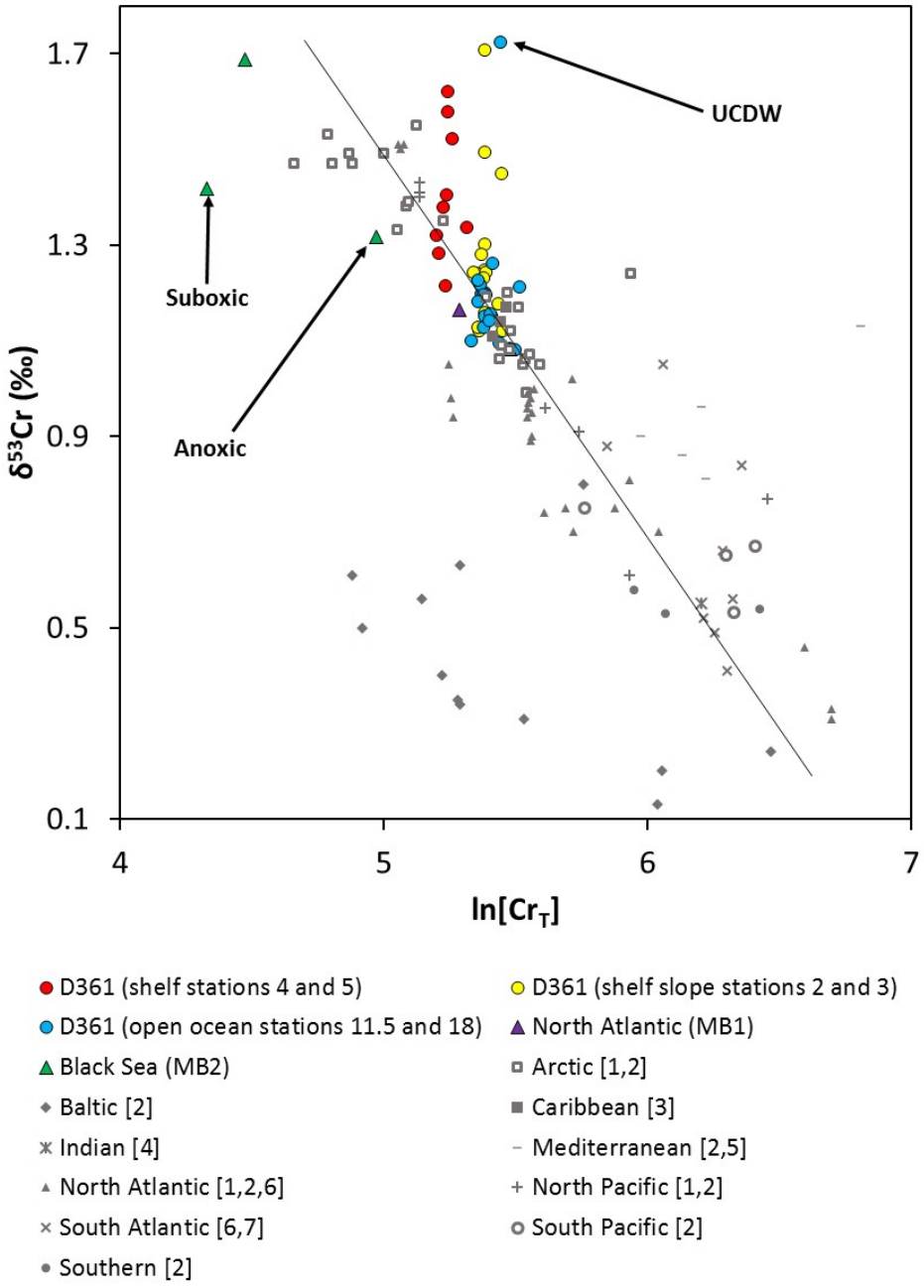

Figure 3.8 - Correlation between $\delta^{53}Cr$ and $lnCr_T$, with our data alongside the global trend line reported by Scheiderich et al. 2015. References are as follows: [1] Scheiderich *et al.* 2015, [2] Paulukat *et al.* 2016, [3] Holmden 2013, [4] Paulukat *et al.* 2015, [5] Economou-Eliopoulos *et al.* 2016, [6] Bonnand *et al.* 2013, [7] Pereira *et al.* 2015.

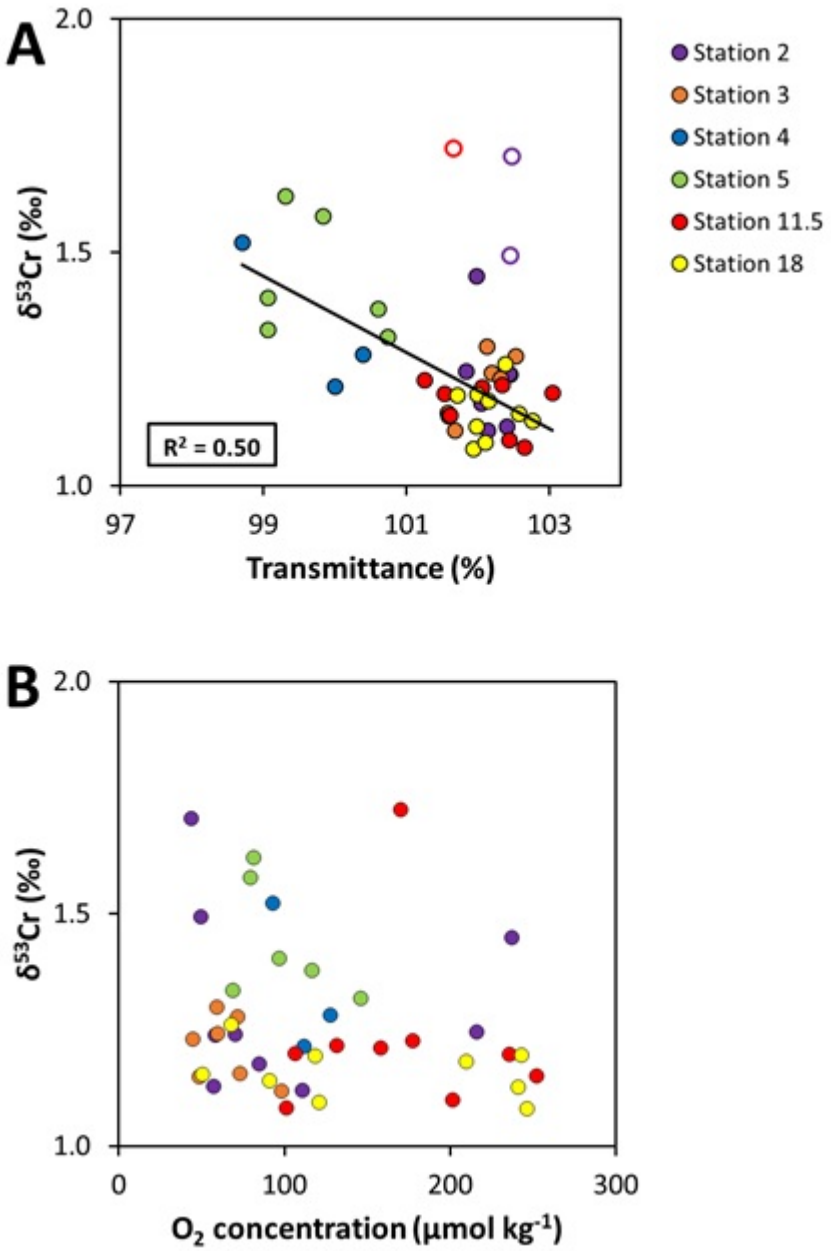

Figure 3.9 - (A) Plot showing $\delta^{53}Cr$ as a function of transmittance – open circles are data points that have been excluded from the trendline because their $\delta^{53}Cr$ values are influenced by inputs from water masses with high $\delta^{53}Cr$ (see Section 3.5.6). (B) Plot showing $\delta^{53}Cr$ as a function of dissolved O_2 concentration. Legend in (A) applies to both plots. Contains data supplied by the Natural Environment Research Council.

0.12‰, 1SD). The deepest samples taken from stations 2 and 18 have slightly higher Cr_T than the other NADW samples that may reflect mixing with ABW (Station 18) and/or input of benthic sedimentary Cr (both stations). These AAIW and NADW $\delta^{53}Cr$ values are higher than those measured for the same water masses in the Argentine Basin (0.56‰ and 0.44‰ respectively) in the western South Atlantic Ocean (Bonnand *et al.*, 2013). The low $\delta^{53}Cr$ values measured in the Argentine Basin may be due to low $\delta^{53}Cr$ inputs from the rivers of the South American continent (Frei *et al.*, 2014) such as the Parana River (average 0.38‰), but whether these inputs are capable of modifying deep water mass $\delta^{53}Cr$ is unclear. Our results are more comparable with other intermediate and deep Atlantic water masses (1.15‰ for Atlantic Water and 1.06‰ for Canada Basin Deep Water; Scheiderich *et al.* 2015). Based on current knowledge it therefore appears that a range of 1.0-1.2‰ is typical for intermediate and deep water masses in the North Atlantic Ocean.

3.5.4 Input of Cr from benthic sedimentary sources

Shelf sediments are an important source of dissolved iron to some parts of the ocean (e.g. Elrod *et al.* 2008; Severmann *et al.* 2010; Siedlecki *et al.* 2012) and shelf waters sampled for D361 have high concentrations of dissolved Fe that may be transported some considerable distance (~950km) off the shelf and into the open ocean within the OMZ (Klar, 2014). Iron isotope analyses indicate that this iron is principally derived from sediment pore waters that have undergone dissimilatory iron reduction (Klar, 2014), which raises the possibility that any Cr adsorbed to Fe oxyhydroxide phases is released as insoluble Fe(III) is reduced to soluble Fe(II). In support of this, analyses of Cr concentrations in pore waters of the California Margin reveal that Cr may be mobilised from sediments at the oxic/suboxic front in marine sediments; if this front lies close to the sediment-seawater interface then Cr may be released into seawater (Shaw *et al.*, 1990). While the highest Cr_T values are found in waters with the highest dissolved Fe, the increase in Cr_T is quite small and, in the context of the wider eastern Atlantic, Cr_T concentrations on the shelf are in fact lower than they are in surface waters off the shelf. However, the sample collected from 107m water depth at station 5 (seabed depth 164m) has notably higher dissolved Fe (6.4nM; Klar 2014) and Cr_T (2.37nmol kg^{-1}), and slightly lower $\delta^{53}Cr$ than the overlying waters. This is consistent with the re-release of low $\delta^{53}Cr$ Cr(III) from biogenic particles during organic matter remineralisation.

Nevertheless, unlike Fe, there is no obvious change in Cr_T within the OMZ which suggests that any shelf sedimentary source of Cr does not persist in the water column and is not transported offshore. Small increases in Cr_T are observed close to the seafloor at stations 2 and 18. The $\delta^{53}Cr$ values at station 18 are not significantly higher or lower than that of NADW, however at station 2 the $\delta^{53}Cr$ value is higher than other NADW $\delta^{53}Cr$ values which may indicate a high $\delta^{53}Cr$ benthic input at this station. It is clear that detailed studies of Cr in sedimentary pore water and seawater within the benthic boundary layer are required to fully assess the importance of benthic sediments as sources (or indeed sinks) of Cr both on and off the shelf.

3.5.5 Elevated $\delta^{53}Cr$ values

Two of our seawater samples had notably higher $\delta^{53}Cr$ values (1.7‰). One of these was collected from ~400m water depth within the OMZ at station 2, while the other was collected from within UCDW at ~1100m water depth.

Although the sample from ~400m at station 2 was taken from within the OMZ, it was characterised by notably lower dissolved Fe (**Figure 3.10**). This is inconsistent with advection of high $\delta^{53}Cr$ and high Fe waters from the shelf (see **Section 3.5.2**), but may be consistent with reduction of Cr(VI) to Cr(III) in the presence of Fe(II), and removal of the Fe(III) and Cr(III) that form. However there is no evidence for removal of Cr(III) as there is little obvious change in Cr_T.

One other potential explanation is the injection of higher salinity surface waters at this depth at station 2 (**Figure 3A**). These surface waters have low dissolved Fe concentrations and must have distinctively high $\delta^{53}Cr$; slightly higher than we observed for shelf waters at stations 4 and 5. This is consistent with the highly variable salinity of upper SACW (**Figure 3.3B**).

The sample from ~1100m water depth at station 11.5 has a similarly high $\delta^{53}Cr$ value (1.72‰). Crucially, this sample is the only one that is located within UCDW. This strongly suggests that the high $\delta^{53}Cr$ value is not the result of in situ Cr cycling but rather it is a

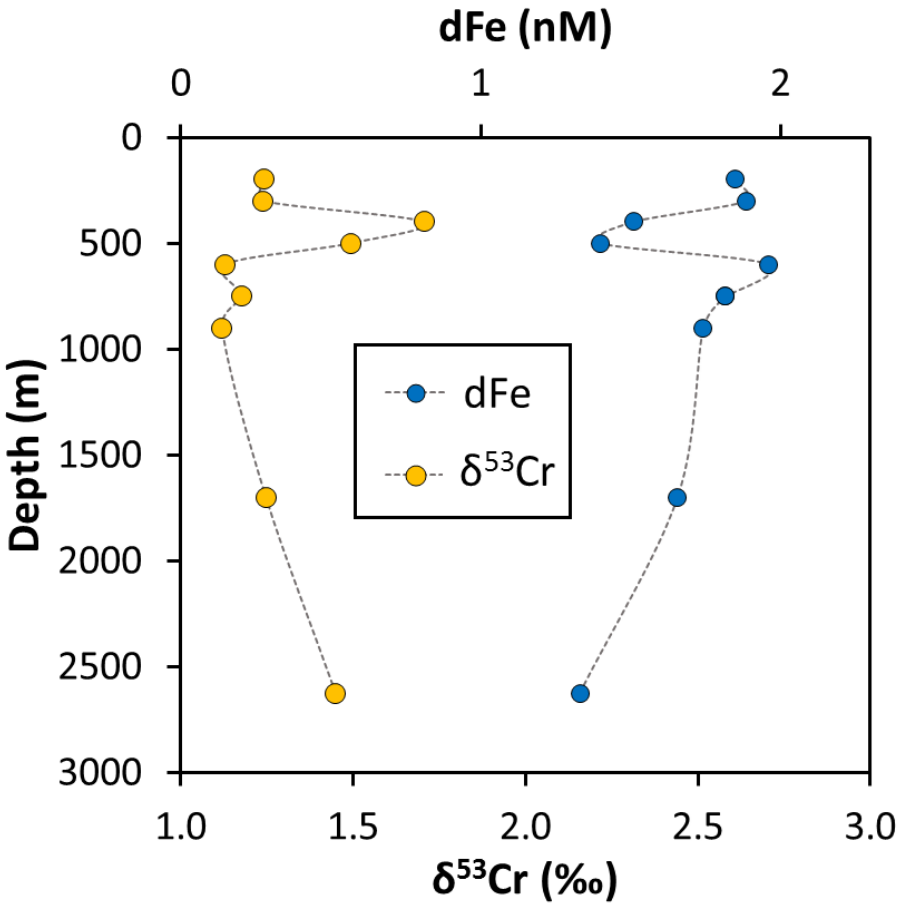

Figure 3.10 - $\delta^{53}Cr$ and dFe profiles for Station 2 (Fe data from Klar 2014).

pre-formed signature that was acquired elsewhere as the water mass formed, and was preserved to some extent during transport.

3.5.6 Behaviour of Cr isotopes in the Black Sea

It has been postulated that high $\delta^{53}Cr$ values created by oxidative weathering should be transferred to marine sediments if reduction of Cr(VI) to Cr(III) is quantitative (e.g. Frei *et al.* 2009). The Black Sea is a modern analogy for such a setting, but concentrations of Cr_T were actually higher (1.67nmol kg^{-1}) in the anoxic layer than they were in the oxic surface layer (1.02nmol kg^{-1}) and quantitative removal was not observed.

The $\delta^{53}Cr$ value (1.69‰) of the oxic surface water was higher than that of adjacent North Atlantic waters (1.16‰) and Cr_T was also lower (1.67nmol kg^{-1} compared to 2.31nmol kg^{-1} in the North Atlantic). This may partly reflect a contribution of freshwater (from rivers) to the surface layer; nearshore waters such as Southampton Water (see **Section 3.4.1** and

Bonnand *et al.* 2013) and the Glenariff estuary (D'Arcy *et al.*, 2016) also have relatively high $\delta^{53}Cr$ and low Cr_T that have been attributed to the preferential removal of ^{52}Cr *via* back-reduction of Cr(VI) in the estuarine environment (Bonnand *et al.*, 2013; D'Arcy *et al.*, 2016). Moreover, the oxic layer of the Black Sea is characterised by high levels of suspended particulate material that is known to be enriched in Cr (Yiğiterhan *et al.*, 2011). This strongly suggests that *in situ* removal processes are important, and, in support of this we note that light attenuance is high at 30m water depth (the depth at which the oxic sample was taken; **Figure 3.7**).

Reduced levels of Cr_T appear to be a distinctive feature of suboxic waters; concentrations of Cr were notably lower at the suboxic interface (~1nmol kg^{-1}) in the Saanich Inlet than they were above it (~1.5nmol kg^{-1}; Emerson *et al.* 1979), and were also lower in the suboxic waters in the North Pacific OMZ than they were in the overlying oxic waters (Rue *et al.*, 1997). Our sample from 100m water depth was taken from within the fine particulate layer that forms as a result of re-oxidation of Mn and Fe, which may variably affect Cr as it is expected to be in its Cr(III) form under suboxic conditions but can also be rapidly oxidised in the presence of Mn oxides (Oze *et al.*, 2007; Schroeder and Lee, 1975). The lower Cr_T of the sample demonstrates that reduction followed by removal *via* adsorption to particles must be occurring, but it is clearly not quantitative. Crucially, the $\delta^{53}Cr$ value of this sample is actually lower than that of the overlying waters (by 0.27‰). This suggests that $\delta^{53}Cr$ is influenced by (i) input of ^{52}Cr enriched Cr(III) from the dissolution of Fe and Mn oxides (either within the suboxic layer or *via* diffusion from the lower anoxic layer), and/or (ii) isotopic exchange between dissolved Cr(III) with a relatively high $\delta^{53}Cr$ value and adsorbed Cr(III) with a relatively low $\delta^{53}Cr$ value, in a similar manner to that observed for Cr(VI) isotopic exchange (Ellis *et al.*, 2004).

Anoxic waters are characterised by higher Cr_T, presumably because particulate Mn and Fe oxides are reduced and dissolved, releasing Cr(III) back into the water column as observed for a number of other trace metals (Lewis and Landing, 1991; Tankéré *et al.*, 2001). As discussed above, this Cr is expected to have low $\delta^{53}Cr$ imparted by reduction reactions occurring in the suboxic and oxic layers, and in support of this the anoxic waters have lower $\delta^{53}Cr$ than the overlying suboxic and oxic layers. Quantitative removal of Cr was not observed despite very high concentrations of dissolved Fe (~300nmol kg^{-1}; Rolison 2016)

which is known to remove Cr(VI) from solution in its Fe(II) form (e.g. Døssing *et al.* 2011; Kitchen *et al.* 2012). However Cr is expected to be present in the Cr(III) form within the suboxic layer and this species does not undergo a redox reaction with Fe(II), which may explain why quantitative removal of Cr did not occur.

3.5.7 Controls on $\delta^{53}Cr$

This work, together with other studies (Bonnand *et al.*, 2013; D'Arcy *et al.*, 2016; Scheiderich *et al.*, 2015) shows that coastal and shelf waters appear to be characterised by higher $\delta^{53}Cr$ (1.2-1.5‰) compared to deeper open ocean waters (typically 0.4-1.2‰). This may be, in part, due to oxidation and back-reduction of Cr in estuaries, but as $\delta^{53}Cr$ values measured in most estuaries to date (see **Chapter 1, Table 1.2**) have lower $\delta^{53}Cr$ values (0.08 – 1.02‰; D'Arcy *et al.* 2016; Frei *et al.* 2014; Paulukat *et al.* 2015), this suggests that further fractionation occurs in the shelf waters themselves. The most plausible process for increased $\delta^{53}Cr$ in surface waters is reduction of Cr(VI), but we find no evidence that this is controlled by biological processes. In particular samples from within the Chl-a maxima at stations 18 and 11.5 do not show any particular isotopic response even though Cr_T is slightly depleted in the surface layers of both stations, in line with the classification of Cr as a recycled element.

In contrast, we suggest that particles play a critical role in defining $\delta^{53}Cr$ at the local scale. The highest $\delta^{53}Cr$ values (>1.2‰) were observed in seawater that contained high particle concentrations in both the Atlantic Ocean and the Black Sea. Particles support the creation of high $\delta^{53}Cr$ signals by providing a surface onto which Cr(III) created by reduction reactions can be removed. Without removal of Cr(III) that has low $\delta^{53}Cr$ there will be no change in the $\delta^{53}Cr$ value of the (total) dissolved fraction. Without separate analyses of the Cr concentration and $\delta^{53}Cr$ values of Cr(III) and Cr(VI) pools, it is not possible to gauge whether Cr(VI) reduction processes are also enhanced on the shelf, or whether the Cr pools are simply better separated by particles.

Importantly, we have shown that suboxic seawater retains Cr that has relatively low $\delta^{53}Cr$ and somewhat deviates from the apparent global trend between $\delta^{53}Cr$ and Cr_T (**Figure 3.8**). We anticipate that a similar effect may also occur in suboxic Indian and Pacific Ocean OMZs, and this has the potential to exert an influence on water masses globally.

3.5.7.1 Seawater Cr isotope budget

To assess the potential effects of internal processes on the Cr isotope composition of seawater, we use our new data to update the global Cr isotope budget of the oceans (**Table 3.5**).

Table 3.5 - Revised Cr budget of seawater.

Input	$\delta^{53}Cr$	Flux Cr (mol yr^{-1})	Fraction total Cr	$\delta^{53}Cr$ contribution to ocean	Reference
Estuaries	0.73	3.75×10^8	0.97	0.71	Bonnand *et al.* 2013, Frei *et al.* 2014, D'Arcy *et al.* 2016, Paulukat *et al.* 2015
Dust	-0.12	8.70×10^6	0.02	0.00	Bonnand *et al.* 2013
Groundwater	3.00	1.00×10^7	0.00	0.01	Bonnand *et al.* 2013
Hydrothermal	-0.15	1.50×10^5	0.00	0.00	Bonnand *et al.* 2013
Total inputs		3.94×10^8		0.72	
Outputs					
Oxic sediment	-0.12	2.51×10^8	0.64	-0.08	Gueguen *et al.* 2016
Anoxic sediment	0.60	1.43×10^8	0.36	-0.29	Reinhard *et al.* 2014, Gueguen *et al.* 2016, Piper and Calvert 2009
Total outputs		3.94×10^8	**Total $\delta^{53}Cr$**	1.09	

A previous budget (Bonnand *et al.*, 2013) estimated that the riverine flux of Cr to the oceans was 5.6×10^8 mol yr^{-1} based on a riverine concentration of 15nM, which does not account for removal of Cr in estuaries. More recent work suggests that the removal of Cr in estuaries could result in a much lower flux of Cr into the oceans (0.75×10^8 mol yr^{-1}; McClain and Maher 2016). This value is based on Cr concentration for estuarine waters of 2nM, which is rather lower than most estuaries measured to date (between 2 and 8nM; Abu-Saba and Flegal 1997; Campbell and Yeats 1984; Cranston and Murray 1980; D'Arcy *et al.* 2016; Paulukat *et al.* 2015) and does not account for potentially large inputs from ultramafic river catchments (e.g. McClain and Maher 2016; Novak *et al.* 2014). For this reason, we use a Cr concentration of 10nM to calculate the contribution of fluvial Cr to the oceans. The average $\delta^{53}Cr$ value of estuaries is taken to be 0.73‰, however, this is based on only a handful of reported measurements (D'Arcy *et al.*, 2016; Frei *et al.*, 2014; Paulukat *et al.*, 2015). The typical $\delta^{53}Cr$ of the ground water pool is thought to be between 2 and 4‰ (Bonnand *et al.*, 2013) so we have selected an intermediate $\delta^{53}Cr$ value of 3‰. Since the contribution of this source to seawater is small it makes little difference to seawater $\delta^{53}Cr$ even if its $\delta^{53}Cr$

value is 1‰ higher or lower than this figure (this is also true of dust and hydrothermal inputs). Hydrothermal and dust fluxes have been kept the same because, to our knowledge, there have been no studies on the $\delta^{53}Cr$ of these pools thus far. Removal of Cr(III) under anoxic conditions and its incorporation into marine sediments is estimated from the authigenic sediment flux and average Cr_T in authigenic sediments from the Cariaco Basin (Gueguen *et al.*, 2016; Piper and Calvert, 2009). The balance of the Cr outputs is attributed to uptake of Cr into oxic sediments *via* adsorption onto particulate material. This is a fairly simplistic calculation, but the result (2.51×10^8 mol yr^{-1}) compares fairly well with the estimated Cr output to oxic sediments based on accumulation rates of Cr in the Pacific (average 0.002-0.004mg cm^2 yr^{-1}; Murray and Leinen 1993), multiplied by the area of the global seafloor, which gives 1.39 to 2.78×10^8 mol yr^{-1}. The area of anoxic seafloor is insignificant for this calculation. It is not possible to calculate the degree of fractionation between dissolved Cr and Cr(III) that is removed into anoxic sediments without knowing the $\delta^{53}Cr$ value of coeval seawater (Gueguen *et al.*, 2016), so we have employed the fractionation factor estimated from the relationship between $\delta^{53}Cr$ and Cr_T for global seawater (0.8‰; Scheiderich *et al.* 2015). Using these figures, the $\delta^{53}Cr$ of seawater unaffected by localised internal processes is ~1.1‰, which is very close to the values we measured for deeper water masses (AAIW, NADW and MOW) in the Atlantic Ocean. Thus, on the global scale, internal processes such as biogeochemical cycling, benthic inputs, and reduction of Cr by inorganic reductants (e.g. Fe(II) or H_2O_2; Kitchen *et al.* 2012; Zink *et al.* 2010) appear to have little effect on the $\delta^{53}Cr$ value of seawater in the deep ocean. Nevertheless, internal processes are clearly important in defining the $\delta^{53}Cr$ value of shallow coastal and shelf waters (that have $\delta^{53}Cr$ >1.1‰). This may partly explain why shelf and surface water samples do not always conform well to the global $\delta^{53}Cr$-Cr_T correlation line (Paulukat *et al.*, 2016).

3.5.8 Implications for the Cr redox proxy

Our Black Sea data show that Cr is not quantitatively removed from seawater under anoxic conditions and the Cr isotopic composition of anoxic waters is different from the overlying oxic waters. Thus it seems likely that the $\delta^{53}Cr$ value of anoxic sediments is likely to provide a lower estimate of the $\delta^{53}Cr$ value of seawater; this would need to be taken into account for reconstructions of seawater $\delta^{53}Cr$ using banded iron formations and black shale

deposits. On the other hand, it may be possible to exploit this sensitivity of Cr to suboxic conditions, since other isotopic redox proxies such as Mo and Fe do not respond until anoxic conditions set in (Algeo and Maynard, 2004). For example $\delta^{53}Cr$ shifts in carbonates that formed at known depths at the same time could be used to estimate the depth of the suboxic boundary in coeval local seawater.

It is also clear that whilst the Cr isotopic composition of seawater is principally defined by fractionation processes occurring during terrestrial weathering, processes occurring within the oceans may also be locally significant. It appears that $\delta^{53}Cr$ values in central and surface waters may change as a result of reactions occurring on the shelf. Though these reactions are not well characterised, they consistently appear to locally raise $\delta^{53}Cr$. This may raise $\delta^{53}Cr$ values in anoxic authigenic sediments formed on the shelf by up to 0.58‰ compared to stable NADW/AAIW values. One way of bypassing local variations in $\delta^{53}Cr$ would be to select sediments which formed in waters of >1000m depth, since intermediate and deep waters appear less affected by local redox reactions.

One final point is that we could not find evidence of biological Cr fractionation in our Atlantic samples. If biological fractionation of Cr makes a relatively insignificant contribution to seawater $\delta^{53}Cr$, this would cement Cr isotopes as a useful indicator of non-biological redox in chemically precipitated sediments. However, more studies of $\delta^{53}Cr$ in the euphotic zone of the water column in different regions are required to determine if biological fractionation is significant in other areas.

3.6 Conclusions

We found that low O_2 concentrations (50-100µmol kg^{-1}) and biological reduction did not have major impacts on $\delta^{53}Cr$ values in Atlantic seawater. Nonetheless Atlantic seawater $\delta^{53}Cr$ varied between 1.08 and 1.72‰, with the majority of variation found in the central and surface waters. High $\delta^{53}Cr$ values on the shelf are thought to arise due to enhanced Cr(III) removal in the presence of high particle concentrations, though the reactions responsible for reducing Cr in these environments are poorly characterised. Benthic shelf Cr sources are also poorly resolved and seem to have variable influence on bottom water $\delta^{53}Cr$. More holistic studies that include measurements of $\delta^{53}Cr$ in seawater, particulate materials, sediments and pore waters as well as dissolved Cr speciation are needed to determine the causes of shelf $\delta^{53}Cr$ fractionation and the impact on underlying sediments.

More consistent $\delta^{53}Cr$ values appear to be held by intermediate and deep ocean waters (>1000m water depth) and these waters therefore likely represent the most reliable indicator of global $\delta^{53}Cr$ in coeval ancient seawater. However, we also found evidence that the presence of a suboxic boundary in the Black Sea lowers anoxic seawater $\delta^{53}Cr$ by 0.38‰ compared to oxic values, potentially due to the dissolution of Fe or Mn oxides that carry Cr with a low $\delta^{53}Cr$ value, or because dissolved Cr(III) with high $\delta^{53}Cr$ and solid phase Cr(III) with low $\delta^{53}Cr$ are able to equilibrate in the suboxic layer. Studies of suboxic Indian and Pacific OMZs and the underlying sediments would be useful to constrain the fractionation caused by marine redox boundaries and further our understanding of how seawater $\delta^{53}Cr$ values translate into underlying ancient sediments.

Chapter 4: Temporal and spatial variations in the chromium isotopic signature of seawater in the Celtic Sea

4.1. Introduction

In oxygenated seawater, chromium (Cr) is expected to be present as Cr(VI) in the chromate oxyanion CrO_4^{2-}, and to a much lesser extent as Cr(III) (Elderfield, 1970). Under mildly reducing (denitrifying) conditions, Cr(VI) may be reduced to Cr(III) forming aquahydroxyl cations and hydroxyl species that readily adsorb onto particle surfaces (Crawford *et al.*, 1993). Chromium isotopes are fractionated during the reduction of Cr(VI) to Cr(III) as the lighter isotopes are preferentially reduced, enriching the remaining Cr(VI) in the heavier isotopes by up to 7.9‰ (e.g. Ball and Bassett 2000; Døssing *et al.* 2011; Ellis *et al.* 2002; Kitchen *et al.* 2012; Sikora *et al.* 2008; Zink *et al.* 2010). By contrast, adsorption does not appear to fractionate Cr isotopes due to rapid isotopic exchange on particle surfaces (Ellis *et al.*, 2004; Wang *et al.*, 2015). Thus sedimentary archives of seawater Cr such as marine carbonates that only incorporate Cr(VI) (Tang *et al.*, 2007) have the potential to record important information about the levels of dissolved oxygen in seawater at the time of deposition (Bonnand *et al.*, 2013; Holmden, 2013; Rodler *et al.*, 2015).

To date however there is limited information as to the processes that regulate the Cr isotopic composition of seawater. Initial studies have shown that there is significant variability in seawater isotopic compositions (δ^{53}Cr calculated relative to the NBS979 Cr standard = 0.13-1.73‰; Bonnand *et al.* 2013; Paulukat *et al.* 2016; Scheiderich *et al.* 2015; **Chapter 3**) even though Cr has a long residence time in seawater (~9500 years; Reinhard *et al.* 2014). This is thought to be mainly caused by partial reduction of Cr in surface waters and oxygen minimum zones (**Chapter 3;** Bonnand *et al.* 2013; Scheiderich *et al.* 2015) which may occur *via* photolytic or biological redox processes, followed by removal of Cr(III) from the dissolved phase due to adsorption onto particles (Bonnand *et al.*, 2013; Scheiderich *et al.*, 2015). This is consistent with speciation analyses that show higher concentrations of Cr(III) in surface waters with concomitant lower concentrations of Cr(VI), and reduced overall concentrations of Cr in surface waters (Achterberg and Berg, 1997; Connelly *et al.*, 2006; Cranston, 1983). Furthermore the vertical distribution of dissolved Cr can be similar to recycled nutrients, particularly silicate (Achterberg and Berg, 1997; Cranston, 1983).

However in other parts of the ocean Cr appears to show more conservative behaviour with little change in concentration with depth (Sirinawin *et al.*, 2000). Overall redox cycling in surface waters appears to impart a negative correlation between Cr concentrations and $\delta^{53}Cr$ (fractionation factor $\Delta_{seawater\text{-}Cr\ removed}$ = 0.8) and it has been suggested that the fractionation resulting from re-oxidation of Cr in marine sediments must be small in order to maintain this correlation (Scheiderich *et al.*, 2015).

It therefore appears likely that in addition to seawater oxygenation, biogeochemical processes may be an important control on seawater $\delta^{53}Cr$. To explore this idea further, we have determined the Cr concentration and Cr isotopic composition of seawater samples collected in different seasons from a highly productive shelf region, the Celtic Sea. We show that although the water column remains oxygenated throughout the year, $\delta^{53}Cr$ varies as a result of seasonal thermal stratification and organic matter cycling. We discuss the potential influence of these $\delta^{53}Cr$ variations, that are unrelated to levels of dissolved oxygen, on the use of $\delta^{53}Cr$ as a tracer for oceanic paleo-redox conditions.

4.2. Sampling location

Seawater samples were collected from the Celtic Sea (NW European shelf) and shelf slope on four research cruises on board the RRS *Discovery* between November 2014 and August 2015 (**Table 4.1**) as part of the Natural Environment Research Council Shelf Sea Biogeochemistry (SSB) programme. The Celtic Sea is situated on a wide continental shelf of less than 200m depth, and is connected along its southern margin to the Atlantic Ocean by a steep shelf slope (**Figure 4.1**). Seasonal stratification occurs in summer, resulting in a shallow surface mixed layer (SML) around 30-50m thick and a seasonal thermocline at ~100m. In the winter months the SML extends to much greater depths (~900m; van Aken and Becker 1996) due to storms and rough seas; this defines the depth of the permanent thermocline. North East Atlantic Central Water (NEACW) is found between 300 and 700m. This water mass has a complex and variable temperature-salinity structure because it consists of waters delivered from sub-tropical and sub-polar regions, and is further modified by deep winter mixing (Pollard *et al.*, 1996; van Aken and Becker, 1996). Below NEACW, Mediterranean Water (MW) can be identified by a salinity maximum which extends to around 1000m. Finally North East Atlantic Deep Water (NEADW) extends to the seafloor at the deepest stations sampled during this study, and contains contributions from

Labrador Sea Water, Iceland-Scotland Overflow Water and MW (McCartney, 1992). The area is also affected by an along slope surface current that flows primarily in a north-westerly direction but may reverse in summer (Pingree and Le Cann, 1989; Porter *et al.*, 2016) and mixing *via* eddies and internal waves can occur at the shelf break (Huthnance *et al.*, 2009; Pingree, 1979; Pingree *et al.*, 1983). Thus, the Celtic Sea is highly dynamic. Over 30 submarine canyons intersect the shelf slope which further complicate its hydrography, and these are also considered to be sediment and suspended particle 'traps' (Amaro *et al.*, 2016; Wilson *et al.*, 2015). The most important phytoplankton taxa in the Celtic Sea are diatoms, dinoflagellates and prymnesiophytes, with the latter two types dominating in summer when surface nutrient concentrations are lowest. Phytoplankton community structures in the Celtic Sea are highly sensitive to spatial and temporal effects produced by seasonal stratification (Joint *et al.*, 2001; Pemberton *et al.*, 2004). Growth is limited by nitrogen (N) availability in the summer and light intensity in the winter, and most of the on-shelf N appears to be provided by recycling of organic material (up to 94%; Kitidis *et al.* 2017).

Water samples were taken from two stations overlying a submarine canyon on the shelf slope in Autumn 2014, and from three stations on the shelf itself during Winter Early 2015. Samples collected in Spring 2015 and Summer 2015 samples were taken from 5 different stations located along a transect off the point of a small spur on the shelf slope.

Table 4.1 - Summary of sampling stations and their locations. Contains data supplied by the Natural Environment Research Council.

Cruise	Station	Sampling date	Latitude	Longitude	Sea floor depth (m)
DY018	Fe03	15th Nov 2014	48.33997	-9.70683	1500
(Autumn 2014)	Fe05	16th Nov 2014	48.37813	-9.60818	731
DY021	G	8th Mar 2015	51.07248	-6.58110	104
(Winter Early 2015)	I	14th Mar 2015	50.57553	-7.10472	113
	CCS	22nd Mar 2015	49.39983	-8.60020	146
DY029	Fe09	8th Apr 2015	48.39950	-9.90133	1856
(Spring 2015)	Fe10	7th Apr 2015	48.41015	-9.88983	1400
	Fe11	8th Apr 2015	48.42550	-9.87900	921
DY033	Fe09	16th Jul 2015	48.39948	-9.90078	1861
(Summer 2015)	Fe12	18th Jul 2015	48.42948	-9.87113	667
	CS2	20th Jul 2015	48.57083	-9.50967	202

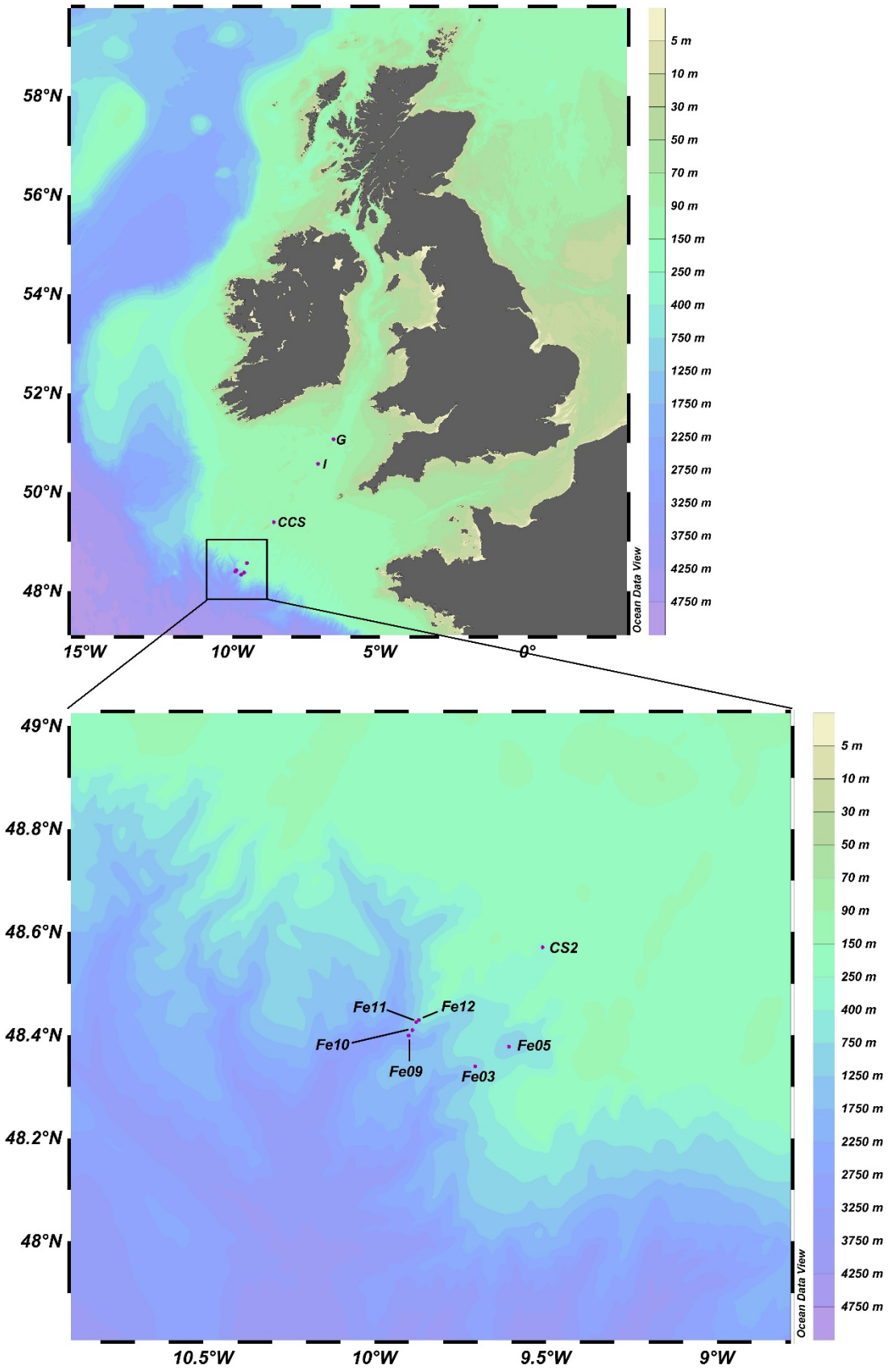

Figure 4.1 - Map of stations sampled.

4.3. Methods

4.3.1. Sample collection

Water samples were collected using Ocean Test Equipment (OTE) bottles mounted on a trace-metal titanium rosette with Kevlar wire. The OTE bottles were transferred to a class 100 clean laboratory on board the RRS Discovery and samples were passed through capsule filters (0.2µm, Sartorius Sartobran 300) into acid-washed, pre-rinsed LDPE bottles. The samples were acidified to pH <2 using sub-boiled HCl on return to the National Oceanography Centre (Southampton, UK) and were then stored for 6-12 months before further processing.

Water samples collected for the analysis of Cr(III) concentrations in Winter Early 2015 were filtered in the same way. However, as Cr(III) is not stable the spiking and pre-concentration steps were carried out immediately on board the ship as described in **Section 4.3.2.2**. These samples were therefore not acidified on return to the laboratory.

4.3.2. Sample processing

4.3.2.1. Analysis of total Cr(VI) + Cr(III): concentration and Cr isotopic composition

Between 1 and 3L of acidified seawater samples (~100-300ng Cr) were spiked with a ^{50}Cr-^{54}Cr double spike which allows isotopic fractionation during sample processing to be accounted for. This double spiked Cr was removed from seawater by co-precipitation with Fe(II) hydroxide as described in **Chapters 2** and **3**. In the presence of Fe(II) hydroxide Cr(VI) is quantitatively reduced to Cr(III) and Fe(II) is oxidised to Fe(III) hydroxide. The Cr(III) which forms during this reaction, together with the Cr(III) which was already present in the sample co-precipitates with the Fe(III) hydroxide (Cranston and Murray, 1978) The Fe(III)-Cr(III) hydroxide is separated from solution by filtration through 1µm Millipore Omnipore filters. The Cr is then separated from the Fe by anion exchange chromatography (Biorad AG1-X8 resin), and residual salts are removed using cation exchange chromatography (Biorad AG50-X12 resin) as detailed in Bonnand *et al.* 2013. The isotopic composition of the purified Cr was determined on a Thermo Fisher Neptune multi-collector inductively coupled plasma mass spectrometer (MC-ICP-MS) equipped with an Aridus 2 Desolvating Nebuliser system. Analyses were performed in medium resolution mode (mass resolution M/ΔM = 5800-6500) and blank-corrected using measurements of 3% nitric acid before and after each sample. The δ^{53}Cr of each seawater sample was obtained by performing a Newton-Raphson

deconvolution calculation on the spiked sample measurement and the raw $\delta^{53}Cr$ values were normalised against the daily $\delta^{53}Cr$ value of the NBS979 standard (true $\delta^{53}Cr$ = 0‰) to account for instrumental drift. Our average normalised $\delta^{53}Cr$ for the NBS979 standard is 0.000 ± 0.041‰ (n = 520); this precision is similar to that of other seawater $\delta^{53}Cr$ studies (Bonnand *et al.*, 2013; Paulukat *et al.*, 2016; Scheiderich *et al.*, 2015). The total Cr concentration (Cr_T) of the sample was obtained *via* isotope dilution calculations. The external precision (2SD) of our seawater technique is ±0.10‰ for $\delta^{53}Cr$ and ±0.03nmol kg^{-1} for total Cr concentration based on repeated analyses of the OSIL Atlantic Seawater salinity standard (n=6; **Chapter 3**).

4.3.2.2. Analysis of Cr(III) concentration

As the speciation of Cr may change rapidly after collection (Kingston *et al.*, 1998), spiking and co-precipitation of seawater samples for Cr(III) analysis was done within 1 hour of sample collection on board the RRS *Discovery*. A single ^{53}Cr spike was used in place of the ^{50}Cr-^{54}Cr double spike and Cr(III) was captured on a Fe(III) hydroxide precipitate; Cr(VI) does not react and is not adsorbed by Fe(III) hydroxide (Cranston and Murray, 1978). Concentrations were calculated using an isotope dilution technique based on the $^{52}Cr/^{53}Cr$ ratio, which was analysed using an Element 2 ICP-MS. This method can be used on relatively small amounts of seawater (200-300mL) since it is not necessary to collect sufficient Cr to quantify the less abundant ^{50}Cr and ^{54}Cr isotopes. The external error for mixed Cr(VI)-Cr(III) standards is 8-10% (**Chapter 5**), thus conservative 10% error bars have been applied to the results of this study. A full description of the technique can be found in **Chapter 5** and Cranston and Murray 1978.

4.4. Results

4.4.1. Seasonal variability in temperature, salinity, nutrient and chlorophyll concentrations in the Celtic Sea

Temperature-salinity plots and profiles of density and nitrate+nitrite for the sites sampled in this study are presented in **Figure 4.2** (all nutrient data supplied by Malcolm Woodward, Plymouth Marine Laboratory). Sections displaying salinity and attenuance for each season can be found in **Figure 4.3**. All CTD sensor data shown in this work was supplied by the British Oceanographic Data Centre, courtesy of the Natural Environment Research Council.

In Autumn 2014 stratification from the summer of that year had not yet broken down and the SML was relatively thin, ~60m. Nutrients were extremely low in the SML (0.2µM phosphate, 1.7µM nitrate at 25m water depth) although concentrations of chlorophyll-a (Chl-a) were lower than in Spring and Summer 2015, never exceeding 0.7mg m^{-3}. Dissolved organic carbon (DOC) production was low and N regeneration was high compared to Spring/Summer 2015 (pers. comms., Claire Mahaffey, University of Liverpool). The depth of the thermocline was ~240m and NEACW was present to 750m. High salinity caused by MW was apparent between 750 and 1100m, but this water mass was significantly diluted by mixing within the canyon; MW waters outside of the canyon were ~0.1 higher than those within it.

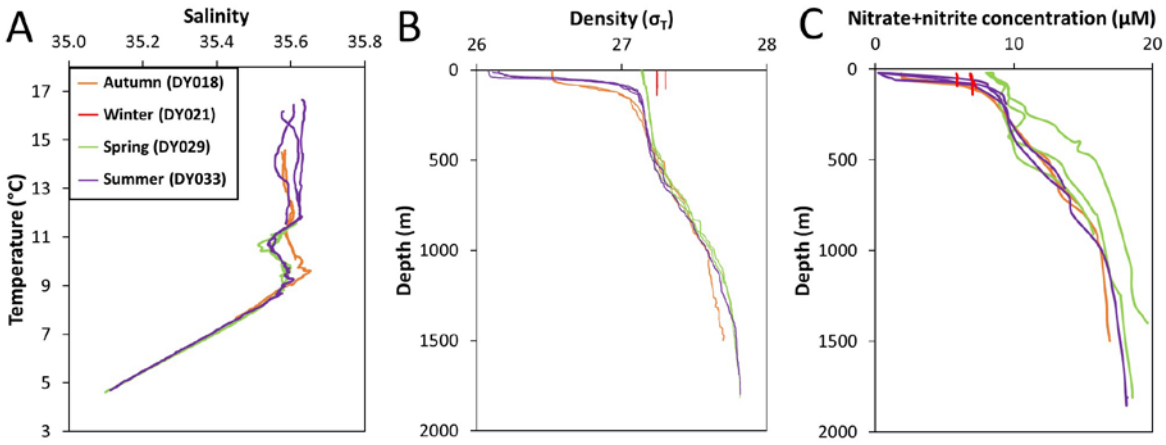

Figure 4.2 - (A) T-S plots for all cruises except DY021 as T-S was homogenous, (B) density profiles for all stations, (C) nitrate+nitrite profiles for all stations. Legend in (A) applies to all. Contains data supplied by the Natural Environment Research Council.

Shelf waters (<200m depth) were well mixed during Winter Early 2015 with no variation in salinity or temperature through the water column at any of the sites sampled for this study. Off-shelf waters were mixed to a depth of 500m. However, salinity increased with increasing distance from the coast from Site G to Site I to CCS, due to decreased contributions of freshwater run-off. Chl-a did not exceed 0.2mg m^{-3} at the sites sampled, indicating that levels of primary production were negligible.

Stratification of the water column had started to develop by Spring 2015 but was not yet fully established. The SML lay at 80m as indicated by salinity and temperature profiles but overall densities were quite homogenous down to 400m, allowing isopycnal mixing

between shelf and Atlantic waters to occur in this part of the water column. This can be seen in the salinity and attenuance sections (**Figure 4.3**) which show a number of lenses over the shelf edge. Mixing is also reflected in the Chl-a profiles which show two peaks, one at 50m (up to 0.9mg m^{-3}) and another smaller one (up to 0.5mg m^{-3}) at 170-250m (**Figure 4.4**). Nutrients were somewhat depleted in surface waters, as low as 0.5µM for phosphate and 7.9µM for nitrate at 20m water depth, but the spring bloom had not yet occurred when the samples were taken.

By Summer 2015 the water column was strongly stratified and the SML was no deeper than 40m at any of the three sampling sites. Atlantic waters were observed to spread over the shelf underneath the SML, and were detectable up to 120km from the shelf edge (pers. comms., Joanne Hopkins, NOC Liverpool). Nutrients were highly depleted within the SML with phosphate concentrations close to zero at 20m (<0.1µM). Chl-a concentrations were highest during this period, reaching up to 1.24mg m^{-3} at CS2. The thermocline extended to 140m, below which NEACW was present.

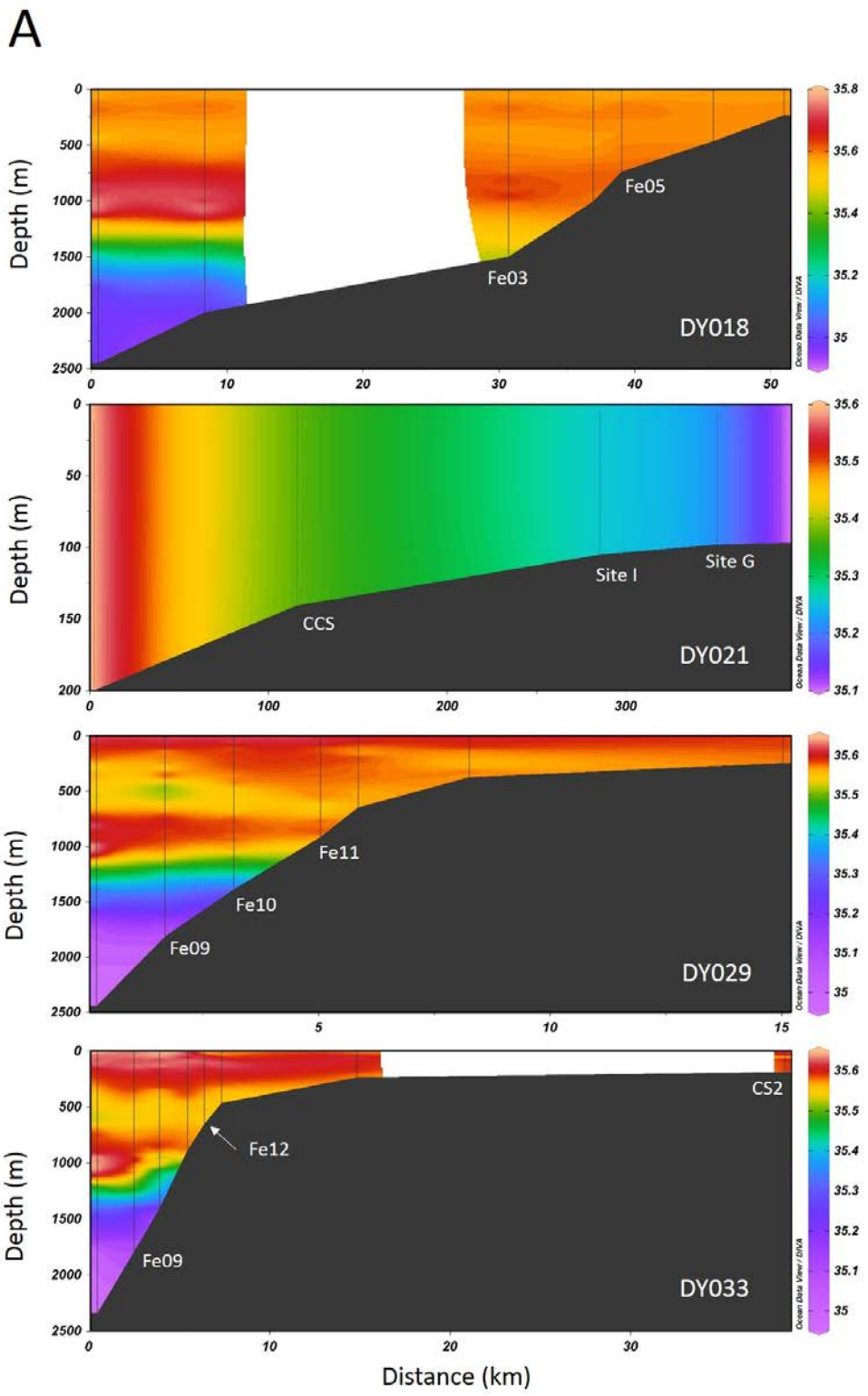

Figure 4.3A - Salinity (PSU) sections for all sampling periods. Note different scale bars are used to accommodate for different sampling locations/depths during each season. Stations sampled for Cr are marked in white text. Contains data supplied by the Natural Environment Research Council.

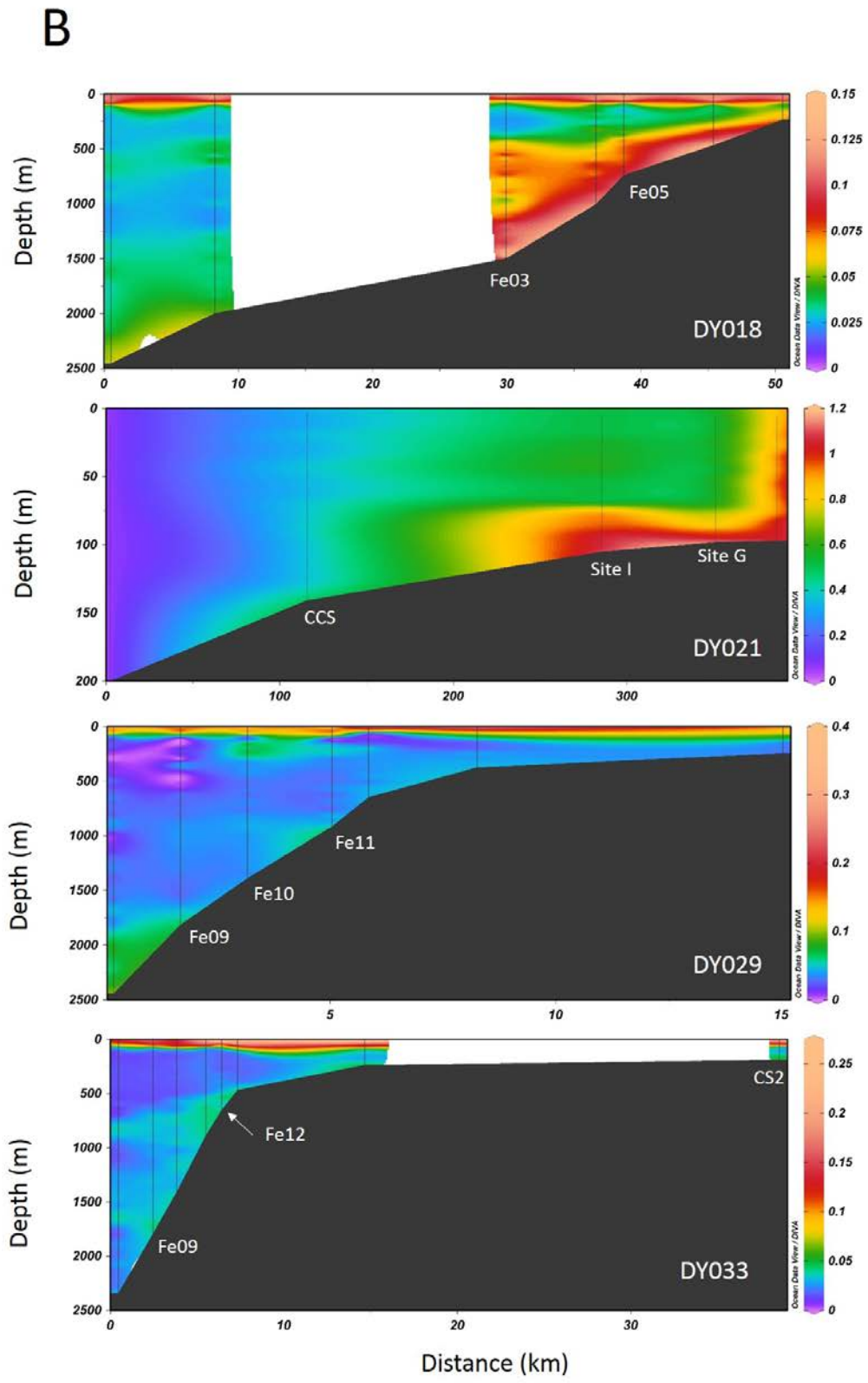

Figure 4.3B - Attenuance (m^{-1}) sections for all sampling periods. Note different scale bars are used to accommodate for different sampling locations/depths during each season. Stations sampled for Cr are marked in white text. Contains data supplied by the Natural Environment Research Council.

4.4.2. Seasonal variations in concentrations of particulate material

Although no samples of particulate material were collected as part of this study, the relative concentration of particulate material and clues as to its provenance can be estimated from profiles of attenuance and Chl-a (**Figure 4.4**).

In Autumn 2014 attenuance was highest in the top 150m of the water column. This corresponds to high concentrations of Chl-a, suggesting that these particles were due to the presence of phytoplankton. Attenuance also increased below 400m towards the seafloor to values far higher than those measured outside of the canyon during the same period or at any of the other off-shelf sites during subsequent sampling periods. High concentrations of particulate material are a year-round feature within canyon settings due to enhanced sedimentary transport processes and nepheloid layer formation (Wilson *et al.*, 2015). Chl-a levels were low in these deeper waters suggesting that the particles mainly consist of sedimentary detrital material. This is substantiated by particulate Mn/Al ratios which indicate that these nepheloid layers mainly consist of lithogenic material (pers. comm., Angela Milne, University of Plymouth).

Attenuance on the shelf during Winter Early 2015 was very high at all stations compared to off-shelf sites, despite low Chl-a concentrations. Therefore much of the shelf particulate matter is likely to have been sedimentary material that was been re-suspended by stormy weather, vigorous mixing and large bed stresses. In support of this, attenuance was highest closest to the seabed (**Figure 4.3B**). Attenuance was lower at CCS than the two shallower sites (Sites G and I). At Site G the sediment consists of permeable sands whereas Site I has a larger mud component. Consequently Site G had exceptionally high oxygen penetration depths (OPDs) due to advective transport of oxygenated seawater into the sediment, whereas OPDs at Site I were shallower (Hicks *et al.*, 2017). The OPD at CCS yet known but the sediment consists of sands, so it is likely to be similar to the OPD at Site G. Shallow OPDs have been linked with higher sedimentary Fe supply to overlying waters in the Celtic Sea (Klar *et al.*, 2017).

The highest concentrations of Chl-a in Spring 2015 were found just below the sea surface, and there was a smaller peak located at ~300m water depth. Attenuance and Chl-a over this depth range showed a similar distribution suggesting that the particles were mainly

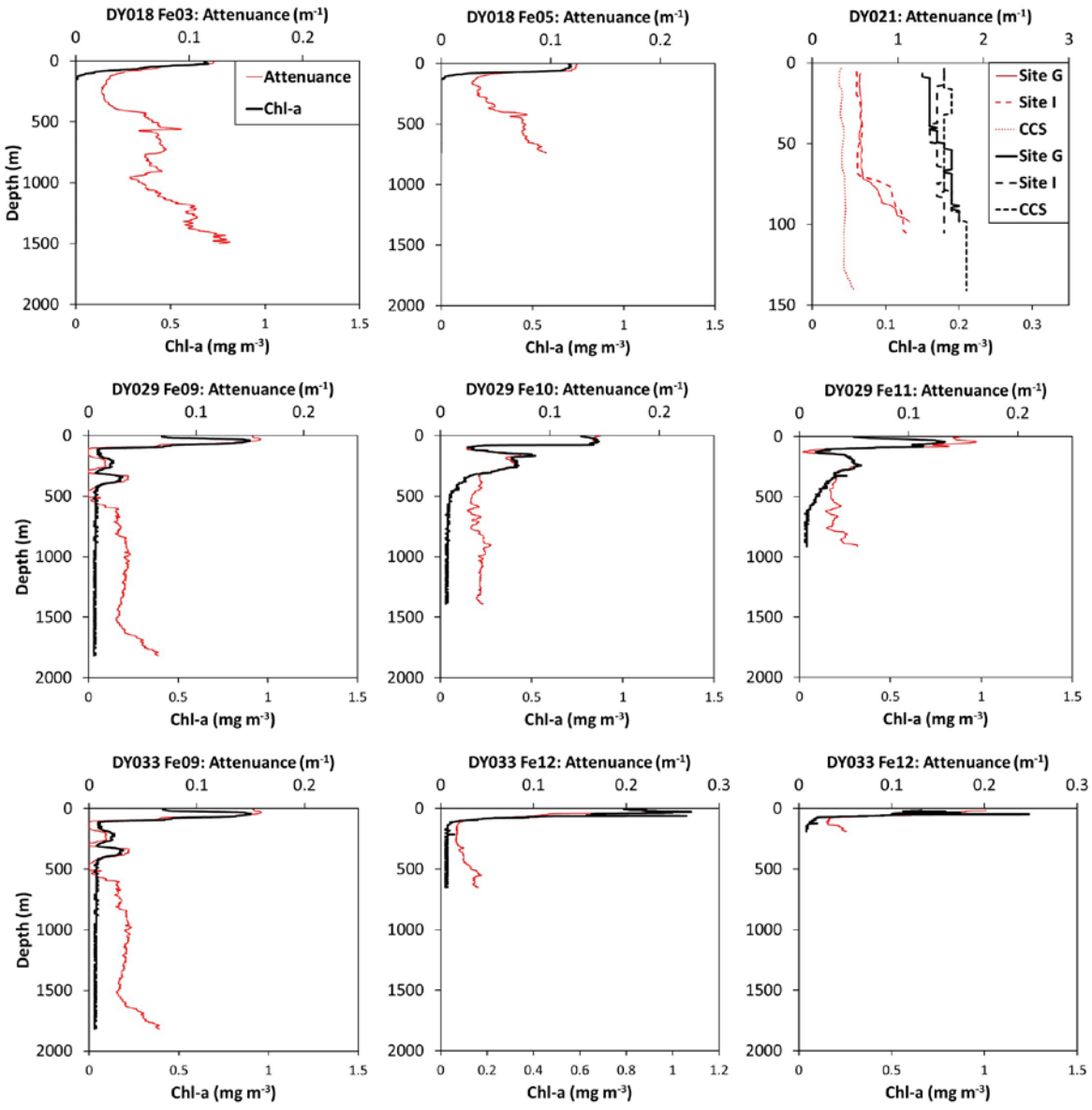

Figure 4.4 - Attenuance and Chl-a profiles for all stations (legend in top left hand graph applies to all). Bottom of profiles denotes seafloor depth. All DY021 stations are shown on the same graph, note different scale bars. Contains data supplied by the Natural Environment Research Council.

biological in origin. Attenuance increased slightly towards the seabed at Site Fe09 and Fe11 but levels of Chl-a remained low pointing to some re-suspension of sedimentary material, though given the higher levels of primary productivity within this period these particles could be re-suspended organic matter.

During Summer 2015, high concentrations of Chl-a were found in the top 80m of the water column and thus biological particles account for the high attenuance in surface waters. Attenuance increased slightly towards the seafloor at all of the sites sampled in this cruise

but was generally lower than in other sampling periods; as for Spring 2015 particles below the SML could be sedimentary material or re-suspended organic matter.

4.4.3. Temporal and spatial variation in total Cr concentrations

Profiles of total Cr concentration (Cr_T) and $\delta^{53}Cr$ are shown in **Figure 4.5** and the data are provided in in **Table 4.2**. Cr_T was highest in Autumn 2014 throughout the water column, ranging from 2.4nmol kg^{-1} in the SML to 2.8nmol kg^{-1} in NEADW at >1000m water depth. Cr exhibits a nutrient-type distribution in Autumn 2014 and in support of this Cr_T is positively correlated with nutrient concentrations, most notably silicate (R^2 = 0.79) (**Figure 4.5A**)**.** This relationship has also been observed in other parts of the ocean (Achterberg and Berg, 1997; Cranston, 1983). Overall the Cr_T concentrations in Autumn 2014 were similar to those reported for other regions of the Atlantic Ocean (typically 2-5nM; e.g. Achterberg and Berg 1997; Bonnand *et al.* 2013; Campbell and Yeats 1981; Connelly *et al.* 2006; Jeandel and Minster 1987; Scheiderich *et al.* 2015; Sherrell and Boyle 1988).

On the shelf in Winter Early 2015, Cr_T values increased with distance from the coast, ranging from ~2.2nmol kg^{-1} at Site G to ~2.3nmol kg^{-1} at Site I, to ~2.4nmol kg^{-1} at CCS. These values are very similar to those previously measured around the south coast of the UK (typically 2nM; Achterberg *et al.* 1999). There is little change in Cr_T with depth as all samples were taken from within the SML. The differences in Cr_T between the sites were principally controlled by salinity (**Figure** 4.**6B**) as Cr_T increased with salinity, i.e. towards the shelf edge. This is consistent with results from the north-west African shelf (**Chapter 3)**, where Cr concentrations were also lower on the shelf itself compared to off-shelf waters. Cr_T was also very well correlated with nitrite and ammonia (R^2 = 0.86 and 0.87 respectively, **Figure 4.6D**), both of which appeared to originate from off-shelf waters (**Figure 4.7**). Note that for 2 samples in this sampling period (marked with an asterisk in **Table 4.2**), Cr_T and $\delta^{53}Cr$ were determined separately due to low level ^{53}Cr contamination during the first analysis that affected the determination of $\delta^{53}Cr$, but not Cr_T.

Cr_T tended towards lower values lower in Spring and Summer 2015 compared to Autumn 2014 and Winter Early 2015 at all water depths, but overall there was more variation in Cr_T even between stations located only a few kilometres apart. No samples were collected from the upper 200m of the water column in Spring 2015 so it is not possible to assess the

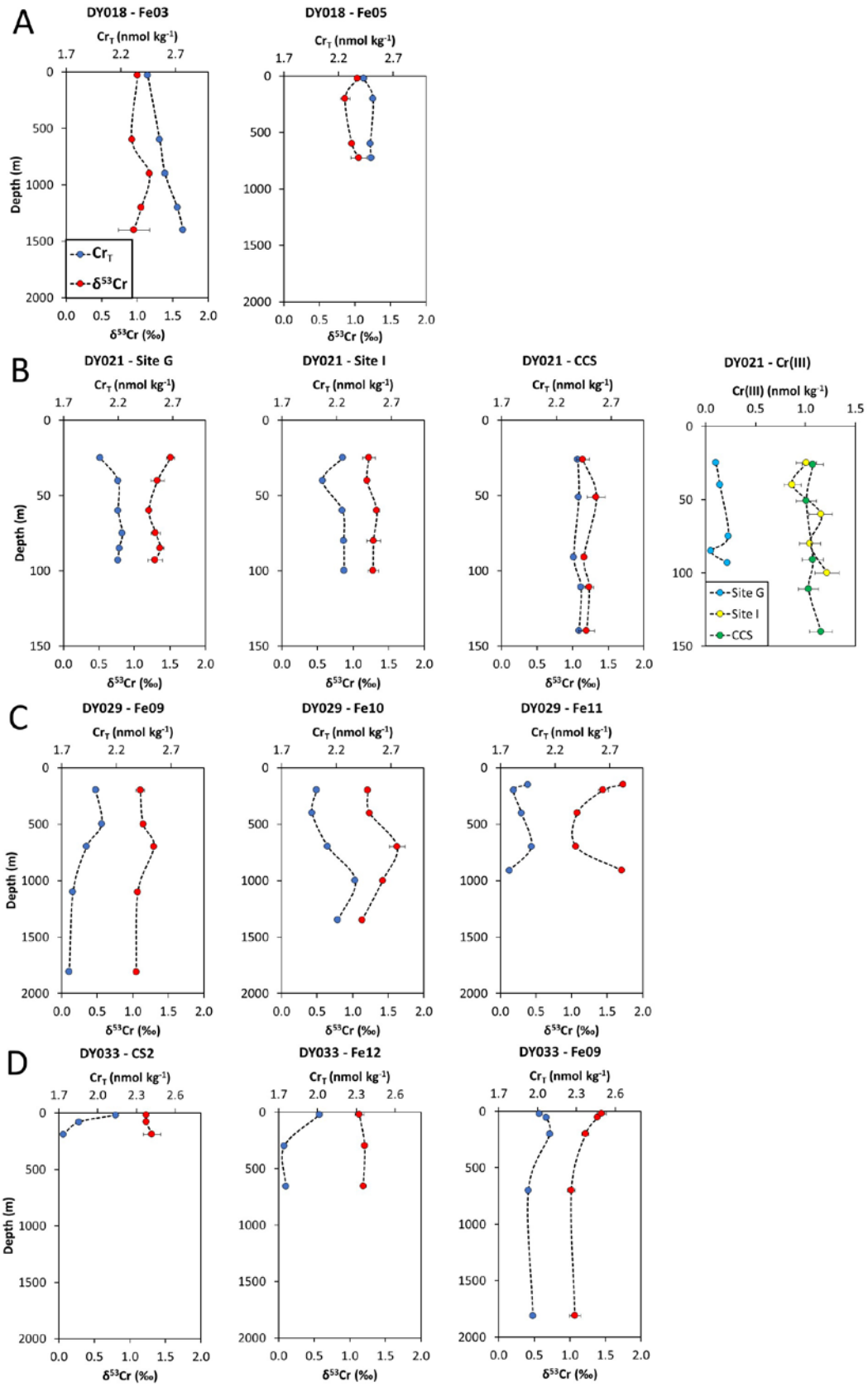

Figure 4.5 - Cr_T and $\delta^{53}Cr$ profiles for all stations. Row (A) Autumn (DY018), row (B) Winter shelf stations (DY021 - note different scale bars), also including Cr(III) data, row (C) Spring (DY029), row (D) summer (DY033). Error bars are analytical error - 2SD for $\delta^{53}Cr$ and 10% for Cr(III) measurements. Error bars for Cr_T are not shown as they are smaller than data points.

effects of biogeochemical nutrient cycling on Cr_T at these sites. In general however, NEACW in Spring 2015 had a Cr_T of ~2nmol kg^{-1} at all sites, whereas Cr_T at Sites Fe09 and Fe11 appeared to be slightly lower (~1.8nmol kg^{-1}) close to the seabed where attenuance is also elevated (**Figure 4.5C**).

The profiles collected in Summer 2015 afford a better perspective on Cr biogeochemical behaviour because samples were taken within the SML, which extended to ~40m below the sea surface. At all of the sites sampled during this cruise, Cr_T was generally higher in the SML (2.0-2.1nmol kg^{-1}) than at 200-300m (1.7-1.9nmol kg^{-1}).

4.4.4. Cr(III) concentrations of shelf waters in Winter Early 2015

Cr(III) concentrations were only determined for sampled collected in Winter Early 2015. Between 42 and 53% of the total dissolved Cr was present as Cr(III) at Sites I and CCS (**Figure** 4.**5B**). This is far higher than predicted by thermodynamic considerations and observations made in some open ocean waters (Cranston, 1983; Elderfield, 1970; Sirinawin *et al.*, 2000), but similar proportions have been observed in the upper waters of the Sargasso and Mediterranean Seas (Achterberg and Berg, 1997; Connelly *et al.*, 2006). By contrast, Site G had significantly less Cr(III) (0-10%) even though Cr_T concentrations were similar to those measured at Site I. Particle and biological influences can be ruled out as the cause for the discrepancy in speciation between these two sites, since Chl-a and attenuance levels were extremely similar at the two sites.

4.4.5. Temporal and spatial variation of seawater $\delta^{53}Cr$

The overall range of $\delta^{53}Cr$ values measured during this study (0.86-1.73‰) was slightly larger than the range found for the sub-tropical Atlantic (1.08-1.72‰) and Canada Basin waters (0.99-1.55‰; **Chapter 3;** Scheiderich *et al.* 2015). Cr_T and $\delta^{53}Cr$ are generally poorly correlated at individual sites, between different sites and seasons, and for the dataset as a whole.

In general, samples collected in Autumn 2014 had the lowest $\delta^{53}Cr$ and highest Cr_T. Although Cr_T was slightly lower in the SML than it was at depth, there was no obvious correlated shift in $\delta^{53}Cr$. There was a small peak in $\delta^{53}Cr$ at 902m at Fe03.

Table 4.2 - All Cr_T, Cr(III) and $\delta^{53}Cr$ data measured for this study. Cr(III) measurements made during DY021 only. 2SD for $\delta^{53}Cr$ is calculated from 2-4 MC-ICP-MS measurements. *Marks samples where Cr_T and $\delta^{53}Cr$ were determined in separate sessions (see text).

Cruise	Station	Depth (m)	Cr_T (nmol kg^{-1})	Cr(III) (nmol kg^{-1})	$\delta^{53}Cr$ (‰)	2SD
DY018 (Autumn 2014)	Fe03	32	2.45		1.01	0.00
		601	2.56		0.93	0.01
		902	2.61		1.17	0.03
		1200	2.72		1.06	0.00
		1403	2.77		0.95	0.22
		22				
	Fe05	186	2.43		1.03	0.02
		601	2.52		0.86	0.06
		737	2.49		0.96	0.00
		32	2.50		1.05	0.11
DY021 (Winter Early 2015)	Site G	27	2.19	0.11	1.51*	0.05
		42	2.20	0.14	1.33	0.09
		62	2.20	NT	1.20	0.01
		77	2.24	0.23	1.30	0.06
		87	2.21	0.06	1.36	0.05
		97	2.20	0.22	1.29	0.10
	Site I	26	2.26	1.01	1.22	0.09
		41	2.24	0.87	1.20*	0.01
		61	2.25	1.16	1.33	0.04
		81	2.27	1.05	1.29	0.10
		104	2.27	1.22	1.28	0.08
	CCS	26	2.40	1.07	1.14	0.09
		51	2.41	1.01	1.33	0.13
		91	2.36	1.07	1.16	0.01
		111	2.43	1.03	1.23	0.06
		141	2.41	1.16	1.20	0.11
DY029 (Spring 2015)	Fe09	200	2.01		1.11	0.06
		500	2.07		1.15	0.03
		699	1.93		1.30	0.02
		1100	1.80		1.07	0.01
		1811	1.77		1.05	0.03
	Fe10	200	2.02		1.21	0.02
		401	1.98		1.24	0.01
		699	2.12		1.63	0.10
		1000	2.38		1.42	0.03
		1348	2.22		1.13	0.02
	Fe11	149	1.95		1.73	0.03
		200	1.82		1.45	0.07
		400	1.89		1.08	0.02
		701	1.98		1.06	0.00
		911	1.78		1.71	0.02
DY033 (Summer 2015)	CS2	20	2.14		1.23	0.11
		80	1.86		1.23	0.05
		190	1.74		1.31	0.14
	Fe12	20	2.02		1.14	0.06
		300	1.74		1.21	0.02
		652	1.76		1.19	0.05
	Fe09	20	2.01		1.45	0.06
		53	2.07		1.39	0.02
		200	2.10		1.22	0.05
		700	1.93		1.02	0.05
		1810	1.97		1.07	0.08

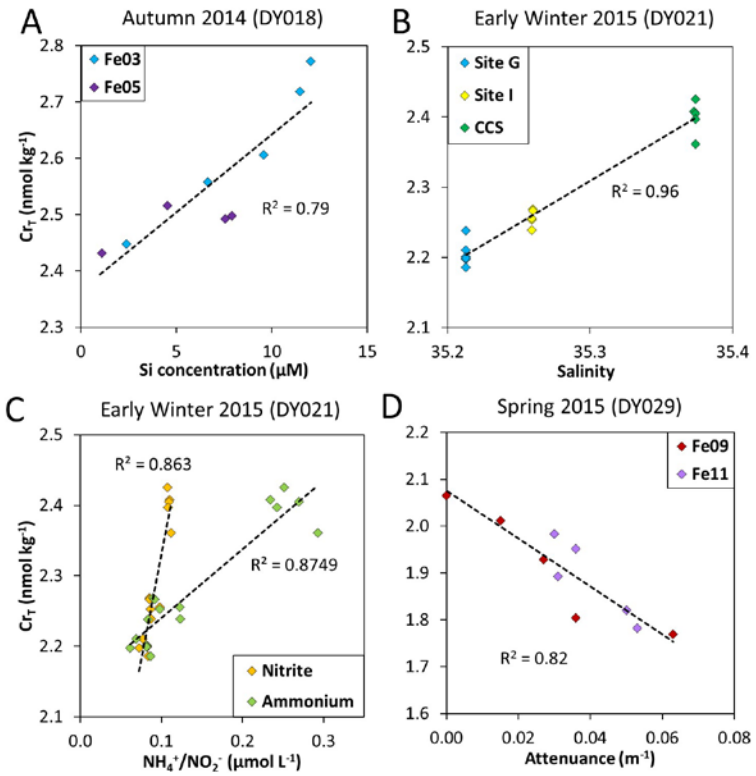

Figure 4.6 - Selected graphs for Cr_T relationships with (A) Silicate concentration during Autumn 2014 (DY018), (B) salinity during Winter Early 2015 (DY021). (C) Nitrite and ammonium concentrations during Winter Early 2015 (DY021), (D) Attenuance during Spring 2015 (DY029). Note different Cr_T scales. Contains data supplied by the Natural Environment Research Council.

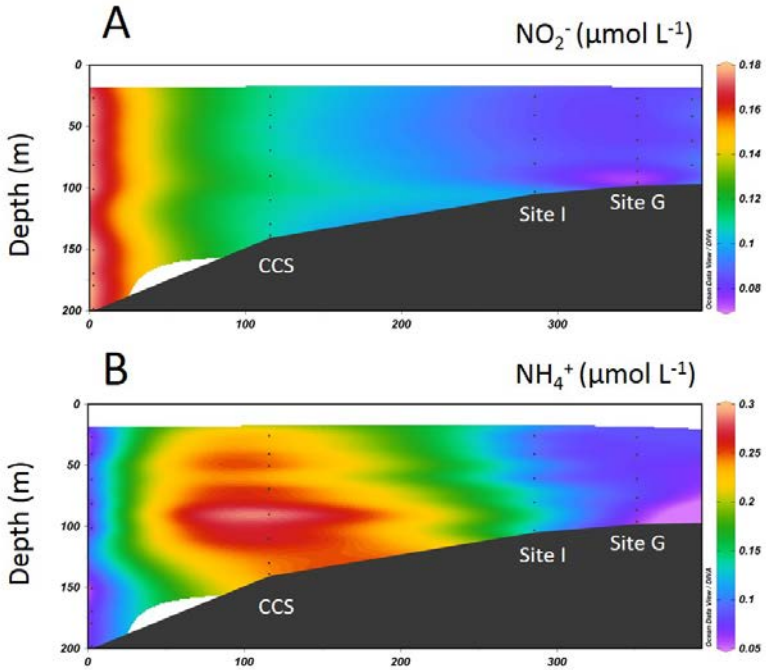

Figure 4.7 - (A) Nitrite concentrations and (B) Ammonium concentrations during Winter Early 2015 (DY021).

During Winter Early 2015, $\delta^{53}Cr$ values of well mixed shelf waters averaged 1.27‰ which is higher than off-shelf waters of comparable depth in this study (average 1.06‰). Between the three sites there was a subtle shift in average $\delta^{53}Cr$ with increasing distance from the coast, from 1.33‰ at Site G, to 1.27‰ at Site I to 1.21‰ at Site CCS.

As for Cr_T, $\delta^{53}Cr$ values showed the greatest variation in Spring 2015. $\delta^{53}Cr$ was notably higher in samples recovered from 699m at Fe09 and Fe10, and at 911m at Fe11. The size of this $\delta^{53}Cr$ anomaly was generally higher at lower salinities. The second notable feature during Spring 2015 was the presence of seawater with high $\delta^{53}Cr$ at 150-200m at station Fe11 (1.45 - 1.73‰).

In Summer 2015, there was little change in $\delta^{53}Cr$ values with depth at Fe12 and CS2, although average $\delta^{53}Cr$ values were slightly higher on the shelf at CS2 (1.26‰) than they were at Fe12, which is slightly off the shelf (1.18‰). At Fe09 there was a clear increase in $\delta^{53}Cr$ at the top of the profile and overall $\delta^{53}Cr$ was well correlated with nitrate+nitrite (R^2 = 0.90), though the correlation between Cr_T and nitrate+nitrite was poor (R^2 = 0.19).

Fe09 was the only site sampled on two separate occasions during this study (Spring and Summer 2015). Unfortunately no samples were recovered from the upper 200m of the water column in Spring, but below 200m water depth average Cr_T and $\delta^{53}Cr$ for NEACW for the two cruises were comparable (2.00nmol kg^{-1} and 1.23‰ in Spring, 2.02nmol kg^{-1} and 1.12‰ in Summer). Average Cr_T and $\delta^{53}Cr$ values for NEADW parameters were also similar (1.79nmol kg^{-1} and 1.06‰ in Spring, 1.97nmol kg^{-1} and 1.07‰ in Summer).

4.5. Discussion

4.5.1. Cr behaviour on the Celtic shelf (Winter Early 2015)

Cr_T values on the Celtic shelf (2.2-2.4nmol kg^{-1}) were similar to those measured along the south coast of the UK (1.3 - 3.3nmol kg^{-1} (**Chapters 3 and 5**; Achterberg *et al.* 1999; Auger *et al.* 1999; Bonnand *et al.* 2013). The increase in Cr_T with salinity during Winter Early 2015 suggests that off-shelf waters represent a source of Cr to the shelf during the winter months. Deep mixing of off-shelf waters (~500m) in winter is also considered to be a source of remineralised N from off the shelf (Hydes *et al.*, 2004) in this connection there is positive correlation between nitrite and ammonium concentrations, salinity and Cr_T during this

period (**Figures 4.6B** and **4.6C**). Thus, it seems likely that organic matter remineralisation is the source of this Cr. This is consistent with studies which have shown that Cr is strongly associated with particulate organic matter in the Celtic Sea and elsewhere (Auger *et al.*, 1999; Connelly *et al.*, 2006; Dauby *et al.*, 1994).

At Sites I and CCS, a large proportion of Cr was present in the reduced form which may suggest that remineralised Cr was returned to the dissolved phase as Cr(III). Furthermore, this Cr appeared to possess lower δ^{53}Cr values than on-shelf Cr, since average δ^{53}Cr values decreased towards the shelf edge. Overall these trends are consistent with the preferential uptake of ^{52}Cr onto/into biological particles (see **Section 4.5.2**) resulting in low δ^{53}Cr within organic matter, and return of this low δ^{53}Cr Cr to the dissolved phase during remineralisation.

At Site G, the proportion of dissolved Cr(VI) was markedly higher than at the other two sites. This is consistent with its position farthest from the shelf edge; it receives the smallest quantities of Cr(III) from off-shelf waters. Based on its position between Sites G and CCS, Site I had a relatively high proportion of Cr(III), though Cr_T was still controlled by salinity. This implies that reduction occurred at Site I, but not removal to sediments as this would decrease Cr_T and increase δ^{53}Cr. The sediments at this site have a large component of mud compared to the other two sites (which both have sand sediments), resulting in less advective transport of seawater through the sediments (Hicks *et al.*, 2017). Consequently oxygen penetration depths (OPDs) at Site I (~7mm) are far lower than at Site G (~47mm). Where OPDs are shallow there is greater opportunity for Fe(II) release into overlying waters (Klar *et al.*, 2017) and indeed dissolved Fe concentrations at Site I are higher than those at Sites G and CCS (pers. comms., Antony Birchill, University of Plymouth). Fe(II) is a highly effective Cr reductant (Døssing *et al.*, 2011; Kitchen *et al.*, 2012) and thus reduction by Fe due to increased sedimentary release of this element may explain the larger proportion of Cr(III) at Site I. It is notable that there is no obvious removal of Cr(III) by adsorption at Site I despite the high levels of particles in the water column; however, these particles are lithogenic in origin (**Section 4.4.2**) and uptake of Cr(III) appears to be largely controlled by adsorption to biological particles (**Chapter 3**; Semeniuk et al. 2016).

Whilst mixing with off-shelf waters appeared to lower δ^{53}Cr values in the shelf edge region, all shelf sites sampled in Winter Early 2015 and CS2 in Summer 2015 had high δ^{53}Cr values

relative to Atlantic waters measured during this study and by others (e.g. **Chapter 3**; Bonnand *et al.* 2013; Scheiderich *et al.* 2015). This suggests that high $\delta^{53}Cr$ values are a year-round feature of the Celtic shelf. It is clear that Cr behaviour is associated with biological uptake and remineralisation in this region, and thus it is likely that Cr is repeatedly cycled on the shelf like carbon and N (Kitidis *et al.*, 2017; Wakelin *et al.*, 2012). Although most organic matter is recycled on the shelf, a small amount is lost *via* transport off the shelf (Wakelin *et al.*, 2012), presumably along with some of the Cr contained within it. This Cr is likely to have low $\delta^{53}Cr$ due to the preferential biological uptake of ^{52}Cr (Han *et al.*, 2012; Sikora *et al.*, 2008) or adsorption of Cr(III) derived from reduction of Cr(VI) (see **Section 4.5.3** and **Chapter 3**) which may explain why $\delta^{53}Cr$ values are persistently higher on the shelf. Given that $\delta^{53}Cr$ values are consistently high in other shelf seas and coastal areas (**Figure 4.8**; **Chapter 3**; Bonnand *et al.* 2013, Scheiderich *et al.* 2015), it is possible that there is a common process which differentiates shelf and open ocean $\delta^{53}Cr$ values.

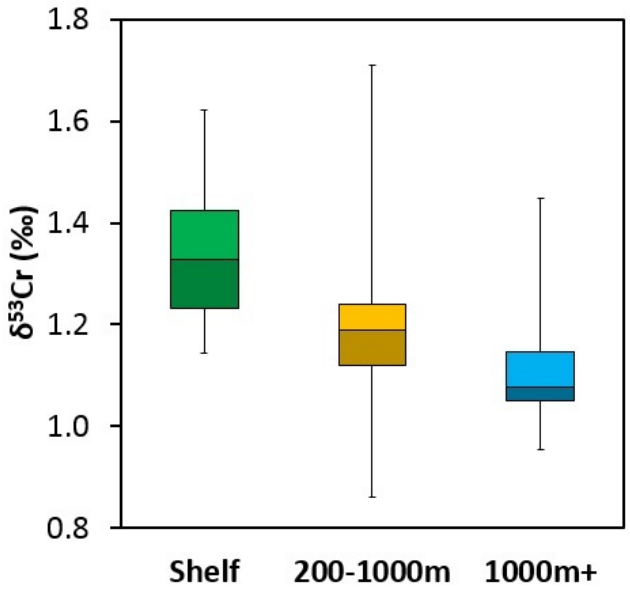

Figure 4.8 - Box and whisker diagram displaying interquartile $\delta^{53}Cr$ ranges for shelf waters, intermediate waters (200-1000m) and deep waters (1000m+) in the North Atlantic, compiled from the datasets of Bonnand *et al.* 2013, Scheiderich *et al.* 2015, Chapter 3 and this work. Capped vertical lines represent full $\delta^{53}Cr$ range, bottom and top boxes represent 2nd and 3rd quartiles respectively, and centre horizontal lines are median values.

4.5.2. Cr behaviour on the shelf slope

Cr_T values were much higher in Autumn 2014 compared to Spring and Summer 2015. Since the samples from Autumn 2014 were taken from a different location (a canyon), either (or both) spatial or seasonal effects could be responsible for this difference. Attenuance is elevated within the canyon due to sedimentary inputs from the shelf slope and this material is a source of particulate Fe and Cr (Angela Milne, pers. comms., University of Plymouth). However, whilst dissolved Fe is positively correlated with attenuance suggesting that nepheloid layers are a source of dissolved Fe to the water column (pers. comms., Antony Birchill, University of Plymouth), there is no correlation between Cr_T and attenuance, suggesting that nepheloid layers do not supply a significant amount of dissolved Cr to the canyon. On the other hand, Cr_T is positively correlated with nutrients during Autumn. At this time of year, respiration usually exceeds production (Joint *et al.*, 2001) and in support of this rates of dissolved organic carbon (DOC) production were low whereas rates of N regeneration were high during Autumn 2014 (pers. comm., Claire Mahaffey, University of Liverpool) meaning that Cr release from organic matter is likely to have been more important than biological uptake. The low $\delta^{53}Cr$ values also support the return of isotopically light Cr to the water column, and are consistent with remineralisation of organic matter with low $\delta^{53}Cr$. Thus we attribute higher Cr_T values on the Celtic slope to seasonal effects involving the remineralisation of organic material, rather than spatially variable sedimentary inputs.

In Spring 2015, Cr_T values within the SML were generally elevated compared to underlying NEACW. This could be explained by either (i) transport of shelf waters with higher Cr_T into the SML off-shelf, or (ii) adsorption of Cr to biological particles (scavenging) through the water column, or both. Cr_T values are higher throughout the water column during Autumn 2014, which suggests that Cr has been removed from the water column during Spring and Summer 2015. This is best explained by scavenging and this is reflected in the strong relationship between Cr_T and attenuance for two of the sites (Fe09 and Fe11; **Figure 4.6D**). This would also explain why Cr_T and $\delta^{53}Cr$ values are not well correlated during this season, since adsorption does not fractionate Cr isotopes (Ellis *et al.*, 2004). On the other hand the elevated $\delta^{53}Cr$ value at the top of the Spring 2015 Fe10 profile (200m, **Figure 4.5C**) is more readily explained by the transport of high $\delta^{53}Cr$ shelf waters; this is made possible through

isopycnal mixing in the thick SML that was present during Spring 2015, but unfortunately since no shelf samples were measured during Spring 2015 this cannot be confirmed.

In Summer 2015, similarly low concentrations of Cr_T were observed below the SML; the lowest Cr_T values measured in this study (1.73-1.75nmol kg^{-1}) were found in the NEACW influenced waters at stations Fe12 and CS2. However during this season there was no relationship between attenuance and Cr_T, suggesting that active removal of Cr was not important during this season. It is possible that Cr removed during Spring 2015 was simply not replenished due to strong stratification during summer and was instead recycled within the thin SML, or removed to sediments.

A distinct feature of the Summer 2015 profiles is the increase in $\delta^{53}Cr$ closer to the shelf. This increase is positively correlated with salinity ($R^2 = 0.66$, discounting the 1810m NEADW sample from Fe09 which was too deep to interact with shelf waters), because lower salinity NEACW has a lower $\delta^{53}Cr$ than high salinity shelf waters. Therefore both our Winter Early 2015 and Summer 2015 data capture the transition from distinctive high shelf $\delta^{53}Cr$ values to lower $\delta^{53}Cr$ Atlantic-derived water values.

Another feature during Autumn 2014 and Spring 2015 was the presence of relatively high $\delta^{53}Cr$ between ~700 and 900m. These are not consistent with the addition of Cr from remineralisation because (i) there is no associated increase in Cr_T and (ii) Cr added from remineralisation should have relatively low $\delta^{53}Cr$ (Han *et al.*, 2012; Sikora *et al.*, 2008). Attenuance is slightly higher over this depth interval, but other nepheloid layers above and below this interval are not associated with elevated $\delta^{53}Cr$. Finally, although this depth interval coincides with input of MW, the size of the $\delta^{53}Cr$ anomaly decreases with distance from the shelf edge whereas the characteristic high salinity of MW increases in that direction, suggesting that this water mass does not carry a high $\delta^{53}Cr$ value. It is possible that Cr with high $\delta^{53}Cr$ from the shelf was adsorbed onto particles and underwent remineralisation at 700-900m, or was transferred in dissolved form from the shelf to these depths *via* deep Ekman transport as has been observed for Fe (Cullen *et al.*, 2009).

4.5.3. Evidence for Cr isotopic fractionation by biological processes

Given the relationship between N and Cr on the shelf in Winter Early 2015 and the nutrient-type profile of Cr_T in Autumn 2014, it is apparent that Cr cycling in the Celtic Sea is linked

with remineralisation processes at certain times of year. Although phytoplankton and microbes have been found to reduce Cr(VI) to Cr(III) and fractionate Cr isotopes in laboratory experiments (Han *et al.*, 2012; Semeniuk *et al.*, 2016; Sikora *et al.*, 2008; Wang and Dei, 2001), it is not clear whether biological processes significantly fractionate Cr isotopes in the natural environment. Inorganic processes such as reduction of Cr(VI) by Fe(II) can also strongly isotopically fractionate the Cr(III) and Cr(VI) pools (Døssing *et al.*, 2011; Kitchen *et al.*, 2012), and adsorption of the resulting Cr(III) to biological particles (e.g. Abu-Saba and Flegal 1997; Semeniuk *et al.* 2016) may occur. Thus, seawater Cr_T and $\delta^{53}Cr$ values may be linked to biological processes even if these biological processes are not the cause of fractionation. This makes it difficult to distinguish between inorganic and biological mechanisms of fractionation using only seawater $\delta^{53}Cr$ data. Separate isotopic analyses of organic and sedimentary particulate material would be useful to determine the importance of biological *versus* lithogenic uptake of Cr(III), but this would not clarify whether reduction occurred before or after Cr was taken up onto organic material. Analyses of the isotopic composition of the dissolved Cr(III) and Cr(VI) pools may help; Cr fractionated during biological reduction should be sequestered within cells during the reduction process leaving remaining dissolved Cr(III) unaffected, whereas Cr reduced and fractionated by inorganic reactions has the potential to remain in the water column for some time before removal if the concentration of organic particles is low. Therefore inorganic processes may lower the $\delta^{53}Cr$ value of dissolved Cr(III) more than biological uptake.

Nevertheless, high $\delta^{53}Cr$ values within the SML together with a small depletion in Cr_T within the high Chl-a zone was observed at station Fe09 in Summer 2015 (**Figure 4.5D**), consistent with preferential ^{52}Cr uptake by cells. The lower $\delta^{53}Cr$ values in the NEACW along with higher Cr_T could also be consistent with the return of remineralised Cr with low $\delta^{53}Cr$. Examination of salinity data (**Figure 4.3A**) suggests that high $\delta^{53}Cr$ shelf waters are not tranported as far as station Fe09, and indeed surface waters are thought to travel onto the shelf when the water column is highly stratified, rather than off the shelf (Huthnance *et al.*, 2009). Therefore the high $\delta^{53}Cr$ values may have arisen from *in situ* reduction of Cr(VI) to Cr(III) due to biological processes given the exceptionally high Chl-a concentrations (up to 1.24 mg m^{-3}) in the SML at this station. Only a very small change (0.09nM) in Cr_T was

observed between 20 and 200m, but the fractionation factors for biologically mediated Cr reduction are quite large ($\Delta_{Cr(VI)-Cr(III)}$ = 4.1; Sikora *et al.* 2008). If we assume the SML initially had Cr_T and $\delta^{53}Cr$ values similar to those found at 200m (2.10nmol kg^{-1}, 1.22‰) and apply a fractionation factor of 4.1‰ to the 0.09nM which has been removed, the estimated $\delta^{53}Cr$ value for the SML is 1.38‰ which is close to the value observed at 20m (1.45 ± 0.06‰). Thus, significant changes in $\delta^{53}Cr$ can occur as a result of biological reduction of Cr(VI) even with very little corresponding loss of Cr. Alternatively Cr may not have been lost to deeper waters and may instead have been recycled within the SML, which would also cause little net loss of Cr whilst still imparting high $\delta^{53}Cr$ values to seawater within the SML. The properly assess the importance of biological processes on global $\delta^{53}Cr$ it is clear that more data need to be obtained, especially for surface waters and particulate material in areas with high levels of biological activity. In addition, the extent and mode (e.g. extracellular or intercellular) of Cr uptake by phytoplankton may be expected to vary considerably for different assemblages (Li *et al.*, 2009; Semeniuk *et al.*, 2016), and the biological fractionation factor may be expected to vary under different environmental conditions (Han *et al.*, 2012; Sikora *et al.*, 2008).

4.5.4. Comparison of Celtic seawater with global ocean seawater

The Cr data from this study are plotted alongside the global correlation line found by Scheiderich *et al.* 2015 in **Figure 4.9**. The correlation between $\delta^{53}Cr$ and Cr_T is thought to arise from the preferential reduction and removal of ^{52}Cr from surface waters and oxygen minimum zones to sediments, and the return of this Cr to the water column following sedimentary Cr oxidation (Scheiderich *et al.*, 2015). Overall the Celtic Sea data fall close to the line but are considerably more scattered than some other data sets, and in fact when the Celtic Sea data are plotted by themselves there is no trend between Cr_T and $\delta^{53}Cr$. This reflects the fact that $\delta^{53}Cr$ and Cr_T values of the Celtic Sea are affected by local processes, such as mixing of waters from isotopically distinct pools (i.e. shelf waters and Atlantic Ocean waters), and adsorption of Cr(III) onto particles.

Seasonal variations in Cr_T and $\delta^{53}Cr$ seemed to be confined to the top 1000m of the water column, and except for one value in Spring 2015 (1.42‰, 1000m Fe10) all samples from below 1000m water depth had a very narrow range of $\delta^{53}Cr$ values (1.05 ± 0.11‰). This is consistent with other studies which show that deep water North Atlantic $\delta^{53}Cr$ values are

generally within the range of 1.0-1.2‰ (**Figure 4.8**; **Chapter 3**; Scheiderich *et al.* 2015). The $\delta^{53}Cr$ of Cr in any water mass is defined by (i) the source of Cr supplied to the ocean and (ii) oceanic processes fractionate Cr isotopes. Obviously deep water masses are prevented from mixing with shelf waters due to density differences and additionally, the vast majority of organic material produced around shelf seas is recycled on the shelf (Wakelin *et al.*, 2012) and does not reach the deep oceans. Therefore shelf sea biological and hydrological processes probably have little effect on the Cr_T and $\delta^{53}Cr$ values of water below ~1000m, and this is supported by North Atlantic seawater data (**Figure 4.8**).

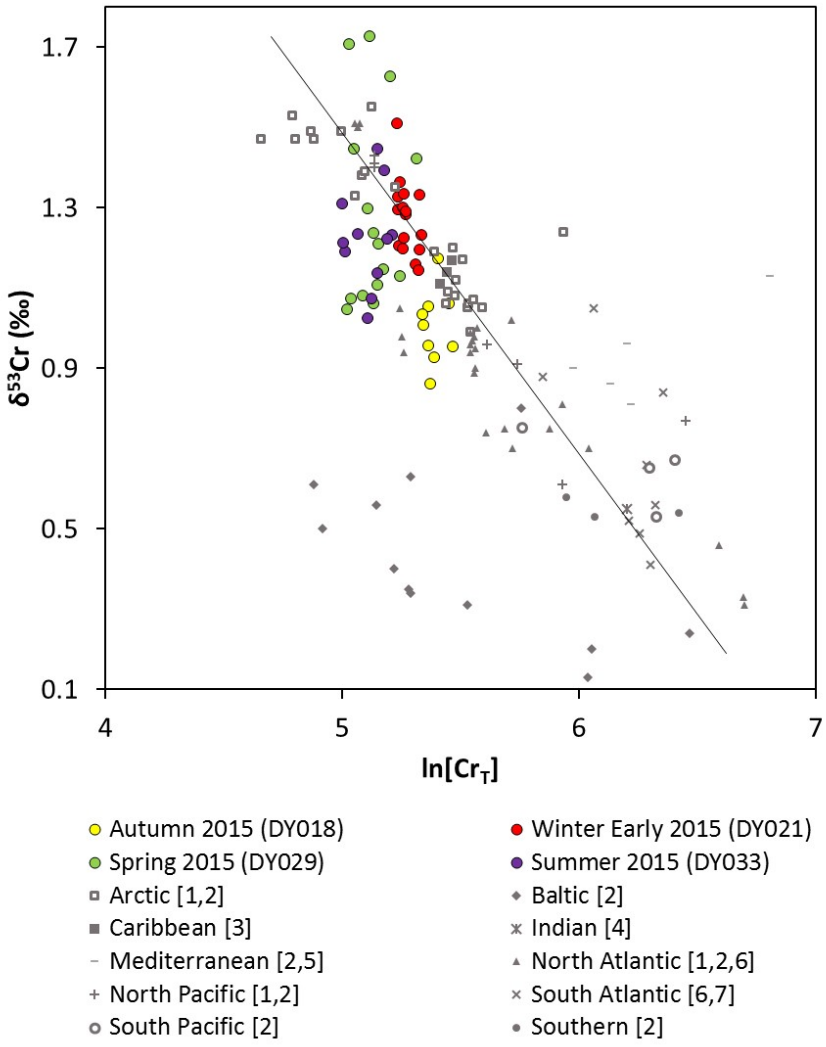

Figure 4.9 - Celtic Sea Cr data plotted alongside Scheiderich *et al.* 2015's global correlation line for $\delta^{53}Cr$-ln[Cr_T]. Ln[Cr_T] was calculated using units of ng kg^{-1} for consistency with previous studies. References are as follows: [1] Scheiderich *et al.* 2015, [2] Paulukat *et al.* 2016, [3] Holmden 2013, [4] Paulukat *et al.* 2015, [5] Economou-Eliopoulos *et al.* 2016, [6] Bonnand *et al.* 2013, [7] Pereira *et al.* 2015.

4.5.5. Implications for Cr isotopes as a tracer of paleoredox in the oceans

The residence time of Cr in seawater is relatively long (~9500 years; Reinhard *et al.* 2014) but it is nevertheless apparent that both Cr concentrations and $\delta^{53}Cr$ are variable in seawater (**Figure 4.5**). The ^{52}Cr isotope is thought to be preferentially reduced to Cr(III) under reducing conditions in seawater and Cr(III) is then removed by precipitation or adsorption, driving seawater to higher $\delta^{53}Cr$ values (Scheiderich *et al.*, 2015). Therefore differences in the $\delta^{53}Cr$ values of marine deposits are thought to partly reflect changes in dissolved oxygen levels (D'Arcy *et al.*, 2016; Gilleaudeau *et al.*, 2016; Rodler *et al.*, 2016). This study, however, demonstrates that $\delta^{53}Cr$ can vary by up to 0.86‰ within a relatively small geographic area despite pervasive oxic conditions throughout the water column. This variation in $\delta^{53}Cr$ is rather attributed to (i) mixing between shelf and off-shelf water masses that have different $\delta^{53}Cr$ and Cr concentrations, and (ii) organic matter cycling.

The variability of 0.86‰ we observed due to hydrological and biological processes implies that $\delta^{53}Cr$ does not necessarily directly scale with processes related to seawater oxygen levels. Shelf processes must, therefore, be considered when interpreting authigenic $\delta^{53}Cr$ signatures from shelf or near-shelf marine deposits. For example, $\delta^{53}Cr$ shifts between 0.40 – 0.91‰ in authigenic sediments from the Peru Margin were interpreted to arise from glacial-interglacial changes in seawater oxygenation (Gueguen *et al.*, 2016), but this range is smaller than that which could be induced by hydrological and remineralisation processes under fully oxic conditions. In that study $\delta^{53}Cr$ values were also positively correlated with $\delta^{15}N$ values and the relationship was interpreted to reflect increasing denitrification under reduced seawater oxygenation conditions (Gueguen *et al.*, 2016). However such a correlation could arise without invoking low dissolved oxygen levels; for instance if the sediments recorded nitrate assimilation (which raises $\delta^{15}N$; Robinson *et al.* 2012) within waters which received Cr with high $\delta^{53}Cr$ from the shelf.

Overall, an oxic $\delta^{53}Cr$ variability of 0.86‰ represents a small but significant portion of the total range measured in the authigenic fraction of marine sediments (-0.36 – 5.00‰; e.g. Frei *et al.* 2009; Frei *et al.* 2011; Gilleaudeau *et al.* 2016; Holmden *et al.* 2016; Rodler *et al.* 2016; Sial *et al.* 2015). This variability should be considered not just for deposits that have $\delta^{53}Cr$ values in the range of the Celtic Sea (i.e. 0.86 – 1.73‰) but for any deposits from a shelf or shelf slope, because the absolute $\delta^{53}Cr$ values recorded in authigenic material may

be skewed from the value of coeval seawater due to fractionation during deposition. For example authigenic carbonate sediments may faithfully record changes in seawater $\delta^{53}Cr$ but not its absolute value, because carbonate precipitation induces some fractionation in its own right (by up to ~0.3‰; Rodler *et al.* 2015). Furthermore the absolute $\delta^{53}Cr$ of seawater may itself change if the Cr flux and/$\delta^{53}Cr$ value of Cr sources to the oceans changes (Lehmann *et al.*, 2016). It may also be worthwhile to consider whether seasonal changes in $\delta^{53}Cr$ could bias the $\delta^{53}Cr$ value of black shale deposits that would primarily deposited in spring/summer. Uptake of ^{52}Cr appears to be higher in spring and summer, and this may decrease $\delta^{53}Cr$ in organic material that is transferred to sediments. Alternatively, adsorption of Cr derived from shelf waters that have high $\delta^{53}Cr$ may be more likely when organic matter concentrations are higher, which may cause transfer of relatively high $\delta^{53}Cr$ values to black shales. Further exploration of $\delta^{53}Cr$ in marine particles is required to understand the role of organic matter in setting the $\delta^{53}Cr$ value of organic-rich sediments.

Shelf slope sedimentary sequences may not represent global scale palaeoceanographic trends because they are affected by local, seasonal processes. The majority of the variability in seawater $\delta^{53}Cr$ values occurs in the first 1000m of the water column but deep water masses appear to have much more consistent $\delta^{53}Cr$ values (~1.0 - 1.2‰ in the modern North Atlantic Ocean (**Figure 4.8**; **Chapter 3**; Scheiderich *et al.* 2015) which means that sediments formed in deep waters are more likely to be representative of global trends.

4.6. Conclusions

Our study shows that there is considerable variability in seawater $\delta^{53}Cr$ both spatially and temporally in the Celtic Sea. The principle causes of these variations are (i) cycling of organic material and (ii) changes in seawater stratification. It appears that ^{52}Cr is preferentially incorporated into particulate organic material in spring and summer when Chl-a concentrations are high, either due to biologically mediated reduction of Cr(VI) to Cr(III) or adsorption of Cr(III) after inorganic reduction processes occur, or both. In autumn, this Cr is returned to the water column due to remineralisation of organic material, which lowers seawater $\delta^{53}Cr$ and increases its Cr concentrations. Atlantic waters appear to act as a source of Cr with low $\delta^{53}Cr$ to the shelf in winter, whereas in spring and summer shelf waters are transported off-shelf and represent a source of Cr to the SML in off-shelf waters due to

strong stratification. Our results also confirm that shelf waters tend to have relatively high $\delta^{53}Cr$ values whereas deep water masses (>1000m water depth) have more consistent and lower $\delta^{53}Cr$ values of 0.95 – 1.13‰ (apart from one anomalous value of 1.42‰).

The impact of shelf processes on seawater $\delta^{53}Cr$ must be considered in the interpretation of the $\delta^{53}Cr$ record of authigenic matieral deposited on or near the shelf. To this end, analyses of the Cr isotopic composition of both the Cr(III) and Cr(VI) fractions of seawater and sediment pore waters, as well as the organic and lithogenic fractions of particulate materials and sediments, would be useful to better resolve the mechanisms of shelf Cr redox cycling and the scale of off-shelf Cr transport.

Chapter 5: Behaviour of chromium and chromium isotopes during estuarine mixing: Beaulieu estuary, UK

5.1. Introduction

Chromium is a redox sensitive element with two oxidation states, Cr(VI) and Cr(III). Partial reduction of Cr(VI) to Cr(III) leads to enrichment of light Cr isotopes in the Cr(III) product, and enrichment of heavier isotopes in the remaining Cr(VI) (Døssing *et al.*, 2011; Han *et al.*, 2012; Kitchen *et al.*, 2012; Sikora *et al.*, 2008; Zink *et al.*, 2010). Conversely, oxidation reactions (Cr(III) → Cr(VI)) are thought to favour the transfer of ^{53}Cr into the Cr(VI) product (Bain and Bullen, 2005; Crowe *et al.*, 2013; Frei *et al.*, 2014; Joshi *et al.*, 2011; Zink *et al.*, 2010). Most samples of ground water and seawater analysed to date have δ^{53}Cr values (δ^{53}Cr = the ^{53}Cr/^{52}Cr ratio of a sample expressed relative to the NBS979 standard; see **Chapter 1**) higher than those of crustal rocks (-0.12 ± 0.10‰; Schoenberg *et al.* 2008). These values are attributed to the preferential release of ^{53}Cr during oxidative weathering of Cr(III) in rocks to soluble Cr(VI), and transfer of the resulting high δ^{53}Cr waters into the oceans *via* rivers. Past changes in seawater δ^{53}Cr, preserved in the authigenic fraction of marine sediments, are therefore considered to provide an important record of the levels of atmospheric oxygen that were present at the time they formed (e.g. Frei *et al.* 2016; Frei *et al.* 2009; Gilleaudeau *et al.* 2016; Planavsky *et al.* 2014). However, redox reactions may also occur post-weathering, during riverine transport, and so preserved δ^{53}Cr values may represent a mixture of redox processes.

Rivers typically contain between 2nM and 20nM of Cr (e.g. Bonnand *et al.* 2013 and references therein), but rivers draining mafic lithologies and rivers contaminated with industrial wastes can contain much higher levels (100-2000nM; McClain and Maher 2016; Novak *et al.* 2014; Paulukat *et al.* 2015). Rivers are the main source of Cr to the oceans, supplying >90% of the total Cr input (Bonnand *et al.* 2013; Chester and Murphy 1990; McClain and Maher 2016). Although Cr(VI) is the thermodynamically stable form of Cr in oxygen-replete waters (Elderfield, 1970), rivers commonly contain both Cr(III) and Cr(VI) in varying proportions (Abu-Saba and Flegal, 1995; Comber and Gardner, 2003; Cranston and Murray, 1980; Dolamore-Frank, 1984; McClain and Maher, 2016; Saputro *et al.*, 2014). Rivers with pH values of >7.5 tend to carry higher proportions of Cr(VI) (Saputro *et al.*,

2014), and this species behaves quite conservatively in some estuaries; i.e. its concentration is mainly determined by the proportion of freshwater to seawater, and it does not undergo any reactions within the estuarine mixing zone (Cranston and Murray, 1980; Dolamore-Frank, 1984; Mayer and Schick, 1981). However in other rivers and estuaries Cr(VI) may be reduced to Cr(III) by organic molecules or by photochemically produced Fe(II) (D'Arcy *et al.*, 2016; Kieber and Helz, 1992; Saputro *et al.*, 2014). The resulting Cr(III) is often removed at low salinities due to the flocculation of organic materials (Campbell and Yeats, 1984; Cranston and Murray, 1980; Mayer and Schick, 1981) and it can also adsorb onto sedimentary particles (Abu-Saba and Flegal, 1995; Jonas and Millward, 2010; Mayer and Schick, 1981). In contrast, complexation of Cr(III) with certain organic molecules may stabilise this species in solution (Abu-Saba and Flegal, 1995; Buerge and Hug, 1998; Dolamore-Frank, 1984; Kaczynski and Kieber, 1994).

Published Cr isotope data for exoreic river waters to date are shown in **Figure 5.1** (data from the Damsal River are not included as the catchment is significantly contaminated from chromite mining activities; Paulukat *et al.* 2015). Rivers with higher Cr concentrations tend to have δ^{53}Cr values slightly higher than igneous crust, and these values are thought to arise primarily from the preferential release of ^{53}Cr during oxidative weathering (D'Arcy *et al.*, 2016; Frei *et al.*, 2014). On the other hand, rivers with lower Cr concentrations have a wider range of δ^{53}Cr values that may be attributed to a combination of oxidative weathering and reduction and removal of Cr(VI) within riverine and/or estuarine waters (D'Arcy *et al.*, 2016). The overall δ^{53}Cr range for rivers (-0.33 – 1.68‰; D'Arcy *et al.* 2016; Frei *et al.* 2014; Wu *et al.* 2017) is similar to that of seawater (0.13 – 1.73‰; Bonnand *et al.* 2013; Economou-Eliopoulos *et al.* 2016; Holmden *et al.* 2016; Paulukat 2015; Paulukat *et al.* 2016; Pereira *et al.* 2015; Scheiderich *et al.* 2015; **Chapters 3** and **4**). These data support the idea that the δ^{53}Cr composition of the river source has a strong influence on the δ^{53}Cr values of seawater. However, the mean river value (0.40‰) is significantly lower than the mean seawater δ^{53}Cr value (1.04‰) suggesting that modifications to the δ^{53}Cr value of river-sourced Cr may occur during transport to, or within, the oceans.

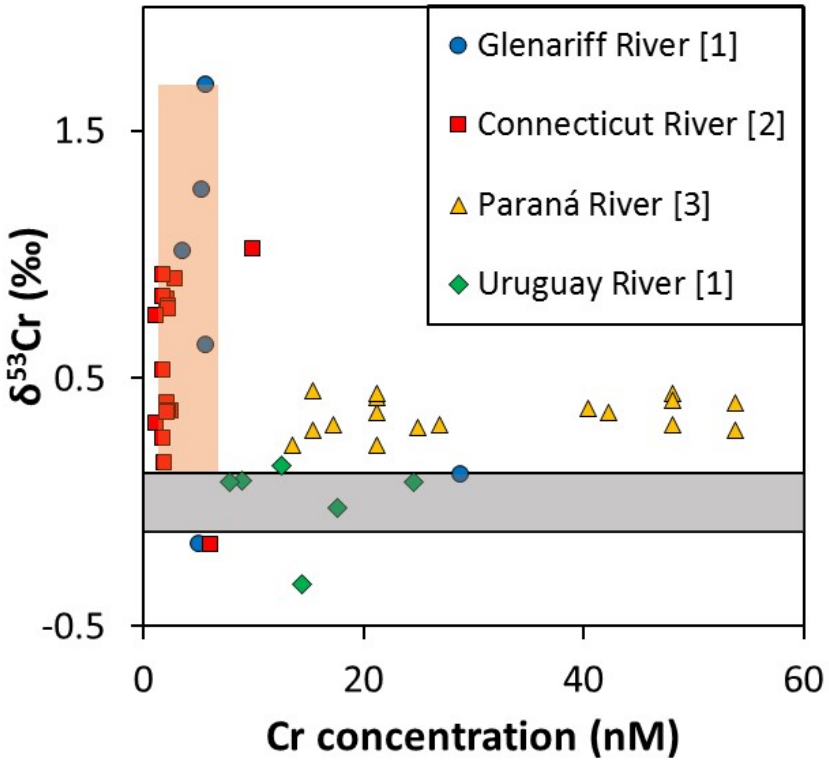

Figure 5.1 - Previously published $\delta^{53}Cr$ data for rivers that drain into the sea. Data includes tributaries to the main rivers for the Glenariff, Connecticut and Paraná Rivers. Horizontal grey bar represents crustal $\delta^{53}Cr$ range. Orange box represents typical $\delta^{53}Cr$ and Cr concentration range for seawater (Bonnand *et al.*, 2013; Paulukat *et al.*, 2016; Scheiderich *et al.*, 2015). References are: [1] D'Arcy *et al.* 2016; [2] Wu *et al.* 2017; [3] Frei *et al.* 2014.

To date, there are only 7 published measurements of $\delta^{53}Cr$ in estuarine waters (D'Arcy *et al.*, 2016; Frei *et al.*, 2014; Paulukat *et al.*, 2015) and they span a range of 0.08 to 1.02‰. An assessment of the variation in $\delta^{53}Cr$ as a function of salinity is not possible because salinity measurements were not provided for any of the analysed samples. In a study of the Glenariff estuary (Ireland), Cr concentrations apparently decreased with increasing total dissolved solids (i.e. as the proportion of seawater to river water increased; D'Arcy *et al.* 2016). However, there were no obvious trends between $\delta^{53}Cr$ and total dissolved solids (TDS), as the $\delta^{53}Cr$ values of waters with low TDS (0.81-0.89‰) were similar to those with higher TDS (0.85-1.01‰).

To fill this gap, we have investigated the processes affecting Cr isotopic signatures within the Beaulieu River and estuary (UK), by measuring both $\delta^{53}Cr$ and Cr speciation with respect to salinity variations. We show that a large proportion of Cr in Beaulieu River water is present as Cr(III), and that unlike most other rivers the $\delta^{53}Cr$ of the Beaulieu River is lower

than that of crustal rocks, possibly due to the preferential mobilisation of ^{52}Cr from pore waters by dissolved organic material. We also show that both Cr(III) and Cr(VI) behave conservatively within the estuary, even in the presence of potential reductants like Fe, and discuss the implications of our findings for interpreting the $\delta^{53}Cr$ record of authigenic phases in marine sediments.

5.1.1. The Beaulieu River and estuary

The Beaulieu River (**Figure 5.2**) is located in the New Forest National Park (UK), and drains into the strait between mainland England and the Isle of Wight known as the Solent. The protected status of the National Park means that it is sparsely populated and there is little industry, so levels of pollution in the Beaulieu River are minimal compared to the rivers that drain the neighbouring city of Southampton (the Rivers Test, Itchen and Hamble).

The New Forest primarily consists of heathlands, woodlands, bogs and wetlands. Surficial deposits are predominantly Paleogene Barton and Headon Group sands, although Quaternary Period alluvia, clays and silts are found around the river and these promote the growth of forest patches (British Geological Society 2017; Gilkes 1968; Tubbs 1969). There are also tidal flats around the mouth of the estuary. The upper limit of the estuary is marked by a sluice gate, upstream of which is a small lake (the Mill Dam; **Figure 5.2**) that sometimes contains a small component of seawater. The depth of the river does not usually exceed ~1m whereas the depth of the estuary changes considerably with the tides, varying between ~0.1 and 4m. The freshwater residence time in the estuary is ~7 days (Fang, 1995), which is similar to the residence time of water in the Solent (~6.25 days; Dyer and Lasta King 1975).

The chemical composition of the Beaulieu River is relatively well characterised (Dolamore-Frank, 1984; Fang, 1995; Holliday and Liss, 1976; Hopwood *et al.*, 2014; Hopwood *et al.*, 2015; Moore *et al.*, 1979). The pH of the river water is fairly neutral (6.5-7.8) and

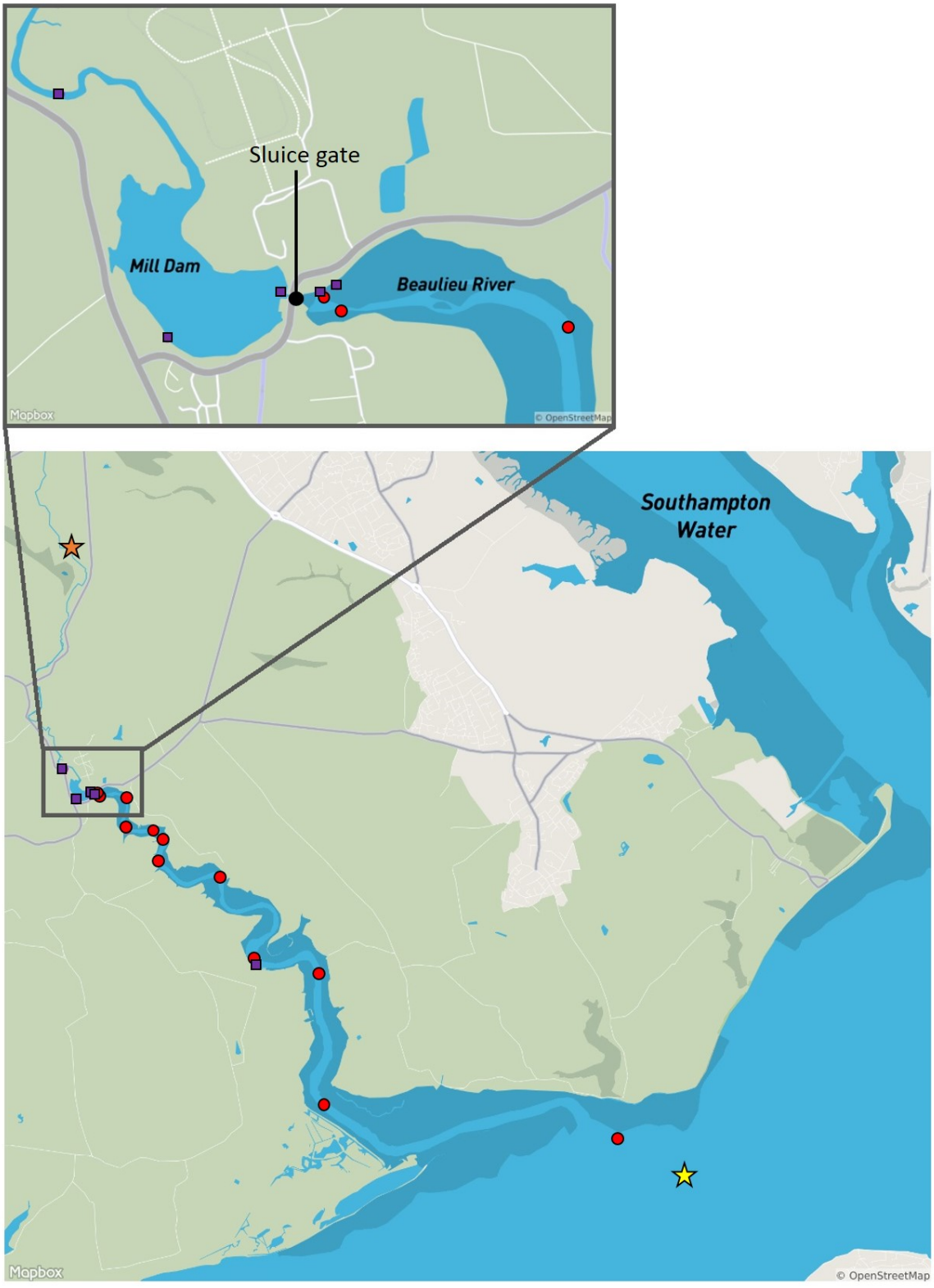

Figure 5.2 - Sampling locations along the Beaulieu River and estuary. Orange star shows freshwater (March 20th 2016) and push core (7th April 2017) collection point. Red circles show 22nd March sample collection points and purple squares show 5th October 2016 collection points. Yellow star shows Bonnand *et al.* 2013 Southampton Water sampling station. Darker blue areas are intertidal flats. See Table 5.2 for sample co-ordinates.

concentrations of dissolved oxygen are high (up to 370µmol L^{-1} dissolved O_2; Hopwood *et al.* 2014). Due to the abundant vegetation in the catchment, the river waters have high levels of dissolved organic carbon (DOC; Moore *et al.* 1979); even at high salinities (*S* = >24), Beaulieu estuarine waters have concentrations of >1mg C L^{-1}. Concentrations of dissolved iron (dFe) in the river are highly variable (8-21µM), and they fall significantly as river waters mix with seawaters, because Fe is incorporated into organic flocculates or forms Fe oxyhydroxide precipitates (Fang, 1995; Holliday and Liss, 1976; Hopwood *et al.*, 2014). Up to ~50% of Fe at low salinities (*S* = <5) is present as Fe(II) (Hopwood *et al.*, 2014); Fe(II) is an effective reductant for Cr(VI) (Døssing *et al.*, 2011; Kitchen *et al.*, 2012).

The concentration of Cr in the Beaulieu River is ~1.5nM (**Chapter 3**; Bonnand *et al.* 2013, although higher concentrations (up to 5nM) have been recorded in the estuary (Dolamore-Frank, 1984). In a previous study chromium appeared to behave conservatively during estuarine mixing, although loss of Cr(VI) was suggested at high salinities, possibly as a result of reduction of Cr(VI) by DOC and removal of the Cr(III) that formed from solution (Dolamore-Frank, 1984). Nevertheless, concentrations of particulate Cr were low even though concentrations of Cr(III) were relatively high, indicating that adsorption of Cr(III) onto particulate material was not an important process in the estuary (Dolamore-Frank, 1984). Although the Cr isotopic compositions of river and estuarine waters of the Beaulieu are unknown, the δ^{53}Cr value of water from Southampton Water (part of the Solent water body) is 1.45-1.51‰, with Cr concentrations of 1.3-1.8nmol kg^{-1} (**Chapter 3**; Bonnand *et al.* 2013; Dolamore-Frank 1984).

5.2. Methods

5.2.1. Sample collection

All containers and sampling/filtration equipment were acid washed before fieldwork began. A river water endmember sample was taken from the King's Hat Enclosure on foot on 20th March 2016 and the estuary was sampled around high tide on 22nd March 2016 from the R.V. *Bill Conway*. A RIB was used access the shallowest waters, but even so waters with low to mid-range salinities (*S* = 1-14) were inaccessible due to low rainfall in the preceding weeks, and the rapid mixing between freshwater and seawater at the sluice gate. A second set of samples targeting a lower salinity range was therefore taken on 5th October

2016 on foot from the river, Mill Dam and upper part of the estuary waters during the early stages of the flood tide.

All samples were collected between 0.1-0.5m depth using a 1L bottle either by (gloved) hand or by deploying a weighted metal free bottle holder. The 1L aliquots were homogenised in a larger container (5-6L total sample volume) and a subsample of this was taken immediately to measure salinity, pH and temperature (WTW Measurement Systems Inc. 340i handheld multimeter).

River pore waters were sampled by insertion of 80mm diameter plastic core liners into the river sediments at the King's Hat Enclosure in April 2017. Cores were immediately transported back to the National Oceanography Centre Southampton (NOCS) and placed in a constant temperature laboratory at 10°C (to approximately match the temperature of the river water) for further processing.

5.2.2. Processing and analysis of water samples

5.2.2.1. Determination of Cr concentration and Cr isotopic composition of river and estuarine waters

As the Cr concentration of river waters and seawater is very low, it was first necessary to pre-concentrate Cr using an Fe co-precipitation method as described in **Chapters 2** and **3**. Critically, this technique is not expected to collect Cr that is bound to organic material, as organically bound Cr is thought to be resistant to reduction and adsorption (Abu-Saba and Flegal, 1997; Nakayama *et al.*, 1981). By contrast, all published analyses of $\delta^{53}Cr$ in river waters to date have been obtained from samples that have been pre-concentrated by evaporation; this is considered to capture all Cr, including the organically bound Cr (Cr_{ORG}) fraction (D'Arcy *et al.*, 2016; Frei *et al.*, 2014; Paulukat *et al.*, 2015). However, it is important to note that a wide range of organic complexes with different binding strengths are present in the Beaulieu River (Hopwood *et al.*, 2015), so our Fe co-precipitation method may incorporate some weakly complexed Cr_{ORG}; thus in these samples the total Cr concentrations (Cr_T, where Cr_T = Cr(VI) + Cr(III)) is operationally defined. Two samples (B1 and B2) were analysed after UV irradiation for ~3 hours in an attempt to oxidise any Cr_{ORG} and assess the contribution of Cr_{ORG} to the total Cr pool (i.e. Cr_T + Cr_{ORG}).

Water samples were filtered within 24 hours of collection in a class 100 clean laboratory using pre-rinsed Sartorius Sartobran 300 capsule filters (0.45µm). The March 2016 samples were then acidified to pH <2 for storage (2ml L^{-1} sub-boiled hydrochloric acid) before further processing, whereas the October 2016 samples were precipitated with Fe on the day of filtration (within ~8 hours). Both of these approaches were expected to successfully capture Cr_T since both immediate precipitation and acidification prevent the adsorption of Cr(III) to the container walls, and adsorption is not thought to be important for Cr(VI) at river water pH (**Chapter 1**; Gaillardet *et al.* 2003).

A ^{50}Cr-^{54}Cr double spike was added to the samples for isotopic analysis to account for any fractionation incurred during sample processing, and to remove the need for sample-standard bracketing during MC-ICP-MS analysis. Based on previous studies (Bonnand *et al.*, 2013; Dolamore-Frank, 1984), Cr_T in the Beaulieu River-estuary system was not expected to exceed ~6nmol kg^{-1}, but around 600nmol kg^{-1} (or ~30 ppb) was required for MC-ICP-MS analysis in medium resolution mode, thus a pre-concentration procedure was employed. Full details of the pre-concentration and purification procedures used for this work can be found in **Chapter 3**. Briefly, the pH of the river water samples (~3L) was adjusted to pH 8-9 ~24 hours after the double-spike was added. Chromium was then removed from solution using an Fe(II) hydroxide precipitate that converts any Cr(VI) to Cr(III) and quantitatively removes the Cr(III) in the form of an Fe(III)-Cr(III) precipitate (Cranston and Murray, 1978). This precipitate was then separated by vacuum filtration. A two stage ion exchange chromatography procedure was carried out to remove the Fe and residual salts using the Biorad AG1-X8 and AG50-X12 resins respectively, and any remaining organic material was oxidised using H_2O_2. The Cr isotopic composition of the purified Cr was determined using a Thermo Fisher Neptune MC-ICP-MS in medium resolution mode. All acids used in the procedure were thermally distilled, while the other chemicals were Romil UpA/Fluka TraceSELECT Ultra/Aristar® Ultra grade to prevent contamination. Newton-Raphson deconvolution and isotope dilution calculations were used to calculate $\delta^{53}Cr$ and Cr_T respectively. This procedure has been shown to give accurate, precise values for $\delta^{53}Cr$ in seawater and estuarine samples by several authors (**Chapter 3**; Bonnand *et al.* 2013; Scheiderich *et al.* 2015).

5.2.3. Determination of Cr speciation in river and estuarine waters

Dissolved Cr(III) concentrations were measured using a modified version of the Fe co-precipitation technique, wherein an oxidised Fe(III) precipitate was used in place of the Fe(II) hydroxide to collect Cr(III) only. Cr(III) is strongly adsorbed to this precipitate, whereas Cr(VI) is not, allowing effective separation of the two species (Cranston and Murray, 1978). The proportions of Cr(III) and Cr(VI) in natural water samples may change rapidly after sample collection (Kingston *et al.*, 1998), so to guarantee the integrity of speciation measurements the Cr(III) subsamples (taken from the bulk 5-6L samples) were filtered, spiked and treated with an Fe(III) precipitate within 4 hours of collection either in a class 100 clean laboratory at NOCS or on board the R.V. *Bill Conway*. Milli-Q (MQ) water blanks were processed alongside the samples in both cases to monitor Cr contamination.

The ^{50}Cr-^{54}Cr double spike was replaced with a ^{53}Cr single spike for Cr(III) analysis and isotope dilution calculations were made using the ^{52}Cr/^{53}Cr ratio. This enabled the use of smaller sample volumes (~500mL) as measurement of the low abundance ^{50}Cr and ^{54}Cr isotopes was not required. Despite the lack of isobaric interferences on ^{52}Cr and ^{53}Cr, large quantities of residual Fe and salts interfere with ICP-MS analysis so an ion exchange procedure similar to that described in **Section 5.2.2** was used to purify the samples after precipitation. ^{52}Cr/^{53}Cr ratios were then measured using an Element 2 ICP-MS. The accuracy of this procedure was tested by processing Cr(III) standards (NBS979) and mixed Cr(III) + Cr(VI) standards (NBS979 and potassium chromate, Fluka TraceCERT®) in MQ water in the same way as samples. Cr(VI) concentrations were subsequently calculated by subtracting Cr(III) from Cr_T.

5.2.4. Analysis of dissolved iron concentrations

Dissolved iron (Fe(II) and Fe(III) in the <0.45µm fraction) concentrations were measured using the ferrozine method (Stookey, 1970). Subsamples (~5mL) were taken from the 5-6L bulk samples and filtered with pre-cleaned 0.45µm syringe filters (Millipore Millex) within 4 hours of collection. 3mL aliquots of these filtered samples were immediately pipetted into vials pre-loaded with 0.2mL of 5mM ferrozine and 0.2mL 10mM ascorbic acid. A series of Fe standards (0-50µM, made with ammonium Fe(II) sulphate) were treated in exactly the same manner. Under these conditions all Fe (Fe(II) + Fe(III)) is converted to Fe(II) and this reacts to form a purple complex with ferrozine. This method collects inorganic Fe and

organically complexed Fe, except for the most strongly bound complexes (Hopwood *et al.*, 2014). The samples and standards were analysed using a Unicom 8625 UV/Visible spectrometer set to measure absorbance at 562nm. A 4cm cell was used to maximise sensitivity and the detection limit was 0.13µM.

5.2.4.1. Processing of push cores and sampling of pore waters

Profiles of dissolved oxygen were measured for two of the four push cores using an optical oxygen meter (Pyroscience FirestingO2 with OX50 needle-type sensor) mounted on a micromanipulator (Pyroscience MU1). The core-top water was then discarded and the top 5cm of sediment from each core was centrifuged to extract the pore water. The pore waters from each of the two sampling locations were then combined before being centrifuged once more. They were then vacuum filtered through pre-cleaned 0.45µm membrane filters (Whatman Polycarbonate). Organic material was oxidised by addition of 0.2mL H_2O_2 and refluxing in 1mL aqua regia at 130°C for ~24 hours. The pore waters were then filtered and any precipitate was digested by refluxing in 0.5mL of hydrogen fluoride at 170°C for 4 days. The samples were finally dried down in 3mL of 7M HCl before being passed through the ion chromatography procedure (i.e. they were not co-precipitated with Fe).

5.3. Results

5.3.1. Method validation for Cr(III) measurements

The average blank for the Cr(III) samples part-processed on board the R.V. *Bill Conway* was 0.08 ± 0.02nmol (n=2) which is well within error of the equivalent long term clean laboratory blank of 0.09 ± 0.06nmol (n=13). This demonstrates that the samples were not compromised by handling outside of a clean laboratory environment. Furthermore two blanks were processed alongside each batch of samples and the 2SD of these blanks did not exceed ±0.02nmol, meaning that the blank subtraction for each processing session was accurate. **Table 5.1** displays the results of method validation tests. Cr(III) standard measurements were within ±4% of the expected value, whereas for mixed Cr(III) + Cr(VI) standards the range was slightly higher at ±10%. The higher error in mixed standards may be due to minor inter-species conversions prior to precipitation, since this was not done until ~24 hours after spiking. Beaulieu samples were precipitated within 4 hours of

collection to circumvent this issue, and the error of the concentration measurements was conservatively taken to be ±10%.

Table 5.1 - Cr(III) results for NBS979 standards in MQ water using Fe(III) precipitation and ^{53}Cr spike.

Standard type	Calculated Cr(III)	Measured Cr(III)	Difference (%)
Cr(III) only	11.00	11.23	2.0
	10.77	11.19	3.8
	10.58	10.48	-2.0
	10.04	10.44	1.9
Cr(III) + Cr(VI)	4.75	5.19	8.6
(1:1 mix)	4.81	5.23	8.0
	5.77	5.25	-9.7
	5.77	5.23	-10.0

5.3.2. Cr and δ^{53}Cr variation in estuarine waters

The range of Cr_T values for samples collected in March 2016 was similar to those measured previously for this location (1.64 - 5.05nmol kg^{-1}; **Table 5.3**; Bonnand *et al.* 2013; Dolamore-Frank 1984) whereas the October samples had very low Cr_T (0.66 - 1.03 nmol kg^{-1}, **Table 5.3**). On both sampling dates Cr_T decreased slightly with salinity; concentrations of Cr(III) decreased with increasing salinity whereas concentrations of Cr(VI) increased (**Table 5.3**; **Figure 5.3**). Between 14 and 16% of Cr was found to be present as Cr(III) in high salinity waters (*S* = >29), whereas low salinity waters (*S* = <5) contained up to 55% of Cr(III). The δ^{53}Cr values increased with increasing salinity (**Figure 5.3**); assuming that the relationship between salinity and δ^{53}Cr was linear, then the δ^{53}Cr of the river endmember (determined by extrapolation of the linear trend) was similar in March (δ^{53}Cr ≈ -0.43‰) and October (δ^{53}Cr ≈ -0.34‰).

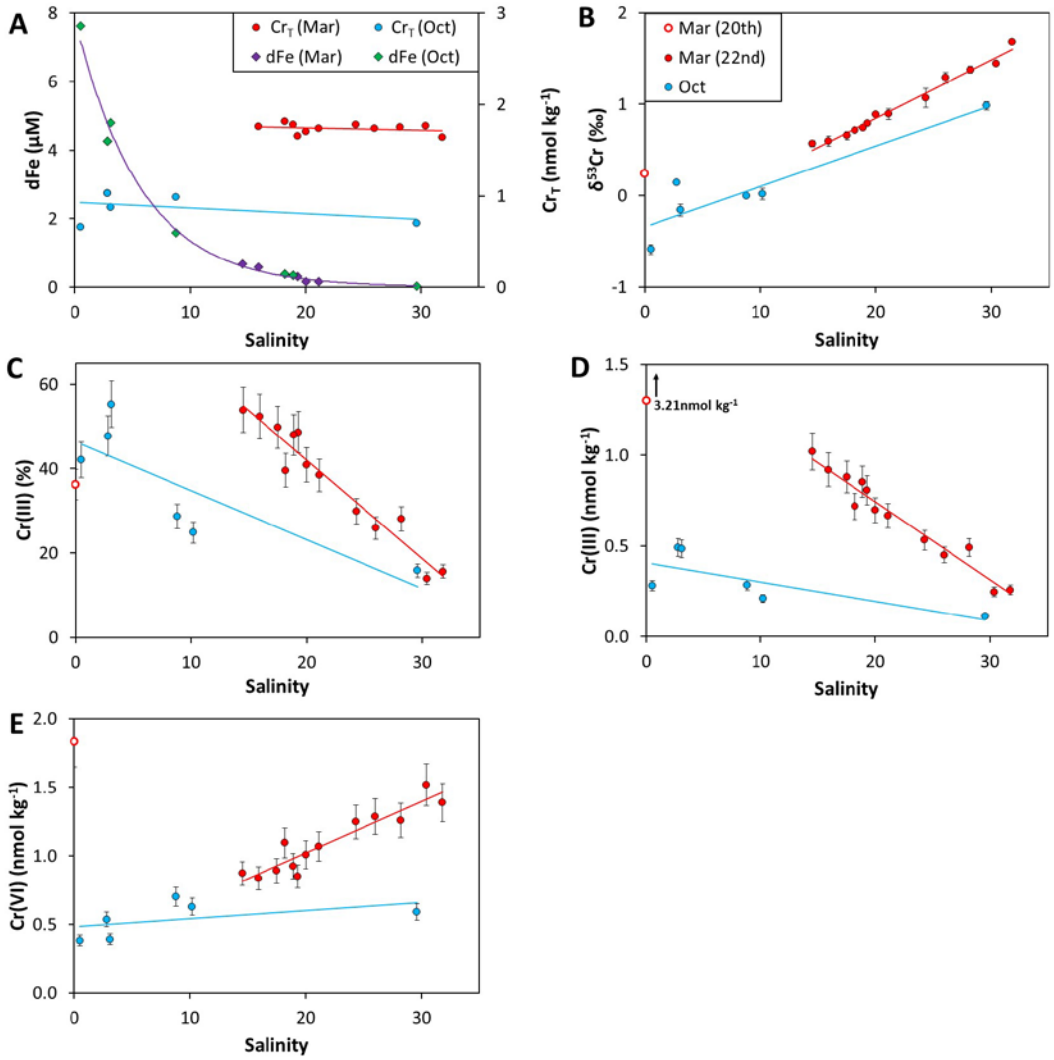

Figure 5.3 - Relationship of salinity in the Beaulieu River with (A) dFe and Cr_T (errors smaller than data points), (B) δ^{53}Cr (2SD error bars, some smaller than data points), (C) Cr(III) as percentage of Cr_T (10% error bars), (D) Cr(III) concentration (10% error bars), (E) Cr(VI) concentration (calculated from Cr(III) and Cr_T concentrations, 10% error bars). The March 20th sample (B1) is excluded from A and from the trend lines in B-E because it is thought to be an outlier (see text).

Table 5.2 - Beaulieu River/estuary sample locations, water measurements ($\delta^{53}Cr$ and Cr_T, Cr(III), Cr(VI) and dFe concentrations), and auxiliary data (salinity, pH, temperature). BDL = Below Detection Limit.

Sampling date	Sample	Latitude	Longitude	Salinity (*S*)	pH	Temperature (°C)	$\delta^{53}Cr$ (‰)	2SD	Cr_T (nmol kg^{-1})	Cr(III) (nmol kg^{-1})	Cr(VI) (nmol kg^{-1})	dFe (µM)
20th March 2016	B1	50.8470	-1.45492	0.0	7.6	8.6	0.24	0.02	5.05	3.21	1.83	12.63
22nd March 2016	B2	50.8189	-1.45039	14.5	7.8	10.4	0.57	0.04	1.89	1.02	0.87	0.68
	B3	50.8192	-1.45045	17.5	7.9	9.6	0.66	0.01	1.77	0.88	0.89	0.17
	B4	50.8184	-1.44563	20.0	8.1	11.3	0.89	0.00	1.70	0.70	1.01	0.30
	B5	50.8147	-1.44441	19.3	8.0	10.2	0.79	0.06	1.66	0.81	0.85	0.17
	B6	50.8150	-1.43885	21.1	8.0	10.3	0.89	0.02	1.74	0.67	1.07	0.59
	B7	50.8134	-1.43790	15.9	7.9	11.1	0.59	0.04	1.76	0.92	0.84	0.39
	B8	50.8134	-1.43790	18.2	8.0	10.3	0.72	0.02	1.81	0.72	1.09	0.34
	B9	50.8110	-1.43908	18.9	8.0	11.4	0.74	0.06	1.78	0.85	0.92	BDL
	B10	50.8087	-1.42809	24.3	8.1	10.7	1.07	0.11	1.78	0.53	1.25	BDL
	B11	50.8005	-1.42216	26.0	8.0	10.3	1.29	0.06	1.74	0.45	1.29	BDL
	B12	50.7978	-1.41076	28.2	8.1	10.3	1.38	0.04	1.75	0.49	1.26	BDL
	B13	50.7828	-1.40701	30.4	8.1	10.3	1.44	0.02	1.77	0.25	1.52	BDL
	B14	50.7835	-1.36943	31.8	8.1	9.9	1.68	0.04	1.64	0.26	1.39	BDL
5th October 2016	B15	50.8192	-1.45078	10.2	7.4	14.7	0.02	0.06	0.84	0.21	0.63	1.37
	B16	50.822	-1.45667	0.5	7.0	13.3	-0.59	0.05	0.66	0.28	0.38	7.55
	B17	50.8184	-1.45384	2.8	7.6	14.7	0.14	0.01	1.03	0.49	0.54	4.22
	B18	50.8192	-1.45135	3.1	7.3	13.7	-0.16	0.07	0.87	0.48	0.39	4.76
	B19	50.8192	-1.45101	8.8	7.3	15.7	0.00	0.01	0.99	0.28	0.70	1.57
	B20	50.7994	-1.42062	29.6	8.1	17.1	0.98	0.04	0.70	0.11	0.59	0.03

Table 5.3 - Pearson correlation co-efficients for various Cr parameters on the two main sampling dates (22nd March and 5th October), with strong correlations (≥ ±0.7) in bold type.

22nd March 2016	$\delta^{53}Cr$	Cr_T	Cr(III)	Cr(VI)	*S*	pH
Cr_T	-0.56					
Cr(III)	**-0.96**	0.56				
Cr(VI)	**0.92**	-0.31	**-0.96**			
S	**0.99**	-0.57	**-0.98**	**0.92**		
pH	**0.72**	**-0.70**	**-0.79**	0.67	**0.77**	
dFe	**-0.74**	0.48	**0.77**	**-0.71**	**-0.78**	**-0.72**
5th October 2016	$\delta^{53}Cr$	Cr_T	Cr(III)	Cr(VI)	*S*	pH
Cr_T	-0.04					
Cr(III)	-0.46	0.62				
Cr(VI)	0.50	0.41	-0.46			
S	**0.92**	-0.35	**-0.76**	0.48		
pH	**0.98**	-0.01	-0.36	0.41	**0.85**	
dFe	**-0.80**	-0.16	0.57	**-0.84**	**-0.80**	**-0.70**

5.3.3. Cr associated with organic material

The results for UV irradiated samples are provided in **Table 5.4**. Both UV irradiated samples showed higher concentrations compared to non-irradiated aliquots, indicating that at least 18-25% of Beaulieu River Cr was organically bound. Both samples also had lower $\delta^{53}Cr$ compared to non-irradiated samples, which demonstrates that the Cr_{ORG} fraction has a lower $\delta^{53}Cr$ than the mostly inorganic Cr_T fraction. Calculated $\delta^{53}Cr$ values for the Cr_{ORG} fraction in samples B1 and B2 are -1.01‰ and -0.66‰ respectively.

Table 5.4 - Results for UV irradiated samples.

Sample	$Cr_T + Cr_{ORG}$ (nmol kg^{-1})	Cr_{ORG} (nmol kg^{-1})	Cr_{ORG} (%)	$Cr_T + Cr_{ORG}$ $\delta^{53}Cr$ (‰)	2SD	Calculated Cr_{ORG} $\delta^{53}Cr$ (‰)
B1	6.17	1.13	18	0.06	0.01	-1.01
B2	2.52	0.63	25	0.40	0.01	-0.66

5.3.4. Cr concentration and Cr isotopic composition of pore waters

The core-top waters contained 230-260µM dissolved O_2, and the pH at approximately 1cm depth (measured in one core only) was 6.9. Oxygen profiles (**Figure 5.4**) revealed a shallow average oxygen penetration depth of 2.9 ± 1.7mm (2SD). Cr_T concentrations of pore waters from the two different locations were 100 and 120nmol kg^{-1} and $\delta^{53}Cr$ values were slightly higher than those of crustal rocks (-0.12 ± 0.10‰; Schoenberg *et al.* 2008), at 0.06 ± 0.05‰ and 0.13 ± 0.05‰ respectively. These analyses included all Cr_{ORG} in the pore waters as the Fe co-precipitation method was not used.

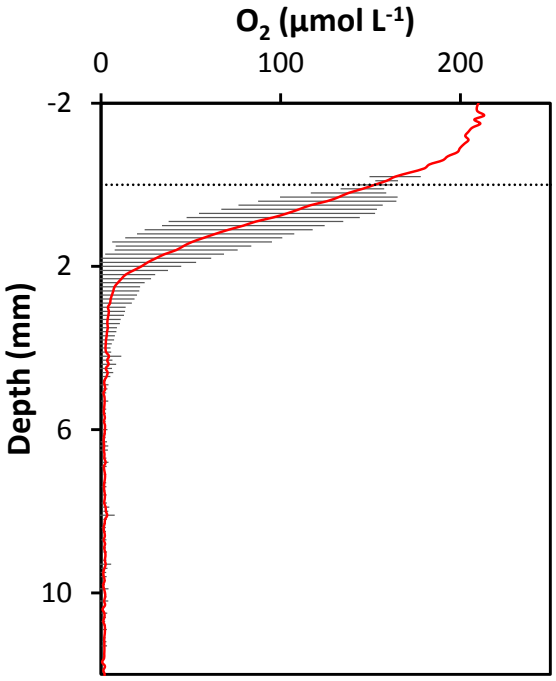

Figure 5.4 - Combined O_2 profile for river sediment push cores (n=3). Solid horizontal lines are error bars (none for -2.0 to -0.2mm as only one set of measurements taken). Dotted line is sediment-water interface.

5.3.5. Behaviour of dFe during estuarine mixing

Concentrations of dFe (**Table 5.3**) were within the range previously measured for the Beaulieu River and estuary (Fang, 1995; Hopwood *et al.*, 2014; Moore *et al.*, 1979). An exponential decrease in dFe with salinity was observed in October 2016 indicating removal at low salinities as found by other studies (Fang, 1995; Holliday and Liss, 1976). In March 2016, dFe was undetectable at S = >21.1 whereas in October a small but detectable amount of Fe was still present at S = 29.8.

5.4. Discussion

5.4.1. Conservative Cr behaviour in the Beaulieu River-estuary system

Assuming that the relationship between Cr_T and salinity is linear throughout the Beaulieu estuary, then the concentrations of inorganic Cr in the river water endmember (S = 0) and the seawater endmember (S = 35) must be similar, but the absolute ranges were distinctly different in March and October (1.6 - 1.9nmol kg^{-1} and 0.7 – 1.0 nmol kg^{-1} respectively). The results for March are consistent with previous studies, which have found concentrations of ~1.5nM in both the Beaulieu River and in Southampton Water (**Chapter 3**; Bonnand *et al.*

2013; Dolamore-Frank 1984). Cr_T concentrations in October, however, were significantly lower than previously measured in the Beaulieu estuary, and were also lower than concentrations measured in most global rivers (e.g. McClain and Maher 2016; Wu *et al.* 2017). In October, a greater proportion of dissolved Cr may have been in the organic fraction that is not captured by our Fe co-precipitation method, due to the release of dissolved organic material during the autumn as a result of the decomposition of deciduous tree leaves. Organic molecules from leaf litter leachates have been shown to bind copper more strongly in the earlier stages of decomposition, because microbes transform or consume the most effective organic ligands (proteins and polyphenol-like compounds) over time (Cuss and Gueguen, 2012). It is possible that a similar situation applies to Cr. In support of this, large amounts of natural foam were observed on the river surface in October, suggesting that concentrations of organic surfactants were high. Additionally, dFe was still detectable at higher salinities in October, also consistent with the presence of more organic ligand stabilised dFe.

Although both Fe and Cr have previously been shown to be removed by flocculation of organic materials at low salinities (Cranston and Murray, 1980; Dolamore-Frank, 1984; Hopwood *et al.*, 2014; Moore *et al.*, 1979; Sholkovitz *et al.*, 1978), there is no relationship between Cr_T and dFe concentrations at low salinities in the Beaulieu estuary (R^2 = -0.01 for October; **Table 5.3**). This may suggest that Cr is unaffected by flocculation of organic material, but it is important to note that while the ferrozine method used to measure dFe in this study includes most organically bound Fe (Hopwood *et al.*, 2015), our Fe co-precipitation technique may not effectively capture organically bound Cr. It is clear, however, that Cr in the (mainly) inorganic fraction behaves conservatively during estuarine mixing in the Beaulieu estuary; the linear relationships between $\delta^{53}Cr$, Cr(III), Cr(VI) and salinity (**Figure 5.3**) can be explained by simple two end-member mixing between high Cr(III)/low Cr(VI), low $\delta^{53}Cr$ river water and low Cr(III)/high Cr(VI), high $\delta^{53}Cr$ seawater.

It is possible that Cr removal occurs at extremely low salinities (<1) as observed for the St Lawrence estuary, Canada (Campbell and Yeats, 1984), as we were unable to sample salinities between 0 and 1 in detail. This could explain why sample B1, that was taken much further upstream than the others, had a much higher Cr_T (5.05nmol kg^{-1}) compared to other samples. However, the most likely reductants of Cr(VI) in the Beaulieu are Fe(II) and DOC,

and the Rayleigh fractionation factors for these processes are large ($\Delta_{Cr(VI)-Cr(III)}$ = 3.6 – 4.2 for reduction by Fe(II) and 3.1 for reduction by organic molecules; Døssing *et al.* 2011; Kitchen *et al.* 2012). Even a relatively small amount of reduction (15-20%) in waters of salinity 0-1 would result in higher δ^{53}Cr values than those actually observed in the estuary (**Figure 5.5**). Thus, aqueous Cr(VI) reduction processes do not appear to be important in the Beaulieu River-estuary system. On the other hand, removal of Cr(III) by adsorption would not be expected to cause significant fractionation (Ellis *et al.*, 2004), so adsorption of Cr(III) to particles could potentially have occurred at very low salinities (<1).

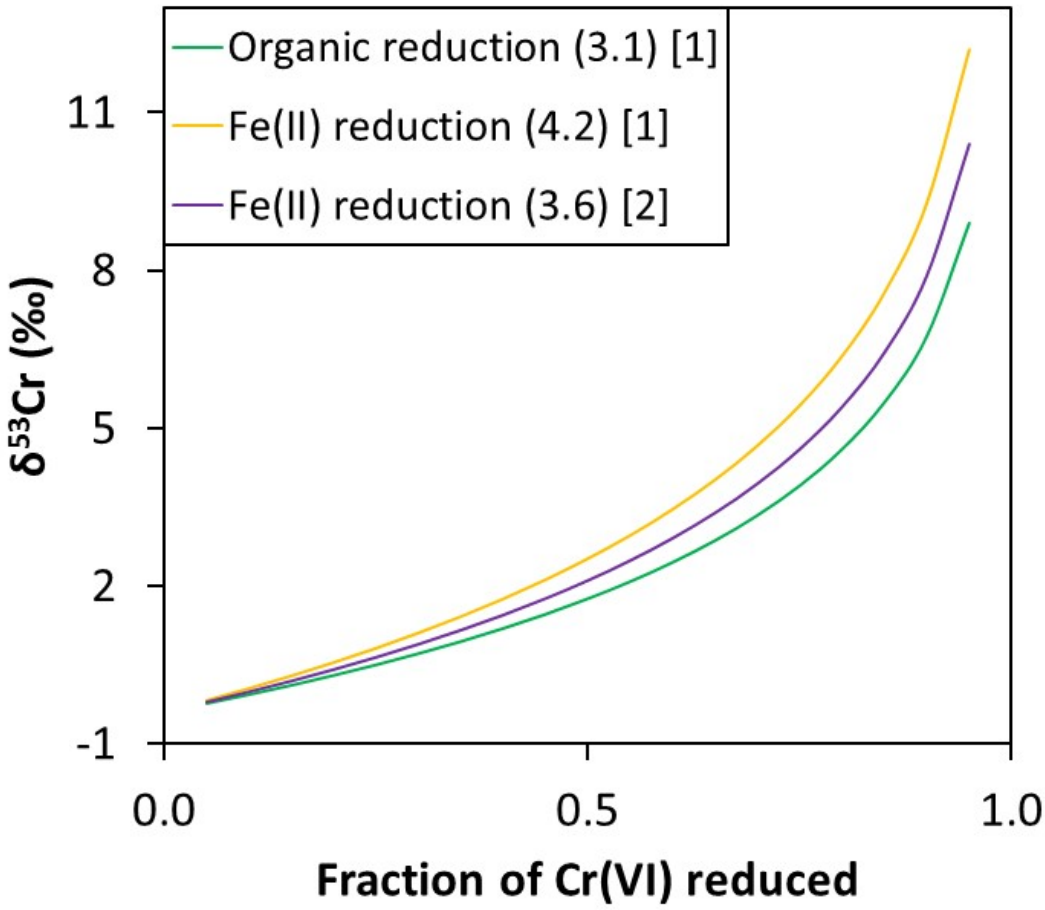

Figure 5.5 - Modelled δ^{53}Cr of residual Cr(VI) when partial reduction to Cr(III) occurs, as a function of the proportion of Cr(VI) reduced. The initial δ^{53}Cr of the Cr(VI) pool was taken to be -0.4‰ to represent the average Cr source to the Beaulieu River (see Section 5.4.2), and the results using three different Rayleigh fractionation factors (in brackets) are shown. References are: [1] (Kitchen *et al.*, 2012); [2] (Døssing *et al.*, 2011).

5.4.2. Controls on the Cr concentration and Cr isotopic composition of the river water endmember

The variation in Cr concentration and $\delta^{53}Cr$ of estuarine waters is higher in the lower salinity samples that were collected from upstream of the sluice gate (*S* = ≥14.5; **Figure 5.3**). In particular, samples B1 and B17 had high $\delta^{53}Cr$, high Cr_T and a low proportion of Cr(III) that may be indicative of input of Cr from a different source. Nevertheless, overall there are linear relationships between $\delta^{53}Cr$, Cr(III), Cr(VI) and salinity that allow us to define the Cr composition of the river water endmember. The estimated $\delta^{53}Cr$ value of the river water endmember (~ -0.43‰ in March and ~ -0.34‰ in October) is lower than the values measured in most other rivers to date (**Figure 5.1**). It is also lower than crustal values (-0.12 ± 0.10‰; Schoenberg *et al.* 2008) and Beaulieu pore water values (0.06 – 0.13‰). Oxidative weathering is expected to produce aqueous Cr(VI) that has higher $\delta^{53}Cr$ than the crustal value (e.g. Frei *et al.* 2014; D'Arcy *et al.* 2016), so oxidative weathering cannot be the principal control on the $\delta^{53}Cr$ of Beaulieu River water.

An alternative mechanism for Cr release is *via* anoxic dissolution of secondary minerals (**Figure 5.6**). Dissolution of Fe (oxy)hydroxides occurs in the Fe reducing zone in sediments and this process has been shown to release Cr into marine pore waters (Rigaud *et al.*, 2013). Isotopic fractionation of Cr during dissolution is not expected (Crowe *et al.*, 2013), so the Cr released by the dissolution of such minerals would likely have $\delta^{53}Cr$ similar to that incorporated into the Fe (oxy)hydroxides. These minerals are a product of weathering and are therefore expected to be enriched in ^{52}Cr (Berger and Frei, 2014; D'Arcy *et al.*, 2016; Frei *et al.*, 2014). Since the anoxic boundary is close to the sediment-water interface at Beaulieu (**Figure 5.4**), and given the high concentration of Cr in the pore waters (100-120nmol kg^{-1}), diffusion of Cr from this source into the river waters could explain their low $\delta^{53}Cr$ values. However, our analyses indicate that the $\delta^{53}Cr$ values of the pore waters are higher than that of the river water endmember, suggesting that further modification of $\delta^{53}Cr$ occurs after release from sediments.

It seems likely that the $\delta^{53}Cr$ value of the Beaulieu River water is controlled by the presence of organic ligands (**Figure 5.6**). Our UV irradiated river samples (B1 and B2) indicate that a significant portion (at least ~18%) of Beaulieu River Cr is present in the organic fraction of the dissolved phase, and the $\delta^{53}Cr$ value of Cr_{ORG} is lower than the $\delta^{53}Cr$ of inorganic Cr.

Organic forms of dissolved Cr are likely to form in the soil solution, and in support of this positive correlations between pore water Cr and DOC have been observed in other studies (Beck *et al.*, 2008; Douglas *et al.*, 1986; Rigaud *et al.*, 2013). As the estimated $\delta^{53}Cr$ value of Cr_{ORG} is lower than the crustal value, this suggests that reduction of Cr(VI) to Cr(III) in the presence of organic material must occur within the sediments/pore waters. This obviously requires the presence of some Cr(VI) to begin with; some Cr(VI) may be produced either *via* oxidation of Cr from minerals in the oxic sediment layer, or from the oxidation of Cr(III) that diffuses into the oxic layer from the underlying anoxic zone. Reduction of Cr(VI) by organic material is associated with a large isotopic fractionation factor ($\Delta_{Cr(VI)-Cr(III)}$ = 3.1; Kitchen *et al.* 2012) compared to oxidation of Cr(III) to Cr(VI) (~ -0.2 to -0.6; Zink *et al.* 2010) and favours the ^{52}Cr isotope, thus Cr(III) produced in this way is likely to have a negative $\delta^{53}Cr$ value. Binding of Cr(III) to organic complexes is known to greatly increase the mobility of Cr(III) (Beck *et al.*, 2008; Brumsack and Gieskes, 1983; Douglas *et al.*, 1986), so organically complexed Cr(III) may be released into river waters. This would explain the low $\delta^{53}Cr$ values in river waters, slightly higher $\delta^{53}Cr$ values in pore waters and the presence of large proportions of dissolved Cr(III) in the river water endmember. Although the Fe co-precipitation method does not capture Cr strongly bound to organic complexes, weakly bound Cr(III) can be released from these complexes by photochemical reactions (Kieber and Helz, 1992) and our method may well have captured this fraction. This seems especially likely considering that we sampled very shallow waters on clear, sunny days. The changing proportion of Cr released *via* this process *versus* Cr released due to oxidative weathering may explain the scatter in the data at low salinities. Many natural organic molecules are acidic in nature, thus a decreased release of these molecules could produce higher pH and $\delta^{53}Cr$ in the overlying river water, which is consistent with the trends observed for samples B1 and B17. It is notable that the $\delta^{53}Cr$ value of the UV irradiated sample B1 (0.06‰) was very similar to that of the pore waters (0.06-0.13‰) that were sampled in very close proximity. This scenario is also consistent with the lower $\delta^{53}Cr$ value of the October high salinity sample (B20, 0.98‰) compared to high salinity samples in March; a larger proportion of ^{52}Cr would have been transported to high salinities within organic complexes and re-released during photochemical reactions, because a greater proportion of Cr was likely to be in the Cr_{ORG} fraction in October (**Section 5.4.1**).

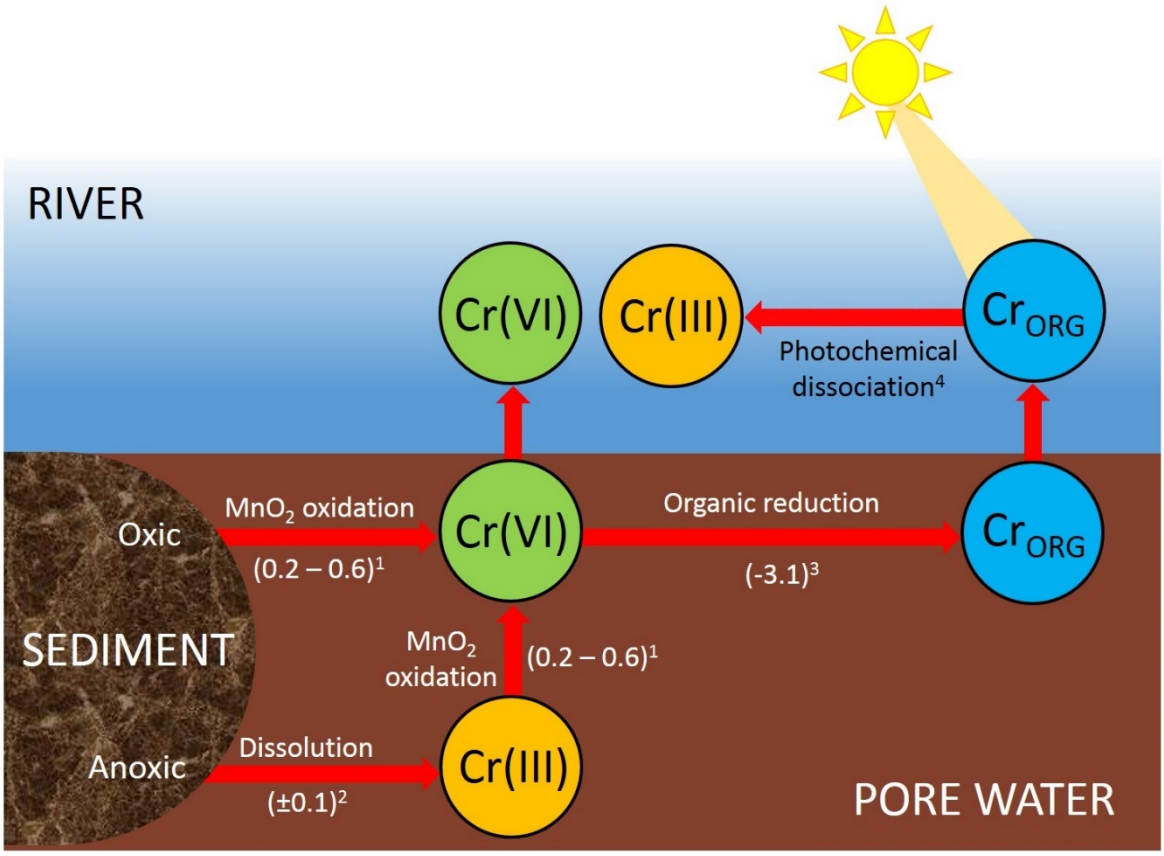

Figure 5.6 - Graphical representation of potential release mechanisms and redox transformations for Cr in the Beaulieu River. Numbers in brackets are isotopic fractionation factors (Δ_{R-P}, see Chapter 1). References are as follows: (1) Zink *et al.* 2010; (2) Crowe *et al.* 2013; (3) Kitchen *et al.* 2012; (4) Kaczynski and Kieber 1994.

Alternatively, it is possible that pre-existing pore water Cr(III) could have been fractionated during complexation with organic molecules. Equilibrium fractionation between Cr(III) and organically bound Cr(III) is theoretically possible (Schauble *et al.*, 2004) but it has not been demonstrated either in the field or in the laboratory. Detailed studies of Cr in soils and soil pore waters over a range of redox settings are required to refine our understanding of the processes that control the δ^{53}Cr values of river water.

5.4.3. Controls on the Cr concentration and Cr isotopic composition of the seawater endmember

Calculated δ^{53}Cr values of the seawater (S = 35) endmember are ~1.8‰ in March and ~1.2‰ in October, close to values previously measured for Southampton Water (1.45-1.51‰; **Chapter 3**; Bonnand *et al.* 2013) and the Celtic shelf sea (**Chapter 4;** 1.20 – 1.51‰),

but higher than the values typically measured in deep water masses (1.1-1.2‰; see **Chapter 4**).

The $\delta^{53}Cr$ values of other rivers that drain into Southampton Water and the Solent (the Rivers Test, Itchen and Hamble) are not known, but the concentrations of reductants such as DOC and Fe(II) which may reduce Cr(VI) and drive up $\delta^{53}Cr$ are much lower in these rivers than in the Beaulieu (Hopwood *et al.*, 2015; Moore *et al.*, 1979). Furthermore, anthropogenic Cr has also been shown to possess low $\delta^{53}Cr$ (-0.07 – 0.50‰; Ellis *et al.* 2002; Novak *et al.* 2014) so the relatively high values in Southampton Water cannot be explained by direct anthropogenic inputs. Cr waste remediation involving Cr reduction could potentially result in residual anthropogenic Cr that has high $\delta^{53}Cr$ (Berna *et al.*, 2010; Wanner *et al.*, 2013), but given that Cr concentrations in Southampton Water are similar to those measured along the rest of the UK south coast (~2nM; Achterberg *et al.* 1999; Bonnand *et al.* 2013), a large anthropogenic contribution of Cr to Southampton Water is unlikely. Therefore it is unlikely that the Cr supplied to Southampton Water *via* rivers has a high $\delta^{53}Cr$ value, and this suggests that Southampton Water $\delta^{53}Cr$ is not controlled by riverine and estuarine processes.

Furthermore, mass balance calculations suggest that the combined input of Cr from all of the rivers that drain into Southampton Water is small. The combined discharge rates of the Test, Itchen, Hamble and Beaulieu Rivers is ~25200 m^3 per day (Fang, 1995; Levasseur *et al.*, 2007). Assuming these rivers have Cr_T concentrations of 1.4nmol kg^{-1} (this study, Dolamore-Frank 1984, Bonnand *et al.* 2013) then ~0.04mol of Cr per day, or ~0.22mol within its 6.25 day flushing time (Dyer and Lasta King, 1975), are added to Southampton Water and the Solent from rivers. The volume of Southampton Water and the Solent is about 27 x 10^8 m^3 (Dyer and Lasta King, 1975) and given that Southampton Water has a Cr_T of ~1.5nmol kg^{-1} (**Chapter 3**, Bonnand *et al.* 2013), the total Cr_T in this region is ~4000mol. Hence <1% of dissolved inorganic Cr in Southampton Water and the Solent comes from these rivers. Input of Cr from submarine ground water is expected to be even lower (Bonnand *et al.*, 2013). Thus, the $\delta^{53}Cr$ of the Southampton Water is controlled by seawater $\delta^{53}Cr$ that, in turn, is regulated by internal cycling of Cr including reduction of Cr(VI) to Cr(III) in surface waters and oxygen minimum zones (Scheiderich *et al.*, 2015).

5.4.4. Implications for the $\delta^{53}Cr$ redox proxy

Whilst we have no information on the behaviour of organically bound Cr, significant quantities of Cr in the Cr_{ORG} fraction are unlikely to be transferred to open ocean settings given that DOC concentrations are extremely low in open ocean waters (of the order ~40-100µmol C L^{-1} compared with up to ~5mmol C L^{-1} in the Beaulieu River; e.g. Carlson and Ducklow 1995; Hansell and Carlson 1998; Miller and Zepp 1995; Moore *et al.* 1979). Furthermore, the fraction of Cr_{ORG} in the Beaulieu is <30% of the total Cr despite the exceptionally high concentrations of DOC found there (Moore *et al.*, 1979), suggesting that Cr_{ORG} may be a less important component in other rivers. Thus, inorganic forms of Cr are most likely to be transferred to the oceans, and hence control the $\delta^{53}Cr$ value of seawater. Our study shows that inorganic forms of dissolved Cr and Cr isotopes behave conservatively during estuarine mixing in the Beaulieu. This suggests that estuarine reduction of the Cr(VI) produced during oxidative weathering may not be an important control on the $\delta^{53}Cr$ of riverine Cr that is delivered to the oceans. However, more studies are required to confirm this, since Cr(VI) has been shown to undergo reduction in some estuaries (Abu-Saba and Flegal, 1995; Cranston and Murray, 1980). If the results of our study are applicable for most river systems, then this would considerably simplify the interpretation of terrestrially derived Cr isotopic signatures since $\delta^{53}Cr$ values generated on land would be faithfully transferred into the oceans.

On the other hand, our study reveals that the principle source of Cr to the Beaulieu River may be anoxic dissolution of sediments rather than oxidative weathering, and in either case the $\delta^{53}Cr$ of the source Cr is controlled by complexation with organic ligands. This may complicate the interpretation of seawater $\delta^{53}Cr$ values in terms of the level of atmospheric oxygenation, although we note that on a global scale, the input of Cr from oxidative weathering in mafic catchments is likely to be far more important than input of Cr from organic rich, non-mafic catchments (McClain and Maher, 2016).

5.5. Conclusions

Knowledge of the behaviour of Cr and Cr isotopes in rivers and during estuarine mixing is essential for our understanding of the Cr isotope redox proxy. Low river $\delta^{53}Cr$ values (-0.59 to 0.24‰) determined in the Beaulieu are thought to have been generated by the release of organically bound Cr(III), which contrasts with previous studies showing that direct

oxidative release generates Cr(VI) with high δ^{53}Cr values in river water (D'Arcy *et al.*, 2016; Frei *et al.*, 2014; Wu *et al.*, 2017). This implies that the isotopic effects of different Cr release processes and organic reactions in river-estuary systems are not well characterised, and further analyses of inorganic and organic Cr within soils, pore waters and estuaries are required to remedy this.

Our results show that Cr behaves rather conservatively in transition from the Beaulieu River to Southampton Water and the Solent. The operationally defined inorganic Cr fraction was surprisingly unreactive in the presence of abundant reductants, and isotope fractionation due to the reduction of aqueous Cr(VI) was not seen. We show that the δ^{53}Cr value of Southampton Water is not affected by estuarine mixing, and that *in situ* seawater processes (such as the reduction of Cr(VI) in surface waters; Scheiderich *et al.* 2015) are more likely to be the primary control. Together these findings suggest that δ^{53}Cr in marine deposits will reflect the combined δ^{53}Cr contributions from global rivers with high Cr concentrations and *in situ* Cr cycling in seawater (as discussed in **Chapters 3** and **4**).

An evaluation of δ^{53}Cr variability in a number of major world rivers would be desirable to fully understand the influence of riverine/estuarine processes on δ^{53}Cr in the global oceans, particularly those which contain high concentrations of Cr. Determination of the average contribution from rivers would substantially improve our understanding of the Cr isotopic composition of the ocean. However, in this connection, it is important to note that many major rivers suffer from anthropogenic Cr contamination. Therefore a more detailed understanding of the mechanisms governing Cr behaviour in pristine rivers combined with modelling may prove more fruitful in refining interpretations of the global effect of rivers and estuaries on δ^{53}Cr, and subsequently the δ^{53}Cr record of seawater preserved in marine deposits.

Chapter 6: Conclusions and further work

The chromium (Cr) isotopic composition of marine authigenic minerals preserved in sedimentary archives is increasingly being used to provide new insight into the oxygenation of the ancient atmosphere and oceans, as its isotopes are fractionated relative to crustal rocks by weathering processes when oxygen is present in the environment (e.g. Frei *et al.* 2009; Planavsky *et al.* 2014). This may lead to a better understanding of the role of oxygen on the evolution of life on Earth, and the causes and consequences of Ocean Anoxic Events. However the biogeochemical cycle of Cr is not fully understood, and so the meaning of ancient Cr isotopic signatures cannot, at present, be fully deciphered. One major reason for this is that the aqueous chemistry of Cr is complex and variable in different environmental settings, and evaluating the isotopic fractionation that results from aqueous reactions in the modern environment is highly challenging due to the low concentrations of Cr in most natural waters (typically 2-20nM in oceans and rivers; e.g. Bonnand *et al.* 2013).

The goals of this work were to develop a precise and accurate method for measuring Cr isotopic signatures and Cr concentrations in natural water samples, and to apply this method to the analysis of waters from a range of settings where Cr isotopic fractionation may be expected to occur; river and estuarine waters, biologically productive shelf seas and seawater with low dissolved oxygen concentrations. This chapter summarises the outcomes of this work and identifies a number of key areas for further research.

6.1. Principle outcomes

6.1.1. Method development

A method that enables the simultaneous measurement of Cr isotopic compositions and Cr concentrations in natural waters has been developed, based on previous work by Cranston and Murray 1978 and Bonnand *et al.* 2013 (**Chapter 2**). A new ^{50}Cr-^{54}Cr double spike was made and calibrated, in order to account for any isotopic fractionation that occurs during sample processing and for mass bias effects that occur during analysis by MC-ICP-MS. An Fe co-precipitation technique was used to remove Cr(III) and Cr(VI) from the aqueous phase in the form of an insoluble Fe(III)-Cr(III) precipitate, and this precipitate was processed

through a two stage ion chromatographic procedure to remove Fe and residual salts. Hydrogen peroxide was used to oxidise organic material that interfered with analysis by MC-ICP-MS.

The method was shown to produce accurate and precise $\delta^{53}Cr$ values for samples in aqueous matrices using a rigorous set of tests. These included (i) doping of seawater with the manufactured Cr standard NBS979 to confirm that the seawater matrix does not affect the measured $\delta^{53}Cr$ values; (ii) standard addition experiments in which the expected $\delta^{53}Cr$ values of seawater-standard mixtures matched those that were actually obtained; (iii) repeated measurements of the OSIL Atlantic Seawater Conductivity Standard that showed that the external reproducibility of $\delta^{53}Cr$ measurements was comparable to that of other laboratories (0.1‰); and (iv) an inter-calibration study with the University of Saskatchewan that demonstrated that this method produces seawater $\delta^{53}Cr$ values which are in excellent agreement with their laboratory (within 2SD error). Cr concentration measurements obtained using this method should be considered minimum estimates, as the values were 0-14% lower than those produced by the University of Saskatchewan in samples measured by both laboratories.

In addition, an isotope dilution method for the measurement of dissolved Cr(III) was developed. This was similar to the method described above, except that a single spike (^{53}Cr) was used and an oxidised Fe(III) precipitate was used to collect Cr(III) but not Cr(VI). This method was advantageous because the sample volume is a factor of 10 smaller (from ~1-3L to ~200-300mL), as measurement of the less abundant ^{50}Cr and ^{54}Cr isotopes is not required. For NBS979 Cr(III) standards in Milli-Q water, this method produced Cr concentrations within ±4% of the expected value, and within ±10% for mixed Cr(III)-Cr(VI) standards. A similar method was used to determine preliminary total Cr concentrations for isotopic analysis as this allowed an optimal amount of double spike to be added.

6.1.2. Chromium isotope systematics in shelf seas

Cr isotopic signatures in the Senegalese and Celtic shelf seas (**Chapters 3** and **4**) were both found to be slightly elevated ($\delta^{53}Cr$ = 1.2 – 1.6‰) relative to open Atlantic waters (1.1 – 1.2‰), and Cr concentrations were also lower (2.1 – 2.4nmol kg^{-1} compared to 2.4 – 2.9nmol kg^{-1}). This is consistent with removal of Cr(III) that is enriched with ^{52}Cr in shelf seas. Although there was little evidence for fractionation of Cr isotopes due to biological

activity in the open Atlantic Ocean (**Chapter 3**), concentrations of Cr appeared to be linked to the cycling of organic matter (**Chapter 4**). In both studies, low Cr concentrations were encountered in waters that had high levels of biogenic particulate material (as indicated by attenuance/transmittance and Chl-a profiles), but this was not the case in waters dominated by lithogenic suspended particulate material (**Chapter 4**). Furthermore, in times of high biological activity in the Celtic Sea, Cr concentrations were as low as 1.74nmol kg^{-1} close to the shelf edge. This implies that Cr(III) that produced by reduction of Cr(VI) adsorbs to organic material, and this is supported by previous work that shows that Cr is incorporated into organic material (Connelly *et al.*, 2006; Dauby *et al.*, 1994), mainly *via* adsorption of Cr(III) (Semeniuk *et al.*, 2016). Significant attenuation of the distinctive high shelf $\delta^{53}Cr$ values occurred on both the Senegalese and Celtic shelf slopes within ~30km of the shelf edge, suggesting that shelf waters do not contribute significantly to the $\delta^{53}Cr$ value of open ocean waters. Waters from the Arctic shelf sea, Southampton Water and the coast of Oregon display similarly high $\delta^{53}Cr$ values and low Cr concentrations (Bonnand *et al.*, 2013; Scheiderich *et al.*, 2015), that may suggest that reduction of Cr(VI) and removal of Cr(III) are important in shallow marine waters worldwide, regardless of O_2 concentrations. Authigenic sediments formed in shelf and shelf slope environments may thus show isotope variability that is related to adsorption to biogenic particles (and therefore to seasonal organic matter production) as well as variations due to O_2 levels in the atmosphere or oceans.

6.1.3. Chromium isotope systematics in oxic Atlantic Ocean waters

Atlantic Ocean seawater samples collected on several cruises were analysed for this work, including GEOTRACES cruise D361 (February-March 2011), GEOTRACES Medblack cruise PE370, and four SSB cruises – DY018, DY021, DY029 and DY033 (November 2014 – July 2015). The $\delta^{53}Cr$ values of these waters was very variable, between 0.86 and 1.72‰ (**Chapters 3** and **4**). Both the highest and lowest $\delta^{53}Cr$ values were observed in Senegalese and Celtic shelf slope environments; whilst some of the high values were attributed to hydrological mixing between shelf and surface waters, the lower values were attributed to the return of Cr with low $\delta^{53}Cr$ to the water column during organic matter remineralisation. Samples taken further away from the shelf had a much narrower range of $\delta^{53}Cr$ values, between 1.08 and 1.26‰ (**Chapter 3**), and deep waters that formed in the North Atlantic

(NADW, NEADW) had similar $\delta^{53}Cr$ values (1.12 ± 0.11‰, 1SD). Notably, one sample from the Upper Circumpolar Deep Water had an exceptionally high $\delta^{53}Cr$ value (1.72‰) which may suggest that certain water masses carry distinctive pre-formed $\delta^{53}Cr$ signatures. However, it seems that authigenic sediments formed in open ocean waters may reflect global seawater $\delta^{53}Cr$ values more accurately than those formed in shallow marine waters, because they are less affected by local processes that are not related to O_2 concentrations.

6.1.4. Chromium isotope systematics in low oxygen seawater

Dysoxic waters (44 – 91µmol kg^{-1} O_2) from the Atlantic Oxygen Minimum Zone (OMZ) along with suboxic (0µmol kg^{-1} O_2) and anoxic (0nmol kg^{-1} O_2, 20µmol kg^{-1} H_2S) waters from the Black Sea were analysed during this work (**Chapter 3**). The O_2 concentrations in the dysoxic OMZ samples were apparently not low enough to induce the reduction of Cr(VI) to Cr(III), as no trends were observed in $\delta^{53}Cr$ values or Cr concentrations as a function of dissolved O_2. However, suboxic and anoxic waters in the Black Sea had lower $\delta^{53}Cr$ values compared to the overlying oxic waters (by up to 0.38‰), possibly due to the dissolution of particulate materials enriched with ^{52}Cr, and/or due to isotopic exchange between adsorbed and aqueous Cr(III) as has been observed for Cr(VI) (Ellis *et al.*, 2004). This means that authigenic sediments formed beneath a suboxic boundary (e.g. Banded Iron Formations and black shales) may have lower $\delta^{53}Cr$ values than the seawater from which the Cr is derived; this may cause an under-estimation of the O_2 levels present in redox stratified basins.

6.1.5. Chromium isotope systematics in an organic-rich river

Samples were collected from the Beaulieu River (UK) and its estuary over two sampling periods (March and October 2016) and chromium isotopic signatures, total Cr concentrations and Cr speciation measurements were made on these (**Chapter 5**). Total (inorganic) concentrations of Cr in the Beaulieu River and estuary (0.7 – 5.0nmol kg^{-1}) were similar to or lower than other rivers and $\delta^{53}Cr$ values spanned a range from -0.58 to 1.68‰. Despite the abundance of potential Cr reductants (Fe and organic molecules) in the Beaulieu River and estuarine waters, Cr behaved conservatively in the estuary, i.e. variations in Cr and $\delta^{53}Cr$ were due to variations in the proportion of freshwater to seawater. If Cr behaves similarly in the majority of rivers globally, this would mean that the Cr isotopic signature of river waters is faithfully transferred to the oceans and is not

modified by processes occurring in estuaries. This would simplify the interpretation of ancient $\delta^{53}Cr$ values in marine authigenic sedimentary rocks.

Although oxidative weathering and aqueous reduction reactions both preferentially retain ^{53}Cr in solution (imparting high $\delta^{53}Cr$ values to natural waters compared to crustal rocks), Beaulieu River waters had $\delta^{53}Cr$ values as low as -0.59‰. Soil pore waters within the Beaulieu River catchment had high concentrations of dissolved Cr (100-120nmol kg^{-1}) and a $\delta^{53}Cr$ value of around 0.1‰. This suggests that ^{52}Cr enriched, organically bound Cr(III) is released from anoxic pore waters into the river, leaving slightly ^{53}Cr enriched Cr behind in the pore waters. This also accounts for the high proportions of Cr(III) in the river waters (up to 55%); it is thought that this Cr(III) must have been released from organic complexes by photolytic reactions in sunlit surface waters in order to be captured by the Fe co-precipitation method. This demonstrates that processes other than oxidative weathering may affect the $\delta^{53}Cr$ of Cr supplied to the oceans *via* rivers, which may in turn affect the $\delta^{53}Cr$ of ancient marine authigenic sediments if the Cr contribution from these processes is large enough on a global scale.

6.2. Key areas for further research

6.2.1. Methodological improvements

Further measurements of $\delta^{53}Cr$ and Cr concentrations in natural samples are needed in order to fully understand the processes that control seawater $\delta^{53}Cr$ values (see **Section 6.2.2**). The method described in **Chapter 2** produces precise and accurate $\delta^{53}Cr$ values for seawater, thus it will be appropriate to use this method for natural waters in future studies. It would be useful to increase the yield of Cr recovered during sample processing (currently ~60-70%), as this would allow for smaller sample sizes; in turn this would make it more practical to increase the sampling resolution of both vertical water profiles and horizontal transects. Yield losses are greatest during the vacuum filtration and cation exchange chromatography stages (~20% and ~10% respectively). Filtration losses may be decreased by introducing a second stage of filtration for capturing very small particles (<1µm) of the Fe-Cr precipitate, and alternative ion exchange procedures that optimise the yield of Cr have recently been described (Larsen *et al.*, 2016).

The determination of total Cr concentrations in seawater samples appear to be slightly under-estimated by our method, or else overestimated by the University of Saskatchewan (by 0-14%); the reasons for this remain unclear, but could be related to the behaviour of Cr(VI) in the samples. Possible aspects for future investigations include reducing Cr adsorption to container walls and improving equilibration between Cr(VI) in the sample and the isotopic spike.

6.2.2. Constraints on natural δ^{53}Cr variability

It is clear that particulate material plays an important role in the cycling of Cr in shelf seas and within suboxic waters (**Chapters 3** and **4**), and the δ^{53}Cr of authigenic marine sediments is very likely to be affected by these interactions. For example, the dissolution of particles that are enriched in ^{52}Cr within suboxic zones and during organic matter remineralisation may lower the δ^{53}Cr of authigenic precipitates (**Chapter 3**). On the other hand, the preferential adsorption of ^{52}Cr(III) onto particles will act to increase the δ^{53}Cr of the remaining seawater Cr even under fully oxic conditions, and this should have the effect of driving up the δ^{53}Cr values of carbonates that precipitate from these waters. Samples of suspended particulate material were collected from Southampton Water (12 samples) and the Celtic Sea shelf stations on cruises DY021, DY030 and DY034 (45 samples in total) to help resolve particulate effects on seawater δ^{53}Cr. A sequential extraction procedure was trialled in order to determine δ^{53}Cr values in the weakly adsorbed, organic, Fe-Mn bound and lithogenic fractions, but unfortunately there were too few particles in the samples to obtain enough Cr to make an isotopic measurement for each fraction (<10ng in each of the adsorbed, organic and Fe-Mn fractions). Furthermore, the recovery of Cr using this sequential extraction method was low compared the recovery in bulk samples (~25%). It may be possible to obtain some δ^{53}Cr values from these samples if the Cr yield of this method can be improved, and it would be worthwhile to target the organic fraction given the link between Cr concentrations and organic matter cycling in the Celtic Sea (**Chapter 4**). The samples from DY030 are most promising for this as they were collected at the end of the spring bloom period and are thus expected to contain a large proportion of organic material.

It will also be important to characterise the mechanism(s) that reduce Cr(VI) to Cr(III) in seawater, and to find out whether the production of Cr(III) is accelerated in some areas

(e.g. shelf seas). It seems that active biological reduction either did not occur or had a small effect on $\delta^{53}Cr$ values in the open Atlantic Ocean (**Chapter 3**), although there was some evidence for biological fractionation in one profile from the Celtic Sea (**Chapter 4**). Biological fractionation may vary temporally and spatially; the fractionation factors for biological reduction may be different under different environmental conditions (Han *et al.*, 2012) and different species may interact differently with Cr (Semeniuk *et al.*, 2016). Additionally, bulk seawater $\delta^{53}Cr$ analyses cannot be used to determine whether Cr(III) is produced by reduction of Cr(VI), because they may instead simply reflect how effectively the existing Cr(III) and Cr(VI) pools are separated (e.g. by particle adsorption). Further seawater analyses from the GEOTRACES D361 cruise are underway to determine the $\delta^{53}Cr$ values of dissolved Cr(III) and total Cr in Atlantic seawater. Additional analyses of this kind on shelf sea waters would also be helpful for comparison.

Between the oxic and anoxic layers of the Black Sea, a $\delta^{53}Cr$ difference of 0.38‰ was observed (**Chapter 3**). Such a shift would be expected to have an impact on the $\delta^{53}Cr$ of authigenic sediments formed in the Black Sea. The Black Sea is a restricted basin so this isotopic shift may not be important at the global scale, but suboxic conditions are also present in the OMZs of the tropical Pacific and northern Indian Oceans. These waters may have the capacity to modify global seawater $\delta^{53}Cr$ values, and could represent an important sink of Cr if Cr(III) removal is increased by adsorption or precipitation within the OMZs. Furthermore, the $\delta^{53}Cr$ values of oxic seawater in the Pacific and Indian Oceans are not as well characterised as the Atlantic Ocean (**Figure 6.1**) and thus our understanding of the global seawater $\delta^{53}Cr$ range is not complete. Therefore seawater measurements should be carried out in both oxic and suboxic waters of the Pacific and Indian Oceans; preferably alongside authigenic sediment analyses from the same area in order to gauge whether seawater $\delta^{53}Cr$ values are faithfully transferred to the sedimentary record.

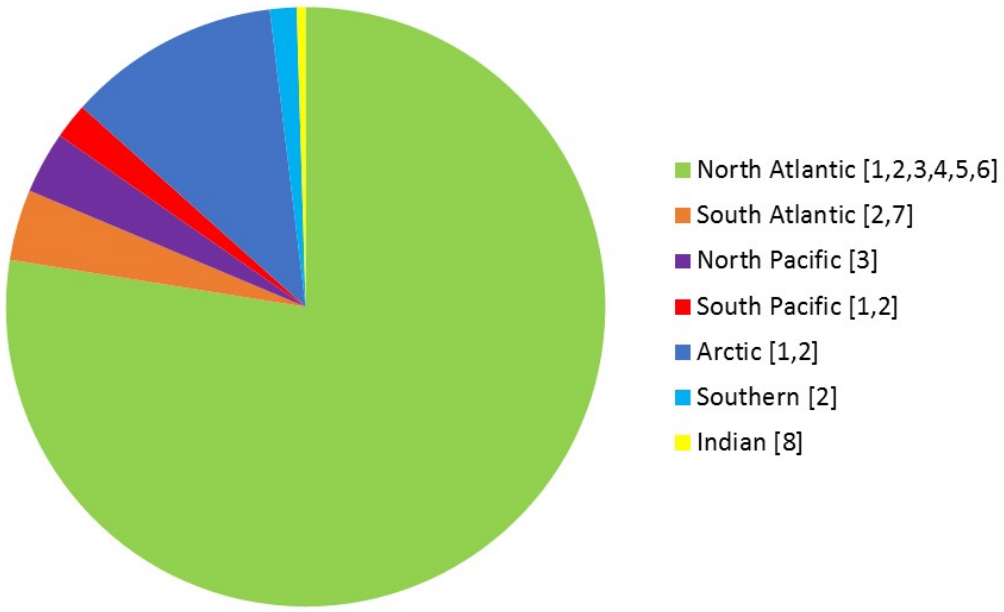

Figure 6.1 - The regional distribution of seawater $\delta^{53}Cr$ values measured to date. References are as follows: [1] Scheiderich et al. 2015; [2] Paulukat et al. 2016; [3] Bonnand et al. 2013, [4] Holmden et al. 2016, [5] Economou-Eliopoulos et al. 2016; [6] Chapters 3 and 4; [7] Pereira et al. 2015; [8] Paulukat et al. 2015.

The Fe co-precipitation method is thought to capture only inorganic Cr species, but organically bound Cr appears to play an important role in regulating the $\delta^{53}Cr$ of some river waters (**Chapter 5**; D'Arcy et al. 2016). In the future, it may be useful to measure both UV digested and non-digested samples to understand how Cr is communicated between organic and inorganic phases in organic-rich environments, and how this impacts $\delta^{53}Cr$. Furthermore, dissolved organic material seems to exert variable effects on Cr; for example it is responsible for removing Cr during flocculation in the Columbia estuary (Cranston and Murray, 1980), for reducing Cr in the Glenariff River, and for mobilising Cr from pore waters in the Beaulieu River (**Chapter 5**). Characterisation of the organic species responsible for these different behaviours would allow $\delta^{53}Cr$ variations in different rivers and their influence on seawater $\delta^{53}Cr$ to be better understood. Furthermore, the mechanisms for Cr release from terrestrial rocks and soils vary under different environmental conditions (**Chapter 5**; D'Arcy et al. 2016; Frei et al. 2014). Analyses of Cr in pore waters and sediments should be done on samples from a range of riverine/estuarine settings in order to improve our understanding in this area. Most of the Cr in seawater is supplied by rivers, so taking

these steps would allow for a more precise Cr isotopic budget for seawater, and would give better insight on the controls on $\delta^{53}Cr$ in ancient marine sedimentary archives.

Oxidation has been shown to induce some Cr isotopic fractionation (e.g. Berger and Frei 2014; Frei *et al.* 2014; Zink *et al.* 2010). However, fractionation factors for oxidation processes are not well constrained, partly due to difficulties with back-reduction in laboratory experiments (Bain and Bullen, 2005; Joshi *et al.*, 2011). It is essential that this is rectified in the future in order to understand the relative contributions of oxidation and reduction reactions to seawater $\delta^{53}Cr$ values.

Finally, in order to better interpret Cr isotopic signatures in terms of past oxygen levels, it would be interesting to compare $\delta^{53}Cr$ values in redox stratified basins and authigenic sediments to other redox sensitive isotope systems, such as $\delta^{56}Fe$, $\delta^{98}Mo$ and $\delta^{238}U$ (e.g. Neubert *et al.* 2008; Pearce *et al.* 2008; Rolison *et al.* 2017; Severmann and Anbar 2009).

Appendices

Appendix A: Sample preparation procedures

Procedure 1: Seawater sample preparation

Author: Heather Goring-Harford (Oct 2016)

COSHH assessments: Ammonium iron(II) sulphate; Ammonium hydroxide; HCl

This procedure describes the preparation of aqueous samples prior to Cr purification by anion and cation columns. An Fe(II) precipitate is generated that reacts with Cr(VI) in the aqueous phase forming a solid precipitate. Any Cr(III) remaining in the solution adsorbs to this precipitate, resulting in near-quantitative collection of Cr from the aqueous phase.

1. Establish concentration of Cr in samples using Element (see **CrConc** procedure).
2. Record sample weights.
3. Add an appropriate amount of double spike (~2.5ppm) to the samples. Allow 24 hours for equilibration, then adjust sample pH to 8-9 using ammonia as necessary. Make up appropriate amount of 2mM ammonium Fe(II) sulphate (10ml per litre of seawater is required). Add sufficient ammonium hydroxide (Romil grade) to 2mM ammonium Fe(II) sulphate solution to produce a solution of pH 8-9. It is best to split the ammonium Fe(II) sulphate solution into batches in case the amount of ammonia needs adjusting (e.g., 4x 25ml batches in clean centrifuge tubes). Add 75µl conc. ammonia per 100ml of ammonium Fe(II) sulphate solution. The desired fine green precipitate should form within a few seconds and remain for about 5 minutes. If the solution turns orange with no green precipitate forming first, do not use. More ammonia should be added to the next batch. If the green precipitate turns orange or black very quickly (<2 minutes), do not use. Add less ammonia to the next batch and make sure the solution is aerated by opening the container and swirling (do not shake vigorously as this will oxidise the Fe(II) too fast).

4. Immediately add 5-10ml/L of the Fe(II) hydroxide solution to samples. This is critical as Fe(II) will oxidise after about 5 minutes.
5. Shake the mixtures and leave to stand for 5-7 days, allowing Fe-Cr precipitate to form and settle.
6. Use clean 1 micron Teflon filters (about 1 per litre of sample) to collect precipitate *via* vacuum filtration. Place all the used filters from each sample into a single clean 15ml Savillex container. Reserve empty sample containers for weighing.
7. Add 5ml 6M HCl to each container and shake vigorously for a few seconds (the acid will turn bright yellow as the precipitate dissolves). Leave for 1 hour to fully dissolve.
8. Remove the filter to a new 15ml Savillex container, draining off as much sample liquid as possible. Rinse the filter with a further 5ml 6M HCl and add this back to the sample.
9. Dry samples down overnight at 100°C.
10. Dissolve the samples in 6ml 7M HCl and reflux at 130°C overnight. Then process the samples through anion columns.

Procedure 2: Anion columns (separation of Cr from Fe)

Author: Christopher Pearce, after Bonnand *et al.* 2013 (Dec 2016); last updated Oct 2016 (Heather Goring-Harford).

COSHH assessments: HCl; HNO_3

This procedure describes the anionic column separation of Cr prior to MC-ICP-MS isotopic analysis. The protocol uses a 10 ml Bio-Rad poly-prep column, loaded with 2 mls of pre-cleaned Bio-Rad AG1-X8 resin (200-400 mesh). The resin can be used multiple times, but it's important to check the resin height and that there are no air bubbles prior to use.

The Cr anion column procedure is used solely to remove Fe from the sample, thus it ***must*** *be followed by the Cr cation column procedure to separate Cr from the rest of the matrix. A single pass through the anion exchange column should be sufficient to remove Fe from most samples.*

NB: It is essential to use separate columns for double and single spiked Cr to avoid contamination of isotopic samples with ^{53}Cr.

1. Clean the resin with 10 ml of 15M HNO_3, then 5 ml of MQ H_2O, then 10 ml of 0.5M HCl, then 5 ml of MQ H_2O, then 5 ml of conc. HCl, then finally 5 ml MQ H_2O. *N.B. Although this cleaning procedure is long, it ensures that the blank contribution from the columns is very low.*
2. Condition the resin with 10 ml 7M HCl. *N.B. This 7M HCl must be accurately titrated.*
3. Ensure the sample is dissolved in 6 ml of 7M HCl and carefully load on to the column. Collect the eluant in a clean 15 ml Savillex vial. *N.B. Unlike Fe(III), Cr(III) does not stick to the resin, so should be collected immediately after loading.*
4. Wash the column with a further 4 ml of 7M HCl and collect the eluant in the same 15 ml Savillex vial.
5. Dry down the sample at ~100^{o}C overnight.
6. Clean the resin with with 10 ml of 0.5M HCl (to remove the Fe).
7. Columns should be stored in 5 mls 0.5M HCl, with the caps and lids firmly sealed.

Procedure 3: Cation columns (separation of Cr from residual salts)

Author: Christopher Pearce, after Bonnand *et al.* 2013 (Dec 2016); last updated Oct 2016 (Heather Goring-Harford).

COSHH assessments: HCl; HNO_3

This procedure describes the cationic column separation of Cr prior to MC-ICP-MS isotopic analysis. The protocol uses Savillex columns with a 30 ml reservoir, loaded with pre-cleaned Bio-Rad AG50W-X12 resin to a height of 9 cm in 0.5M HCl. The resin can be used multiple times, but it's important to check the resin height and that there are no air bubbles prior to use.

For most samples, a single pass through this cation exchange column is sufficient to separate Cr cleanly from the sample matrix. However, samples that are Fe-rich must be passed through the anion column procedure ***before*** *running the cation columns.*

1. Clean the resin with 10 ml of 8M HNO_3, then 30 ml of 6M HCl, then 30 ml of MQ H_2O. *N.B. This cleaning step takes a long time, so should be done the day before running samples (once clean the resin can be left in the preconditioning 0.5M HCl of step 2).*
2. Condition the resin with 12 ml of 0.5M HCl. *N.B. This 0.5M HCl must be accurately titrated.*
3. When the columns are clean, dissolve the sample in 0.5ml titrated 6M HCl. Add 5.5ml MQ water to make a 0.5M solution and immediately load sample onto the column. Collect the elutant in a clean 15 ml Savillex vial. *N.B. Cr does not stick to the resin, so should be collected immediately after loading.*
4. Wash the column with another 4 ml of titrated 0.5M HCl and collect the eluant in the same 15 ml Savillex vial.
5. Dry down the sample at ~100˚C overnight.
6. Clean the resin with 30 ml of 6M HCl then with 30 ml of MQ H_2O.
7. Pipette 50µL conc. H_2O_2 onto the dry sample. Dry down at 100˚C.
8. Pipette 50µL conc. HNO_3 onto the dry sample. Dry down at 100˚C.

9. Reconstitute in 60µl conc. HNO_3 and then add 1.94ml MQ H_2O for a 3% HNO_3 solution.
10. Columns should be stored in 15mls 0.5M HCl.

Appendix B: Method development

Table B.1 - Chromium yields for NBS979 standards in Milli-Q water processed using the seawater method (Appendix A).

Expected Cr concentration (nmol kg^{-1})	Cr concentration determined by ^{52}Cr counts (nmol kg^{-1})	Estimated Cr recovery (%)
10.98	7.60	69
10.95	8.44	77
11.22	5.68	51
11.19	6.03	54
10.52	6.22	59
10.59	5.95	56
	Average	61

Table B.2 - Blank measurements for chemical solutions used for seawater sample processing.

Solution	Concentration (mol L^{-1})	Grade	Cr conc. (ppb)	2SD	n
LDPE bottle leachate[1]	N/A	N/A	0.00	0.00	6
Nitric acid	0.5	Sub-boiled (in house)	0.08	0.03	6
Hydrochloric acid	10.5	Sub-boiled (in house)	0.02	0.02	2
Ammonium hydroxide	11.4	Romil UltraPure	0.00	0.00	2
Hydrogen peroxide	10.0	Fluka TraceSELECT Ultra	0.05[2]	N/A	N/A

[1]Milli-Q water acidified to pH 2 using sub-boiled HCl, stored for 3-8 weeks before analysis.
[2]Value taken from manufacturer's Certificate of Analysis.

Table B.3 – Experiments performed to investigate inaccurate Cr(VI) concentrations obtained using single (^{53}Cr) spike method.

Purpose of experiment	Cr(VI) standard used	Treatment of Cr(VI)	$^{52}Cr/^{53}Cr$	Concentration determined (nM)	Concentration expected (nM)	Proportion of expected value achieved (%)
Initial test	Ammonium bichromate[1]	In Milli-Q	0.44	8.02	10.88	74
		In Milli-Q	0.44	7.95	10.81	73
Does acidification allow recovery of adsorbed Cr(VI)?	Ammonium bichromate[1]	In acidified Milli-Q	0.47	8.59	10.87	79
		In acidified Milli-Q	0.47	8.75	10.98	80
Is more Fe(II) required to recover all Cr(VI)?	Ammonium bichromate[1]	3ml Fe(II) added	0.44	7.47	11.09	67
		3ml Fe(II) added	0.43	7.46	11.16	67
		6ml Fe(II) added	0.44	7.41	11.05	67
		6ml Fe(II) added	0.44	7.48	11.12	67
Does chromate ion behave differently to bichromate?	Potassium chromate[2]	In Milli-Q	0.29	4.89	9.98	49
		In Milli-Q	0.30	5.05	9.91	51
Is the problem reproducible?	Potassium chromate[2]	In Milli-Q	0.25	3.67	10.29	36
		In Milli-Q	0.25	3.48	10.09	35
		In Milli-Q	0.25	3.53	10.22	35
Is Cr(VI) lost on anion column?	Potassium chromate[2]	Anion column calibration	0.26	NT	NT	N/A
Is Cr(VI) lost on cation column?	Potassium chromate[2]	Cation column calibration	0.28	NT	NT	N/A
Is Cr(VI) lost during or before co-precipitation?	Potassium chromate[2]	No co-precipitation	0.24	228	567	40
		No co-precipitation	0.24	230	567	40
Is Cr(VI) volatile?	Potassium chromate[2]	Dried down (with spike)	0.26	2168	5926	37
		Dried down (with spike)	0.25	7071	20147	35
		Not dried	0.23	6385	20147	32
Can adsorbed Cr(VI) be recovered through reflux with HCl?	Potassium chromate[2]	Refluxed in 7M HCl for 48 hours	0.30	2601	5926	44
Can equilibration of spike and Cr(VI) be improved by oxidising spike?	Potassium chromate[2]	Added H_2O_2 and allowed to react overnight	0.25	6939	20147	34
		Added H_2O_2 and immediately dried down	0.25	6919	20147	34

[1]Supplied by Inorganic Ventures (1000ppm Certified Reference Material); [2]Supplied by Sigma-Aldrich (1000ppm standard).

Appendix C: Neptune MC-ICP-MS analysis

Author: Hélène Planquette; revised Apr 2017 (Heather Goring-Harford)

Preparation before the run

3 days before: Soak 2mL and 20mL scintillation vials and 50ml centrifuge tubes in 10% SB HNO_3 to clean. Clean 2mL vials are also available in the instrument lab.

2 days before: Prepare 1L of 10% SB HNO_3 and heat overnight at 130°C. Use it to clean the Aridus following the protocol located in the instrument lab.

1 day before:

- Check if cones require cleaning.
- Make up 500mL of 3% SB HNO_3 in a clean FEP bottle. This acid will be used to make standards and blanks for consistency.
- Make 125mL 33ppb unspiked NBS979 tuning solution and 125mL 53ppb double spiked NBS979 standard in separate FEP bottles. The double spiked NBS979 standard must be centrifuged to remove particles which can develop in the double spike.

Cleaning Ni X-cones:

1. Sonicate for 10 minutes in 10% Decon, then rinse with Milli-Q.
2. Sonicate for 2 minutes only in 3% HNO_3, then rinse with Milli-Q.
3. Sonicate in Milli-Q for 5 minutes.
4. Dry in the oven at 60°C.
5. Check cone tips under a microscope.

Unspiked 33ppb NBS979 standard:

- 125ml 3% HNO_3
- 138µL 30ppm NBS979

Double-spiked 53ppb NBS979 standard:

- 125ml 3% HNO_3
- 138µL 30ppm NBS979
- 50µL 50ppm Soton double spike

Centrifuging spiked NBS979 standard:

1. Pour the standard into clean centrifuge tubes and seal with Parafilm.
2. Centrifuge for 20 minutes at 3500rpm (there is a centrifuge in 781/05).
3. Pipette standard into clean labelled 20mL vials, leaving the last 5mL behind.

Note: Particles may re-develop over time. Standard should be used within 1 week of centrifugation.

Start-up

1. Check that skimmer and sample Ni X-cones are mounted properly, and that the torch is in position.
2. Check that the Aridus introduction system is connected, and that the 'quick wash' valve at the back is closed. The Temperature setting must not be touched. Before starting the plasma, make sure that N_2 = 0 and and Ar = 0L/min.
3. Check hardware system status. All lights must be green (incl. cool gas flow, coil cooling, interface pump, skimmer valve and analyzer gate, high voltage).
4. Go to the 'Neptune Software' folder.
5. Open 'Acquisition' application, which opens up the communication between the computer and the Neptune. The 'System OK' box will appear. The connection status should be blue (lower right corner on the screen).
6. Open Tune application and click 'On' in 'Start and Stop plasma'. A message will appear: 'Do you want to start peristaltic pump?' Click 'No'.

7. There will be a ‘clunk’ sound from the instrument as the pump turns on. Slowly increase Ar gas flow on the Aridus to ~4mL/min after you hear this. Watch the torch – if it flickers, turn gas up more slowly.
8. Open up the cup configuration ‘Cr4’ (or other most recent cup configuration file). Click ‘Select Collection’.
9. Go to the ‘Detector Calibration’ tab and do a Gain Calibration. Then do a Baseline Calibration.
10. Send the Autosampler into the wash and check that solution is being taken up.

Troubleshooting for start-up:

- If the ‘System OK’ symbol is grey, reconnect the instrument by re-opening ‘Acquisition’. Wait until the system status turns red (not ready) or blue (ready). If it is red, open the software application Tune in folder ‘Neptune software’ on desktop. Turn HV on. System status should go blue.
- If the Autosampler doesn’t move when given a command, switch it off and on at the front of the machine. Give it about 1 minute to settle, and then try giving it another command. Alternatively, restart the computer.

Tuning

It takes at least 1 hour for the signal to stabilise after the plasma is switched on. The Autosampler should be left in the wash while you wait (when the torch is on the probe should always be placed in the wash when not running). When the signal appears reasonably stable, make sure the guard electrode is on and tune the machine using the 33ppb unspiked NBS979 tuning solution. Typically 5-9V on the ^{52}Cr beam is achievable (see ‘Troubleshooting’ section for more info).

1. Adjust the following parameters in Tune at least twice to ensure the best combination of settings is achieved for good signal:
    - **Ar sweep gas on front of Aridus:** Ar flow will usually need to be increased up to ~4L/ min. Select the lowest flow rate which gives good signal.

- **Inlet system:** Sample gas: 0.9-1L/min. Torch position: X-; Y- and Z-. Note: 'Z-position' moves in and out. Be careful not to move it too close to the cones.
- **Source lenses:** 'Focus', 'X-deflection', 'Y-deflection', 'Shape'.
- Do not adjust 'Cool Gas', 'Auxiliary Gas', 'Add Gas 1', 'Add Gas 2', 'Peri-Pump', 'RF Power', 'Extraction' or 'Source Offset'. 'Rot. Quad' should be zero.

2. When you are reasonably satisfied with the signal, check the signal of the wash and your blank. A good starting value for ^{56}Fe and ^{52}Cr is <0.005V. Often these values will creep up throughout the run so you need to start with optimal values. Wash values >0.03V are considered sub-optimal. Blank signals needs to be checked regularly throughout tuning and the run.
3. Click on 'mass scan' and make sure the 'echo function' is selected in order to see differences between readjustment attempts. Adjust the following parameters in order to obtain accurate measurements.
    - **Zoom optics**: Adjust focus quad to get a peak as steep as possible - the mass resolution should be >4800. Typically the optimal focus is about -1V. Align ^{50}Cr, ^{56}Fe and ^{52}Cr together using the dispersion focus (see **Fig. 1**). Typically, the dispersion focus is set at ~-3.5V.

Calculating mass resolution:

1. Read the maximum voltage of the ^{52}Cr peak. Calculate 95% and 5% of this value.
2. Read the masses (M) at the 95% and 5% voltage levels from the x-axis. A ruler is helpful for this.
3. Mass resolution = 51.996 / $M_{95\%}$ - $M_{5\%}$

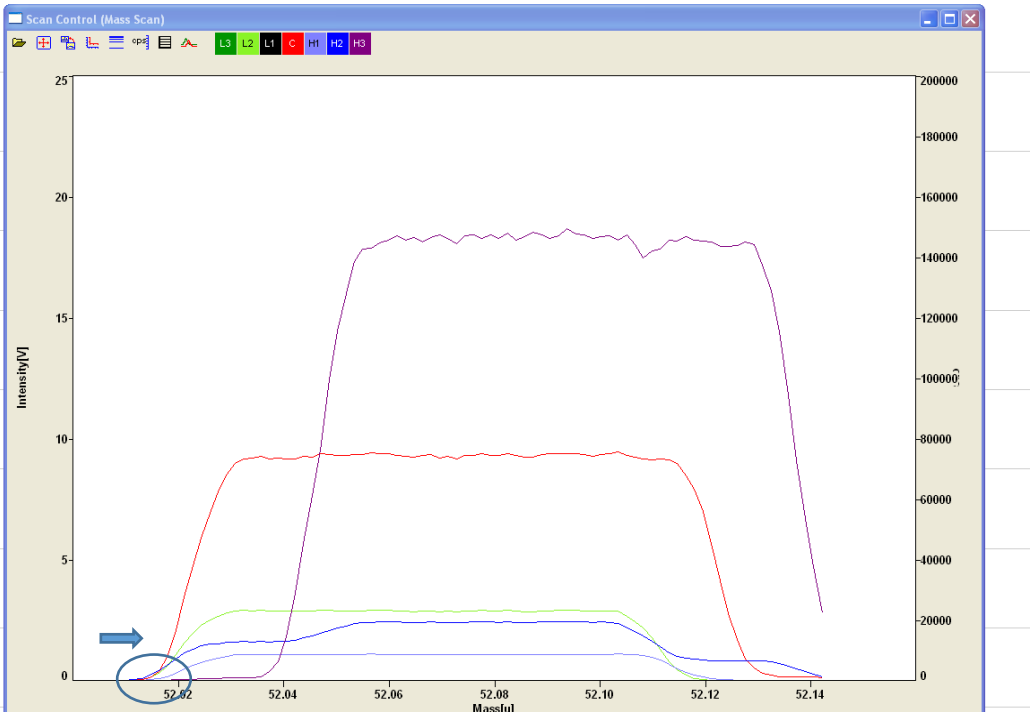

Figure C.1 - Correct peak alignment for MC-ICP-MS analysis.

- **Interferences:** Change the y-axis maximum value to 50V so that you can see the top of the interference peaks. If these interferences are too large (>35V) they cause the ^{56}Fe peak to take on a 'domed' shape, which has a very significant effect on measurement accuracy. Zoom in on the ^{56}Fe peak to check that it has a flat top. If not, reduce the Aridus gas flow. Some ^{52}Cr signal may be sacrificed to achieve a flat top on ^{56}Fe.
- **Determine the optimum position for the C cup (^{52}Cr):** The optimal position is where all peaks are flat before the interferences on H2 and H3 begin (see **Fig 2 and 3**). Usually the peak with the narrowest flat shoulder is that of the ^{56}Fe peak so zoom in to make sure your chosen position is aligned well with it.
- **Set the optimum position:** In Tune, go to 'Cup Configuration' and change the C mass to the desired value. Click on 'Set' then save the cup configuration. Finally open Method Editor in the 'Neptune Software' folder. Open the method files you will use in your run and click 'save' so that the new cup configuration is recognised properly by the software.

Figure C.2 - Selecting the correct measurement position (in this case mass 52.01 is appropriate).

Figure C.3 - Zoomed in from Figure C.2. Refining the measurement position (in this case to 52.007).

Troubleshooting for tuning:

High wash/blank voltages:

- Change the 3% HNO_3 in the wash carboy using SB acid from the university clean lab. There is a bottle in the instrument lab for diluting this acid in the correct proportions.
- Make sure the black tube within the probe does not come into contact with the wash solution, as Fe sometimes leaches out of it. Adjust the height of the probe using the ESI software.

No ^{52}Cr signal:

- Mass range may have shifted. Set 'mass scan' range to 51.5 to 52.5 and run to find peaks. Adjust 'Selected Mass' in 'Peak Control' window (Scan Control tab) and C cup position accordingly.
- 'Extraction' on the right hand side of the Tune software under 'Watch Parameter' should have a consistent value of -2000V. When the instrument is not taking data, the extraction voltage is switched off and this value appears red. If this lens turns red during a measurement, try changing the tuning configuration as a particular combination of tuning settings can lead to poor extraction. Alternatively, the extraction lens may require replacement. Cr analyses wear out the extraction lens quicker than other elements so if it is not in optimal condition it can often become damaged during tuning.
- If the LED for guard electrode has turned red, un-tick it and tick it again.

Low ^{52}Cr signal:

- Check the sample uptake rate. If it is <1mL every 15mins then not enough sample is being aspirated into the instrument to generate the desired signal. The nebuliser can be changed to rectify this. The signal takes about 1 hour to stabilise again afterwards.

- If the ^{52}Cr signal becomes unstable or drops significantly (>2V) during the day, adjust the gas flow on the Aridus and re-check the size of the interference peaks in 'mass scan'. If the problem persists, check the Aridus tubing.

Note: Do not get too hung up on achieving the highest possible ^{52}Cr signal. A signal as low as 5V can produce accurate and precise (2SE = <0.020) isotopic measurements if the stability is good. It is *relative* changes in the size of the peaks that usually disrupt isotopic measurements, and high signal-to-noise ratios that drive up measurement errors.

Misaligned peaks:

- If adjustments in the 'Zoom Optics' tab do not allow the peaks to be aligned, then it is possible to readjust each cup position by changing each position under the 'Cup Configuration' menu. Carefully alter either H3 or H2 to better align the cups. Then select 'Set' to move the cup (not always successful). Make sure you save any changes.

Standard tests

1. Go into the 'Neptune Software' folder and open Sequence Editor.
2. Create a standard sequence.
3. Each standard will take about 30 minutes to complete. It is a good idea to process each standard as the data becomes available (See 'Data Processing'), as this will save time if there is an obvious problem. Check the 2SE value of each standard - this should be <0.020. Also check the 2SD of the standard measurements. This should be similar to the long term reproducibility (currently 0.04‰).

Standard sequence:

1. The sequence should contain at least 3 spiked NBS979 standards alternated with blanks before and after.
2. Set the wash time in each blank to 5 minutes (0 in the standards).
1. Select the correct method file for each row (e.g. 'Cr4 blank' and 'Cr4 sample').

2. Set the correct rack number (usually 1) and vial position for standard and sample vials.
3. Save the sequence.
4. Go to 'Execute' menu and untick 'Switch plasma off at end'.
5. Click the 'Play' button. Select the 'ASCII' output option and then 'OK'.

Troubleshooting for standards:

- Check for signal instability. Plot $\delta^{53}Cr$ of the individual cycles in a scatter graph (column 'EE' of the deconvolution spreadsheet). The scatter should be normal around 0‰. If the average value changes significantly through the standard run, the signal is unstable. Re-tune, check the measurement position carefully and run a few more standards. If the scatter is normal around 0‰ but too large, the signal-to-noise ratio is high. Take steps to increase size of signal as in 'Tuning', or change nebuliser to reduce noise.
- Check for particles in the standard. Particles produce inaccurate individual isotopic ratios (always too high for $^{50}Cr/^{52}Cr$, always too low for $^{54}Cr/^{52}Cr$) (**Fig. 4**). Plot one of these ratios (row DN or DP) in deconvolution spreadsheet. One or two unusual ratios is ok but if there are several which have moved away from the average in the same direction, the standard needs to be re-centrifuged.

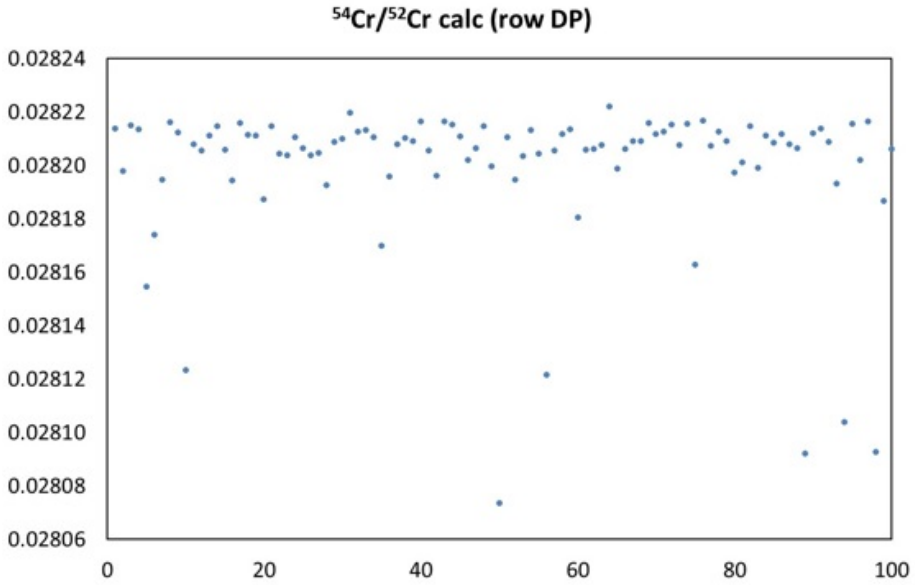

Figure C.8 - Particles in double spike create low ratios at random.

Sample Run

1. Prior to sample analysis, dip test your samples. Pour them into 2mL vials and place them in the same rack position they will be in for the run. This allows you to check that the Autosampler is correctly aligned for each vial as you go along. Send the probe to each sample and measure the ^{52}Cr voltage. Send the probe back to the wash and allow the ^{52}Cr and ^{56}Fe signals to drop back to their background values between each sample. Dilute your samples using the 3% HNO_3 blank solution so that the signal will be within ±10% of the standard ^{52}Cr signal. Check the depth of the probe in one of the vials. It should be 2-3mm from the bottom. Adjust using the ESI software if necessary.
2. Write a sequence. This should start with 3 spiked NBS979 standards and another after every 3 samples (along with a secondary reference material if possible/appropriate, e.g. carbonate or OSIL seawater). Sample and standards should always be alternated with blanks. The wash time on the blank should be 12 minutes to allow adequate wash-out between samples. Ensure sample positions correspond with rack numbers and file names in the sequence.
3. A typical sample/standards takes 40 minutes including blanks. Calculate how long your run is (runs longer than 12 hours require regular checks).
4. If you want the torch to switch off automatically at the end of a run, tick 'Switch plasma off at the end' under the 'Execute' menu in Sequence Editor.
5. Click 'Play' button and tick 'ASCII' output option.
6. Check standards whenever possible throughout the run. Watch the analysis of the first couple of samples in the 'Evaluation' tab (click the graph icon to see a visual representation). It is normal for the signal to fluctuate or drop off somewhat during a standard/sample analysis (particularly natural water samples). However see 'Troubleshooting' for major signal drop-offs.
7. Run each sample 2-3 times and check the 2SD. It should be <0.1 for samples.

Turning off the Neptune:

1. Send the Autosampler to 'Home'. When the torch is off the probe should sit out of the wash (in air).
2. On 'Stop and Start Plasma', select 'Off'.
3. Turn the Aridus Ar flow down to zero.
4. Tidy up your sample vials and remove from the instrument lab.
5. Fill in Andy's lab book for billing if necessary.

Troubleshooting for samples:

- If the ^{52}Cr signal drops by more than 30% and does not show signs of recovery within ~20 individual measurement cycles, the sample may contain too much dissolved organic matter. In this case affected samples need to be dried down and treated with hydrogen peroxide before further analysis.
- If all signals drop to extremely low values (<0.0001) check for blockages in the probe tubing. Blockages are visible as air bubbles within the tubing. They can be fixed in two ways:

1. Take the probe out of the Autosampler arm and attach a syringe containing Milli-Q water to the probe tip using flexible tubing (a suitable syringe is usually kept next to the instrument). Pulse gently to shift a minor blockage. A large signal peak will be observed as the blockage passes through.
2. If this doesn't work, slowly drop 'sample gas' in the Tune application to 0. Then drop the Aridus sweep gas to 0. Pull the nebuliser tip out of the Aridus then increase 'sample gas' to 1. Place the probe into the wash – if it bubbles there is no blockage. If it does not bubble, check that the inner and outer tubes of the probe are flush with one another and then place a gloved finger over the end of the probe to flush the blockage. Hold the nebuliser tip close to a dark background (the base of the Autosampler works well). A fine spray should be visible – this indicates the blockage is fixed. Turn 'sample gas' back to 0 and replace the nebuliser tip.

Slowly increase the sample gas back to 1 and finally increase the Aridus gas to its previous value.

Data Processing

1. Open the deconvolution spreadsheet (most up-to-date file is currently 'DS deconvolution Soton spike HGH'). This file is set up for samples spiked with the double spike made at Southampton ('Soton spike').
2. Open the 'Neptune data' folder and find your data files. Sort by 'Date modified' from oldest-newest.
3. Open the two blank EXP files which bracket your first standard. Paste the blank data into the 'Background' section, starting at cell C44.
4. Plot the blank data and check for atypical values. Clear these values (don't delete).
5. Paste your sample data into the 'Sample' section starting at cell K44.
6. On the 'View' menu, click 'Macro' then select Macro1 and click 'Run'.
7. View results in blue bar (starting in cell B155). Check that the $\delta^{53}Cr$ looks reasonable and the 2SE error is no higher than 0.02.
8. Go to the 'ID' tab in the deconvolution spreadsheet. Enter the exact weight of the sample and spike and the concentration of the spike in cells C10-13. The sample concentration is given in cell F10.
9. Paste all standard values for the day into the 'NBS979 Cr Std reproducibility' file (both the 'Unnormalised' and 'Normalisation' tabs). In the 'Normalisation' tab make sure the correct calculations are applied in cells Z-AE and in the green bar underneath the samples (check previous session values for comparison). Cells Z, AD and AB in the green bar should be exactly 0 when the calculations are done correctly. The value in the S cell of the green bar (del 53/52) should be subtracted from all sample and standard $\delta^{53}Cr$ values to normalise them for daily drift.
10. Apply appropriate blank corrections to $\delta^{53}Cr$ and concentration values (e.g. blank Fe(II) correction for seawater).

Troubleshooting for data processing:

1. If the results say #DIV/0! after running the macro, check that all of your data is realistic. If voltages are extremely low in either the sample or blank values there may have been a blockage, or else the probe was not in the solution for the whole analysis. You can remove a single bad data point or a bad block of data by clearing all cells in the appropriate row after (and including) column DH. Also check that the macro calculation worked properly – 'del f mix' values in column CV (6th iteration) should be 0.
2. If the δ^{53}Cr 2SE is high, check for outlier values which were missed by the 2SD reject function. Plot column 'EE' and remove outliers as described in step 1.
3. If δ^{53}Cr is extremely high or low (e.g. 30‰), check which spike you used in your samples. The OU/Bristol spike has a different composition and this needs to be pasted into the appropriate cells at the top of the 'Deconvolution' and 'ID' tabs.

References

Abu-Saba, K. E. and Flegal, A. R. Chromium in San Francisco Bay: superposition of geochemical processes causes complex spatial distributions of redox species. *Mar. Chem.* **49** (2–3), 189-199 (1995).

Abu-Saba, K. E. and Flegal, A. R. Temporally variable freshwater sources of dissolved chromium to the San Francisco Bay estuary. *Environ. Sci. Technol.* **31**, 3455-3460 (1997).

Achterberg, E. P. and Berg, C. M. G. v. d. Chemical speciation of chromium and nickel in the western Mediterranean. *Deep Sea Res. (II Top. Stud. Oceanogr.)* **44** (3-4), 693-720 (1997).

Achterberg, E. P., Colombo, C. and van den Berg, C. M. G. The distribution of dissolved Cu, Zn, Ni, Co and Cr in English coastal surface waters. *Cont. Shelf Res.* **19** (4), 537-558 (1999).

Achterberg, E. P., Holland, T. W., Bowie, A. R., Mantoura, R. F. C. and Worsfold, P. J. Determination of iron in seawater. *Anal. Chim. Acta* **442** (1), 1-14 (2001).

Albarède, F. and Beard, B. Analytical methods for non-traditional isotopes. *Reviews in Mineralogy & Geochemistry* **55**, 113-152 (2004).

Algeo, T. J. and Maynard, J. B. Trace-element behavior and redox facies in core shales of Upper Pennsylvanian Kansas-type cyclothems. *Chem. Geol.* **206** (3–4), 289-318 (2004).

Amaro, T., Huvenne, V. A. I., Allcock, A. L., Aslam, T., Davies, J. S., Danovaro, R., De Stigter, H. C., Duineveld, G. C. A., Gambi, C., Gooday, A. J., Gunton, L. M., Hall, R., Howell, K. L., Ingels, J., Kiriakoulakis, K., Kershaw, C. E., Lavaleye, M. S. S., Robert, K., Stewart, H., Van Rooij, D., White, M. and Wilson, A. M. The Whittard Canyon – A case study of submarine canyon processes. *Prog. Oceanogr.* **146**, 38-57 (2016).

Anbar, A. D. and Rouxel, O. Metal stable isotopes in paleoceanography. *Earth. Planet. Sci. Lett.* **35**, 717-746 (2007).

Auger, Y., Bodineau, L., Leclercq, S. and Wartel, M. Some aspects of vanadium and chromium chemistry in the English Channel. *Cont. Shelf Res.* **19** (15–16), 2003-2018 (1999).

Babechuk, M. G., Kleinhanns, I. C. and Schoenberg, R. Chromium geochemistry of the ca. 1.85 Ga Flin Flon paleosol. *Geobiology*, n/a-n/a (2016).

Bain, D. J. and Bullen, T. D. Chromium isotope fractionation during oxidation of Cr(III) by manganese oxides. *Geochim. Cosmochim. Acta* **69** (10) (2005).

Ball, J. W. and Bassett, R. L. Ion exchange separation of chromium from natural water matrix for stable isotope mass spectrometric analysis. *Chem. Geol.* **168** (1–2), 123-134 (2000).

Basu, A. and Johnson, T. M. Determination of hexavalent chromium reduction using Cr stable isotopes: Isotopic fractionation factors for permeable reactive barrier materials. *Environ. Sci. Technol.* **46** (10), 5353-5360 (2012).

Basu, A., Johnson, T. M. and Sanford, R. A. Cr isotope fractionation factors for Cr(VI) reduction by a metabolically diverse group of bacteria. *Geochim. Cosmochim. Acta* **142** (0), 349-361 (2014).

Beck, M., Dellwig, O., Schnetger, B. and Brumsack, H.-J. Cycling of trace metals (Mn, Fe, Mo, U, V, Cr) in deep pore waters of intertidal flat sediments. *Geochim. Cosmochim. Acta* **72** (12), 2822-2840 (2008).

Bedson, P. (2007). Guidelines for achieving high accuracy in isotope dilution mass spectrometry (IDMS). Cambridge, GBR, Royal Society of Chemistry.

Berger, A. and Frei, R. The fate of chromium during tropical weathering: A laterite profile from Central Madagascar. *Geoderma* **213** (0), 521-532 (2014).

Berna, E. C., Johnson, T. M., Makdisi, R. S. and Basu, A. Cr stable isotopes as indicators of Cr(VI) reduction in groundwater: A detailed time-series study of a point-source plume. *Environ. Sci. Technol.* **44**, 1043-1048 (2010).

Bonnand, P. (2011). Potential of Chromium Isotopes as a Tracer of Past Oxygenation. PhD, Open University (Centre for Earth, Planetary, Space and Astronomical Research).

Bonnand, P., James, R. H., Parkinson, I. J., Connelly, D. P. and Fairchild, I. J. The chromium isotopic composition of seawater and marine carbonates. *Earth. Planet. Sci. Lett.* **382**, 10-20 (2013).

Bonnand, P., Parkinson, I. J., James, R. H., Karjalainena, A.-M. and Fehra, M. A. Accurate and precise determination of stable Cr isotope compositions in carbonates by double spike MC-ICP-MS. *J. Anal. At. Spectrom.* **26**, 528-535 (2011).

Bratsch, S. G. Standard Electrode Potentials and Temperature Coefficients in Water at 298.15K. *J. Phys. Chem. Ref. Data* **18** (1), 1-21 (1989).

Brumsack, H. J. and Gieskes, J. M. Interstitial water trace-metal chemistry of laminated sediments from the Gulf of California, Mexico. *Mar. Chem.* **14** (1), 89-106 (1983).

Buerge, I. J. and Hug, S. J. Influence of organic ligands on chromium(VI) reduction by iron(II). *Environ. Sci. Technol.* **32** (14), 2092-2099 (1998).

Buerge, I. J. and Hug, S. J. Kinetics and pH dependence of chromium(VI) reduction by iron(II). *Environ. Sci. Technol.* **31**, 1426-1432 (1997).

Campbell, J. A. and Yeats, P. A. Dissolved chromium in the northwest Atlantic Ocean. *Earth. Planet. Sci. Lett.* **53** (3), 427-433 (1981).

Campbell, J. A. and Yeats, P. A. Dissolved Chromium in the St. Lawrence Estuary. *Estuar. Coast. Shelf Sci.* **19**, 513-522 (1984).

Carlson, C. A. and Ducklow, H. W. Dissolved organic carbon in the upper ocean of the central equatorial Pacific Ocean, 1992: Daily and finescale vertical variations. *Deep Sea Research Part II: Topical Studies in Oceanography* **42** (2), 639-656 (1995).

Chester, R. and Murphy, K. J. T. (1990). Metals in the marine atmosphere. Heavy Metals in the Marine Environment. R. Furness and P. Rainbow. Boca Raton, FL, CRC Press**:** 27-49.

Cole, D. B., Reinhard, C. T., Wang, X., Gueguen, B., Halverson, G. P., Gibson, T., Hodgskiss, M. S. W., McKenzie, N. R., Lyons, T. W. and Planavsky, N. J. A shale-hosted Cr isotope record of low atmospheric oxygen during the Proterozoic. *Geology* (2016).

Comber, S. and Gardner, M. Chromium redox speciation in natural waters. *J. Environ. Monit.* **5**, 410-413 (2003).

Connelly, D. P. (1997). Occurrence and behaviour of trace metals in coastal waters of Bermuda, and chromium in the Sargasso Sea. PhD, University of Southampton.

Connelly, D. P., Statham, P. J. and Knap, A. H. Seasonal changes in speciation of dissolved chromium in the surface Sargasso Sea. *Deep Sea Res. (I Oceanogr. Res. Pap.)* **53**, 1975-1988 (2006).

Cranston, R. E. Chromium in Cascadia Basin, northeast Pacific Ocean. *Mar. Chem.* **13** (2), 109-125 (1983).

Cranston, R. E. and Murray, J. W. Chromium species in the Columbia River and estuary. *Limnol. Oceanogr.* **25** (6), 1104-1112 (1980).

Cranston, R. E. and Murray, J. W. The determination of chromium species in natural waters. *Anal. Chim. Acta* **99**, 275-282 (1978).

Crawford, R. J., Harding, I. H. and Mainwaring, D. E. Adsorption and coprecipitation of single heavy metal ions onto the hydrated oxides of iron and chromium. *Langmuir* **9** (11), 3050-3056 (1993).

Crowe, S. A., Døssing, L. N., Beukes, N. J., Bau, M., Kruger, S. J., Frei, R. and Canfield, D. E. Atmospheric oxygenation three billion years ago. *Nature* **535-539** (2013).

Cullen, J. T., Chong, M. and Ianson, D. British Columbian continental shelf as a source of dissolved iron to the subarctic northeast Pacific Ocean. *Global Biogeochem. Cycles* **23** (4), n/a-n/a (2009).

Cullen, J. T. and Sherrell, R. M. Techniques for determination of trace metals in small samples of size-fractionated particulate matter: phytoplankton metals off central California. *Mar. Chem.* **67** (3–4), 233-247 (1999).

Cuss, C. and Gueguen, C. Impacts of Microbial Activity on the Optical and Copper-Binding Properties of Leaf-Litter Leachate. *Frontiers in Microbiology* **3** (166) (2012).

D'Arcy, J., Gilleaudeau, G. J., Peralta, S., Gaucher, C. and Frei, R. Redox fluctuations in the Early Ordovician oceans: An insight from chromium stable isotopes. *Chem. Geol.* (2016).

D'Arcy, J., Babechuk, M. G., Døssing, L. N., Gaucher, C. and Frei, R. Processes controlling the chromium isotopic composition of river water: Constrains from basaltic river catchments. *Geochim. Cosmochim. Acta* **186**, 296-315 (2016).

Dauby, P., Frankignoulle, M., Gobert, S. and Bouquegnou, J. Distribution of POC, PON, and particulate Al, Cd, Cr, Cu, Pb, Ti, Zn and 813C in the English Channel and adjacent areas. *Oceanol. Acta* **17** (6), 643-657 (1994).

Deng, B. and Stone, A. T. Surface-catalyzed chromium(VI) reduction: Reactivity comparisons of different organic reductants and different oxide surfaces. *Environ. Sci. Technol.* **30**, 2484-2494 (1996).

Dolamore-Frank, J. A. (1984). The analysis, occurrence and chemical speciation of zinc and chromium in natural waters. PhD, University of Southampton.

Døssing, L. N., Dideriksen, K., Stipp, S. L. S. and Frei, R. Reduction of hexavalent chromium by ferrous iron: A process of chromium isotope fractionation and its relevance to natural environments. *Chem. Geol.* **285** (1–4), 157-166 (2011).

Douglas, G. S., Mills, G. L. and Quinn, J. G. Organic copper and chromium complexes in the interstitial waters of Narragansett Bay sediments. *Mar. Chem.* **19** (2), 161-174 (1986).

Dyer, K. R. and Lasta King, H. The Residual Water Flow through the Solent, South England. *Geophysical Journal International* **42** (1), 97-106 (1975).

Dzomback, D. A. and Morel, F. M. M. (1990). Surface Complexation Modelling: Hydrous Ferric Oxide. New York, USA, John Wiley and Sons.

Economou-Eliopoulos, M., Frei, R. and Megremi, I. Potential leaching of Cr(VI) from laterite mines and residues of metallurgical products (red mud and slag): An integrated approach. *Journal of Geochemical Exploration* **162**, 40-49 (2016).

Elderfield, H. Chromium speciation in seawater. *Earth. Planet. Sci. Lett.* **9**, 10-16 (1970).

Ellis, A. S., Johnson, T. M. and Bullen, T. D. Chromium isotopes and the fate of hexavalent chromium in the environment. *Science* **295**, 2060-2062 (2002).

Ellis, A. S., Johnson, T. M. and Bullen, T. D. Using chromium stable isotope ratios to quantify Cr(VI) reduction: Lack of sorption effects. *Environ. Sci. Technol.* **38**, 3604-3607 (2004).

Elrod, V. A., Johnson, K. S., Fitzwater, S. E. and Plant, J. N. A long-term, high-resolution record of surface water iron concentrations in the upwelling-driven central California region. *Journal of Geophysical Research: Oceans* **113** (C11), n/a-n/a (2008).

Emerson, S., Cranston, R. E. and Liss, P. S. Redox species in a reducing fjord: equilibrium and kinetic considerations. *Deep Sea Research Part A. Oceanographic Research Papers* **26** (8), 859-878 (1979).

Fandeur, D., Juillot, F., Morin, G., Olivi, L., Cognigni, A., Webb, S. M., Ambrosi, J.-P., Fritsch, E., Guyot, F. and Brown, J. G. E. XANES Evidence for Oxidation of Cr(III) to Cr(VI) by Mn-Oxides in a Lateritic Regolith Developed on Serpentinized Ultramafic Rocks of New Caledonia. *Environ. Sci. Technol.* **43** (19), 7384-7390 (2009).

Fang, T.-H. (1995). Studies of the behaviour of trace metals during mixing in some estuaries of the Solent region. PhD, University of Southampton.

Fanning, J. C. The chemical reduction of nitrate in aqueous solution. *Coord. Chem. Rev.* **199** (1), 159-179 (2000).

Fantoni, D., Brozzo, G., Canepa, M., Cipolli, F., Marini, L., Ottonello, G. and Zuccolini, M. Natural hexavalent chromium in groundwaters interacting with ophiolitic rocks. *Environ. Geol.* **42** (8), 871-882 (2002).

Farkaš, J., Chrastný, V., Novák, M., Čadkova, E., Pašava, J., Chakrabarti, R., Jacobsen, S. B., Ackerman, L. and Bullen, T. D. Chromium isotope variations (δ53/52Cr) in mantle-derived sources and their weathering products: Implications for environmental studies and the evolution of δ53/52Cr in the Earth's mantle over geologic time. *Geochim. Cosmochim. Acta* **123** (0), 74-92 (2013).

Fendorf, S. E. and Li, G. Kinetics of Chromate Reduction by Ferrous Iron. *Environ. Sci. Technol.* **30** (5), 1614-1617 (1996).

Frei, R., Crowe, S. A., Bau, M., Polat, A., Fowle, D. A. and Døssing, L. N. Oxidative elemental cycling under the low O(2) Eoarchean atmosphere. *Scientific Reports* **6**, 21058 (2016).

Frei, R., Gaucher, C., Døssing, L. N. and Sial, A. N. Chromium isotopes in carbonates — A tracer for climate change and for reconstructing the redox state of ancient seawater. *Earth. Planet. Sci. Lett.* **312** (1–2), 114-125 (2011).

Frei, R., Gaucher, C., Poulton, S. W. and Canfield, D. E. Fluctuations in Precambrian atmospheric oxygenation recorded by chromium isotopes. *Nature* **461**, 250-253 (2009).

Frei, R., Gaucher, C., Stolper, D. and Canfield, D. E. Fluctuations in late Neoproterozoic atmospheric oxidation — Cr isotope chemostratigraphy and iron speciation of the late Ediacaran lower Arroyo del Soldado Group (Uruguay). *Gondwana Res* **23** (2), 797-811 (2013).

Frei, R., Poiré, D. and Frei, K. M. Weathering on land and transport of chromium to the ocean in a subtropical region (Misiones, NW Argentina): A chromium stable isotope perspective. *Chem. Geol.* **381** (0), 110-124 (2014).

Frei, R. and Polat, A. Chromium isotope fractionation during oxidative weathering—Implications from the study of a Paleoproterozoic (ca. 1.9 Ga) paleosol, Schreiber Beach, Ontario, Canada. *Precambrian Res.* **224** (0), 434-453 (2013).

Gaillardet, J., Viers, J. and Dupré, B. (2003). 5.09 - Trace elements in river waters. Treatise on Geochemistry. H. D. Holland and K. K. Turekian. Oxford, Pergamon**:** 225-272.

Gardner, M. J. and Ravenscroft, J. E. Determination of chromium(III) and total chromium in marine waters. *Fresenius J. Anal. Chem.* **354**, 602-605 (1996).

German, C. R., Campbell, A. C. and Edmond, J. M. Hydrothermal scavenging at the Mid-Atlantic Ridge: Modification of trace element dissolved fluxes. *Earth. Planet. Sci. Lett.* **107** (1), 101-114 (1991).

Gilkes, R. J. Clay Mineral Provinces in the Tertiary Sediments of the Hampshire Basin. *Clay Minerals* **7**, 351-361 (1968).

Gilleaudeau, G. J., Frei, R., Kaufman, A. J., Kah, L. C., Azmy, K., Bartley, J. K., Chernyavskiy, P. and Knoll, A. H. Oxygenation of the mid-Proterozoic atmosphere: clues from chromium isotopes in carbonates. *Geochemical Perspectives Letters* **2** (2), 179-187 (2016).

Gómez, V. and Callao, M. P. Chromium determination and speciation since 2000. *TrAC, Trends Anal. Chem.* **25** (10), 1006-1015 (2006).

Gueguen, B., Reinhard, C. T., Algeo, T. J., Peterson, L. C., Nielsen, S. G., Wang, X., Rowe, H. and Planavsky, N. J. The chromium isotope composition of reducing and oxic marine sediments. *Geochim. Cosmochim. Acta* **184**, 1-19 (2016).

Han, R., Qin, L., Brown, S. T., Christensen, J. N. and Beller, H. R. Differential Isotopic Fractionation during Cr(VI) Reduction by an Aquifer-Derived Bacterium under Aerobic versus Denitrifying Conditions. *Appl. Environ. Microbiol.* **78** (7), 2462-2464 (2012).

Hans Wedepohl, K. The composition of the continental crust. *Geochim. Cosmochim. Acta* **59** (7), 1217-1232 (1995).

Hansell, D. A. and Carlson, C. A. Deep-ocean gradients in the concentration of dissolved organic carbon. *Nature* **395** (6699), 263-266 (1998).

Heikoop, J. M., Johnson, T. M., Birdsell, K. H., Longmire, P., Hickmott, D. D., Jacobs, E. P., Broxton, D. E., Katzman, D., Vesselinov, V. V., Ding, M., Vaniman, D. T., Reneau, S. L., Goering, T. J., Glessner, J. and Basu, A. Isotopic evidence for reduction of anthropogenic hexavalent chromium in Los Alamos National Laboratory groundwater. *Chem. Geol.* **373** (0), 1-9 (2014).

Helly, J. J. and Levin, L. A. Global distribution of naturally occurring marine hypoxia on continental margins. *Deep Sea Research Part I: Oceanographic Research Papers* **51** (9), 1159-1168 (2004).

Hicks, N., Ubbara, G. R., Silburn, B., Smith, H. E. K., Kröger, S., Parker, E. R., Sivyer, D., Kitidis, V., Hatton, A., Mayor, D. J. and Stahl, H. Oxygen dynamics in shelf seas sediments incorporating seasonal variability. *Biogeochemistry*, 1-13 (2017).

Holland, H. D. The oxygenation of the atmosphere and oceans. *Phil. Trans. R. Soc. B* **361**, 903-915 (2006).

Holliday, L. M. and Liss, P. S. The behaviour of dissolved iron, manganese and zinc in the Beaulieu Estuary, S. England. *Estuarine and Coastal Marine Science* **4** (3), 349-353 (1976).

Holmden, C., Jacobson, A. D., Sageman, B. B. and Hurtgen, M. T. Response of the Cr isotope proxy to Cretaceous Ocean Anoxic Event 2 in a pelagic carbonate succession from the Western Interior Seaway. *Geochim. Cosmochim. Acta* **186**, 277-295 (2016).

Holmden, C. E. B., A. (2013). Tracing paleo-ocean redox using Cr isotopes in carbonates spanning the Great Oxidation Event. American Geophysical Union, Fall Meeting 2013

Hopwood, M. J., Statham, P. J. and Milani, A. Dissolved Fe(II) in a river-estuary system rich in dissolved organic matter. *Estuar. Coast. Shelf Sci.* **151**, 1-9 (2014).

Hopwood, M. J., Statham, P. J., Skrabal, S. A. and Willey, J. D. Dissolved iron(II) ligands in river and estuarine water. *Mar. Chem.* **173**, 173-182 (2015).

Hough, M. L., Shields, G. A., Evins, L. Z., Strauss, H., Henderson, R. A. and Mackenzie, S. A major sulphur isotope event at c. 510 Ma: a possible anoxia–extinction–volcanism connection during the Early-Middle Cambrian transition? *Terra Nova* **18** (4), 257-263 (2006).

Hug, S. J., Laubscher, H.-U. and James, B. R. Iron(III) catalyzed photochemical reduction of chromium(VI) by oxalate and citrate in aqueous solutions. *Environ. Sci. Technol.* **31**, 160-170 (1997).

Huthnance, J. M., Holt, J. T. and Wakelin, S. L. Deep ocean exchange with west-European shelf seas. *Ocean Sci.* **5**, 621-634 (2009).

Hydes, D. J., Gowen, R. J., Holliday, N. P., Shammon, T. and Mills, D. External and internal control of winter concentrations of nutrients (N, P and Si) in north-west European shelf seas. *Estuar. Coast. Shelf Sci.* **59** (1), 151-161 (2004).

Izbicki, J. A., Ball, J. W., Bullen, T. D. and Sutley, S. J. Chromium, chromium isotopes and selected trace elements, western Mojave Desert, USA. *Appl. Geochem.* **23** (5), 1325-1352 (2008).

Jamieson-Hanes, J. H., Gibson, B. D., Lindsay, M. B. J., Kim, Y., Ptacek, C. J. and Blowes, D. W. Chromium isotope fractionation during reduction of Cr(VI) under saturated flow conditions. *Environ. Sci. Technol.* **46** (12), 6783-6789 (2012).

Jeandel, C. and Minster, J. F. Chromium behaviour in the ocean: Global versus regional processes. *Global Biogeochem. Cycles* **1** (2), 131-154 (1987).

Jeandel, C. and Minster, J. F. Isotope dilution measurement of inorganic chromium(III) and total chromium in seawater. *Mar. Chem.* **14** (4), 347-364 (1984).

Johnson, C. A., Sigg, L. and Lindauer, U. The chromium cycle in a seasonally anoxic lake. *Limnol. Oceanogr.* **37** (2), 315-321 (1992).

Joint, I., Wollast, R., Chou, L., Batten, S., Elskens, M., Edwards, E., Hirst, A., Burkill, P., Groom, S., Gibb, S., Miller, A., Hydes, D., Dehairs, F., Antia, A., Barlow, R., Rees, A., Pomroy, A., Brockmann, U., Cummings, D., Lampitt, R., Loijens, M., Mantoura, F., Miller, P., Raabe, T., Alvarez-Salgado, X., Stelfox, C. and Woolfenden, J. Pelagic production at the Celtic Sea shelf break. *Deep Sea Research Part II: Topical Studies in Oceanography* **48** (14–15), 3049-3081 (2001).

Jonas, P. J. C. and Millward, G. E. Metals and nutrients in the Severn Estuary and Bristol Channel: Contemporary inputs and distributions. *Mar. Pollut. Bull.* **61** (1–3), 52-67 (2010).

Joshi, S., Wang, D., Ellis, A. S., Johnson, T. M. and Bullen, T. D. (2011). Stable Isotope Fractionation during Cr(III) oxidation by manganese oxides. American Geophysical Union, Fall Meeting 2011, abstract #EP41B-0622.

Kaczynski, S. E. and Kieber, R. J. Hydrophobic C18 bound organic complexes of chromium and their potential impact on the geochemistry of chromium in natural waters. *Environ. Sci. Technol.* **28**, 799-804 (1994).

Keeling, R. F., Kortzinger, A. and Gruber, N. Ocean deoxygenation in a warming world. *Ann. Rev. Mar. Sci.* **2**, 199-229 (2010).

Kent, D. B., Davis, J. A., Anderson, L. C. D. and Rea, B. A. Transport of chromium and selenium in a pristine sand and gravel aquifer: Role of adsorption processes. *Water Resour. Res.* **31** (4), 1041-1050 (1995).

Kieber, R. J. and Helz, G. R. Indirect photoreduction of aqueous chromium(VI). *Environ. Sci. Technol.* **26**, 307-312 (1992).

Kim, C., Zhou, Q., Deng, B., Thornton, E. C. and Xu, H. Chromium(VI) Reduction by Hydrogen Sulfide in Aqueous Media: Stoichiometry and Kinetics. *Environ. Sci. Technol.* **35** (11), 2219-2225 (2001).

Kingston, H. M., Huo, D., Lu, Y. and Chalk, S. Accuracy in species analysis: speciated isotope dilution mass spectrometry (SIDMS) exemplified by the evaluation of chromium species. *Spectrochim. Acta, Part B* **53**, 299-309 (1998).

Kitchen, J. W., Johnson, T. M., Bullen, T. D., Zhu, J. and Raddatz, A. Chromium isotope fractionation factors for reduction of Cr(VI) by aqueous Fe(II) and organic molecules. *Geochim. Cosmochim. Acta* **89** (0), 190-201 (2012).

Kitidis, V., Tait, K., Nunes, J., Brown, I., Woodward, E. M. S., Harris, C., Sabadel, A. J. M., Sivyer, D. B., Silburn, B. and Kröger, S. Seasonal benthic nitrogen cycling in a temperate shelf sea: the Celtic Sea. *Biogeochemistry*, 1-17 (2017).

Klar, J. K. (2014). Iron isotopes in seawater: method development and results from the Atlantic Ocean. PhD, University of Southampton.

Klar, J. K., Homoky, W. B., Statham, P. J., Birchill, A. J., Harris, E. L., Woodward, E. M. S., Silburn, B., Cooper, M. J., James, R. H., Connelly, D. P., Chever, F., Lichtschlag, A. and Graves, C. Stability of dissolved and soluble Fe(II) in shelf sediment pore waters and release to an oxic water column. *Biogeochemistry*, 1-19 (2017).

Konhauser, K. O., Lalonde, S. V., Planavsky, N. J., Pecoits, E., Lyons, T. W., Mojzsis, S. J., Rouxel, O. J., Barley, M. E., Rosiere, C., Fralick, P. W., Kump, L. R. and Bekker, A. Aerobic bacterial pyrite oxidation and acid rock drainage during the Great Oxidation Event. *Nature* **478** (7369), 369-373 (2011).

Larsen, K. K., Wielandt, D., Schiller, M. and Bizzarro, M. Chromatographic speciation of Cr(III)-species, inter-species equilibrium isotope fractionation and improved chemical purification strategies for high-precision isotope analysis. *J. Chromatogr. A* **1443**, 162-174 (2016).

Lehmann, B., Frei, R., Xu, L. and Mao, J. Early Cambrian Black Shale-Hosted Mo-Ni and V Mineralization on the Rifted Margin of the Yangtze Platform, China: Reconnaissance Chromium Isotope Data and a Refined Metallogenic Model. *Economic Geology* **111** (1), 89-103 (2016).

Levasseur, A., Shi, L., Wells, N. C., Purdie, D. A. and Kelly-Gerreyn, B. A. A three-dimensional hydrodynamic model of estuarine circulation with an application to Southampton Water, UK. *Estuar. Coast. Shelf Sci.* **73** (3–4), 753-767 (2007).

Lewis, B. L. and Landing, W. M. The biogeochemistry of manganese and iron in the Black Sea. *Deep Sea Research Part A. Oceanographic Research Papers* **38, Supplement 2**, S773-S803 (1991).

Li, S.-X., Zheng, F.-Y., Hong, H.-S., Deng, N.-s. and Lin, L.-X. Influence of marine phytoplankton, transition metals and sunlight on the species distribution of chromium in surface seawater. *Mar. Environ. Res.* **67**, 199-206 (2009).

Lyons, T. W. and Reinhard, C. T. Early Earth: Oxygen for heavy-metal fans. *Nature* **461** (7261), 179-181 (2009).

Magar, V. S., Martello, L., Southworth, B., Fuchsman, P., Sorensen, M. and Wenning, R. J. Geochemical stability of chromium in sediments from the lower Hackensack River, New Jersey. *Sci. Total Environ.* **394** (1), 103-111 (2008).

Marqués, M. J., Salvador, A., Morales-Rubio, A. and de la Guardia, M. Chromium speciation in liquid matrices: a survey of the literature. *Fresenius J. Anal. Chem.* **367** (7), 601-613 (2000).

Martello, L., Fuchsman, P., Sorensen, M., Magar, V. and Wenning, R. J. Chromium Geochemistry and Bioaccumulation in Sediments from the Lower Hackensack River, New Jersey. *Arch. Environ. Contam. Toxicol.* **53** (3), 337-350 (2007).

Masscheleyn, P. H., Pardue, J. H., DeLaune, R. D. and Patrick, J. W. H. Chromium redox chemistry in a lower Mississippi Valley bottomland hardwood wetland. *Environ. Sci. Technol.* **26** (6), 1217-1226 (1992).

Mayer, L. M. and Schick, L. L. Removal of hexavalent chromium from estuarine waters by model substrates and natural sediments. *Environ. Sci. Technol.* **15** (12), 1482-1484 (1981).

McCartney, M. S. Recirculating components to the deep boundary current of the northern North Atlantic. *Prog. Oceanogr.* **29** (4), 283-383 (1992).

McClain, C. N. and Maher, K. Chromium fluxes and speciation in ultramafic catchments and global rivers. *Chem. Geol.* **426**, 135-157 (2016).

Miller, W. L. and Zepp, R. G. Photochemical production of dissolved inorganic carbon from terrestrial organic matter: Significance to the oceanic organic carbon cycle. *Geophys. Res. Lett.* **22** (4), 417-420 (1995).

Moore, R. M., Burton, J. D., Williams, P. J. L. and Young, M. L. The behaviour of dissolved organic material, iron and manganese in estuarine mixing. *Geochim. Cosmochim. Acta* **43** (6), 919-926 (1979).

Murray, J. W., Spell, B. and Paul, B. (1983). The Contrasting Geochemistry of Manganese and Chromium in the Eastern Tropical Pacific Ocean. Trace Metals in Sea Water. C. S. Wong, E. Boyle, K. W. Bruland, J. D. Burton and E. D. Goldberg. Boston, MA, Springer US**:** 643-669.

Murray, J. W., Top, Z. and Özsoy, E. Hydrographic properties and ventilation of the Black Sea. *Deep Sea Research Part A. Oceanographic Research Papers* **38, Supplement 2**, S663-S689 (1991).

Murray, R. W. and Leinen, M. Chemical transport to the seafloor of the equatorial Pacific Ocean across a latitudinal transect at 135°W: Tracking sedimentary major, trace, and rare earth element fluxes at the Equator and the Intertropical Convergence Zone. *Geochim. Cosmochim. Acta* **57** (17), 4141-4163 (1993).

Nakayama, E., Kuwamoto, T., Tsurubo, S., Tokoro, H. and Fujinaga, T. Chemical speciation of chromium in sea water: Part 1. Effect of naturally occurring organic materials on the complex formation of chromium(III). *Anal. Chim. Acta* **130** (2), 289-294 (1981).

Nameroff, T. J., Calvert, S. E. and Murray, J. W. Glacial-interglacial variability in the eastern tropical North Pacific oxygen minimum zone recorded by redox-sensitive trace metals. *Paleoceanography* **19** (1), n/a-n/a (2004).

Neubert, N., Nägler, T. F. and Böttcher, M. E. Sulfidity controls molybdenum isotope fractionation into euxinic sediments: Evidence from the modern Black Sea. *Geology* **36** (10), 775-778 (2008).

Novak, M., Chrastny, V., Cadkova, E., Farkas, J., Bullen, T. D., Tylcer, J., Szurmanova, Z., Cron, M., Prechova, E., Curik, J., Stepanova, M., Pasava, J., Erbanova, L., Houskova, M., Puncochar, K. and Hellerich, L. A. Common occurrence of a positive δ53Cr shift in central European waters contaminated by geogenic/industrial chromium relative to source values. *Environ. Sci. Technol.* **48** (11), 6089-6096 (2014).

O'Connor, A. E., Luek, J. L., McIntosh, H. and Beck, A. J. Geochemistry of redox-sensitive trace elements in a shallow subterranean estuary. *Mar. Chem.* **172**, 70-81 (2015).

Ohata, M., Ichinose, T., Furuta, N., Shinohara, A. and Chiba, M. Isotope dilution analysis of Se in human blood serum by using high-power nitrogen microwave-induced plasma mass spectrometry coupled with a hydride generation technique. *Anal. Chem.* **70** (13), 2726-2730 (1998).

Oze, C., Bird, D. K. and Fendorf, S. Genesis of hexavalent chromium from natural sources in soil and groundwater. *Proceedings of the National Academy of Sciences* **104** (16), 6544-6549 (2007).

Oze, C., Fendorf, S., Bird, D. K. and Coleman, R. G. Chromium geochemistry in serpentinized ultramafic rocks and serpentine soils from the Franciscan complex of California. *Am. J. Sci.* **304**, 67-101 (2004).

Paulmier, A. and Ruiz-Pino, D. Oxygen minimum zones (OMZs) in the modern ocean. *Prog. Oceanogr.* **80** (3), 113-128 (2009).

Paulukat, C. (2015). Chromium stable isotope fractionation in modern biogeochemical cycling: Insights from continental weathering flux to the ocean, and chromium incorporation into carbonate shells. PhD, University of Copenhagen.

Paulukat, C., Døssing, L. N., Mondal, S. K., Voegelin, A. R. and Frei, R. Oxidative release of chromium from Archean ultramafic rocks, its transport and environmental impact – A Cr isotope perspective on the Sukinda valley ore district (Orissa, India). *Appl. Geochem.* **59** (0), 125-138 (2015).

Paulukat, C., Gilleaudeau, G. J., Chernyavskiy, P. and Frei, R. The Cr-isotope signature of surface seawater — A global perspective. *Chem. Geol.* **444**, 101-109 (2016).

Pearce, C. R., Cohen, A. S., Coe, A. L. and Burton, K. W. Molybdenum isotope evidence for global ocean anoxia coupled with perturbations to the carbon cycle during the Early Jurassic. *Geology* **36**, 231-234 (2008).

Pelegrí, J. L. and Benazzouz, A. (2015). Coastal upwelling off North-West Africa. Oceanographic and biological features in the Canary Current Large Marine Ecosystem. Paris, IOC-UNESCO**:** 93-103.

Pemberton, K., Rees, A. P., Miller, P. I., Raine, R. and Joint, I. The influence of water body characteristics on phytoplankton diversity and production in the Celtic Sea. *Cont. Shelf Res.* **24** (17), 2011-2028 (2004).

Pereira, N. S., Voegelin, A. R., Paulukat, C., Sial, A. N., Ferreira, V. P. and Frei, R. Chromium-isotope signatures in scleractinian corals from the Rocas Atoll, Tropical South Atlantic. *Geobiology*, n/a-n/a (2015).

Pettine, M. and Millero, F. J. Chromium speciation in seawater: The probable role of hydrogen peroxide. *Limnol. Oceanogr.* **35** (3), 730-736 (1990).

Pettine, M., Millero, F. J. and La Noce, T. Chromium (III) interactions in seawater through its oxidation kinetics. *Mar. Chem.* **34** (1–2), 29-46 (1991).

Pingree, R. D. Baroclinic eddies bordering the Celtic Sea in late summer. *J. Mar. Biol. Assoc. U.K.* **59** (3), 689-703 (1979).

Pingree, R. D., Griffiths, D. K. and Mardell, G. T. The structure of the internal tide at the Celtic Sea shelf break. *J. Mar. Biol. Assoc. U.K.* **64**, 99-113 (1983).

Pingree, R. D. and Le Cann, B. Celtic and Armorican slope and shelf residual currents. *Prog. Oceanogr.* **23** (4), 303-338 (1989).

Piper, D. Z. Seawater as the source of minor elements in black shales, phosphorites and other sedimentary rocks. *Chem. Geol.* **114** (1–2), 95-114 (1994).

Piper, D. Z. and Calvert, S. E. A marine biogeochemical perspective on black shale deposition. *Earth-Sci. Rev.* **95** (1–2), 63-96 (2009).

Planavsky, N. J., Cole, D. B., Reinhard, C. T., Diamond, C., Love, G. D., Luo, G., Zhang, S., Konhauser, K. O. and Lyons, T. W. No evidence for high atmospheric oxygen levels 1,400 million years ago. *Proceedings of the National Academy of Sciences* **113** (19), E2550-E2551 (2016).

Planavsky, N. J., Reinhard, C. T., Wang, X., Thomson, D., McGoldrick, P., Rainbird, R. H., Johnson, T., Fischer, W. W. and Lyons, T. W. Low Mid-Proterozoic atmospheric oxygen levels and the delayed rise of animals. *Science* **346** (6209), 635-638 (2014).

Pollard, R. T., Grifftths, M. J., Cunningham, S. A., Read, J. F., Pérez, F. F. and Ríos, A. F. Vivaldi 1991 - A study of the formation, circulation and ventilation of Eastern North Atlantic Central Water. *Prog. Oceanogr.* **37** (2), 167-192 (1996).

Porter, M., Inall, M. E., Hopkins, J., Palmer, M. R., Dale, A. C., Aleynik, D., Barth, J. A., Mahaffey, C. and Smeed, D. A. Glider observations of enhanced deep water upwelling at a shelf break canyon: A mechanism for cross-slope carbon and nutrient exchange. *Journal of Geophysical Research: Oceans* **121** (10), 7575-7588 (2016).

Raddatz, A. L., Johnson, T. M. and McLing, T. L. Cr stable isotopes in Snake River Plain aquifer groundwater: Evidence for natural reduction of dissolved Cr(VI). *Environ. Sci. Technol.* **45** (2), 502-507 (2010).

Rai, D., Sass, B. M. and Moore, D. A. Chromium(III) hydrolysis constants and solubility of chromium(III) hydroxide. *Inorg. Chem.* **26**, 345-349 (1987).

Reinhard, C. T., Planavsky, N. J., Robbins, L. J., Partin, C. A., Gill, B. C., Lalonde, S. V., Bekker, A., Konhauser, K. O. and Lyons, T. W. Proterozoic ocean redox and biogeochemical stasis. *Proceedings of the National Academy of Sciences* **110** (14), 5357-5362 (2013).

Reinhard, C. T., Planavsky, N. J., Wang, X., Fischer, W. W., Johnson, T. M. and Lyons, T. W. The isotopic composition of authigenic chromium in anoxic marine sediments: A case study from the Cariaco Basin. *Earth. Planet. Sci. Lett.* **407** (0), 9-18 (2014).

Remoundaki, E., Hatzikioseyian, A. and Tsezos, M. A systematic study of chromium solubility in the presence of organic matter: consequences for the treatment of chromium-containing wastewater. *Journal of Chemical Technology & Biotechnology* **82** (9), 802-808 (2007).

Rigaud, S., Radakovitch, O., Couture, R.-M., Deflandre, B., Cossa, D., Garnier, C. and Garnier, J.-M. Mobility and fluxes of trace elements and nutrients at the sediment–water interface of a lagoon under contrasting water column oxygenation conditions. *Appl. Geochem.* **31**, 35-51 (2013).

Robbins, L. J., Lalonde, S. V., Planavsky, N. J., Partin, C. A., Reinhard, C. T., Kendall, B., Scott, C., Hardisty, D. S., Gill, B. C., Alessi, D. S., Dupont, C. L., Saito, M. A., Crowe, S. A., Poulton, S. W., Bekker, A., Lyons, T. W. and Konhauser, K. O. Trace elements at the intersection of marine biological and geochemical evolution. *Earth-Sci. Rev.* **163**, 323-348 (2016).

Robinson, R. S., Kienast, M., Luiza Albuquerque, A., Altabet, M., Contreras, S., De Pol Holz, R., Dubois, N., Francois, R., Galbraith, E., Hsu, T.-C., Ivanochko, T., Jaccard, S., Kao, S.-J., Kiefer, T., Kienast, S., Lehmann, M., Martinez, P., McCarthy, M., Möbius, J., Pedersen, T. F., Quan, T. M., Ryabenko, E., Schmittner, A., Schneider, R., Schneider-Mor, A., Shigemitsu, M., Sinclair, D., Somes, C., Studer, A., Thunell, R. and Yang, J.-Y. A review of nitrogen isotopic alteration in marine sediments. *Paleoceanography* **27** (4), PA4273 (2012).

Rodler, A., Sánchez-Pastor, N., Fernández-Díaz, L. and Frei, R. Fractionation behavior of chromium isotopes during coprecipitation with calcium carbonate: Implications for their use as paleoclimatic proxy. *Geochim. Cosmochim. Acta* **164** (0), 221-235 (2015).

Rodler, A. S., Frei, R., Gaucher, C. and Germs, G. J. B. Chromium isotope, REE and redox-sensitive trace element chemostratigraphy across the late Neoproterozoic Ghaub glaciation, Otavi Group, Namibia. *Precambrian Res.* **286**, 234-249 (2016).

Rodler, A. S., Hohl, S. V., Guo, Q. and Frei, R. Chromium isotope stratigraphy of Ediacaran cap dolostones, Doushantuo Formation, South China. *Chem. Geol.* **436**, 24-34 (2016).

Rolison, J. (2016). The biogeochemistry of trace metals and their isotopes in the Mediterranean and Black Seas. PhD, University of Otago.

Rolison, J. M., Stirling, C. H., Middag, R. and Rijkenberg, M. J. A. Uranium stable isotope fractionation in the Black Sea: Modern calibration of the 238U/235U paleo-redox proxy. *Geochim. Cosmochim. Acta* **203**, 69-88 (2017).

Rudnick, R. L. and Gao, S. (2003). 3.01 - Composition of the Continental Crust A2 - Holland, Heinrich D. Treatise on Geochemistry. K. K. Turekian. Oxford, Pergamon**:** 1-64.

Rue, E. L., Smith, G. J., Cutter, G. A. and Bruland, K. W. The response of trace element redox couples to suboxic conditions in the water column. *Deep Sea Res. (I Oceanogr. Res. Pap.)* **44** (1), 113-134 (1997).

Sander, S., Koschinsky, A. and Halbach, P. Redox speciation of chromium in the oceanic water column of the Lesser Antilles and offshore Otago Peninsula, New Zealand. *Mar. Freshwat. Res.* **54**, 745-754 (2003).

Saputro, S., Yoshimura, K., Matsuoka, S., Takehara, K., Narsito, Aizawa, J. and Tennichi, Y. Speciation of dissolved chromium and the mechanisms controlling its concentration in natural water. *Chem. Geol.* **364**, 33-41 (2014).

Sass, B. M. and Rai, D. Solubility of amorphous chromium(III)-iron(III) hydroxide solid solutions. *Inorg. Chem.* **26** (14), 2228-2232 (1987).

Schauble, E., Rossman, G. R. and Taylor Jr, H. P. Theoretical estimates of equilibrium chromium-isotope fractionations. *Chem. Geol.* **205** (1–2), 99-114 (2004).

Scheiderich, K., Amini, M., Holmden, C. and Francois, R. Global variability of chromium isotopes in seawater demonstrated by Pacific, Atlantic, and Arctic Ocean samples. *Earth. Planet. Sci. Lett.* **423**, 87-97 (2015).

Schoenberg, R., Zink, S., Staubwasser, M. and Blanckenburg, F. v. The stable Cr isotope inventory of solid Earth reservoirs determined by double spike MC-ICP-MS. *Chem. Geol.* **249**, 294-306 (2008).

Schroeder, D. C. and Lee, G. F. Potential transformations of chromium in natural waters. *Water, Air, Soil Pollut.* **4**, 355-365 (1975).

Semeniuk, D. M., Maldonado, M. T. and Jaccard, S. L. Chromium uptake and adsorption in marine phytoplankton – Implications for the marine chromium cycle. *Geochim. Cosmochim. Acta* **184**, 41-54 (2016).

Severmann, S. and Anbar, A. D. Reconstructing paleoredox conditions through a multitracer approach: The key to the past is the present. *Elements* **5**, 359-364 (2009).

Severmann, S., McManus, J., Berelson, W. M. and Hammond, D. E. The continental shelf benthic iron flux and its isotope composition. *Geochim. Cosmochim. Acta* **74** (14), 3984-4004 (2010).

Shaw, T. J., Gieskes, J. M. and Jahnke, R. A. Early diagenesis in differing depositional environments: The response of transition metals in pore water. *Geochim. Cosmochim. Acta* **54**, 1233-1246 (1990).

Sherrell, R. M. and Boyle, E. A. Zinc, chromium, vanadium and iron in the Mediterranean Sea. *Deep Sea Research Part A. Oceanographic Research Papers* **35** (8), 1319-1334 (1988).

Sholkovitz, E. R. Flocculation of dissolved organic and inorganic matter during the mixing of river water and seawater. *Geochim. Cosmochim. Acta* **40** (7), 831-845 (1976).

Sholkovitz, E. R., Boyle, E. A. and Price, N. B. The removal of dissolved humic acids and iron during estuarine mixing. *Earth. Planet. Sci. Lett.* **40** (1), 130-136 (1978).

Sial, A. N., Campos, M. S., Gaucher, C., Frei, R., Ferreira, V. P., Nascimento, R. C., Pimentel, M. M., Pereira, N. S. and Rodler, A. Algoma-type Neoproterozoic BIFs and related marbles in the Serido Belt (NE Brazil): REE, C, O, Cr and Sr isotope evidence. *J South Am Earth Sci* **61**, 33-52 (2015).

Siedlecki, S. A., Mahadevan, A. and Archer, D. E. Mechanism for export of sediment-derived iron in an upwelling regime. *Geophys. Res. Lett.* **39** (3), n/a-n/a (2012).

Sikora, E. R., Johnson, T. M. and Bullen, T. D. Microbial mass-dependent fractionation of chromium isotopes. *Geochim. Cosmochim. Acta* **72** (15), 3631-3641 (2008).

Sirinawin, W., Turner, D. R. and Westerlund, S. Chromium(VI) distributions in the Arctic and the Atlantic Oceans and a reassessment of the oceanic Cr cycle. *Mar. Chem.* **71** (3–4), 265-282 (2000).

Sirinawin, W. and Westerlund, S. Analysis and storage of samples for chromium determination in seawater. *Anal. Chim. Acta* **356** (1), 35-40 (1997).

Smillie, R. H., Hunter, K. and Loutit, M. Reduction of chromium(VI) by bacterially produced hydrogen sulphide in a marine environment. *Water Res.* **15** (12), 1351-1354 (1981).

British Geological Society (2017). *GeoIndex Onshore*, http://www.bgs.ac.uk/geoindex [Accessed 13 June 2017].

Sperling, M., Xu, S. and Welz, B. Determination of chromium(III) and chromium(VI) in water using flow injection on-line preconcentration with selective adsorption on activated alumina and flame atomic absorption spectrometric detection. *Anal. Chem.* **64** (24), 3101-3108 (1992).

Stookey, L. L. Ferrozine---a new spectrophotometric reagent for iron. *Anal. Chem.* **42** (7), 779-781 (1970).

Stramma, L., Brandt, P., Schafstall, J., Schott, F., Fischer, J. and Körtzinger, A. Oxygen minimum zone in the North Atlantic south and east of the Cape Verde Islands. *Journal of Geophysical Research: Oceans* **113** (C4), n/a-n/a (2008).

Stramma, L. and England, M. On the water masses and mean circulation of the South Atlantic Ocean. *Journal of Geophysical Research* **104** (C9), 20863-20883 (1999).

Stramma, L., Hüttl, S. and Schafstall, J. Water masses and currents in the upper tropical northeast Atlantic off northwest Africa. *Journal of Geophysical Research: Oceans* **110** (C12), n/a-n/a (2005).

Stramma, L., Johnson, G. C., Sprintall, J. and Mohrholz, V. Expanding Oxygen-Minimum Zones in the Tropical Oceans. *Science* **320** (5876), 655-658 (2008).

Stramma, L. and Schott, F. The mean flow field of the tropical Atlantic Ocean. *Deep Sea Research Part II: Topical Studies in Oceanography* **46** (1), 279-303 (1999).

Stueber, A. M. and Goles, G. G. Abundances of Na, Mn, Cr, Sc and Co in ultramafic rocks. *Geochim. Cosmochim. Acta* **31** (1), 75-93 (1967).

Sunda, W. G. and Huntsman, S. A. Photoreduction of manganese oxides in seawater. *Mar. Chem.* **46** (1), 133-152 (1994).

Tang, Y., Elzinga, E. J., Jae Lee, Y. and Reeder, R. J. Coprecipitation of chromate with calcite: Batch experiments and X-ray absorption spectroscopy. *Geochim. Cosmochim. Acta* **71** (6), 1480-1493 (2007).

Tankéré, S. P. C., Muller, F. L. L., Burton, J. D., Statham, P. J., Guieu, C. and Martin, J. M. Trace metal distributions in shelf waters of the northwestern Black Sea. *Cont. Shelf Res.* **21** (13–14), 1501-1532 (2001).

Tourtelot, H. A. Black shale - its deposition and diagenesis. *Clays Clay Miner.* **27** (5), 313-321 (1979).

Tribovillard, N., Algeo, T. J., Lyons, T. and Riboulleau, A. Trace metals as paleoredox and paleoproductivity proxies: An update. *Chem. Geol.* **232**, 12-32 (2006).

Tubbs, C. R. (1969). The New Forest: An Ecological History. UK, David & Charles.

Tyson, R. V. and Pearson, T. H. Modern and ancient continental shelf anoxia: an overview. *Geological Society, London, Special Publications* **58** (1), 1-24 (1991).

van Aken, H. M. The hydrography of the mid-latitude Northeast Atlantic Ocean: II: The intermediate water masses. *Deep Sea Research Part I: Oceanographic Research Papers* **47** (5), 789-824 (2000).

van Aken, H. M. and Becker, G. Hydrography and through-flow in the north-eastern North Atlantic Ocean: the NANSEN project. *Prog. Oceanogr.* **38** (4), 297-346 (1996).

Viers, J., Dupré, B. and Gaillard, J. Chemical composition of suspended sediments in World Rivers: New insights from a new database. *Sci. Total Environ.* **407**, 853-868 (2009).

Villalobos-Aragón, A., Ellis, A. S., Armienta, M. A., Morton-Bermea, O. and Johnson, T. M. Geochemistry and Cr stable isotopes of Cr-contaminated groundwater in León valley, Guanajuato, México. *Appl. Geochem.* **27** (9), 1783-1794 (2012).

Wakelin, S. L., Holt, J. T., Blackford, J. C., Allen, J. I., Butenschön, M. and Artioli, Y. Modeling the carbon fluxes of the northwest European continental shelf: Validation and budgets. *Journal of Geophysical Research: Oceans* **117** (C5), n/a-n/a (2012).

Walsh, A. R. and O'Halloran, J. Chromium speciation in tannery effluent—I. An assessment of techniques and the role of organic Cr(III) complexes. *Water Res.* **30** (10), 2393-2400 (1996).

Wang, W.-X. and Dei, R. C. H. Influences of phosphate and silicate on Cr(VI) and Se(IV) accumulation in marine phytoplankton. *Aquat. Toxicol.* **52** (1), 39-47 (2001).

Wang, X., Johnson, T. M. and Ellis, A. S. Equilibrium isotopic fractionation and isotopic exchange kinetics between Cr(III) and Cr(VI). *Geochim. Cosmochim. Acta* **153** (0), 72-90 (2015).

Wang, X., Planavsky, N. J., Reinhard, C. T., Zou, H., Ague, J. J., Wu, Y., Gill, B. C., Schwarzenbach, E. M. and Peucker-Ehrenbrink, B. Chromium isotope fractionation during subduction-related metamorphism, black shale weathering, and hydrothermal alteration. *Chem. Geol.* **423**, 19-33 (2016).

Wang, X., Reinhard, C. T., Planavsky, N. J., Owens, J. D., Lyons, T. W. and Johnson, T. M. Sedimentary chromium isotopic compositions across the Cretaceous OAE2 at Demerara Rise Site 1258. *Chem. Geol.* **429**, 85-92 (2016).

Wang, X. L., Planavsky, N. J., Hull, P. M., Tripati, A. E., Zou, H. J., Elder, L. and Henehan, M. Chromium isotopic composition of core-top planktonic foraminifera. *Geobiology*, n/a-n/a (2016).

Wanner, C., Zink, S., Eggenberger, U. and Mäder, U. Unraveling the partial failure of a permeable reactive barrier using a multi-tracer experiment and Cr isotope measurements. *Appl. Geochem.* **37**, 125-133 (2013).

White, A. F. and Peterson, M. L. Reduction of aqueous transition metal species on the surfaces of Fe(II)-containing oxides. *Geochim. Cosmochim. Acta* **60** (20), 3799-3814 (1996).

Wille, M., Nebel, O., Van Kranendonk, M. J., Schoenberg, R., Kleinhanns, I. C. and Ellwood, M. J. Mo–Cr isotope evidence for a reducing Archean atmosphere in 3.46–2.76Ga black shales from the Pilbara, Western Australia. *Chem. Geol.* **340** (0), 68-76 (2013).

Wilson, A. M., Raine, R., Mohn, C. and White, M. Nepheloid layer distribution in the Whittard Canyon, NE Atlantic Margin. *Mar. Geol.* **367**, 130-142 (2015).

Wu, W., Wang, X., Reinhard, C. T. and Planavsky, N. J. Chromium isotope systematics in the Connecticut River. *Chem. Geol.* (2017).

Xu, F., Ma, T., Zhou, L., Hu, Z. and Shi, L. Chromium isotopic fractionation during Cr(VI) reduction by Bacillus sp. under aerobic conditions. *Chemosphere* **130** (0), 46-51 (2015).

Yeats, P. A. Trace metals in sea water: Sampling and storage methods. *ICES*. 1-8 (1987).

Yiğiterhan, O., Murray, J. W. and Tuğrul, S. Trace metal composition of suspended particulate matter in the water column of the Black Sea. *Mar. Chem.* **126** (1–4), 207-228 (2011).

Zachara, J. M., Cowan, C. E., Schmidt, R. L. and Ainsworth, C. C. Chromate Adsorption by Kaolinite. *Clays Clay Miner.* **36** (4), 317-326 (1988).

Zachara, J. M., Girvln, D., Schmidt, R. and Resch, C. T. Chromate Adsorption on Amorphous Iron Oxyhydroxide in the Presence of Major Groundwater Ions. *Environ. Sci. Technol.* **21**, 589-594 (1987).

Zenk, W., Klein, B. and Schroder, M. Cape Verde Frontal Zone. *Deep Sea Research Part A. Oceanographic Research Papers* **38**, S505-S530 (1991).

Zhang, S., Wang, X., Wang, H., Bjerrum, C. J., Hammarlund, E. U., Costa, M. M., Connelly, J. N., Zhang, B., Su, J. and Canfield, D. E. Sufficient oxygen for animal respiration 1,400 million years ago. *Proceedings of the National Academy of Sciences* **113** (7), 1731-1736 (2016).

Zink, S., Schoenberg, R. and Staubwasser, M. Isotopic fractionation and reaction kinetics between Cr(III) and Cr(VI) in aqueous media. *Geochim. Cosmochim. Acta* **74** (20), 5729-5745 (2010).